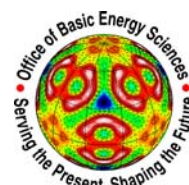


Renewable Energies for a Global Economy

The U.S. Department of Energy Experimental Program to Stimulate Competitive Research



DOE EPSCoR
State/National Laboratory
Program Review Workshop
July 23-25, 2007
Golden, Colorado



Executive Summary

The review of the U.S. Department of Energy's Experimental Program to Stimulate Competitive Research (DOE EPSCoR) program was held on July 22-25, 2007 in Golden, Colorado. The review was hosted by the National Renewable Energy Laboratory (NREL) and was attended by over 60 faculty, students and research scientists from 44 states. A record number of twelve DOE National Laboratories participated in the review to stimulate networking and partnership with these DOE crown jewels. The program was designed to achieve three major objectives: 1) Review projects currently funded by the DOE EPSCoR program, 2) Identify and stimulate interaction between the EPSCoR university community and the DOE National Laboratories, and 3) Provide a forum for exchange of information and ideas regarding the opportunities for renewable energies to contribute to the world's future energy needs.

DOE EPSCoR Program Review – A poster session was held on the afternoon and evening of Monday, July 23rd where over 40 posters representing DOE funded EPSCoR projects were displayed. There was a lively exchange of information on a wide variety of topics ranging from photonics and electro-optic materials, magneto-inertial fusion of plasmas, coal syngas and solid oxide fuel cells, nanomagnetism, grid computing, and high-energy physics. More poster topics included cutting-edge topics on novel battery systems, wind-hydrogen energy systems, solar cells and thermochemical conversion of woody biomass to fuel, all of which were funded by DOE EPSCoR. In addition DOE National Laboratories represented some of their user facilities in poster or booth form. Oak Ridge National Laboratory highlighted the recently completely DOE Spallation Neutron Source and demonstrated how neutrons can be used for renewable energy research and development. Five students from Los Alamos Neutron Scattering Center taught participants about their current research and instruments available at the Manuel Lujan Jr. Neutron Scattering Center (Lujan). The poster session was a great venue for informal exchanges between students, faculty and research scientists.

University/ DOE Laboratory Interactions – A major goal of the EPSCoR meeting was to stimulate interactions between the University Community and the DOE National Laboratories. On Tuesday a panel discussion chaired by Richard Bajura, Director of the West Virginia DOE EPSCoR program, provided overviews of partnering opportunities from the perspective of four universities. Ray Teller, a seasoned DOE Laboratory partnership leader and Director of the Argonne National Laboratory's Intense Pulsed Neutron Source gave a comprehensive overview of the DOE National Laboratory system, with highlights of the national x-rays and neutrons centers, including the five DOE Nanoscale Science Research Centers. In addition, brief presentations were provided by twelve National Laboratories with an emphasis on the user facilities at each laboratory.

On Wednesday morning DOE's Eric Rohlfing, Division Director of the Chemical Sciences, Geosciences and Biosciences Division, Office of Basic Energy Sciences, Office of Science, provided an encompassing overview of the *Strategic Planning and Energy Initiatives* in DOE Basic Sciences with a bird's-eye view of the Basic Research Needs, and planning. Later in the morning, the DOE National Laboratory representatives participated in informal discussions where attendees could participate in one-on-one discussions with Laboratory representatives. This provided an opportunity to discuss specific opportunities for collaboration and identify points of contact at individual Labs and at intersections of research topics to pursue further discussion.

The global agenda was designed to provide numerous opportunities for informal discussions among participants during lunch and coffee breaks as well as during the opening reception Sunday evening and the Bar-b-Que on Tuesday evening. We want to express a particular thanks to Midwest Research Institute and Battelle Memorial Institute for hosting the social events of the workshop. A highlight of the Tuesday evening Bar-b-Que was the music provided by the Grass Roots Review Band from Clemson University, South Carolina.

Renewable Energies for the Global Economy- was the theme for the workshop. The goal was to provide the meeting attendees with an overview of the world's future energy demands, and opportunities for renewable energies to meet current and future demands. The opening plenary on Monday morning was highlighted by an overview of *The Global Energy Challenge* presented by George Crabtree, Argonne National Laboratory; and a review of *Energy and Nano-structured Materials- Scientific Challenges in the Hydrogen Economy* presented by Mildred Dresselhaus, Massachusetts Institute of Technology. These were excellent presentations providing a perspective on future world energy demand and the challenges to achieve a hydrogen economy. The Monday morning session also featured an overview of DOE's Office of Energy Efficiency and Renewable Energy research portfolio presented by Bob Hawsey of Oak Ridge National Laboratory and an overview of the research at NREL presented by Bobi Garrett, Associate Laboratory Director for Renewable Electricity. The overview presentations were followed by more detailed presentations on Solar, Biomass, Wind and Ocean Energy technologies. These overview presentations set the stage for tours of NREL's solar and biomass research facilities on Monday afternoon and the Laboratory's National Wind Technology Center on Tuesday afternoon. The combination of the presentations and laboratory tours provided an excellent introduction to renewable energy technologies and an introduction to on-going research programs in four key renewable energy areas important to DOE and the nation.

A major driver for energy technologies is the relationship between energy conversion and use, and the emission of green house gases. Tuesday morning featured presentations by Warren Washington of the National Center for Atmospheric Research (NCAR) describing climate modeling, and Susan Solomon of the National Oceanic & Atmospheric Administration (NOAA) describing results of the Intergovernmental Panel on Climate Change (IPCC) working group on climate assessment. These two excellent presentations gave the audience an overview of the state-of-the-art in modeling climate change and a summary of recent IPCC assessment of human influence on climate change.

In summary the workshop met its three goals by providing an excellent venue for DOE funded researchers to highlight their work and demonstrate the breadth of the DOE EPSCoR program in energy-related basic and applied research. The meeting stimulated University and National Laboratory interaction, and provided a basis for new partnerships for ground-breaking energy research across the entire nation. Participants came away from the meeting with ideas for future energy research and an appreciation of the challenges and research opportunities in the area of renewable energy.

Acknowledgements:

We would like to thank NSF EPSCoR for their support and collaboration on the meeting with special thanks to Jim Gosz, NSF. Special thanks are due to the NREL administrative staff Barbara Ferris, David Glickson and Melody Mountz whose experience, professionalism and attention to detail made the meeting truly a grand success. DOE EPSCoR would also like to thank Sophia Kitts and Barbara Cohen, ORISE for their continued commitment to excellence in support of the DOE EPSCoR office.

DOE/NSF EPSCoR Program Review 2007

U.S. Department of Energy

Experimental Program to Stimulate Competitive Research (DOE-EPSCoR)

*Sponsored by U.S. Department of Energy & the National Science Foundation
“Renewable Energies for a Global Economy”*

July 22 – 25, 2007

Denver Marriott West, Golden, CO

Hosted by the National Renewable Energy Laboratory (NREL)

Agenda

Sunday, July 22, 2007

3:00 pm – 6:00 pm Early Registration

5:00 pm– 7:00 pm Reception/Mixer
Hosted by Battelle

Monday, July 23, 2007

7:00 am – 8:00 am Registration/ Continental Breakfast

8:10 am – 8:30 am Welcome and Introductory Remarks
Welcome to NREL – **Ray Stults**, Associate Director Energy Sciences,
National Renewable Energy Laboratory

Kristin Bennett, Program Manager, U. S. Department of Energy
EPSCoR Office

8:30 am – 9:10 am Opening Plenary Session
The Global Energy Challenge – **George Crabtree**, Argonne National
Laboratory

9:10 am – 9:50 am Energy and Nanostructured Materials – Scientific Challenges in the
Hydrogen Economy – **Mildred S. Dresselhaus**, Massachusetts Institute
of Technology

9:50 am – 10:15 am Break

10:15 am – 10:45 am Overview of Department of Energy’s Energy Efficiency and Renewable
Energy Program – **Robert Hawsey**, Director Energy Efficiency and
Renewable Energy Program, Oak Ridge National Laboratory

10:45 am – 11:15 am National Renewable Energy Laboratory Overview –
Bobi Garrett, Associate Director Strategic Development & Analysis,
National Renewable Energy Laboratory Director, National Renewable
Energy Laboratory

- 11:15 am – 11:45 am NREL Biomass Program Overview –**Tom Foust**, Biomass Program Manager, National Renewable Energy Laboratory
- 11:45 am – 12:00 pm Tour Logistics – **Ray Stults**
- 12:00 pm – 1:15 pm Luncheon Speaker – **Art Vailas**, President, Idaho State University
- 1:15 p.m. – 2:00 p.m. The Challenges and Opportunities for Solar Research – **Larry Kazmerski**, Director, National Center for Photovoltaics, National Renewable Energy Laboratory
- 2:00 pm – 5:00 pm Concurrent Activities
Poster Set-up
- 2:00 – 3:00 Tour of NREL Biomass and Solar R&D Facilities
- 3:30 – 5:00 Tour of NREL Biomass and Solar R&D Facilities
- 5:00 pm – 7:00 pm Poster Session/Networking Mixer
-Students/Faculty/Staff Poster Session
-NREL Lab S&T and Staffing recruiting displays
-EPSCoR State Displays
-Lab, Facilities and Center Displays

*****Dinner on Own*****

Tuesday, July 24, 2007

- 7:30 am – 8:20 am Registration/Continental Breakfast
- 8:30 am – 9:15 am Climate Modeling: A Tool for Examining Climate Change Options for Mitigation and Adaptation - **Warren Washington**, Senior Scientist and Head of Climate Change Research, National Center for Atmospheric Research
- 9:15 am – 10:00 am Climate Change 2007: Key Results of The IPCC Working Group One Assessment - **Susan Solomon**, Senior Scientist, National Oceanic & Atmospheric Administration /Earth System Research Laboratory (NOAA/ESRL) Chemical Sciences Division
- 10:00 am – 10:30 am Break
- 10:30 am – 12:30 pm **Panel – Partnering with National Laboratories and Centers**
Introduction: Opportunities in the ‘Post-Academic’ World – **Thomas Vogt**, University of South Carolina, Director, USC NanoCenter
- Panel Discussion/Question & Answer**
Chair: Richard Bajura, West Virginia University – Director, West Virginia DOE EPSCoR

Laboratory Introduction: “Working with DOE National Laboratories” –
Ray Teller, Argonne National Laboratory

Laboratory Representatives

Jim Brainard – National Renewable Energy Laboratory
Marie Garcia – Sandia National Laboratory
Bruce Harmon – Ames Laboratory
Alan Hurd/Everett Springer – Los Alamos National Laboratory
Dave Koppenaal – Pacific Northwest National Laboratory
Harold Myron – Argonne National Laboratory
Robert Neilson – Idaho National Laboratory
Christie Nelson – Brookhaven National Laboratory
Frank Ogletree – Lawrence Berkeley National Laboratory
Bob Romanosky – National Energy Technology Laboratory
Judy Trimble/Robert Hawsey – Oak Ridge National Laboratory
John Ziagos – Lawrence Livermore National Laboratory

Panel Members for Q & A

State Representatives

Gary April – Alabama
Stephen Borleske – Delaware
Fred Choobineh – Nebraska
Barbara Kimball – New Mexico

*Panel Discussion/Question & Answer session will be continued Wednesday
10:30-12:00 pm with Concurrent Laboratory Breakout Sessions*

12:30 pm – 1:30 pm	Luncheon Speaker - From Carbon Sequestering to Landmine Detection, Pollinators Do It All - Jerry Bromenshenk , Adjunct Research Professor, Biological Sciences, University of Montana, Missoula
1:30 pm – 2:30 pm	Wind Technology Program Overview – Michael Robinson , Deputy Director, National Wind Technology Center, National Renewable Energy Laboratory Ocean Renewable Technology – Walter Musial , Lead, Marine and Offshore Energy, National Wind Technology Center, National Renewable Energy Laboratory
2:30 pm- 5:00 pm	Tour – National Wind Technology Center
6:00 pm – 9:00 pm	*****Dinner ***** Outdoor Barbeque – Genesee Park Featuring the Grass Roots Review Band Hosted by Midwest Research Institute

Wednesday, July 25

- 7:30am – 8:20 am Networking – Continental Breakfast

- 8:30 am – 9:15 am Strategic Planning and Energy Initiatives in DOE Basic Sciences –
Eric Rohlfig, Division Director of the Chemical Sciences,
Geosciences and Biosciences Division, Office of Basic Energy
Sciences, Office of Science, U. S. Department of Energy

- 9:15 am – 10:00 am Supporting the Convergence of National Energy Needs with
Agricultural Sector Energy Capabilities – **Eldon Boes**,
AAAS/ASME Congressional Fellow, Senate Committee on
Agriculture, Nutrition and Forestry

- 10:00 am – 10:10 am Breakout Orientation – **Kristin Bennett**

- 10:10 am – 10:30 am *****Coffee Break*****

- 10:30 am – 11:30 am Concurrent Breakout Sessions -Partnering with National Labs
[Discussions on user facilities and successful lab/university
collaborations]

- 11:30 am - Noon Summary Remarks and Meeting Adjourns – **Kristin Bennett &**
Ray Stults

**DOE EPSCoR Program Directors Working Group
Satellite Meeting
Wednesday, July 25
1:00 pm – 5:00 pm
Lunch – Provided**

- 1:00- 1:15 pm DOE/EPSCoR

- 1:15- 2:15 pm New Implementation Award Presentations
Eric Grulke - University of Kentucky
Hemant Pendse - University of Maine
John Xiao - University of Delaware
Bob Dalton - University of New Hampshire

- 2:15- 3:00 pm DOE EPSCoR News & Updates, Website, Reporting, Budget,
New Solicitations & Awards - Kristin Bennett, DOE EPSCoR
Program Manager

- 3:00- 5:00 pm Program Director Discussion/Questions & Answer

- 5:00 pm Meeting Adjourns

Table of Contents

Executive Summary	i
Agenda	iii
Table of Contents	vii
Abstracts	
Lignocellulosic Waste Degradation Using Extremophiles from the Homestake Mine, South Dakota <i>Sookie S. Bang and Rajesh K. Sani</i>	1
Investigation of Electron Transfer-Based Photonic and Electro-Optic Materials and Devices <i>Jerry Bromenshenk</i>	4
Numerical Modeling Studies of Plasma Driven Magnetoinertial Fusion <i>Jason T. Cassibry, Charles Knapp, Ron Kirkpatrick, and S. T. Wu</i>	5
Direct Utilization of Coal Syngas in High Temperature Solid Oxide Fuel Cells <i>Ismail Celik</i>	10
Nanomagnetism <i>Siu-Tat Chui and Sam Bader</i>	14
Peer-to-Peer Checkpointing Arrangement for Mobil Grid Computing Systems <i>Paul J. Darby III and Nian-Feng Tzeng</i>	18
A Polychromatic Approach to White Light Generation Using Colloidal Nanocrystals <i>E. A. DeCuir, Jr., T. A. Bond, E. Fred, and M. O. Manasreh</i>	22
Applications of Computational Artificial Intelligence <i>Richard P. Donovan</i>	25
Neutrons – A Tool for Renewable Energy Research at ORNL <i>A. E. Ekkebus and J. L. Trimble</i>	29
High Efficiency Photovoltaic Devices Based on Nanocrystal/Polymer Nanocomposites <i>Emil Fred, Kaushik Y. Narsingi, Omar Manasreh, Simon Ang, and Andrew Wang</i>	30

High Temperature Resonant Ultrasound Spectroscopy Studies <i>Gary A. Lamberton, Jr., Rasheed Adebisi, Joseph R. Gladden, and Henry E. Bass</i>	33
Scattering of Ultra Cold Neutrons on Nano-Size Bubbles <i>Vladimir Gudkov</i>	36
Transforming Wastewater Treatment Facilities into Biocrude Centers <i>Rafael Hernandez, Todd French, Mark White, Kaiwen Liang, William Holmes, Earl Alley, Tracy Benson, Andro Mondala, and Jaclyn Hall</i>	37
Novel Energy Sources – Material Architecture and Charge Transport in Solid State Ionic Materials for Rechargeable Li ion Batteries <i>Ram S. Katiyar</i>	38
Resonant Ultrasound Studies of Spin Glasses and Geometrically Frustrated Magnets <i>Veerle Keppens, Yanbing Luan, Manuel Angst, and David Mandrus</i>	42
Analysis and Development of a Robust Fuel for Gas-Cooled Fast Reactors <i>Travis W. Knight, Thad M. Adams, Gokul Vasudevamurthy, Sergiy Y. Lobach, Devon R. Berry and Jenny M. Watts</i>	46
High Throughput Analysis of the Low Dose Radiation Transcriptome <i>Michael A. Langston, Elissa J. Chesler, and Brynn H. Voy</i>	48
A Grid-Enabled Framework for Ensemble Inverse Modeling <i>Zhou Lei, Gabrielle Allen, Tevfik Kosar, Guan Qin, Frank Tsai, and Christopher White</i>	52
Properties of Ferroelectric Nanostructures: A Combined Theoretical and Experimental Approach <i>Sergey Lisenkov, Laurent Bellaiche, and Huaxiang Fu</i>	56
Addressing System Integration Issues Required for the Development of Distributed Wind-Hydrogen Energy Systems <i>Michael D. Mann, Hossein Salehfar, Nilesh Dale, Christian Biaku, Andrew Peters, Tae-hee Han, Kevin Harrison, and Eduardo Hernandez Pacheco</i>	60
Novel Quantum Phenomena in Layered Ruthenates <i>Zhiqiang Mao</i>	64

Homestake Ultra-Low Background Counting Facility and Detection of Double-Beta Decay to Excited States <i>Dongming Mei, Christina Keller, Yongchen Sun, Zhongbao Yin, Kevin Lesko, Yuen-dat Chan, Al Smith, Gersende Prior, Robert McTaggart, Barbara Szczerbinska, Andrew Alton, and William M. Roggenthen</i>	68
Optoelectronic Properties of Carbon Nanostructures <i>John W. Mintmire and Thushari Jayasekera</i>	72
Surface Anchoring of Nematic Phase on Carbon Nanotubes: Nanostructure of Ultra-High Temperature Materials <i>Amod A. Ogale, Rebecca Alway-Cooper, Marlon Morales, and Daniel Sweeney</i>	76
Preparation and Study of Novel Ru Dyes for Dye Sensitized Solar Cells (DSSCs) <i>Joshua J. Pak, Dominic X. Denty, Stephanie Pritchard, Lisa Lau, Anna Hoskins, Alan W. Hunt and Rene G. Rodriguez</i>	79
Preparation and Study of I-III-VI₂ Nanoparticles and Thin Films <i>Joshua J. Pak, Joseph Gardner, Endrit Shurdha, Ian Kihara, Lisa Lau, Anna Hoskins, Alan W. Hunt and Rene G. Rodriguez</i>	82
Impact of Atmospheric Aerosols on Nocturnal Boundary Layer Temperatures <i>Falguni Patadia, U. S. Nair, R. T. McNider, S. A. Christopher, K. A. Fuller, R. M. Welch, D. A. Bowdle, and M. Newchurch</i>	84
Thermochemical Conversion of Woody Biomass to Fuels and Chemicals <i>Hemant P. Pendse, M. Clayton Wheeler, William J. DeSisto, Brian G. Frederick, and Adrian van Heiningen</i>	86
Design and Implementation of Multi-Hop Wireless and Sensor Networks for the Ubiquitous Computing and Monitoring System (UCoMS) <i>Hongyi Wu, Dmitri Perkins, Nian-Feng Tzeng, and Magdy Bayoumi</i>	89
Dynamic and Deterministic Lightpath Scheduling in Next-Generation WDM Optical Networks <i>Byrav Ramamurthy</i>	93
Advances in the Fundamental Understanding of Coal Combustion Emission Mechanisms <i>Wayne S. Seames, Mark R. Hoffmann, John Hershberger, Uwe Burghaus, Michael D. Mann, Frank Bowman, David T. Pierce, and Evguenii I. Kozliak</i>	97

Ro-vibrational Relaxation Dynamics of PbF Molecules <i>Neil Shafer-Ray, Greg Hall, and Trevor Sears</i>	101
Fabrication of Cu-In-S Nanoparticles and Clusters <i>Pamela Shapiro</i>	105
Key Physical Mechanisms in Nanostructured Solar Cells <i>Valeria Gabriela Stoleru, Christiana B. Honsberg, Andrew G. Norman, A. Pancholi, and Y. C. Zhang</i>	109
EPSCoR Program at OCHEP <i>Flera Rizatdinova and Mike Strauss</i>	113
Phase II: The Next Generation Thermoelectric Materials for Solid State Cooling & Power Generation Applications <i>Terry M. Tritt, Joe Kolis, Murray Daw, Fivos Drymiotis, Catalina Marinescu and Apparao Rao</i>	117
Ubiquitous Computing and Monitoring System (UCoMS) for Discovery and Management of Energy Resources <i>Nian-Feng Tzeng, Magdy Bayoumi, Hongyi Wu, Gabrielle Allen, Dmitri Perkins, Chris White, Zhou Lei, Boyun Guo, Edward Seidel, John Smith, Douglas Moreman, and Michael Khonsari.</i>	121
Experimental and Numerical Investigation of Flows in Expanding Channels <i>Peter Vorobieff and Vakhtang Putkaradze</i>	125
Delaware Research Cluster: The Center for Spintronics and Biodetection <i>John Q. Xiao, Yi Ji, James Kolodzey, Branislav K. Nikolic, Edmund R. Nowak, and Shouheng Sun</i>	129
Estimating Soil Hydraulic Parameter Uncertainty and Heterogeneity Using Bayesian Updating and Neural Network Methods <i>Jianting Zhu, Ming Ye, Philip D. Meyer, Yanxia Zhao, Ahmed E. Hassan, and Feng Pan</i>	133
Author Index	137
Participant List	139

Lignocellulosic Waste Degradation Using Extremophiles from the Homestake Mine, South Dakota

Sookie S. Bang and Rajesh K. Sani

sookie.bang@sdsmt.edu, rajesh.sani@sdsmt.edu

South Dakota School of Mines & Technology, Rapid City, SD 57701

Program Scope

One of the major challenges in biomass degradation is its recalcitrance to chemicals or enzymes due to the presence of complex polymer composites consisting of cellulose, hemicellulose and lignin. Cellulose and hemicellulose degradation rates are significantly higher under thermophilic conditions than under mesophilic, mainly because thermophile cellulases function well at relatively high temperature (50 – 70°C), where substrate solubility and mass transfer rates increase.^{1,2} Recently, extremophiles isolated from deep subsurface, hot springs and compost piles have shown high potential in degradation of recalcitrant biomass.³ Researchers at the Sandia National Laboratories have been working on genetically manipulated hydrolytic “extremozymes” originated from an extreme thermoacidophile, *Sulfolobus solfataricus*.⁴ The scope of our research encompasses a fundamental spectrum of applied extreme microbiology focusing on biomass fermentation, genomics and genetic manipulation of extremophiles. In particular, this research program is based on bioprospecting of novel extremophiles that produce high-quality cellulases and hemicellulases from the Homestake Gold Mine, Lead, South Dakota.

On July 10, 2007, this deepest mine in North America (44°35'2074"N, 103°75'082"W) was chosen by the National Science Foundation as the site for a potential national deep underground science and engineering laboratory (DUSEL). Microbial communities in the geographically isolated deep subsurface (down to 8,000 ft.) of the Homestake Mine have survived under nutrient-limited, extreme environmental conditions, leading their evolutionary lineage to be distinct from the surface-dwelling microorganisms. During active mining operations over 125 years until closure in 2001, surface microbes and lignocellulosic substrates (e.g., mining construction materials) had been introduced into the subsurface environments with high humidity and temperature (close to 65°C at 8,000 ft.). Interactions between introduced and existing microorganisms through horizontal genetic transfer might have been inevitable and caused genome-altering events.⁵ It is therefore possible that genetically distinct microbes including thermophiles with diverse, novel metabolic activities might be present in the biofilms, decaying timbers, and soils of Homestake Mine. Thus, it is believed that the DUSEL represents a potential source of high-value microbial enzymes (e.g. cellulases, xylanases, glucanases, peroxidases, amylases, proteases and lipases) that have optimal activity at high temperatures.

Recent Progress

In 2006, while the Homestake was being transformed to be an NSF-designated DUSEL, water and soil samples from the 4,850 ft. level of the mine were collected and enriched

for cellulose and sawdust-degrading mesophilic (37°C) and thermophilic (60°C) microorganisms under aerobic conditions in our laboratories. These DUSEL microbial consortia as well as pure isolates were examined for phylogenetic diversity of microbial community using 16S rDNA amplification and sequence analysis and biodegradation of cellulose and sawdust using pure and mixed cultures of new isolates.

BLAST analyses were carried out with 63 and 72 bacterial rDNA sequences from clone libraries of mesophiles and thermophiles consortia, respectively. Phylogenetic trees were constructed by the neighbor-joining method with 1000 bootstrappings using MEGA v 3.1.⁶ The mesophile clones were identified as belonging to two clusters, *Clostridiales* and *Bacillales*, of phylum *Firmicutes*, while the thermophile clones to one cluster, *Bacillales*. We isolated several colonies in the presence of cellulose and sawdust as the sole source of carbon and energy at both temperatures. Each of the three isolates (DUSEL G10, G12 and G16) was growing well at 37°C in the presence of cellulose or sawdust. Interestingly, individuals of three isolates (DUSEL R7, R11 and R13) at 60°C were not growing separately, but growing well as a mixed culture in cellulosic media. This observation suggests a potential metabolic dependence among DUSEL thermophiles in cellulose and sawdust degradation.⁷ Currently, kinetics of microbial degradation of cellulosic substrates is being studied.

Future Plans

With the NSF support, the Homestake DUSEL will become one of the top national laboratories. This underground laboratory will allow access to depths of 4,850 and 8,000 ft. in 2007 and 2008, respectively. Accordingly, our future research plans will be synchronized with the mine re-entry schedule. Our future research will focus on both culturable and non-culturable lignocellulose-degrading DUSEL extremophiles utilizing agricultural and forestry waste that are abundant throughout the state of South Dakota including the Black Hills. Based on the experimental procedures established in our laboratories, we plan to conduct microbial, biochemical and DNA-based tasks using samples of soil, biofilms, and timbers from the deep mine.

In detail, microorganisms from the DUSEL samples (soil, biofilms, and timbers) taken from different depths (4,850, 6,000, and 8,000 ft.) will be grown in corn stover, switch grass, and woodchips as sole carbon and energy source. The enrichment and isolation conditions will include variations of temperature (50 – 70°C), pH (3 – 10) and e^- acceptors (aerobic and anaerobic).^{8,9} With extremophile isolates, the robotic workcell system will be used to screen expression of cellulose-degrading enzymes from DUSEL isolates, to select optimum lignocellulases from the isolates and to identify high-value co-metabolites and byproducts.¹⁰ Further, we plan to construct clone expression libraries using culture-based genomic DNA and metagenomic DNA of DUSEL microorganisms to identify novel thermotolerant hydrolytic enzymes.¹¹ These extremozymes will be subsequently cloned into expression vectors and engineered into industrial yeast strains for seamless processing of lignocellulosic biomass into biofuel ethanol.^{12,13}

The robust, genetically engineered super microorganisms should be able to overcome difficulties associated with biomass degradation and to produce ethanol and co-metabolic products from lignocellulose. We expect that successful outcomes of our proposed research will establish a critical milestone to efficient, economic and sustainable biofuel production. The ultimate goal of the proposed research is to achieve a cost-effective production technology of ethanol and value-added chemicals.

References

1. Feitkenhauer, H. et al. 2003. *Water Sci. Technol.* 47, 123-130
2. Viamajala, S. et al. 2007. *Chemosphere.* 66, 1094-1106
3. Turner, P. et al. 2007. *Microbial Cell Factories.* in press
4. Simmons, B.A. et al. 2007. Abstract submitted to the 2007 Annual Meeting of the American Institute of Chemical Engineers, Salt Lake City, UT
5. Martinez, R.J. et al. 2006. *Appl. Environ. Microbiol.* 72, 3111-3118
6. Kumar, S. et al. 2004. *Briefings in Bioinformatics.* 5, 150-163
7. Moller, S. et al. 1998. *Appl. Environ. Microbiol.* 64, 721-732
8. Sani, R.K. et al. 2005. *Environ. Sci. Technol.* 39, 2059-2066
9. Sani, R.K. et al. 2007. Poster presented at the 107th General Meeting of the American Society of Microbiology, Toronto, Canada
10. Hughes, S.R. et al. 2005. *J. Assoc. Lab. Autom.* 10, 287-300
11. Edwards, R.A. et al. 2006. *BMC Genomics.* 7, 57
12. Hughes, S.R. et al. 2006. *Proteome Science.* 4, 10
13. Panavas, T. et al. 2005. *Proc. Natl. Acad. Sci. USA.* 102, 7326-7331

DUSEL-Related Research Presentations

- Muppidi, G.L., Sani, R.K., Bang, S.S., and Rastogi, G. Characterization of cellulose- and sawdust-degrading thermophilic microorganisms in deep subsurface of Homestake Mine, Lead, South Dakota. Poster presentation at the 36th annual Biochemical Engineering Symposium, Kansas State University, Manhattan, KS, April 20 – 21, 2007
- Sani, R.K., Muppidi, G.L., Sefa, F., and Bang, S.S. Presence of culturable cellulose- and sawdust-degrading thermophilic microorganisms in deep subsurface of Homestake Mine, Lead, South Dakota. Poster presentation at the American Society of Microbiology 107th General Meeting, Toronto, ON, Canada, May 21 – 25, 2007
- Sani, R.K., Rastogi, G., Muppidi, G.L., and Bang, S.S. Culturable cellulose- and sawdust-degrading mesophilic and thermophilic microbial diversity in deep subsurface of Homestake Mine, Lead, South Dakota. Poster presentation at the Society for Industrial Microbiology Annual Meeting, Denver, CO, July 29 – August 2, 2007

Montana Program Abstract:

Investigation of Electron Transfer-Based Photonic and Electro-Optic Materials and Devices

- Montana's current state program finished its sixth and final year in December 2006. Most projects have been completed, with a few in final wrap up stage. The project's research cluster focuses on physical, chemical, and biological materials that exhibit unique electron-transfer properties. In 2006, the first of a broad series of patents were filed. These patents protect the concept and implementation of Fractional Order Control (FOC), including nanostructured materials; while two other patent applications address materials and methods of incorporating conductive polymer electrodes on a flexible piezoelectric sheet. Recent project advances include push-pull phthalocyanines for optical storage and potentially quantum storage and quantum computing, photochromes to achieve terabyte storage capacity, growth of nanowires in 2-100 micron channels as circuit components, development of a novel finite element approach for the piezoelectric bending response of a bimorphic cantilever driven by AC voltage, advances in electrical rectification in metal, a finding that endgroups need to be permanently covalently tethered together in order to introduce order on polyaminoamine (PAMAM) stardust dendrimers and virion protein cages used as breadboards for molecular circuitry, devolving synthetic methodologies for new luminescent molecules for use as probes of biomolecular structure and dynamics, and developing the use of Artificial Neural Networks for calculating the material properties of advanced composite materials and for distributed sensor arrays. In addition, this program leveraged funds to assemble a 28-processor (64-bit AMD Opteron) Linux cluster, that uses PNNLs NWChem software suite and ECCE visualization software to support quantum chemical calculations. Montana investigators also have published and presented nearly 300 papers, won numerous additional grants and contracts averaging \$2-3M/year, and have established five spin-off businesses (3 MSU, 2 UM) and a research center (MT Tech). In addition, in its final year, this project included 13 faculty at three campuses (UM, MSU, MT Tech), 2 professional staff, 13 graduate students, 20 undergraduate students, and 4 post doctoral fellows. Of these, 15 are under-represented students, including 10 women and 5 Native Americans.

NUMERICAL MODELING STUDIES OF PLASMA DRIVEN MAGNETOINERTIAL FUSION

Jason T. Cassibry¹

Propulsion Research Center, University of Alabama in Huntsville, Huntsville, AL 35899

Charles Knapp, Ron Kirkpatrick²

Los Alamos National Laboratory, Los Alamos, New Mexico, 87545

S. T. Wu³

Center for Space Plasma and Aeronomy Research, University of Alabama-Huntsville, Huntsville, AL 35899

1. Introduction

In magneto-inertial fusion (MIF), an imploding material liner is used to compress a magnetized plasma to fusion ignition and to inertially confine the resulting burning plasma to obtain the necessary energy gain. The approach attempts to combine the strengths of both magnetic and inertial confinement, and it offers a low-cost development path for fusion energy[1]. Plasma liner-driven MIF (PJMIF) has the potential for liners to be formed in a repeatable, standoff manner using plasma accelerators, and allows for the possibility of secondary fusion burn in the liner[2, 3]. The physics basis for doing plasma-jet plasma liner research has been established by simulations performed by Thio, Kirkpatrick, and Knapp[4]. The modeling results indicate that the jets can form a stable, imploding liner both in a cylindrical and spherical distribution and compress a target to thermonuclear conditions[4].

Additional computational and theoretical studies are required to firmly establish its theoretical foundation in detail. As a first step, the numerical models used to study the PJMIF problem must be verified as much as possible against known solutions, to bring confidence to the numerical output. We performed an assessment of two separate numerical models, one based on finite volume discretization and one based on smoothed particle hydrodynamics. Specifically, we compared numerical output from these codes with two known problems in cylindrical and spherical symmetry, the Noh problem and a self-similar solution of converging shocks. In section 2, we summarize the analytic solutions and numerical models used in the study. Section 3 covers the technical approach followed, including flow parameters and approach to the analysis. Results are given in section 4.

2. Numerical Models

2.1. The Noh Problem

The Noh problem[5] is a verification problem involving a gas with uniform properties and ideal gas behavior. The solution consists of the properties of a reflected shock which depends on the initial conditions, and exists in planar, cylindrical and spherical geometries. For cylindrical and spherical geometries, the velocity is purely radial and directed inward, and the reflected shock begins at the origin.

¹ UAH Mechanical & Aerospace Engineering Assistant Research Professor, AIAA Member

² LANL Research Scientist

³ UAH Mechanical & Aerospace Engineering Distinguished Professor Emeritus, AIAA Fellow

2.2. Self Similar Converging Shock

For a uniform gas at rest obeying constant gamma ideal gas law, there is a similarity solution for an infinite MACH number shock converging on the origin in cylindrical and spherical symmetry[6, 7]. This problem provides a verification of a high temperature, high velocity gas converging on a stationary target gas, which provides strong overlap with MIF-related problems.

2.3. MACH2

Two dimensional hydrodynamic simulations are performed with MACH2[8]. MACH2 is a 2½D multiblock, Arbitrary Lagrangian Eulerian (ALE), resistive, single fluid magnetohydrodynamic (MHD) code was used to develop the model. MACH2 carries all three spatial components of vectors, but allows no quantity to depend on the coordinate that is normal to the computational plane. All computations were performed on a Dell dual processor dual core Xenon workstation with 4 GB of RAM running Suse 10.1 linux.

2.4. Smoothed Particle Hydrodynamics

Smooth Particle Hydrodynamics (SPH) is a gridless Lagrangian technique [9], in which a differential interpolant of a function can be constructed from its values at the particles by using a differentiable kernel, whereby derivatives are obtained by ordinary differentiation[10]. In this paper, all SPH calculations are performed using the SPHC code[11].

3. Technical Approach

For Noh problem, the density, velocity, atomic weight, and specific heat ratio were set uniformly to 1 kg/m^3 , $-10,000 \text{ m/s}$, 2 kg/kmol , and $5/3$, respectively. We chose the molecular weight to be 2 because we are interested in the dynamics of deuterium. Flow properties for both MACH2 and SPHC were plotted against the exact solution. For the 2D MACH2 calculations, data were extracted along radial lines through the computational domain. For the spherical case, data were extracted along the lines making angles of $\pi/8$, $2\pi/8$, and $3\pi/8$, providing a means of assessing the symmetry in the model.

For the converging shock test, we chose the parameters as given in Table 1. α has to be quite close to the values shown for a given symmetry value ν and γ chosen, discussed in Lazarus and Richtmyer[6]. To set up the initial conditions in MACH2 and SPHC, the exact model was run to 10^{-7} s , close to shock collapse. The data from that run was extracted, and a number of points were put through the data as a piecewise linear curve fit. These points were read into MACH2 and SPHC, and actual initial value for the flow properties of velocity, temperature, and density were linearly interpolated based on these points. We chose 25 points, which provided SPHC and MACH2 with initial conditions within 1% of the exact method.

Table 1. Parameters for exact converging shock test.

Geometry	ν	α	A	γ	$\rho_0 (\text{kg/m}^3)$
cylindrical	1	0.8156250	10000	5/3	6.642×10^{-4}
spherical	2	0.68837682	2000	5/3	5.0×10^{-4}

4. Results

Figure 1 shows the comparison of the reflected shock conditions for the cylindrical (left) and spherical (right) Noh test case. SPHC gives very good agreement in both cases, except for on axis (~5 to 10% error). MACH2 agreement is only qualitative. We observed excessive

compression in cylindrical case, which resulted in low temperatures. The pressure was fairly accurate in the cylindrical case, although there were oscillations from the origin to the shock boundary. The temperature was high by about 80% at the origin in the spherical case, but good agreement was achieved near the shock boundary. The reasons for the poor MACH2 agreement are not understood at this time. We will investigate the impact of various input file controls on the model in a future work to address this issue, and may switch to full Lagrangian mode to see if it is due to the stationary grid.

Results from the cylindrical and spherical converging shock test are given in Figure 2. SPHC gives very good agreement in the cylindrical case, except for pressure and density on axis (50% error, but 1% error at the shock). MACH2 gave very good agreement with density and temperature. The Gibbs phenomena was observed for density and pressure, with the shocked pressure high by 20%. For SPHC in the spherical test, shock values for density and velocity within 5%. There was an observed density spike/temperature dip at liner/target interface. Temperature and pressure agreement was only qualitative. It must be noted that the initial density profile was not set up in the model as specified in the input deck, so it is possible that some of the numerical problems were caused by a bug in the setup algorithm.

MACH2 gave extremely good agreement with the exact solution for the spherical test case. In fact, it was almost hard to tell the difference between exact and MACH2 solutions, except on axis. This brings confidence to using MACH2 to study MIF problems with spherical symmetry.

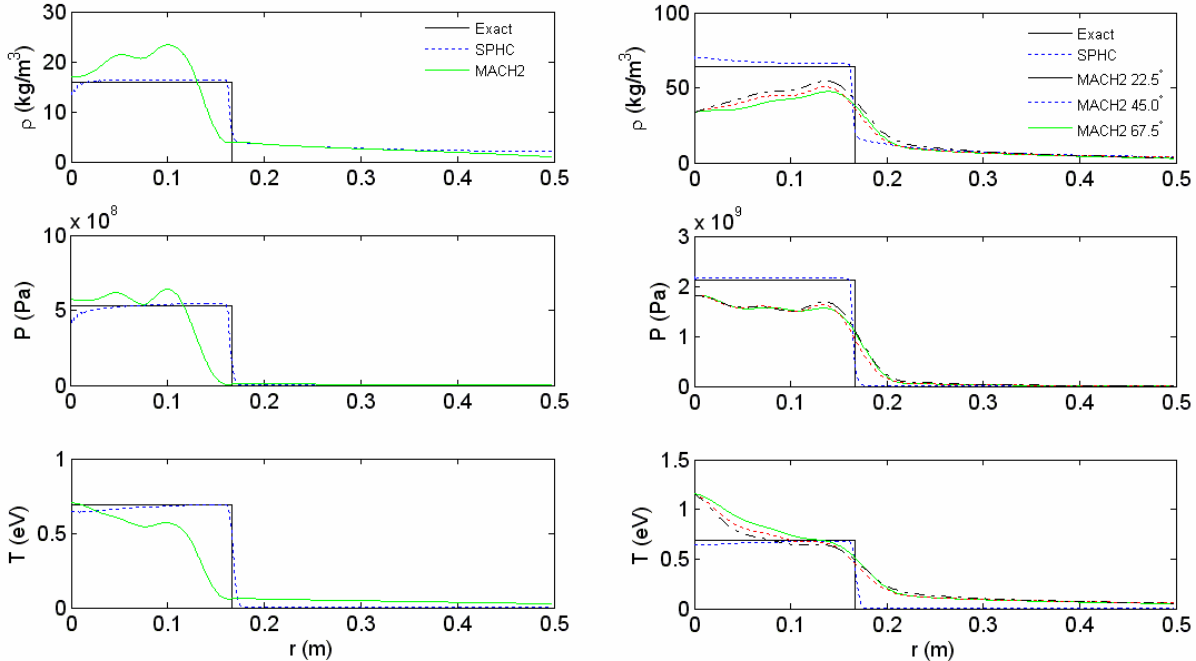


Figure 1. Comparisons of cylindrical (left) and spherical (right) Noh tests for all models.

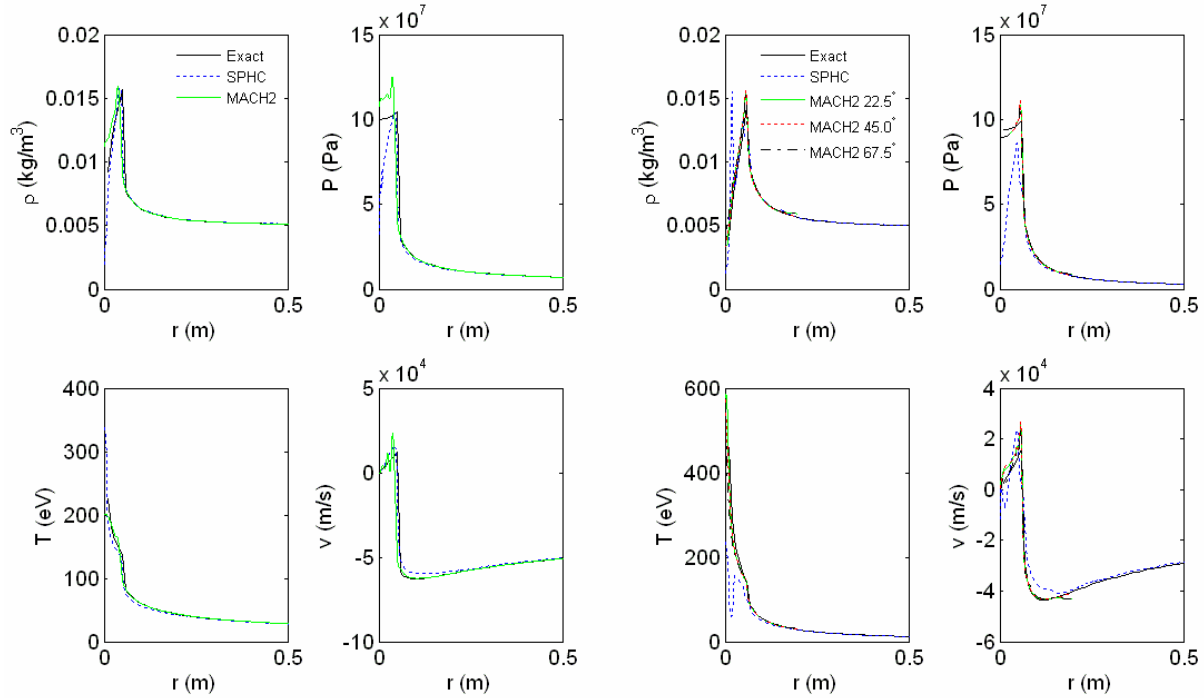


Figure 2. Comparison of reflected shock flow properties for all models for cylindrical (left) and spherical (right) converging shock.

In a future study, we will investigate reasons for poor prediction of shocked density and temperature for MACH2 in Noh case, investigate the cause of excessive pressure in the MACH2 cylindrical shock test. For SPHC, we will investigate reasons for poor on axis performance for SPH in Noh tests and attempt to correct the density overshoot problem at the liner/target interface. Finally, we will set up test cases for ideal MHD and finite thermal conduction in cylindrical and spherical geometries

5. Acknowledgments

This work is primarily funded by the DOE EPSCoR program. The authors would like to thank Dr. Y. C. Francis Thio of DOE for his support of this work. We thank Clark Hawk (UAH PRC) for providing some funding in this effort. Finally, we wish to sincerely thank Bob Stellingwerf (Stellingwerf Consulting) for providing SPHC, his invaluable technical assistance in running the code, and providing the idea for using the Noh tests.

References

- [1] Siemon RE, Lindemuth IR, Schoenberg KF. Why Magnetized Target Fusion Offers a Low-Cost Development Path for Fusion Energy. *Comments on Plasma Physics and Controlled Fusion*. 1999;18:363.
- [2] Thio YCF, Knapp CE, Kirkpatrick RC, Siemon RE, Turchi PJ. A Physics Exploratory Experiment on Plasma Liner Formation. *J Fusion Energy*. 2001;20(1/2):1-11.
- [3] Thio YCF, Panarella E, Kirkpatrick RC, Knapp CE, Wysocki FJ. Magnetized Target Fusion in a Spheroidal Geometry With Standoff Drivers. In: Panarella E, editor. *Current Trends*

in International Fusion Research -- Proceedings of the Second Symposium; 1999; Ottawa, Canada: NRC Research Press; 1999.

[4] Thio YCF, Kirkpatrick RC, Knapp CE. Progress in Magnetized Target Fusion Driven by Plasma Liners. In: Panarella E, ed. *Current Trends in International Fusion Research Proc of the 4th Symposium*. Ottawa, Canada: Physics Essay 2002.

[5] Noh WF. Errors for calculations of strong shocks using an artificial viscosity and an artificial heat flux. *Journal of Computational Physics*. 1987 September;72:78-120.

[6] Lazarus RB, Richtmyer RD. Similarity Solutions for Converging Shocks. Informal Report. Los Alamos, New Mexico: Los Alamos Scientific Laboratory of the University of California; 1977 June 1977. Report No.: LA-6823-MS.

[7] Zel'dovich YB, Raizer YP. *Physics of Shock Waves and High-Temperature Hydrodynamic Phenomena*. Meneola, New York: Dover Publications, Inc. 2000.

[8] Peterkin REJ, Frese MH, Sovinec CR. Transport of Magnetic Flux in an Arbitrary Coordinate ALE Code. *Journal of Computational Physics*. 1998;140:148-71.

[9] Bonet J, Lok T-SL. Variational and Momentum Preservation Aspects of Smooth Particle Hydrodynamic Formulations. *Computer Methods in Applied Mechanics and Engineering*. 1999(180):97-114.

[10] Monaghan JJ. An Introduction to SPH. *Computer Physics Communications*. 1988;48:89-96.

[11] Wingate CA, Stellingwerf RF. Smooth Particle Hydrodynamics - The SPHYNX and SPHC codes. Los Alamos, New Mexico: Los Alamos National Laboratory; 1993 November 28. Report No.: LA -UR-93-1938.

Direct Utilization of Coal Syngas in High Temperature Solid Oxide Fuel Cells

Ismail Celik, ismail.celik@mail.wvu.edu, Mechanical and Aerospace Engineering Department, West Virginia University, Morgantown, WV.

Program Scope

Our vision is to establish an internationally recognized fuel cell research center for coal-based clean power generation which serves as a technology resource for the emerging fuel cell industry in West Virginia. Our strengths are in applying cutting-edge technology to develop and fabricate materials for advanced coal-based fuel cells; establishing a state-of-the-art material characterization and fuel cell testing laboratory; and modeling fuel cells from atomistic to continuum scales using high performance computing. We have formed a multidisciplinary team of researchers who have worked together for several years and have strong credentials in their respective areas of expertise. Under the present project, we will develop a laboratory infrastructure, solidify interactive working relationships, and attain national recognition for the work conducted by the center in the area of coal-based clean power generation via fuel cells. Our project will be conducted in collaboration with the National Energy Technology Laboratory (NETL). This project is to be funded for a 3-year effort. The project effectively started in December 2006.

The research cluster is based on a multi-scale, multi-disciplinary approach conducted by nine faculty members and 3 post doctoral fellows in addition to at least 6 graduate students in four departments at West Virginia University (WVU). The work is organized under four integrated projects: (1) anode material development and experimental characterization of anodes, (2) sub-micro-scale modeling, (3) multi-scale continuum modeling, and (4) laboratory testing. The strength of the research cluster is in the integration of knowledge obtained from experiments (Projects 1 and 4) with multi-scale computational models (Projects 2 and 3). At all stages, information, predictions, and data will be exchanged among researchers in different projects. At the end of three years, we anticipate four outcomes. First, we will have identified the fundamental processes characterizing the operation of SOFC anodes from the atomic level to the level of the operating fuel cell. Second, strategies will be developed for constructing SOFCs that exhibit stable operation with coal syngas. Third, the research infrastructure (equipment for analysis and for cell fabrication, computers for modeling) and collaborations across disciplines and departments at WVU will be well developed for future research on fuel cells. Fourth, a program of educating and training students in the area of fuel cell technology will be established.

Results

A literature review on the effects of coal syngas contaminants has been conducted and data was gathered on possible contaminants in coal syngas, and their typical concentrations. The majority of coal syngas is H_2 , CO_2 , H_2O , CH_4 and N_2 with trace amounts of many naturally occurring elements [1]. Experimental results (Krishnan [2], [3]) show the effect of HCl, CH_3Cl , Zn, P, As, Cd and Hg found in syngas on SOFC performance. Our literature review [O.6] provides insight into the effects of coal syngas contaminants on the performance of an SOFC. Based on this knowledge, our initial testing will be performed with syngas containing As and P.

We also completed a literature review on the effects of sulfur. There are two primary sulfur-degradation mechanisms for the anode materials: (1) physical absorption of sulfur that blocks the hydrogen reaction sites; and, (2) chemical reaction that forms nickel sulfide. The results of our review will appear in **Journal of Power Sources** [O.1].

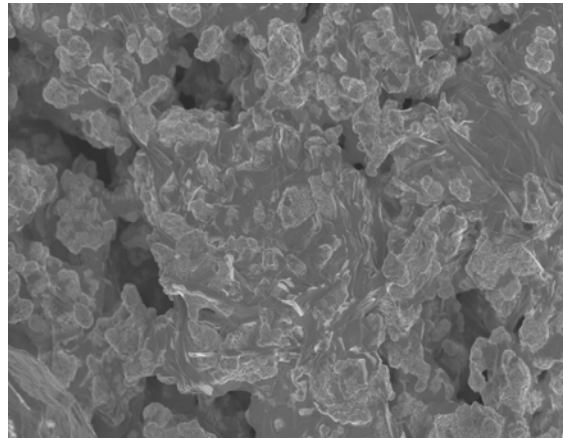
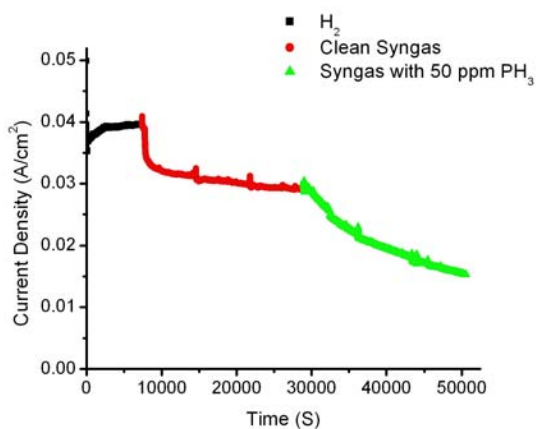


Figure 1: (a) Current density variations with time for a button cell operating on various fuels. (b) Scanning Electron Microscope (SEM) image of the anode microstructure after PH₃ exposure

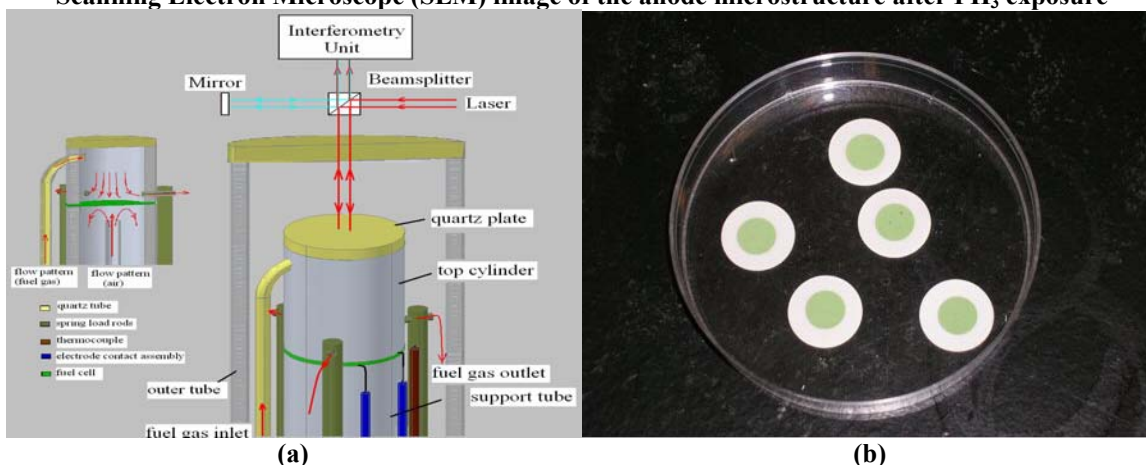


Figure 2. Button cell Testing (a) Schematic of apparatus designed for in-situ electrochemical and structural measurements (b) Button SOFCs manufactured at WVU

Project 1: Anode Materials Development and Characterization

This research project investigates the electro-chemical and structure degradation of SOFC anode materials due to the effect of impurities in coal syngas and develops new materials that would reduce such degradation. We have designed and built a unique button cell testing apparatus that is capable of half cell or full cell testing including EIS (electrochemical impedance spectroscopy) and ASR (anelastic strain recovery) measurements. This testing apparatus includes three main components: (a) testing, (b) mass-flow-control (MFC) and (c) furnace assembly. This is an automated rig in which a computer can control the temperature and the gas flow through programming. Figure 1 shows preliminary results of tests performed to assess the effect of PH₃, a common coal syngas contaminant, on the performance of an SOFC. The cell current decreased significantly (Fig 1a) within 30 min of operation on contaminated syngas and the SEM image of the anode microstructure (Fig 1b) shows that the surface morphology became coarser after PH₃ exposure. We must note that the actual composition of PH₃ in clean coal-syngas may be much less than 50 ppm.

A second test bench is constructed (Fig 2a) for in-situ surface deformation monitoring of the anode side of the button cell subjected to attack from impurities in coal syngas. Most likely, the structural degradation will only occur on surface which may cause a change in the structural

mechanical properties. We shall apply suitable pressure loading to the cell to “amplify” the state of surface structural degradation coupled with simultaneous EIS and ASR measurements to correlate the linkage between mechanical and electro-chemical degradation. An analytical model is developed to predict deformation of a multilayer laminate under uniform pressure and the model was validated against a multi-dimensional model.

A fuel cell manufacturing lab has been set up with a total area of 280 ft². The following equipment has been purchased: tape caster with single-blade (TTC-1200, Richard E. Mistler Inc.), jar-mill (755RMV, U.S. Stoneware); spin-coater (KW4A, Chemat Technology Inc.), screen printer (3230B, Aremco), and low-temperature furnace (Carbolite). Figure 2b. shows some of the button cells manufactured in our lab. These cells are being tested with different levels of contaminant exposure; results will be available soon.

Project 2: Sub-Micro-Scale Modeling

Modeling efforts progressed in two fronts: (i) atomistic level and (ii) molecular level modeling. Using *ab-initio* FP-LMTO techniques based on density functional theory, we calculated the electronic structures for a hydrogen molecule adsorbed on the Ni (1,0,0) surface. Detailed analysis reveals the properties and features of chemical bonding, charge transfer, and Ni surface electronic states. This will serve as a comparison basis to analyze the bonding mechanisms of trace elements on catalysts in our future work. We have also developed an *ab-initio* tight-binding parameter base for Ni/S/H, Ni/P/H and Ni/As/H which will be used in tight-binding based molecular dynamics simulations involving larger scale and longer time. Molecular dynamics modeling will provide the necessary statistical data to retrieve macroscopic properties of the substance, such as effective diffusion coefficient, thermal expansion coefficients and heat capacities, as well as molecular kinetic parameters of importance for determining reaction rates.

Project 3: Multi-Scale Continuum Modeling

The button cell being used in the laboratory was simulated using our in house code: DREAM SOFC. Figure 3a shows the calculated temperature distribution on the top (anode) and bottom (cathode) surfaces of the cell. These simulations are being refined to match the experimental conditions. The results will provide information such as temperature and current distribution that can be measured. Transient mass transport calculations for a typical coal syngas operated anode revealed that chemical kinetics play a critical role in cell performance. This model will be expanded to include the trace species with detailed reaction mechanisms.

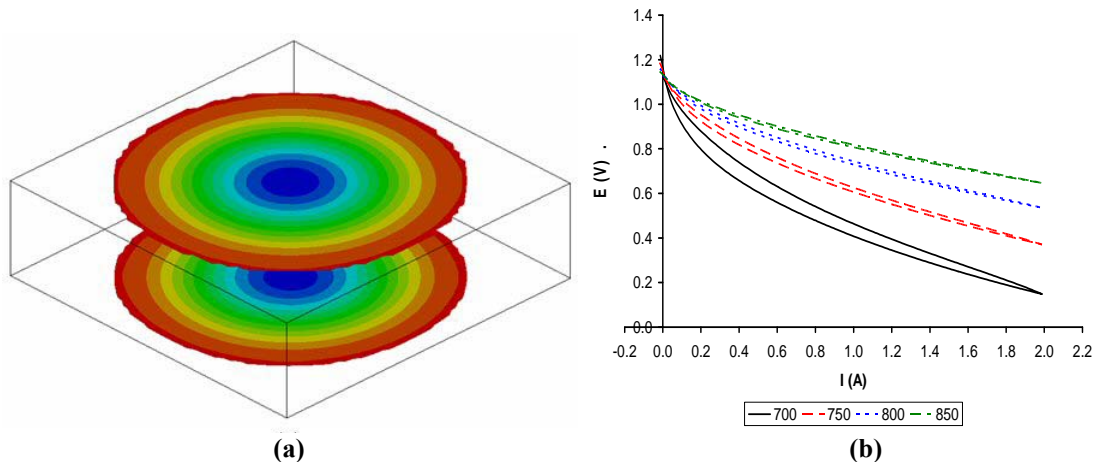


Figure 3. (a) Computed temperature distribution on top and bottom surfaces of a button cell , red indicates hotter region and blue indicates colder region (b) Current vs. Voltage during cyclic voltammetry tests.

Project 4: Cell and System Laboratory Testing

A survey of chemical literature was done for relevant information on measurements of electron transfer kinetics. A complete impedance spectroscopy set up (Solartron Model 1287 potentiostat, Model 1252 frequency response analyzer, ZPlot and ZView software for electrochemical impedance spectroscopy and CorrWare and CorrView software for other electrochemical measurements) was installed in the lab. This system is capable of performing the three electrochemical methods: (1) electrochemical impedance spectroscopy, (2) cyclic voltammetry, and (3) current-interrupt measurements. Cyclic Voltammetry results shown in Figure 3(b) exhibit hysteresis, with higher voltage on the return scan. The possible reason could be that the cell is at a slightly higher temperature during return scan. Also current interrupt and impedance spectroscopy measurements were performed to isolate the contributions of various mechanisms to the overall cell losses. An SOFC test stand has also been made operational and both commercial and in house cells are being tested.

Future Plans

- Cell manufacturing capability will be perfected and new types of materials will be evaluated.
- Cell and anode testing using the three set ups will continue with simulated syngas with trace contaminants to characterize the effects of various contaminants.
- Atomistic and molecular dynamics modeling will first focus on sulfur mechanisms to validate our approach against literature, and then mechanisms for contaminants such as As and P will be investigated.
- Continuum modeling will proceed towards full simulation of conditions being tested in the laboratory.
- A degradation model will be developed for SOFC operating on coal syngas

References

- [1] Trembly, J.P., Gemmen, R.S. and Bayless, D.J. (2007), "The effect of IGFC warm gas cleanup system conditions on the gas-solid partitioning and form of trace species in coal syngas and their interactions with SOFC anodes", vol. 163, pp. 986-996.
- [2] Krishnan, G. (2006), 7th Annual SECA Review Meeting September 12-14, Philadelphia, PA.
- [3] Dr. Gopala N. Krishnan (2007), Private communication, Seminar presentation at National Research Center for Coal and Energy (NRCCE) at WVU, March 21.

DOE Publications/Presentations in 2007

- [O.1] M. Gong, X. Liu, J. Trembly, C. Johnson: Sulfur-Tolerant Anode Materials for Solid Oxide Fuel Cell Application, Accepted J. of Power Sources (2007).
- [O.2] X. Liu, C. Johnson, C. Li, J. Xu, C. Cross: Developing TiAlN Coatings for Intermediate Temperature SOFC Interconnects Applications, submitted, Int. J. of Hydrogen Energy (2007).
- [O.3] R. Dastane, C. Johnson, X. Liu: Degradation of SOFC Metallic Interconnect in Coal Syngas, abstract submitted to Materials Science & Technology 2007 conference.
- [O.4] J. Wu, Y. Jiang, C. Johnson, M. Gong, X. Liu: Pulse Plating of Manganese-Cobalt Alloys for SOFC Interconnect Application, abstract submitted to Materials Science & Technology 2007 conference.
- [O.5] S. R. Pakalapati, F. Elizalde-Blancas, I. Celik (2007): Numerical Simulation of SOFC Stacks: Comparison between a Reduced Order Pseudo Three-dimensional Model and a Multidimensional Model, proceedings of the Fifth Int. Fuel Cell Sci., Eng. and Tech. Conference, June 18-20, NY.
- [O.6] N. Cayan, M. Zhi, S. R. Pakalapati, I. Celik, N. Wu: Coal Syngas contaminants and their effect on operation of SOFC: a literature review, in preparation.

Nanomagnetism

Siu-Tat Chui, Bartol Research Institute, University of Delaware, Newark, DE 19716, chui@udel.edu

Collaborator: Sam Bader, Argonne National Lab.

Program Scope:

We have focused on three classes of physics in magnetic nanostructures:

- (I) Electromagnetic waves in magnetic nanostructures: We propose to study new classes of artificially nanostructured materials with previously unattainable electromagnetic properties over a wide range of frequencies through the incorporation of nanoscale magnetic components. Examples include a new design of circulators, magnetic photonic crystals and materials with negative susceptibilities.
- (II) Controlling the switching of the magnetization of nano structures. We propose to exploit our combined expertise in finite temperature micromagnetics simulation with the Argonne expertise in high precision magnetic imaging in conjunction with hysteresis measurements to study the switching behavior of nanostructures such as the elements in a MRAM chip.
- (III) Spin polarized transport in small structures.

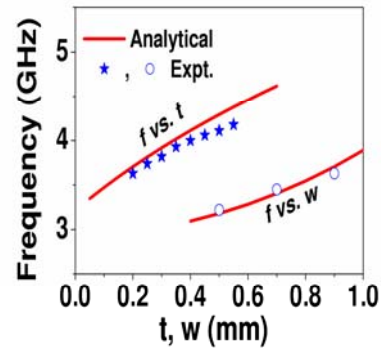
Nanotechnology is one of the priority area of DOE. Our experience and expertise in theoretical studies of nanomagnetism will complement and enhance the exciting experimental work carried out at Argonne.

Recent progress

(1) *Analytic solution of the resonance of split ring systems:* As the building blocks of recently discovered left-handed meta-materials (LHM) [1], metallic ring systems have attracted considerable attention recently [2]. Although the full-wave simulations [3] provided highly reliable results, the computations were usually time-consuming. In addition, it was not easy to extract the polarizabilities of a building block directly from the obtained results [3], usually presented as transmission spectra. Recently, we established an approach for metallic ring systems and applied it to study the electromagnetic (EM) eigenmodes of a single split ring resonator (SRR) [4]. We showed that the theory included the inductive/capacitive effects *completely* and calculated the involved circuit parameters *rigorously*, and provided the structure's responses to arbitrary external fields [4].

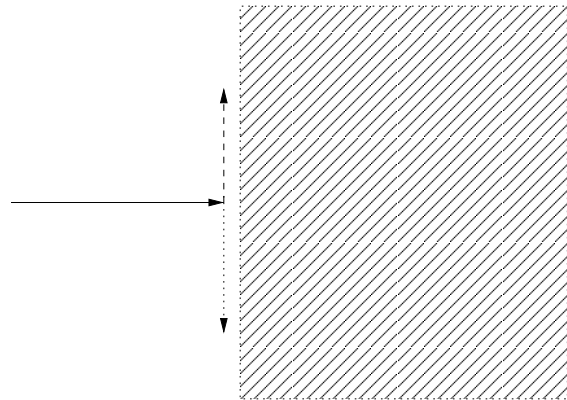
Since most LHM's were built upon the principle of effective medium theory, to realize an LHM sample with a good quality, one requires the building block to be as *subwavelength* as possible and its *bi-anisotropy* as small as possible. We recently extended our theory [4] to study the EM resonances in a double-ring SRR, with attention mainly focused on the above two properties. We found that the ring-ring interactions split each

single-ring mode to two modes with different symmetries, and the bi-anisotropy of each mode decreases significantly as two rings approach. We derived analytical formulas to estimate the resonance frequency of the fundamental (magnetic) mode, and showed how to lower this frequency via tuning the structural parameters. Our formulae are explicit functions of various geometrical parameters. The validities of our formulae are supported not only by finite-difference-time-domain (FDTD) simulations, but also by experimental data published previously [5]. This is shown in the above figure where we compare the theoretical results (lines) of the resonance frequencies of split rings as a function of its width w and separation t to experimental data (points).



(2) *Magnetic photonic crystals*: Over the last ten years there has been much activity on the Hall effect for electrons in heterostructures in which a longitudinal voltage induces a transverse component of the electrical current in the presence of an external magnetic field. This is motivated by the novel physics due to the breakdown of time reversal invariance. The Hall current is believed to be carried by edge states with macroscopic circulations.

Concurrently, there is much activity studying the effects of resonances on the propagation of electromagnetic (EM) waves. This includes such phenomena as negative refraction, the slowing down and the storage of light. We recently investigated if a scattering resonance that lacks time reversal symmetry can create novel effects on the propagation of EM waves in magnetic photonic crystals (MPC). We predict that in the presence of an external beam onto a MPC (Fig., solid line), there is a grazing component of the reflected beam that is **parallel** to the surface of the MPC (dashed line). The magnitude of this grazing component can be changed by an external field. The direction of this parallel component is reversed (dotted line) as the direction of the magnetization is reversed. This provides for a way to probe states with macroscopic circulations inside the MPC. The effect we described is different from the Goos-Hanchen effect[6] in which the mean position of a wave packet is shifted upon reflection. In the present effect, the direction of propagation becomes parallel to the interface.



Future Plans

Split rings: A theme in current research is the development of resonators so that their geometrical size is much smaller than the wavelength at resonance. Miniaturization of

resonators will open the door to different technological applications such as the subwavelength ultra-compact dipole antennas and filters. We showed that for two rings of radii R placed on the same plane, made by wires possessing a circular cross-section with radius a , the resonance frequency can be made to approach zero as $\ln(R/a)$. In practice, the rate of approach to zero frequency is slow, because of the nature of the log function. Furthermore it is not possible to greatly reduce a because this will increase the resistance of the wire and hence the damping of the structure. The SRR has other properties, say, the bianisotropy, that are undesirable for negative index applications. This bianisotropy can increase the damping of the system and reduce the frequency range in which the structure is useful as negative index material. We shall investigate how to reduce both the resonance frequency and the bianisotropy of structures made with rings. Our calculation suggests that the entire spectrum of the SRR (both single- and double-ring) may be determined exactly. We shall further investigate this. When the rings are on the same plane, d is always larger than $2a$, so that this difference *never* approaches zero. However, when the rings are made by flat wires of a film-like rectangle cross-section, and are placed on different planes, their separation d need only be larger than the thickness t of the rings which can be much smaller than width $2a$ of the wires that make up the ring. For such structures, the difference between the self- and the mutual capacitances, and hence the resonance frequency, may be much smaller.

Magnetic photonic crystals: There is much recent interest in spintronics, which involves manipulating the transport of spin-polarized electrons in magnetic structures. This is motivated by the fast spin switching time, the ease with which the external magnetic field can be controlled and the big changes in physical quantities that can result from a small change of the magnetic field. We shall examine possible dramatic changes of the electromagnetic (EM) waves in magnetic photonic crystals (MPCs) with external magnetic fields. Novel ways of manipulating EM waves for different applications are currently being pursued. Left-handed material with negative refraction has been proposed and demonstrated.[1] The stopping and storage of light in atomic systems was observed.[7] Subsequently storage of EM waves with shock waves in photonic crystals was proposed.[8] In these works, a resonance is involved. In magnetic materials, there is a ferromagnetic resonance (FMR). Our focus in this paper is on what the FMR does in the MPC. With the MPC, we shall investigate possible new giant magneto-reflectivity and giant magneto-refractivity (including negative refraction[9]) effects: With an external magnetic field of magnitude much smaller than the anisotropy field of the ferromagnet, the MPC can be changed from non-reflecting to completely reflecting with corresponding changes in the angle of refraction.

Spin polarized transport: We shall investigate if the coupling of the charge and spin degrees of freedom will produce novel unexpected results in recent spin pumping experiment for tunnel junctions.

References

- [1] V. C. Veselago, Sov. Phys. Usp. **10**, 509 (1968); D. R. [Smith](#), *et. al.*, Phys. Rev. Lett. **84**, 4184 (2000); R. A. Shelby, D. R. Smith, S. Schultz, Science **292**, 77 (2001).
- [2] J.B. Pendry, *et. al.*, IEEE Trans. Microwave Theory Tech. **47**, 2075 (1999).
- [3] D. R. Smith, *et. al.*, Phys. Rev. B **65**, 195104 (2002).
- [4] L. Zhou and S. T. Chui, Phys. Rev. B. **74**, 035419 (2006).

- [5] K. Aydin *et.al.*, *New. J. Phys.*, **7**, 168 (2005).
[6] M. Onoda, S. Murakami and N. Nagaosa, *Phys. Rev. Lett.* **93**, 083901 (2004).
[7] Phillips, D., A. Fleischhauer, A. Mair, R. Walsworth, and M. D. Lukin, *Phys. Rev. Lett.* **86**, 783, (2001); Z. Liu, Z. Dutton, C. H. Behroozi and L. Hau, *Nature*, **409**, 490 (2001). A. V. Turukhin, V. S. Sudarshanam, M. S. Shahriar, J. A. Musser B. S. Ham and P. R. Hemmer, *Phys. Rev. Lett.* **88**, 023602 (2002).
[8] E. J. Reed, M. Soljacic, and J. D. Joannopoulos, *Phys. Rev. Lett.* **90**, 203904 (2003).
[9] M. Notomi, *Phys. Rev. B* **62**, 10696 (2000).

DOE sponsored publication in 2007

- L. Zhou and S. T. Chui, *Appl. Phys. Lett.* **94**, 041903 (2007).

Peer-to-Peer Checkpointing Arrangement for Mobile Grid Computing Systems

Paul J. Darby III and Nian-Feng Tzeng
pauldarby@aol.com, tzeng@cacs.louisiana.edu

Center for Advanced Computer Studies, University of Louisiana at Lafayette, Lafayette, LA 70504

Program Scope

Grid computing systems have seen their widespread adoption lately in not only academia but also in industry. Grid computing systems are becoming increasingly important in the efficient discovery, extraction, delivery, and utilization of energy resources. Traditional Grid computer systems consist of multiple individual computers (hosts), usually interconnected by a network, such as the Internet, or high-speed wired backbone, operating collaboratively as a coordinated entity to perform application computations. Applications often can be quite computationally intensive requiring many hours or days of computation time. These applications benefit from grid computation in that the workload is distributed and shared among grid system hosts, resulting in computations being performed concurrently, thus speeding time to computation completion.

However, while most existing Grids refer to clusters of computing and storage resources which are wire-interconnected for offering utility services collaboratively, Mobile Grids (MoGs) have started to receive growing attention and they are expected to become an integral and critical part of a future computational Grid involving mobile hosts (MHs) that facilitate user access to the Grid and also offer computing resources for applications. A MoG can be comprised of a number of MHs, i.e., laptop computers, PDAs, wearable computing gear, cell phones, or even sensors, having wireless interconnections among one another or to network backbone access points. MoGs are envisioned to add value to Grid computations, not only because the workload is shared among the MHs, but also because data (possibly from sensors or other sources) may be inherently distributed, and mobile, requiring localized collaborative computation and timely results. In these scenarios, mobility is often an essential component and access to a wired backbone may or may not always be available. The distributed applications, likely to run on these MoGs are not the traditional long-running heavy computation jobs commonly found in their wired counterparts. Instead, what is envisioned are scenarios involving distributed applets with moderate execution durations (such as address book or data table synchronization), interactive and automated business negotiations based on dynamic localized and mobile data, and distributed microcode sensor applications. The ability to access and process this mobile wireless data locally is seen as adding value to Grid computing systems in general.¹

Whenever an application is distributed among multiple hosts for collaborative computation, it is always possible that one or more hosts will experience some failure during the course of application processing. This is particularly true in Grid computing applications where applications run for days or even longer. Checkpointing forces each host involved in a job execution to save its intermediate states, registers, process control blocks, message logs, etc. at a safe point of stable storage periodically. This stored checkpointing information can then be used to resume job execution at a host chosen to substitute the affected failed host, allowing job

This project was supported in part by the U.S. Department of Energy under Award Number DE-FG02-04ER46136, and by the Board of Regents, State of Louisiana under Contract No. DOE/LEQSF(2004-07)-ULL.

execution to continue to completion, without having to be restarted from the beginning. But in the wireless environment, due to mobility, frequent intermittent disconnections and failures in wireless connectivity (MH to MH), checkpointing in MoGs is even more crucial than in the wired Grid.

In the MoG, even applications of short duration will not complete unless some robust checkpointing mechanism is provided. Where checkpointed data from each MH is stored, referred to as a *checkpointing arrangement*, will determine the probability of successfully retrieving that data when it is needed to resume the application. As base stations (BSs), acting as MH access points, with connections to the wired Grid, may not always be available, neighboring MHs must be utilized in the MoG to provide safe storage. In order to make good decisions, promoting superior checkpointing arrangements, the MoG must be aware of MH-to-MH dynamically varying link strengths, and thus must be QoS-aware.

The focus of this research has been to provide a novel, distributed, QoS-aware, peer-to-peer checkpointing arrangement component for Mobile Grid (MoG) computing systems middleware called ReD (Reliability Driven Protocol). Specific goals were to demonstrate that our ReD protocol, employing QoS-Aware heuristics, constructs superior peer-to-peer checkpointing arrangements efficiently and is a viable and crucial component in MoG middleware. However, the entire program scope further includes additional MoG middleware components, promoting both efficient checkpointing and recovery, so that distributed applications in execution on the MoG, can be successfully resumed and thus completed in the presence of MH or link failures.

Recent Progress

This research work resulted in the development of a functional QoS-aware, distributed peer-to-peer checkpointing arrangement middleware component for Mobile Grids (MoGs). Traditional research pertaining to checkpointing methodologies for wireless MHs has assumed the support of BSs, serving as stable storage points for checkpointed data. This methodology has drawbacks, however, when not all MHs are adjacent to BSs or when BSs do not exist. This is because mobility itself presents major impediments to moving checkpointed data from the MHs to the BSs, often over multiple unreliable wireless links which are experiencing dynamic and time varying connections and disconnections. Such a methodology can result in severe latency, and excessive power consumption to transmit and retransmit over multiple hops, making it infeasible in many scenarios.

The MoG of our interest contains no BS, and its constituent MHs are not adjacent to any BS. Thus, our checkpointing strategy for the MoG aims to keep checkpointed data at immediate neighboring MHs. In order to limit the use of relatively unreliable wireless links, while minimizing consumption of wireless MH memory resources and energy, each MH sends its checkpointed data to *one and only one* neighboring MH, and also serves to take checkpointed data from exactly one neighboring MH, realizing the novel wireless peer-to-peer checkpointing methodology. When a given peer MH, say A, sends its checkpointed data to another peer MH, say B, for safe storage, A is called the “consumer” and B is called the “provider” of checkpointing services. We symbolize this relationship via $A \rightarrow B$. Obviously, given any significant number of MHs, there are numerous ways to assign checkpointing consumers and providers among the constituent MHs comprising the MoG, referred to as checkpointing arrangements. Because of varying link reliabilities between neighboring MHs, resulting in some

MHs being much better connected to other MHs, not all checkpointing arrangements are equal from the standpoint of accessing checkpointed data, once a failure has occurred, and that data is needed for recovery, in order to resume the application. Some checkpoint arrangements are superior, in that they are “more reliable,” meaning that the MoG has a greater probability of recovering checkpointed data with such arrangements, and thus resuming the application from the failure point. Having determined the globally optimum checkpoint arrangement to be NP-complete, we consider ReD, our Reliability Driven (ReD) protocol, employing QoS-aware heuristics, for constructing superior peer-to-peer checkpointing arrangements efficiently. In order to support rapid convergence in scenarios with large numbers of MHs, we assume MHs can be grouped into smaller clusters of size k , so that ReD can operate concurrently within the confines of each MH cluster. For the MoG, ReD seeks to maximize $R_A = \max \prod_{i=0}^{n-1} [1 - (1 - C_i)(1 - P_j L_{ij})]$, $i \neq j$, where C_i is defined as the connectivity (parallel reliability of connections to all neighboring MHs) of consumer i and P_j is the connectivity of its corresponding provider, j , L_{ij} is the reliability of the link from consumer i to provider j , and R_A is the checkpoint arrangement reliability.

The novel nature of our research meant that we found no existing competing protocols for comparison to ReD. Therefore we have utilized both extensive simulation and actual wireless MoG testbed studies to compare ReD to a Baseline Neutral Algorithm (BaNA) employing neutral heuristics. The data evaluated in these studies included the reliabilities of the resulting checkpointing arrangements, time to converge, message counts, and performance with respect to variations in MH relative position, produced by both ReD and BaNA.

Our discrete event-driven simulator, employing physical, link state, connectivity, and clustering functional layers, allowed evaluation of both ReD and BaNA for of up to 100 mobile or stationary hosts. The testbed MoG included six wireless laptop computers (MHs) and software making the system aware of MH-to-MH link strengths. The QoS-aware testbed was utilized to compare ReD which made use of QoS-aware functionality, to BaNA which did not.

The simulation results showed that ReD outperformed BaNA with respect to all metrics under study. ReD produced checkpointing arrangements which were statistically more reliable than did BaNA, and did so utilizing fewer checkpointing arrangement messages. This statistical advantage of ReD over BaNA was shown to increase with increasing numbers of nodes committed to service in the MoG. Figure 1 is an excerpt of this data and depicts the increase in checkpoint arrangement reliability of ReD over BaNA for from 31 to 39 nodes. ReD is clearly shown to outperform BaNA in arrangement reliability by nearly 400 % for MoG node commitment levels of 39 nodes. Likewise, results obtained in the testbed implementation, confirm the performance increase of ReD versus BaNA as shown in Figure 2. As a result, ReD is shown to exceed BaNA in the resulting reliabilities of checkpointing arrangements produced, while utilizing fewer checkpoint arrangement messages to establish those arrangements.

Future Plans

Traditional checkpointing approaches in wired Grid computing systems have assumed that constituent nodes are connected by high-speed wired links with low latency and small link and node failure rates. In general, these approaches assume that the computation interval and checkpoint overhead are much smaller than the “mean time between failures” (MTBF). In such an environment, little attention is given to network latency, link failures and the resulting need

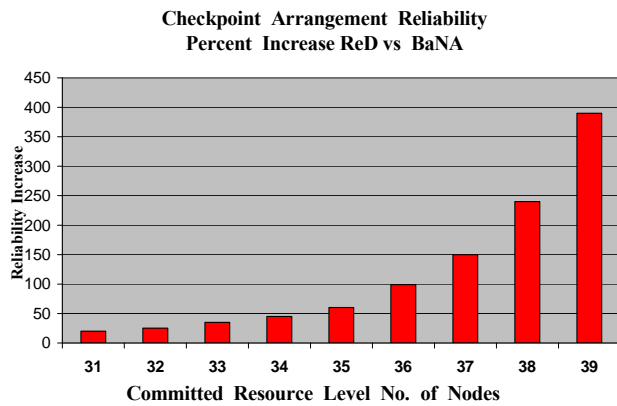


Figure 1. Simulator ReD vs. BaNA.

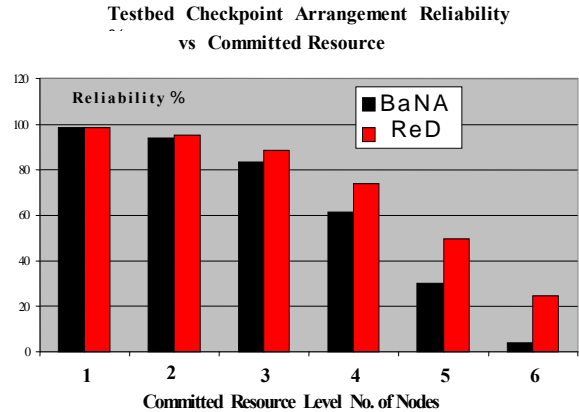


Figure 2. Testbed Checkpoint Arrangement Reliability.

to retransmit checkpointed data. Further, in that environment, checkpoint data message and file size are not of particular concern since high speed wired links and large disk arrays are readily available. In wired Grids, coordinated recovery is easier to achieve and multiple rollbacks are less likely, since replication and other augmenting resources are usually available.

The MoG environment, on the other hand, desires checkpoint transmissions over the fewest hops possible, with the sizes of checkpoint messages kept small to yield short transmission times. In addition, MHs with relatively limited resources can support only fewer and smaller checkpoint data files. The focus of our future research is therefore the development of an efficient mechanism which greatly minimizes checkpoint message transmission times and resource utilization, and which employs localized decision methodologies for execution recovery. In essence, the developed mechanism is to achieve fast, light-weight checkpointing and recovery with high resource-efficiency, ideally suitable for the MoG environment. We intend to implement such a mechanism on a working testbed for assessment, taking two steps: (1) efficient asynchronous checkpointing with checkpointed file derivation, transmission, and management, and (2) speedy execution recovery using checkpointed files and message logs.

References

- [1] S. Wesner *et al.*, "Mobile Collaborative Business Grids – A Short Overview of the Akogrimo Project," White Paper, Akogrimo Consortium, 2006.
- [2] N. Neves and W. Fuchs, "Coordinated Checkpointing without Direct Coordination," *Proceedings of International Computer Performance and Dependability Symposium*, Sept. 1998, pp. 23-31.
- [3] W. Gao, M. Chen, and T. Nanya, "A Faster Checkpointing and Recovery Algorithm with a Hierarchical Storage Approach," *Proceedings of 8th International Conference on High-Performance Computing in Asia-Pacific Region*, Nov. 2005, pp. 398-402.
- [4] N. Neves and W. Fuchs, "Adaptive Recovery for Mobile Environments," *Communications of the ACM*, vol. 40, no. 1, Jan. 1997, pp. 68-74.
- [5] P. Ghosh, N. Roy, S. Das, and K. Basu, "A Game Theory Based Pricing Strategy for Job Allocation in Mobile Grids," *Proceedings of the 18th International Parallel and Distributed Processing Symposium (IPDPS04)*, Apr. 2004, pp. 82-91.
- [6] S. Wong, and K. Ng, "A Middleware Framework for Secure Mobile Grid Services," *Proceedings of the 6th IEEE International Symposium on Cluster Computing and the Grid Workshops (CCGRIDW 06)*, Nov. 2006, pp. 2 – 12.

DOE Sponsored Publications in 2005-2007

- P. Darby and N.-F. Tzeng, "Efficient Checkpointing for Mobile Grid Computing Systems," *Proceedings of 2005 DOE/NSF EPSCoR Conference*, June 2005.
- P. Darby and N.-F. Tzeng, "Peer-to-Peer Checkpointing Arrangement for Mobile Grid Computing Systems," *accepted for presentation in 16th IEEE International Symposium on High Performance Distributed Computing (HPDC-16)*, June 2007.

A Polychromatic Approach to White light Generation using Colloidal Nanocrystals

E. A. DeCuir Jr., T. A. Bond, E. Fred, and M.O. Manasreh
edecuir@uark.edu, txb010@uark.edu, efred@uark.edu, manasreh@uark.edu
Department of Electrical Engineering, University of Arkansas, Fayetteville, AR. 72701

Program Scope

Solid state lighting has gained considerable momentum in the past few years due to current goals to cut energy consumption, reduce green house emissions, and reduce dependence on fossil fuels. Consideration of this technology has also been largely linked to the increasing efficiency of current LED technologies and the projected efficiency gains in ensuing years. There are various options that are currently being used or investigated for the creation of white light using solid state resources. These techniques include the use of UV LEDs in combination with YAG phosphors, visible LEDs in conjunction with yellow and multi-color phosphors, and more recently UV and blue LEDs in conjunction with colloidal nanocrystals. This is of particular interest in that improved color rendering may be achieved by using blue or UV LED in conjunction with polychromatic nanocrystals mixes. This effort will largely focus on achieving broadband visible light from polychromatic nanocrystals embedded in a UV curable epoxy resin which may later be incorporated into the molded LED package itself.

This program will investigate the viability of both blue and UV LEDs employing polychromatic nanocrystal mixes and their subsequent incorporation into an LED package. It is believed that intelligent incorporation of polychromatic nanocrystals in an epoxy LED package, i.e., embedding nanocrystals in the molded package itself, will greatly simplify the generation of broadband light from monochromatic LEDs. The specific goals of this research will be to characterize the emission of various polychromatic nanocrystal blends to achieve broadband visible white light yielding various specific color correlated temperatures. Currently, commercially available prepackaged LEDs (either UV or blue) are used as a monochromatic excitation sources to evaluate the viability of white light generation from custom polychromatic nanocrystal mixes. This study will then investigate methods to characterize and incorporate custom mixes into the molded LED packages, i.e., the creation of an embedded nanocrystal LED package.

Recent Progress

To date, color converting phosphors have been extensively used in the generation of white light LEDs.¹⁻³ Recently, there has been growing interest in the use of nanocrystal technologies for the fabrication of white light LEDs because of their high quantum efficiencies, ease of tuning, and narrow bandwidths.⁴⁻¹³ Additionally, there have also been documented approaches using single color and multiple color nanocrystals with III-nitride based LEDs for creation white light.¹⁰⁻¹³ This interest in pursuing white light generation using nanocrystal systems stems from the perceptible weaknesses of currently used phosphors, which include reduced quantum efficiencies, lack of tuning, broad

emission spectra, and poor stability with respect to photooxidation.¹⁶ It has been shown that nanocrystals enable white LEDs with adjustable tristimulus coordinates, adjustable correlated color temperature, and adjustable color rendering index.¹⁰

Future Plans

While there has been various works establishing the legitimacy of white light created from nanocrystals mixtures, addressing the viability of incorporating these nanocrystals into current LED packages is project of significant merit as it may aid in the adoption of this technology into current LED manufacturing schemes. As with any mature processing scheme, incorporation of new steps in a mature process flow generates large costs involved in equipment retooling and down time. This obviates the need for easy assimilation of nanocrystals into modern, well defined LED manufacturing schemes. It is through the development of an intelligent method aimed at incorporating characterized polychromatic nanocrystal mixes into the molded LED package that will enable easier integration into current manufacturing models. Experimental studies are focusing on characterizing a collection of nanocrystals compositions in conjunction with currently available blue and UV LED products. Evaluation and generation of techniques aimed at incorporating these polychromatic nanocrystals mixes into the LED package itself will be investigated to develop a range of solid state white light models that can uphold high efficiency, good color rendering, and adjustable color correlated temperatures.

References

- (1) Nakamura S and Fasol G **1997** *The Blue Laser Diode* (Berlin: Springer)
- (2) Schubert E F **2006** *Light-Emitting Diodes* (Cambridge: Cambridge University Press)
- (3) Yamada M, Narukawa Y, Tamaki H, Murazaki Y and Mukai T **2005** IEICE Trans. Electron. E88–C 1860–71
- (4) A. Moazzam, S. Chattopadhyay, A. Nag, A. Kumar, S. Sapra, S. Chakraborty and D.D. Sarma, *Nanotech* **2007** 18 075401.
- (5) A. H. Mueller, M. A. Petruska, M. Achermann, D. J. Werder, E. A. Akhadov, D. D. Koleske, M. A. Hoffbauer and V. I. Klimov. *Nano Lett.* **2005** 5 1039
- (6) J. H. Park, J. Y. Kim, B. D. Chin, Y. C. Kim, J. K. Kim and O. Ok. Park. *Nanotech* **2004** 15 1217.
- (7) H. S. Chena, S. J. J. Wang, C. J. Lo and J. Y. Chi. *Appl. Phys. Lett.* **2005** 86 131905.
- (8) M. J. Bowers, J. R. McBride and S. J. Rosenthal. *J. Am. Chem. Soc.* **2005** 127 15378.

(9) H. Chen, D. Yeh, C. Lu, C. Huang, W. Shiao, J. Huang, C. C. Yang, I. Liu and W. Su. **2006 IEEE Photon. Technol. Lett.** 18 1430–2

(10) S. Nizamoglu, T. Ozel, E. Sari and H. V. Demir. *Nanotech* **2007** 18 065709

(11) H. Chen, C. Hsu and H. Hong **2006 IEEE Photon. Technol. Lett.** 18 193–5

(12) M. A. Petruska, D. D. Koleske, M. H. Crawford and V. I. Klimov **2006 Nano Lett.** 6 1396.

(13) C. N. R. Rao, G. Gundiah, F. L. Deepak, A. Govindaraj and A. K. Cheetham. *J. Mater. Chem.* **2004** 14 440.

(14) R. H. Friend, R. W. Gymer, A. B. Holmes, J. H. Burroughes, R. N. Marks, C. Taliani, D. D. C. Bradley, D. A. Dos Santos, J. L. Bredas, M. Logdlund and W. R. Salaneck. *Nature* **1999** 397 121.

Recent Publications

Optical properties of colloidal InGaP/ZnS core/shell nanocrystals, A. Joshi, M. O. Manasreh, E. A. Davis and B. D. Weaver, *Appl. Phys. Lett.*, **2006** 89 111907.

Temperature dependence of the band gap of colloidal CdSe/ZnS core/shell nanocrystals embedded into an ultraviolet curable resin, A. Joshi, K. Y. Narsingi, M. O. Manasreh, E. A. Davis and B. D. Weaver, *Appl. Phys. Lett.*, **2006** 89 131907.

Near-infrared wavelength intersubband transitions in GaN/AlN short period superlattices, E. A. DeCuir, E. Fred, B. S. Passmore, A. Muddasani, M. O. Manasreh, J. Xie, H. Morkoc, M. E. Ware and G. J. Salamo, *Appl. Phys. Lett.*, **2006** 89 151112.

Intersubband transitions in proton irradiated InGaAs/GaAs multiple quantum dots, Y. C. Chua, E. A. DeCuir Jr., M. O. Manasreh and B. D. Weaver, *Appl. Phys. Lett.*, **2005** 87 091905.

P. P. Neupane, M. O. Manasreh, B. D. Weaver, R. P. Rafaelle and B. J. Landi, "Proton irradiation effect on single-wall carbon nanotubes in a poly(3-octylthiophene) matrix," *Appl. Phys. Lett.*, vol. 86, pp. 221908, 2005.

Applications of Computational Artificial Intelligence

Dr. Richard P. Donovan, rdonovan@mtech.edu

Department of General Engineering, Montana Tech, Butte MT 59701

Program Scope

This program is directed at developing unique applications for artificial intelligence (AI) algorithms. The current project is specifically focused on the use of Artificial Neural Networks (ANNs) for calculating the material properties of advanced composite materials and classification of anomalous activities at regional airports. An ANN application was developed that dramatically reduces the cpu time required to calculate the material properties of advanced composite materials. In addition, ANN applications have been developed and deployed to detect and classify the activities of vehicles approaching the terminal at Bert Mooney Airport Authority (BMAA). In support of these efforts, DOE funding was utilized to deploy significant cyber-infrastructure consisting of a 28 processor cluster computer and a smart sensor network at BMAA.

Progress

ANNs have been utilized in voice recognition, pattern recognition, sensor networks, and other complex applications such as constitutive modeling. For example, ANNs have been used to determine constitutive relations for viscoelastic materials [Qingbin, et. al.] as well as aluminum alloys [Sen, et. al.]. Research has also shown that the global elastic constants of a composite material using the eigenvectors of experimental Lamb waves can be predicted [Yang]. The development of an ANN consists of establishing the underlying network topology, training the network with a set of known inputs and corresponding outputs, and validation against a set of known inputs and corresponding outputs. The validation set is not used in the training process. This approach to constitutive modeling was validated with applications to the Ideal Gas Law, control of talc processing and predicting the global properties of advanced composite materials.

The Ideal Gas Law is a constitutive law relating the four variables and one constant of the familiar: $PV = nRT$. We use the ANN to solve for the output (target), which in this case is Temperature (T). The complete data set for 1 Mole of gas was calculated using the following data: Temperature (T) = 100°-500° Kelvin in increments of 10°; Volume (V) = 1-7.5 meters³ in increments of 0.5; R (Gas constant) = 8.315 Joules/(mol*°K); and $P = nRT/V$. The final data set consists of 201 data points. The data was separated into training (80 %) and validation (20 %) sets. The training data are used to 'train' the network to adequately learn the known system. The test data are used to confirm that sufficient training occurred and that the ANN is able to predict the correct outcome (Temperature) using new data inputs. The network accurately predicted the temperature within 8° Kelvin, which is less than ±1 % error (see Figure 1).

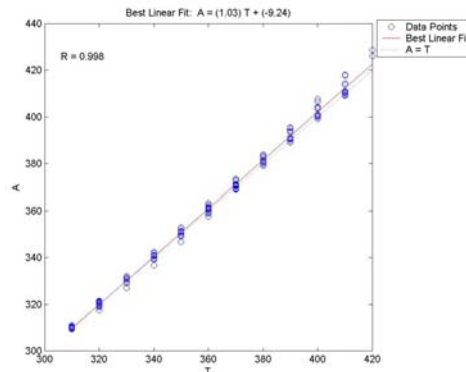


Figure 1: Linear Regression of the Error

ANNs were also used to model the processing of talc at the Luzenac America talc plant in Three Forks MT. The goal of this application is to model the plant (predict the current data set value(s)) and also predict how the plant processes are changing (the future data set value(s)). If this can be done it will prove that the network can predict the present state (constitutive law) and the future state (aid in the control of the system). The *modified* (changed to work with the ANN) control system could then use the predicted values from the ANN to make changes to the plant to keep the process from going unstable. In doing this the ANN will also be used to find the minimum energy state for the process to help control the process and minimize energy costs.

Seventeen independent process parameters such as material feedrates, ambient air temperature, compressed air pressure and power consumption were modeled. The data was provided by Industrial Automation Consulting of Three Forks MT and consisted of samples taken every minute over a twenty four hour time window. Several types of transfer functions and ANN network topologies were investigated to determine the optimum performance.

The network consisted of one input layer, two hidden layers and an output layer. The network utilized a tansig transfer function and a Bayesian Regulation Backpropagation training algorithm. The effectiveness of the network in predicting these values is shown in Figure 2. In this figure the vertical axis represents network predicted values and the horizontal axis represents the actual data. The best performing network was found to be a ANN that used all 17 sets of data as the inputs and one set as the target, the inputs and targets scaled from 0 and 1 or -1 and 1 with the use of satlin and purelin as transfer functions, and only one hidden layer is needed for the problem to solve. When using trainbr or other training algorithms you must use an ANN with at least 15 free parameters to adequately begin to fully learn the data set given by the Luzenac plant.

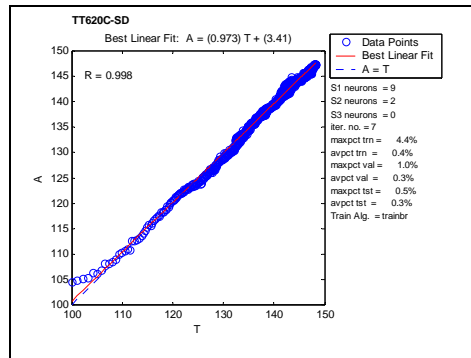


Figure 2. Network Iteration Regression

Because of the complex interactions between constituent properties and micro-structural geometry, the constitutive modeling of advanced composite materials requires a significantly more advanced approach. Data were collected from seven isotropic materials that were arranged in various configurations of a four-cell unit cube representing a longitudinally-reinforced composite. A finite element micro-mechanics analysis was used to generate the ANNs inputs and outputs. The network inputs (eight total) consist of the Young's modulus and Poisson's ratio for the four constituents arranged in the input vector in an order directly corresponding to the geometry of the unit cell. The targets (outputs) of the network are the global elastic constants for the composite material, which are the three elastic moduli and the six corresponding Poisson's ratios. This topology requires significant computational resources in order to sufficiently generalize to the total data set. The training performance and generalization ability of the ANNs can be greatly enhanced by using a network architecture based on the concept of stacked neural networks (SNNs) [Wolpert] in combination with one based upon multiple neural networks (MNNs) [Nguyen]. Rather than training one complex network to predict all nine outputs we suggest training nine smaller networks (each predicting one output) and combining them into one composite network. For example, if we want to just predict E_{1G} (global

Young's modulus in the one direction) and $E2_G$ given the same inputs as before. We could do this in one big network (see Figure 3b) or we could train two separate networks (see Figure 3a) and then combine the two networks into one that accomplishes the same task.

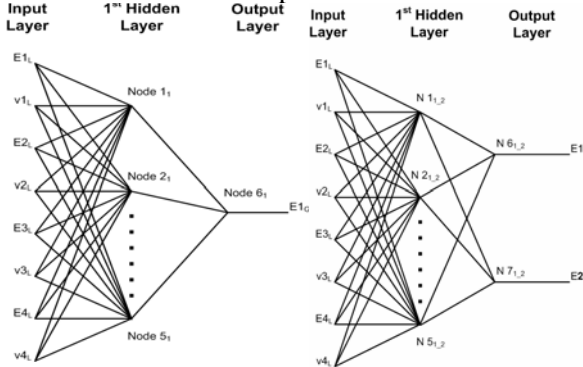


Figure 3a and 3b. $E1_G$ only network (4a). $E1_G$ and $E2_G$ network (4b)

The results of this approach are shown in Figure 4 for the prediction of $E1_G$. The ANNs have been able to learn and predict with reasonable error (less than 5 percent) the global outputs of the system (see Figure 4, which is a linear regression of the network output “A” and the actual target “T”). By creating new MNNs based off the SNNs design we have been able to achieve tighter accuracy than by training a single ANN to predict the system

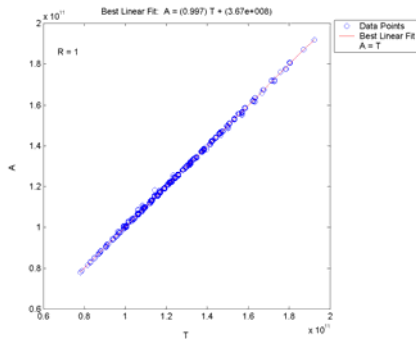


Figure 4. Network Regression of the error of $E1_G$

DOE EPSCoR support was used to develop and deploy a sensor network at BMAA (Butte MT) in order to detect and classify anomalous vehicular traffic approaching the terminal curbside at BMAA. The overall sensor network is illustrated in Figure 5a and 5b. It consists of “weigh-in-motion” systems, video tracking/classification systems, ultra wide band (UWB) radar tracking.

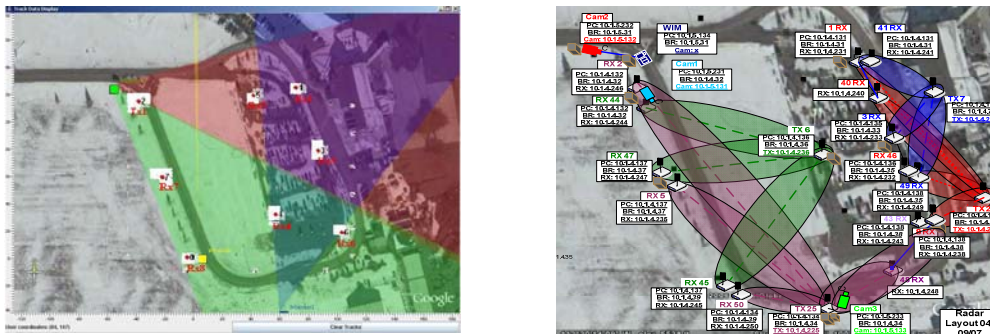


Figure 5a and 5b. Intelligent video and UWB radar layout

The colored triangular areas superposed onto the airport image in Figure 6a represents coverage of three independent video cameras used for tracking vehicles. The ellipses of Figure 6b represent possible locations of objects detected by the UWB radar tracking systems.

Figure 6a and 6b illustrate IEI's Self Training Artificial Neural Network Object (STANNO) approach to classification. Figure 7a illustrates that the camera view of the terminal building is segmented into sixteen individual scenes each of which is assigned a STANNO. The overall anomaly detection is performed by a separate STANNO that combines the results of the sixteen individual STANNOs (network-of-networks approach).

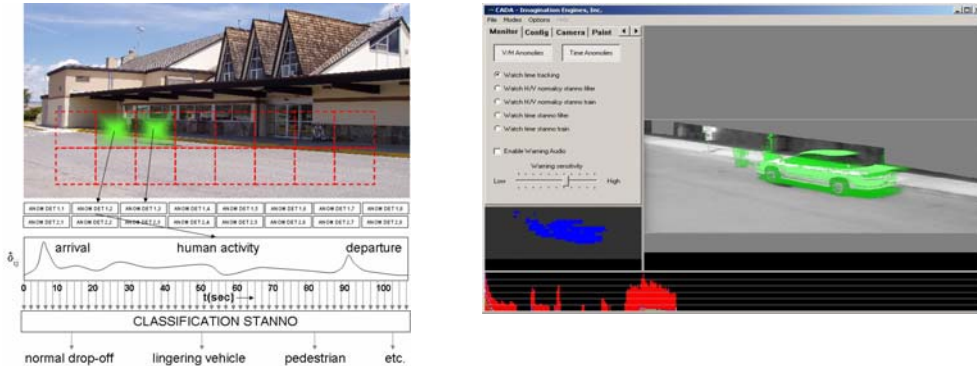


Figure 6a and 6b. Terminal Curbside Anomaly Detection

Future Plans

To support future development of high performance computing and sensor networks the Montana Institute for Sensor and Simulation Technologies (MISST) has been established with funding from the Montana State government. The fundamental goal of MISST is to build upon these programs initiated with DOE EPSCoR funding to create sensor network test beds and a High Performance Computing and Visualization center. These testbeds and the HPC center will be connected via Access Grid Node technology to form a statewide cyber infrastructure system.

The sensor network test beds will be utilized to develop accurate classifications systems of anomalous behavior at small regional airports such as BMAA. This work will require significant computing power (HPC) to accurately and quickly train ANNs to perform a variety of tasks within the sensor network. The HPC and Visualization Center will be utilized for development of computational material science, natural resource modeling and complex system design.

References

- Nguyen, Hanh. H., Christine W. Chan. (April 2004). "Multiple neural networks for a long term time series forecast." *Neural Computing & Applications*, v13 n1, 90-98
- Qingbin, Liu, Et al. (1996) "Acquiring the constitutive relationship for a thermal viscoplastic material using an artificial neural network." *Materials Processing Technology*. 206-210
- Sen, Senjeev., Janet M. Twomey. (2002). "Parameter estimation using a connectionist constitutive model for aluminum 7075 alloy." *Smart Engineering System Design*. v12 889-894
- Wolpert, D. H. (1992). Stacked generalization. *Neural Networks*, 5(2) 241-259
- Yang, Jing. Jian-Chun Cheng. (2001). "A New Inverse Method of Elastic Constants for a Fibre Reinforced Composite Plate from Laser-Based Ultrasonic Lamb Waves." *Chinese Physics Letters*. V18 n12 1620-1623

DOE Sponsored Publications

- An Artificial Neural Network Approach to Multiphase Continua Constitutive Modeling*, Lucon, Peter A, and Donovan, Richard P. *Composites Part B*, **2007**, 38, 817-823
- Application and Testing of a Cougar Agent -Based Architecture*, Mike Emery, John Paxton, Richard P. Donovan. Proceedings of the Fourth IASTED International Conference on Computational Intelligence, Calgary, Alberta, Canada. July 4-6, 2005
- Vehicle Identification Smart Sensor Web: An AI Approach to Screening for Intent*, Donovan, Richard P, Wirth Aaron, Overcast, Desiree. Proceedings of the 2007 IEEE Conference on Technologies for Homeland Security.

EPSCoR State/National Laboratory Program Review Workshop
Renewable Energies for a Global Economy
July 22-25, 2007

Neutrons – A Tool for Renewable Energy Research at ORNL

A. E. Ekkebus, J. L. Trimble,
Neutron Scattering Science Division, Oak Ridge National Laboratory

Oak Ridge National Laboratory desires to work with EPSCoR colleagues to provide the research and development base to advance renewable energy technologies. Managed by UT-Battelle, LLC, for the U.S. Department of Energy, ORNL is home to two of the world's most advanced neutron scattering scientific research facilities. The Spallation Neutron Source is an accelerator-based pulsed neutron source; at full power, it will provide the most intense pulsed neutron beams in the world for basic and applied research. The High Flux Isotope Reactor provides one of the highest steady-state neutron fluxes of any of the world's research reactors. ORNL's research areas include energy, high-performance computing, systems biology, nanoscale materials science, and national security.

These facilities provide intense neutron beams for research on the structure and dynamics of materials in fields such as physics, chemistry, materials science, and biology. Scientists and engineers from universities, industries, and government laboratories are invited to use these facilities for experiments that are typically free of charge subject to conditions such as site access and peer-review publication of research results.

Neutron scattering is a useful source of information about the positions, motions, and magnetic properties of solids. When a beam of neutrons is aimed at a sample, many neutrons will pass through the material. But some will interact directly with atomic nuclei and "bounce" away at an angle, like colliding balls in a game of pool. This behavior is called neutron diffraction, or neutron scattering. Using detectors, scientists can count scattered neutrons, measure their energies and the angles at which they scatter, and map their final position (shown as a diffraction pattern of dots with varying intensities). In this way, scientists can glean details about the nature of materials ranging from liquid crystals to superconducting ceramics, from proteins to plastics, and from metals to micelles to metallic glass magnets. The importance of neutron scattering to the scientific community was recognized by the awarding of the 1994 Nobel Prize for Physics to Clifford Shull and Bertram Brockhouse. Shull pioneered the use of neutron scattering at Oak Ridge to decipher the structure of materials, and Brockhouse found ways to use it in his Canadian laboratory to learn about the motions of atoms in materials.

The intent of the ORNL Neutron Scattering Science User Program is to provide a system that operates seamlessly for users, whether they want to conduct research at SNS, HFIR, or both. This program also accommodates users at the Center for Nanophase Materials Sciences and the Shared Research Equipment Program. The combined proposal system for these facilities allows users to easily submit multiple and combined-facility proposals. Meeting the needs of users is paramount at these facilities. To find out more or to provide input on the Neutron Scattering Science User Program, contact neutronusers@ornl.gov or visit our web site at <http://neutrons.ornl.gov>.

High Efficiency Photovoltaic Devices based on Nanocrystal/Polymer Nanocomposites

Emil Fred¹, Kaushik .Y. Narsingi¹, Omar Manasreh¹, Simon Ang¹, Andrew Wang²

¹Department of Electrical Engineering, University of Arkansas, Fayetteville, AR

²Ocean NanoTech LLC, 700 Research Center Blvd., Fayetteville, AR 72701

Program Scope

Nanocomposites consisting of nanocrystals and electrically conducting conjugated polymers are studied for their use in cheap and highly efficient photovoltaic devices. In previous research work, photovoltaic devices based on silicon and other solid state semiconductor technologies have exhibited power conversion efficiencies upto 40%¹. These devices however, involve highly expensive and complex fabrication techniques. This factor is a major hurdle in the successful commercialization of such devices.

Use of novel materials such as nanocrystals and conducting polymers has yielded devices which are cheaper and easier to fabricate. The power conversion efficiencies of these devices however are less than 5%^{2, 3, 4} which is mainly attributed to the difficulties in charge separation and transport. The possibilities of using nanocomposites for photovoltaic devices are currently being investigated. Materials with Type II band structure is one of the main focus of the current research. Different device designs, tuned to absorb a broad range of solar radiation are being considered. The current research venture can be categorized into three main phases:

Phase I involves the investigation and characterization of the potential materials to be used for the fabrication of the photovoltaic devices.

Phase II investigates different design and fabrication techniques for photovoltaic device and the mechanism of charge transport in these device.

Phase III comprises of efficiency and lifetime measurements of the fabricated devices.

Recent Progress

Significant advances were made into Phase I of the research. Different nanocrystal materials were part of this study and were characterized using optical absorption and photoluminescence (PL) techniques.

Absorption spectra from the CdSe/ZnS core/shell nanocrystals⁵ of different sizes from 2.1nm to 4.5nm diameters, embedded in UV curable resin exhibited first exciton peaks from 498nm to 600nm wavelengths. These measurements help in understanding the absorption wavelength tunability of the nanocrystals. Furthermore, the radiation hardness

of these nanocrystals was investigated using optical absorption and PL techniques. These measurements are applicable to space photovoltaic studies.

Temperature dependent absorption and PL measurements of InGaP/ZnS core shell nanocrystals⁶ embedded in a UV curable resin were recorded. However, the absorption spectra did not show any considerable excitonic peak even at 10K. The bandgap of InGaP nanocrystals was calculated to be 1.970 eV (10K) and 1.930 eV (10K) for the two different samples obtained from Evident Technologies⁷. The mole fraction of In in InGaP nanocrystals samples were estimated to be 0.45 and 0.48. The estimation of the In composition shows that the nanocrystals are direct bandgap materials.

Ongoing research in the current phase includes the synthesis techniques and characterization of CdTe/CdSe core/shell nanocrystals^{8, 9} and GaN@GaP core/shell nanowires^{10, 11}. Interest into this type of materials stems from the fact that type II band structure helps in the separation and transport of charge carriers. The nanocrystals are synthesized using colloidal techniques while the nanowires are produced using a chemical vapor deposition technique.

Future

The next phase will explore different photovoltaic device designs. One possible device structure will have different nanocomposite layers which are spin casted on an appropriate substrate and tuned to absorb different wavelengths in the solar radiation spectrum. This design is based on the Gratzel cell^{12, 13} and multi-junction solar cells^{1, 14} which have shown high power conversion efficiencies. Improvements in the nanocomposite design will also be made by pairing suitable nanocrystal/polymers which exhibits better absorption to desired wavelength and charge transport.

The design and fabrication phase will be followed by testing and measurement of the efficiencies of the devices. Further improvements will be implemented to the earlier phases based on the results of this phase to tune the devices for better performance. Improvements in the quality of the material and the fabrication technique will ultimately lead to the development of photovoltaic devices which are cost effective and have high power conversion efficiency.

References

- (1) R. R. King, D. C. Law, K. M. Edmondson, C. M. Fetzer, *Appl. Phys. Lett.* **90**, 183516 (2007)
- (2) S. E. Shaheen, D. S. Ginley, G. E. Jabbour, *MRS Bull.* **30**, 10 (2005)
- (3) Ilan Gur, Neil A. Fromer, Michael L. Geier, A. Paul Alivisatos, *Science* **310**, 5747, pp. 462 – 465 (2005)
W. U. Huynh, J. J. Dittmer, A. P. Alivisatos, *Science* **295**, 2425 (2002)
- (4) B. Q. Sun, H. J. Snaith, A. S. Dhoot, S. Westenhoff, N. C. Greenham, *J. Appl. Phys.* **97**, 014914 (2005).
- (5) Abhishek Joshi, K. Y. Narsingi, M. O. Manasreh, E. A. Davis, B. D. Weaver *Appl. Phys. Lett* **89**, 131907 (2006)

- (6) Abhishek Joshi ,M. O. Manasreh,E.A.Davis and B.D. Weaver *Appl. Phys. Lett.* **89**, 111907 (2006)
- (7) See www.evidenttech.com
- (8) Hung-Min Lin, Jian Yang, Yong-Lin Chen, Yau-Chung Liu *Mat. Res. Soc. Symp. Proc.* **776** (2003)
- (9) Hung-Min Lin, Yong-Lin Chen, Jian Yang, Yao-Chung Liu *Nano Letters*, **3** (4), 537 -541, 2003.
- (10) Renguo Xie, Xinhua Zhong, and Thomas Basché , *Adv. Mater* **17**, 2741–2745 . 2005
- (11) Haizheng Zhong, Yi Zhou, Yi Yang, Chunhe Yang, and Yongfang Li, *J. Phys. Chem. C*, **111**, 6538-6543,(2007)
- (12) Tingying Zeng, Elizabeth Gladwin and Richard O. Claus *Mat. Res. Soc. Symp. Proc.* **764** (2003)
- (13) Robert F. Service *Science* **300**. 5623, p. 1219(2003)
- (14) Masafumi Yamaguchi , *Physica E* , **14**, pp. 84-90 (2002)

Publications in the last two years

Abhishek Joshi, K. Y. Narsingi, M. O. Manasreh, E. A. Davis, B. D. Weaver *Appl. Phys. Lett* **89**, 131907 (2006)

Abhishek Joshi ,M. O. Manasreh,E.A.Davis and B.D. Weaver *Appl. Phys. Lett.* **89**, 111907 (2006)

High Temperature Resonant Ultrasound Spectroscopy Studies

Gary A. Lamberton, Jr., Rasheed Adebisi, Joseph R. Gladden, and Henry E. Bass
ncpagary@olemiss.edu, radebisi@olemiss.edu, jgladden@olemiss.edu, pabass@olemiss.edu
National Center for Physical Acoustics, University of Mississippi, University, MS 38677

Program Scope:

Resonant Ultrasound Spectroscopy (RUS) is a novel technique in which the free body resonances of a solid are used to determine all of the material's elastic constants in a single measurement. Given a sample's composition, dimensions, and elastic constants, a spectrum of resonance frequencies can be calculated for a given set of boundary conditions (the forward problem). RUS is employed to measure these resonance frequencies and use them along with sample properties and a nonlinear least squares fitting algorithm to compute elastic constants (the inverse problem). These elastic constants are very valuable as probes to study phase transitions, and are closely related to thermodynamic properties such as specific heat and thermal expansion.

In an RUS measurement the sample is held between piezoelectric transducers. One transducer is used to excite the sample while the other measures its response. The driving frequency is typically swept from about 100 kHz to 1 MHz or more until a sufficient number of resonances are obtained to provide a reliable solution to the inverse problem, typically 20-40. A minimal amount of pressure is used to avoid perturbing the resonances of the sample, though this presents a challenge in high temperature work. Transducers cannot be heated significantly or they will lose their piezoelectric properties. As such, in the high temperature apparatus, the transducers are removed from direct contact with the sample and mounted on buffer rods of low acoustic attenuation that allow them to be outside the furnace and cool enough to maintain their function. The weight of these buffer rods is a concern as sample loading can affect the measured spectrum. We have shown that in our current configuration buffer rod loading shifts the frequencies of the peaks by amounts less than or equal to typical errors in the fitted values ($\sim 0.1\%$) for almost all modes, and that good signal to noise ratios can be obtained through the buffer rods (see Figure 1). The apparatus currently shows good thermal stability up to 400 C and with minor adjustments should be stable up to 600 C.

Recent Progress:

We've recently completed a renovation of the apparatus in an effort to enhance our gas-handling control. Operating at elevated temperatures, it is imperative to avoid oxygen in the sample chamber or we risk adverse effects to the system itself and the materials under investigation. The initial design incorporated a low flow (less than 2L/min) of Argon through the measurement chamber during heating and the measurement cycle. At elevated temperatures this led to a difficulty maintaining a stable temperature. The current renovation includes vacuum tight seals and valves in effort to reduce the risk of oxygen leaks into the sample chamber and also to halt the flow of Argon at elevated temperatures for the duration of the measurement cycle. Temperature control has been improved significantly without additional risk of oxygen to the sample chamber.

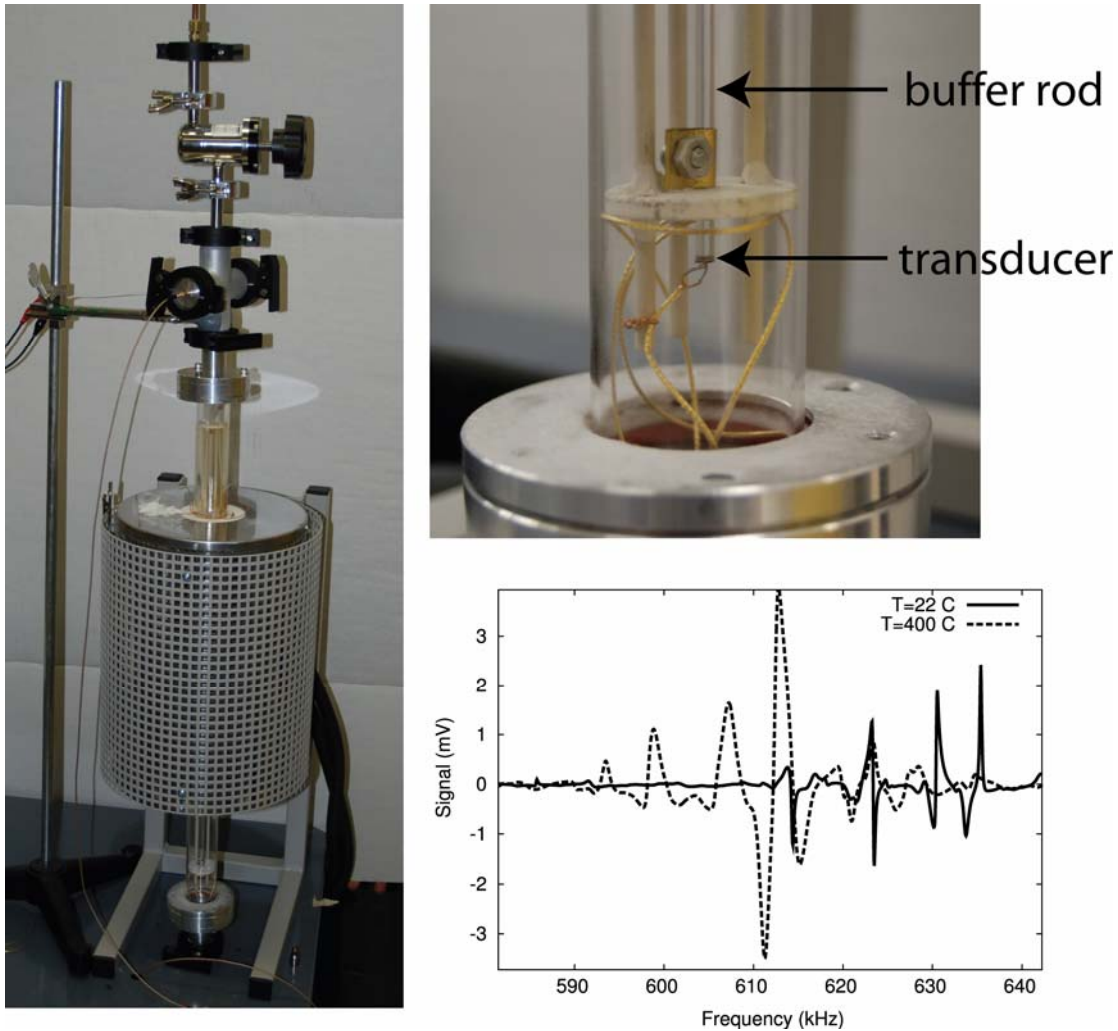
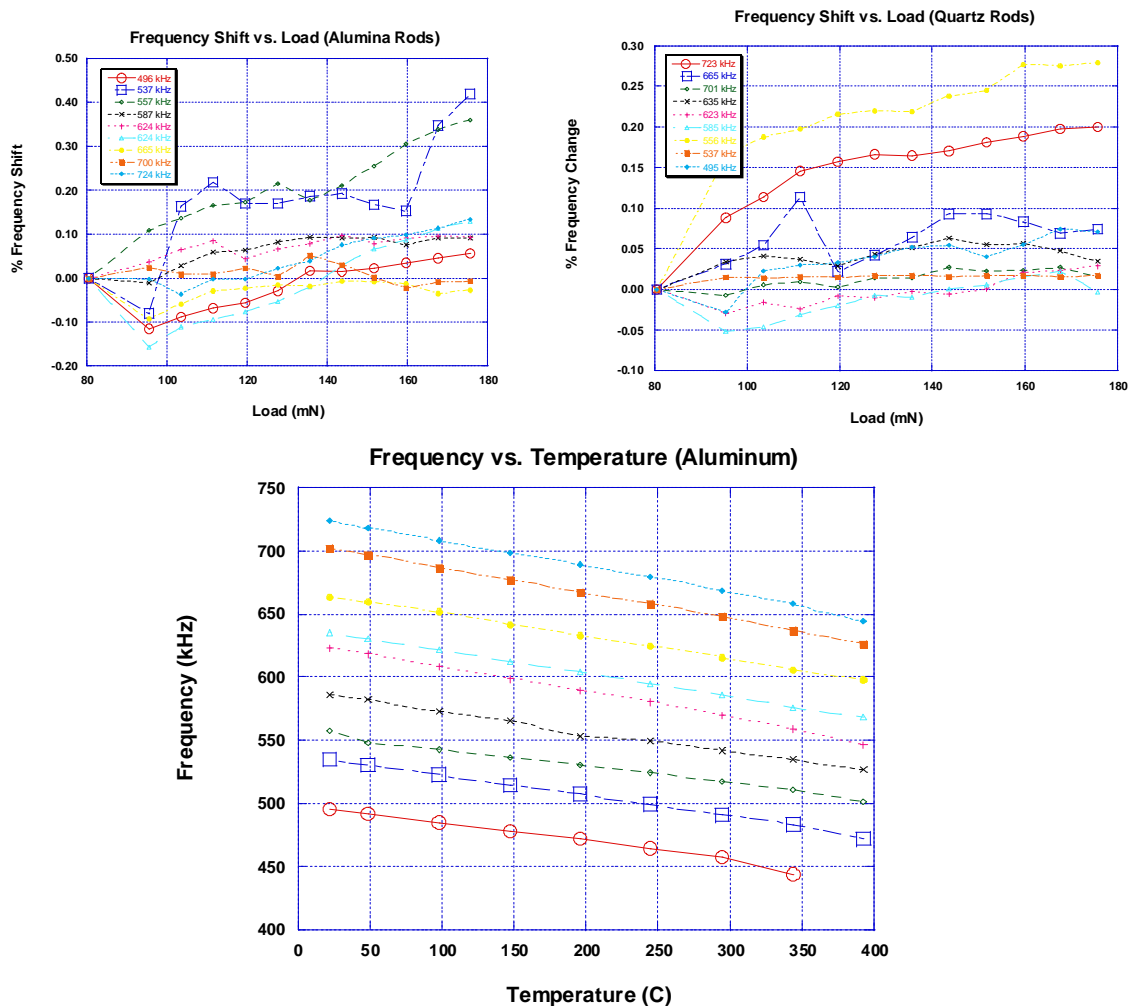


Figure 1: Photos of the oven and gas handling system. The plot shows several resonances of an aluminum sample acquired with the buffer rods at room temperature and 400 C.

In effort to quantify effects of sample loading and effects on the resonant spectrum, we have investigated the frequency shift as a function of load on two different sets of buffer rods (alumina and quartz). As evident in the graphs shown below, the magnitude of the frequency shift is less than 0.1% for almost all resonant modes measured using fused quartz buffer rods for loads up to twice the buffer rod weight (80 mN). We also investigated the effects of loading on the quality factor of the measured modes with similar results for both rods. The quartz rods were chosen for use in the apparatus due to slightly better performance and ease of use.

In addition to clarifying the results of loading on the measured resonant mode frequency and quality, we have performed measurements on a sample of Aluminum and compared our results to literature values. Included in this study is the affect of temperature on the resonant modes of the specimen. The plot below tracks several resonant modes through a temperature difference of approximately 350 degrees C.



Future Plans:

There are a number of interesting phenomena at elevated temperatures to which RUS can be applied. Given the sensitivity of resonant ultrasound it is a useful probe for phase transitions including the glass transition. There is currently a significant body of work accumulating in bulk metallic glass (BMG) compounds due to their high strength and corrosion resistance. In the majority of these materials, the glass transition temperature is well above room temperature. Applying RUS to samples undergoing the glass transition will give us some insight into this important phase transition. The high temperature RUS system provides the capability to investigate the glass transition in a wider variety of BMGs.

Other systems of interest include potential thermoelectric materials such as new SiGe alloys and zintl compounds being developed at the Jet Propulsion Laboratory. The designated use of these compounds is in Radioisotope Thermal Generators (RTGs) for deep space missions. High temperature RUS measurements will provide important mechanical property data for these materials at their application temperature.

Additional studies are planned in collaboration with Oak Ridge National Laboratory investigating new materials such as Fe_2OBO_3 and LuFe_2O_4 which exhibit charge ordering transitions. Such transitions occur in strongly correlated electron systems which are still poorly understood.

Abstract

Scattering of Ultra Cold Neutrons on Nano-size Bubbles

Vladimir Gudkov

*Department of Physics and Astronomy, University of South Carolina, Columbia,
SC 29208*

Inelastic scattering of ultra cold neutrons on bubbles with the size of nanometers is considered. It is shown that neutron-bubble cross section is large and sensitive to different vibration modes of bubbles. This process could be used for the study of dynamics of nano-size bubbles, and for new methods of ultra cold neutron production if appropriately sized bubbles with sufficient density can be created.

Transforming Wastewater Treatment Facilities into Biocrude Centers

Rafael Hernandez, Todd French, Mark White, Kaiwen Liang, William Holmes, Earl Alley, Tracy Benson, Andro Mondala, and Jaclyn Hall,

Renewable Fuels and Chemicals Laboratory
Dave C. Swalm School of Chemical Engineering
Mississippi State University, Mississippi State MS.

Wastewater treatment facilities could be used for oil production, in addition to treating water to conform to Environmental Protection Agency (EPA) standards. Sewage sludge generated at conventional wastewater water treatment facilities could be extracted and converted into biofuels or wastewater could be treated with oleaginous microorganisms, which can convert part of the biochemical oxygen demand of the wastewater into oils and store between 20% and 60% of their mass as oil. To achieve the latter, elimination of indigenous microorganisms present in the wastewater effluent from the primary clarifier while improving the biodegradability of the wastewater is necessary. The oil extracted from oleaginous or conventional microorganisms could be converted into biodiesel or green diesel.

In this work, primary and secondary sludges were collected from a municipal wastewater treatment plant located in Tuscaloosa, AL. After collection, sludges were concentrated by centrifugation, and dried using a freeze dryer. Sludges were also homogenized prior to each experiment. Lipids in dry sludge (~5% moisture) were converted to biodiesel by *in-situ* transesterification. Gas chromatography was used to analyze the fatty acid methyl esters in the sample. It was estimated that wastewater treatment facility could provide approximately 800 million gallons of feedstock for biodiesel production. The presentation will include an economic analysis of the generation of biodiesel from sewage sludge.

An alternative to overcome production of unwanted by-products and expand the inventory of oils available for producing fuels is the application of a more robust conversion process. Green diesel could be produced via cracking of crude lipids using catalytic processes currently employed in the petroleum refining industry. In contrast to biodiesel, green diesel could be distributed via diesel pipelines. And its production does not generate glycerine as a by-product.

Mono-, di-, and triglycerides of oleic acid were cracked over H-ZSM-5 solid catalyst at 400°C in a micro-bed reactor coupled with online GC/MS analysis. H-ZSM-5 was selected due to its high Bronsted acidity and its shape selective characteristics. The operating conditions during the experiments minimized the formation of secondary cracking products.

Novel Energy Sources -Material Architecture and Charge Transport in Solid State Ionic Materials for Rechargeable Li ion Batteries

Ram S. Katiyar (rkatiyar@speclab.upr.edu)

Department of Physics, University of Puerto Rico, San Juan, PR-00931

(DoE Award # DE-FG02-01ER45868)

Program Scope

Technological improvements in rechargeable solid-state batteries are being driven by an ever-increasing demand for portable electronic devices. Lithium-ion batteries are the systems of choice, offering high energy density, flexible and lightweight design, and longer lifespan than comparable battery technologies. Current trends in Li-ion battery research are aimed towards achieving higher capacity, better cycleability and improved rate capability (synthesizing new active materials and improving existing ones). In an other approach of increasing energy density of Li-ion batteries, replacing liquid electrolyte by light weight, flexible polymer electrolytes has attracted considerable attention in recent past. However, polymer electrolytes with suitable conductivities (better than 10^{-3} S/cm) for practical applications have not been obtained yet. Apart from the cathode/electrolyte research, identifying suitable anode is also important as this allows various cathode-electrolyte-anode combinations.

There has been an influx of research activities in order to replace Co based cathode materials, which are being used in commercial Li ion batteries with cheap, environmentally benign, naturally abundant materials. Several alternate candidates to LiCoO_2 have been proposed as potential cathode materials for Li ion batteries, of which spinel LiMn_2O_4 is particularly promising. The specific goals of this program are to (i) optimize the synthesis conditions, (ii) use multi-pronged approaches to stabilize LiMn_2O_4 structure to improve cycleability, (iii) explore coupling between segmental relaxations and ion transport in polymer electrolytes using broadband dielectric spectroscopy, which is still not completely understood, yet crucial for the development of all-solid-state lithium batteries. The work on cathode materials and electrolytes will provide an in-depth study to understand the charge transport in lithium intercalation oxides and its effect on the cell voltage, crystal structure, thermal, and phase stability, which in turn will lead to advanced Li-ion batteries with a longer cycle life, higher capacity/energy, safety, and temperature/rate performance, at lower costs than those currently available

Recent Progress

One of the areas of initial phase of the project was to understand the spinel LiMn_2O_4 cathode materials and optimize process parameters for improving structural stability and electrochemical properties. Another area considered in this period was the improvement in the ionic conductivity of electrolytes by introducing nanoparticles, which were otherwise on the basic underlying mechanism of ionic conduction in polymer electrolytes. In the second phase, information gathered from the first phase was used to improve the electrolyte properties and cathode works continued with various dopings in the spinel compounds. In what follows we briefly summarize our recent achievements in this area.

Cathode materials

It is well known that the cycle life of Li ion cells depends critically upon the structural stability of the host electrode structure upon charge-discharge cycling and $\text{Li}_x\text{Mn}_2\text{O}_4$ cathode is in no way different as it suffers from severe capacity fading in the 3V region due to the anisotropic (Jahn-Teller) distortion. As a result, the cubic symmetry of $\text{Li}[\text{Mn}_2]\text{O}_4$, in which the lithium ions occupy tetrahedral sites, is reduced to tetragonal $\text{Li}_2[\text{Mn}_2]\text{O}_4$ (space group $F4_1/ddm$), in which the lithium ions occupy octahedral sites in an ordered rock salt structure. This crystallographic distortion is too severe for the electrode to maintain its structural stability during cycling. Hence, for good cycle life, the composition of the $\text{Li}_x[\text{Mn}_2]\text{O}_4$ spinel electrode must be kept within the

limits of the cubic structure ($0 < x < 1$) and strict voltage control is required to keep the lower discharge limit above 3V to prevent the onset of the Jahn-Teller distortion. However, $\text{Li}/\text{Li}_x[\text{Mn}_2]\text{O}_4$ cells still lose capacity slowly at 20°C, and more rapidly at 55°C between 4.5 and 3.0 V.¹

Several factors have been speculated for capacity fading of LiMn_2O_4 in the 4V range in the literature¹. Our experimental results clearly shed light on the dominant mechanism responsible for poor cyclability of LiMn_2O_4 . The reason for the severe capacity fading of nano-crystalline LiMn_2O_4 was likely due to the onset of the Jahn-Teller distortion towards the end of the discharge. So, the cation co-doping (replacing Mn partially in the octahedral site by Li and Al simultaneously increased the average oxidation state of Mn thereby delaying the onset of cubic to tetragonal transition, which dramatically improved the cycleability of LiMn_2O_4 .² Also, by substituting Mn ions with transition metals, such as Cr, Fe, Co, Ni the capacity retention was, in general, improved. Recently, it has been found by our group that $\text{LiMn}_{1.5}\text{Ni}_{0.5}\text{O}_4$ has very good initial discharge capacity (148 mAh/gm) as well as excellent capacity retention (of about 94%) after 50 cycles.³ First principle calculations using Vienna *ab initio* simulation package (VASP) confirmed a thermodynamically stable $\text{Li}(\text{NiMnRh})\text{O}$ system and the computed density of states suggested the participation of Ni and Rh during charge-discharge cycles.⁴ Our recent results on $\text{LiMn}_{1.5}\text{Ni}_{0.46}\text{Rh}_{0.04}\text{O}_4$ are very encouraging in the sense that it showed higher discharge capacity (153mAh/gm) and excellent cycleability, the best reported value (to our knowledge) in the literature so far.⁵

Electrolytes

Electrolyte is one of the key components in batteries. Solid electrolyte polymers are stronger contenders over crystals and glasses because of their flexibility and lightweight; thereby increasing process compatibility and energy density, respectively. Ambient temperature lithium-ion conductivities of in currently available candidate solid polymeric electrolyte materials are in the range 10^{-4} - 10^{-6} S/cm, too low for effective room temperature operation. Ion transport takes place in the amorphous phase of polymer electrolyte, therefore lowering the glass transition temperature, T_g (ensuring the amorphous phase at room temperature) is the effective way to improve room temperature conductivity. The most common approach to lower T_g is the addition of liquid plasticizers (small organic molecules). However, the gain in conductivity is adversely accompanied by a loss of the solid state configuration and lithium metal anode compatibility. An alternate approach is to add solid (liquid free) plasticizers, e.g. nanosized inorganic fillers (TiO_2 , SiO_2 , Al_2O_3 , etc.), which increases the conductivity.⁶ Although it has been widely accepted that the segmental motion of the host polymer chain is mainly responsible for the observable macroscopic conductivity in polymer electrolytes⁷, the coupling between segmental relaxation and ion transport in polymer electrolytes is still not completely understood⁸; yet it holds the key to the development of all-solid-state lithium ion batteries.

In order to understand better the role of segmental relaxation dynamics in ion transport process, the glass transition and dielectric relaxation processes of polyethylene oxide (PEO) based polymer salt complexes (PSCs) have been investigated using broadband dielectric spectroscopy. Pure PEO and PSCs consisting of PEO, LiClO_4 or LiCF_3SO_3 were synthesized with and without nano-particulate TiO_2 by solution casting method. The dielectric and ac-conductivity studies, over broad range of temperatures and frequencies, suggest that the polymer segmental dynamics play a crucial role in controlling ion transport in polymer electrolyte systems.⁹ Also, the ion dynamical process in polymer electrolytes has been studied in detail. The frequency dependence of the conductivity showed two regions, namely, Region I (high temperature) and Region II (low temperature). In Region I, the conductivity exhibited a plateau at low frequencies, followed by the dispersion at higher frequencies. In Region II, the conductivity is less sensitive to temperature and exhibits nearly linear frequency dependence. This contribution to ac conductivity from nearly constant dielectric loss has been observed, for the first

time, in polymer electrolytes.¹⁰ Furthermore, a cross over from nearly constant loss to cooperative ion hopping at higher temperatures is noticed from the frequency dependence of the conductivity.

Immediate Future Plans

A Li-ion battery with economically attractive, ecologically friendly, and safety is the main aim of the present research. Our works on the three research fronts, cathode, anode, and electrolytes is progressing well and we are focused in converging the understanding acquired over the years of battery research to a feasible outcome.

(i) *Ab Initio calculation*

Continue theoretical calculations that have already been initiated using VASP to optimize Ni doped spinel structure in order to correlate the improved electrochemical properties with structure.

(ii) *Olivine structure cathode materials*

Even though LiFePO₄ is being considered the most promising alternate cathode material, the major disadvantage for its practical implementation is the lower electronic conductivity. A composite cathode comprising of LiFePO₄ and layered LiMO₂ (M=Co, Ni, Mn) is expected to give better electrochemical properties along with higher electronic conductivity. The phase pure LiFePO₄ has already been synthesized by solid state route, and the effect of composite cathode particle size on the electrochemical properties are proposed to be studied.

(iii) *Thin film coating and nanorods*

Layered coating on spinal structures and nano-rods with higher surface area to increase the capacity between 180-200 m Ah/g is also our goal.

References

- 1) M. M. Thackeray, Y. S. Horn, A. J. Kahaian, K. D. Kepler, E. Skinner, J. T. Vaughey, and S. A. Hackney, *Electrochem. Solid state Lett.*, **1**, 7, (1998)
- 2) S. Nieto, S. B. Majumder and R. S. Katiyar, *J. Power Sources*, **136**, 88, (2004)
- 3) R. Singhal, S. R. Das, O. Ovideo, M. S. Tomar and R. S. Katiyar, *J. Power Sources*, **160**, 651 (2006)
- 4) S. P. Singh, M. S. Tomar and Y. Ishikawa, *Microelectron. J.*, **36**, 491, (2005)
- 5) R. Singhal, M. S. Tomar, S. R. Das, J. G. Burgos, S. P. Singh, A. Kumar and R. S. Katiyar, *Electrochem. Solid state Lett.*, **10**, A163, (2007)
- 6) F. Croce G. B. Appetecchi, L. Persi and B. Scrosati, *Nature*, **394**, 456 (1998)
- 7) S. Zhang and J. Runt, *J. Phys. Chem. B* **108**, 6295, (2004)
- 8) G. Mao, R. F. Perea, W. S. Howells, D. L. Price and M. L. Saboungi, *Nature*, **405**, 163, (2000)
- 9) B. Natesan, N. K. Karan, M. B. Rivera, F. M. Aliev, and R. S. Katiyar, *J. Non-Crystalline Solids*, **352**, 5205 (2006)
- 10) B. Natesan, N. K. Karan, and R. S. Katiyar, *Physical Review E*, **74**, 042801(2006)

DOE sponsored publication list in 2005 -2007

Advances in the design of cathode materials for rechargeable Li-ion batteries, Rahul Singhal, Maharaj S. Tomar, Ram S. Katiyar, Research Signpost **37/661**, (2), (2007)

Li-ion Rechargeable battery with LiMn_{1.5}Ni_{0.46}Rh_{0.04}O₄ spinel cathode material, R. Singhal, M. S. Tomar, S. R. Das, J. G. Burgos, S. P. Singh, A. Kumar and R. S. Katiyar, *Electrochem. Solid state Lett.*, **10**, A163, (2007)

Synthesis and characterization of Nd doped LiMn₂O₄ cathode for Li-ion rechargeable batteries, R. Singhal, S. R. Das, M. S. Tomar, O. Ovideo, S. Nieto, R. E. Melgarejo and R. S. Katiyar, *J. Power Sources*, **164**, 857 (2007)

Improved electrochemical properties of a coin cell using $\text{LiMn}_{1.5}\text{Ni}_{0.5}\text{O}_4$ as cathode in the 5V range, R. Singhal, S. R. Das, O. Ovideo, M. S. Tomar and R. S. Katiyar, *J. Power Sources*, **160**, 651 (2006)

Structural and electrochemical properties of nanocrystalline $\text{Li}_x\text{Mn}_2\text{O}_4$ thin film cathodes ($x=1.0-1.4$), S. R. Das, I. R. Fachini, S. B. Majumder and R. S. Katiyar, *J. Power Sources*, **158**, 518 (2006)

Synthesis and electrochemical properties of $\text{LiNi}_{0.80}(\text{Co}_{0.20-x}\text{Al}_x)\text{O}_2$ ($x=0.0$ and 0.05) cathodes for Li-ion rechargeable batteries, S. B. Majumder, S. Nieto and R. S. Katiyar, *J. Power Sources*, **154**, 262 (2006)

Segmental Relaxation and Ion Transport in Polymer Electrolyte Films by Dielectric Spectroscopy, B. Natesan, N. K. Karan, M. B. Rivera, F. M. Aliev, and R. S. Katiyar, *J. Non-Crystalline Solids*, **352**, 5205 (2006)

Ion Relaxation Dynamics and Nearly Constant Loss Behavior in Polymer Electrolytes, B. Natesan, N. K. Karan, and R. S. Katiyar, *Physical Review E*, **74**, 042801, (2006)

Structural and Lithium Ion Transport Studies in Borophosphate Glasses, N. Karan, B. Natesan, and R. S. Katiyar, *Solid State Ionics*, **177**, 1429-1436 (2006)

Synthesis, structure, and field emission properties of sulfur-doped nanocrystalline diamond, G. Morell, A. González-Berríos, B.R. Weiner, *Journal of Materials Science*, **17**, 443-451 (2006).

Oxygen effect on the electrochemical behavior of n-type sulfur-doped diamond, Ileana González-González, Joel De Jesús, Donald A. Tryk, Gerardo Morell, Carlos R. Cabrera, *Diamond and Related Materials*, **15**, 221-224 (2006)

Synthesis of polycrystalline diamond at low temperature on temperature sensitive materials of industrial interest, F. Piazza, J.A. González, R. Velázquez a, J. De Jesús, S.A. Rosario, G. Morell, *International Journal of Refractory Metals & Hard Materials*, **24**, 24-31, (2006).

Kinetic analysis of the Li^+ ion intercalation behavior of solution derived nano crystalline lithium manganate thin films, S. R. Das, S. B. Majumder and R. S. Katiyar, *J. Power Sources*, **139**, 261 (2005)

Formation of Lithium Clusters and Their Effects on Conductivity in Diamond: a Density Functional Theoretical Study, Hulusi Yilmaz, Brad R. Weiner, Gerardo Morell, *Diamond and Related Materials* (2007) (accepted)

Effect of ZnO coating on the electrochemical performance of $\text{LiMn}_{1.5}\text{Ni}_{0.5}\text{O}_4$ cathode material, Rahul Singhal, Maharaj S. Tomar, Juan G. Burgos, Arun Kumar, Ram S. Katiyar, *Proceedings of Materials Research Society Fall 2006 Meeting*, 2007 (Accepted)

Role of rare-earth element doping in the cycleability of LiMn_2O_4 cathodes for Li-ion rechargeable batteries, Rahul Singhal, Maharaj S. Tomar, Osbert Ovideo, Suprem R. Das, Ram S. Katiyar, *Proceedings of Materials Research Society Fall 2006 Meeting*, 2007 (Accepted)

Resonant Ultrasound Studies of Spin Glasses and Geometrically Frustrated Magnets

P.I.: **Veerle Keppens**, The University of Tennessee

Student supported by DOE EPSCoR grant: **Yanbing Luan**, The University of Tennessee

External collaborators: **Manuel Angst** and **David Mandrus**, Oak Ridge Nat. Laboratory

Program Scope

In this program, the powerful technique of Resonant Ultrasound Spectroscopy (RUS) is brought to bear on spin glasses and geometrically frustrated magnets. As only the canonical spin glasses (dilute magnetic alloys of a noble metal host (Cu, Au, Ag) and a magnetic impurity (Cr, Mn, Fe)) have been subjected to ultrasonic studies, and no elastic measurements have been reported for geometrically frustrated magnets, we have the unique opportunity to start a systematic study of the elastic response of new and less conventional spin glasses. The elastic properties of a material provide information about how a material responds to strain. Near a phase transition, the temperature dependence of the elastic moduli will provide information about the coupling of the order parameter to the strain. Since RUS is extremely sensitive to transitions and ordering phenomena, we also expect effects like orbital ordering (that are easily missed with other experimental techniques) to show up in our measurements.

Recent Progress

i) LuFe_2O_4

Mixed valence LuFe_2O_4 is considered to be a charge-frustrated system, consisting of the alternate stacking of triangular lattices of rare-earth elements, iron and oxygen [1]. An equal amount of Fe^{2+} and Fe^{3+} coexists at the same site in the triangular lattice. Compared with the average iron valence of $\text{Fe}^{2.5+}$, Fe^{2+} and Fe^{3+} are considered as having an excess and a deficiency of half an electron, respectively. The coulombic preference for pairing of ‘oppositely’ signed charges (Fe^{2+} and Fe^{3+}) is considered to cause the degeneracy in the lowest energy for the charge configuration in the triangular lattice, similarly to the triangular antiferromagnetic Ising spins. Recently, a giant magneto-dielectric effect has been reported near room temperature in LuFe_2O_4 [2], due to the ordering of the Fe^{2+} and Fe^{3+} .

Under the current DOE-EPSCoR research grant, we have started a study of the elastic response of LuFe_2O_4 as a function of temperature. Figure 1 shows a representative resonant frequency¹ as measured using Resonant Ultrasound Spectroscopy (RUS) [3]. Whereas the temperature-dependence of the elastic response of “conventional” materials shows a gradual increase or “stiffening” with decreasing temperatures [4], the result

¹ The resonant frequencies of a given sample are directly proportional to the square-root of its elastic moduli, and give therefore clear information about the elastic response of the material.

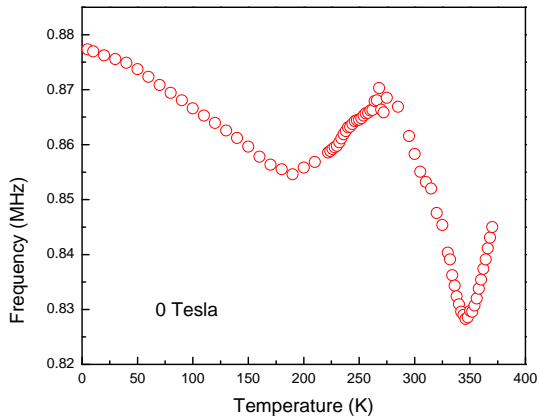


Fig. 1: Temperature-dependence of a representative resonant frequency for LuFe_2O_4 , measured in zero magnetic field.

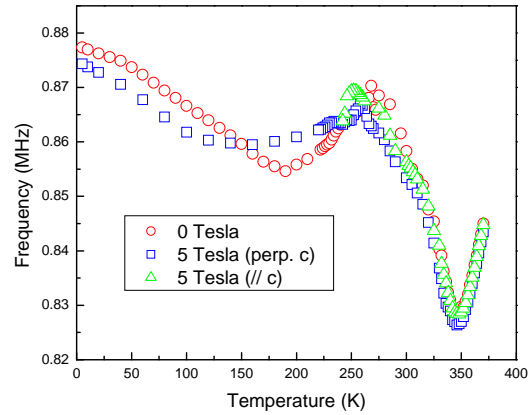


Fig. 2: Temperature-dependence of a representative resonant frequency for LuFe_2O_4 , measured in zero magnetic field (\circ) and a field of 5 Tesla, applied parallel to the trigonal c-axis (Δ) and perpendicular to the c-axis (\square).

shown in figure 1 clearly illustrate how unusual the behavior of LuFe_2O_4 is. Whereas the sudden decrease with decreasing temperature below 250K is believed to be related to the so-called ΔE effect, which is typically observed in ferromagnetic materials, the deep minimum observed around 350 K has to be related to the charge-ordering transition that takes place above room temperature. Figure 2 shows that application of a magnetic field does not seem to have a major influence on the resonant frequencies (and thus the elastic response) above room temperature, but seems to affect the behavior below room temperature. This is in agreement with the drop in magnetization that is observed when a small magnetic field ($H = 1000$ Oe) is applied at 270 K (see figure 3). Careful measurements of the resonant frequencies as a function of magnetic field (Figures 4 and 5) show that the application of a small magnetic field has indeed a small but nevertheless significant effect on the elastic behavior below 300K.

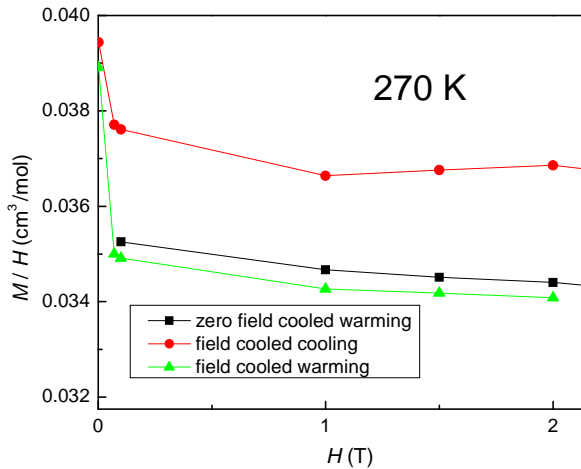


Fig. 3: Magnetization vs. magnetic field for LuFe_2O_4 , measured at 270 K.

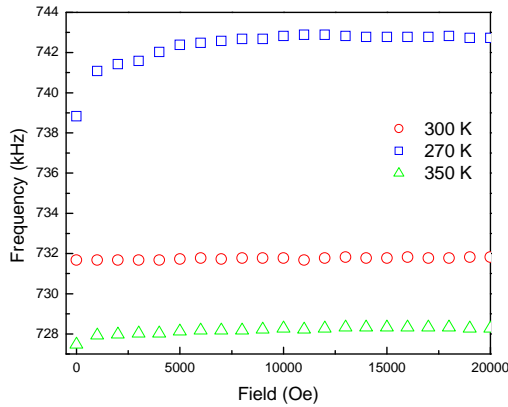


Fig. 4: Field-dependence of a representative resonant frequency for LuFe_2O_4 , measured at 270K (\square), 300 K (\circ), and 350 K (\triangle).

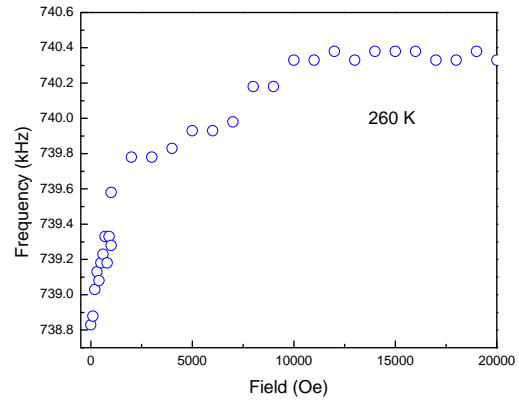


Fig. 5: Field-dependence of a representative resonant frequency for LuFe_2O_4 , measured at 260 K.

ii) MnV_2O_4

This frustrated vanadium spinel exhibits ferrimagnetic ordering at approximately 56 K, and the spin-reorientation is believed to be associated with a structural phase transition from a cubic to a tetragonal phase. It has been demonstrated that switching of crystal structure, as well as domain rotation, occur in this spinel with applied magnetic field. Such large magnetoelastic effects arise from a strong coupling between spin and orbital degrees of freedom for the V ions in this compound.

Our preliminary RUS measurements illustrate how the phase transition MnV_2O_4 is observed in the elastic response of the material. The fast drop in the resonant frequency with decreasing temperature followed by a steep rise below 50 K hints that the strain could be the order parameter that describes this transition [5].

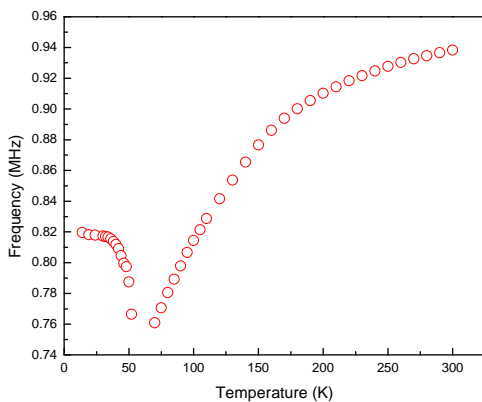


Fig. 6: Temperature-dependence of a representative resonant frequency for MnV_2O_4 .

Future Plans

The results above clearly show that the elastic response of LuFe_2O_4 and MnV_2O_4 is very unusual. In order to elucidate this intriguing behavior, a full analysis with determination of the elastic tensor will be essential. This will be our main focus in the next few months. In addition, we will initiate the growth of frustrated sulpho-spinels such as CdCr_2S_4 , FeCr_2S_4 , MnSc_2S_4 , and FeSc_2S_4 . How these materials will respond elastically is an open question, and RUS measurements as a function of temperature and field are expected to yield insights into the coupling of the lattice to the spin and orbital degrees of freedom.

References

- [1] N. Ikeda et al., *Nature* **436**, 1136 (2005).
- [2] M. Subramanian et al., *Adv. Mater.* **18**, 1737 (2006).
- [3] A. Migliori and J. Sarrao, *Resonant ultrasound spectroscopy*, (Wiley & Sons, 1997).
- [4] Y.P. Varschni, *phys. Rev. B* **2**, 3592 (1970).
- [5] W. Rehwald, *Adv. Physics* **22**, 721 (1973).

Analysis and Development of A Robust Fuel for Gas-Cooled Fast Reactors

Abstract of Progress To Date:
1 January 2006 to 16 July 2007

Contract: DE-FG02-06ER46270
Grant Number: ER46270
Office of Basic Energy Science
U.S Department of Energy
SC-22.2/Germantown Building
1000 Independence Avenue, SW
Washington, DC 20585-1290

Under Program
Experimental Program to Stimulate Competitive Research (EPSCoR),
Building EPSCoR-State/National Laboratory Partnerships

Principal Investigator:
Travis W. Knight, Ph.D.
University of South Carolina
Department of Mechanical Engineering
300 Main Street
Columbia, SC 29208
Tel: (803)777-1465
FAX: (803)777-0106
twknight@sc.edu

Collaborating Lab Partner:
Thad M. Adams, Ph.D.
Savannah River National Laboratory
Materials Applications and Process Technology Group

Graduate Students:
Gokul Vasudevamurthy
Sergiy Y. Lobach

Undergraduate Students:
Devon R. Berry
Jenny M. Watts

July 16, 2007

SUMMARY

Ceramic-ceramic (cercer) composites are a candidate fuel form for gas-cooled fast reactor (GFR) applications. A promising cercer design under investigation consists of mixed carbide fuel kernels coated with a uniform, high density ZrC layer for fission product retention at high temperature and dispersed in a ZrC matrix. The choice of ZrC was selected for its high temperature properties including good thermal conductivity and improved retention of fission products to temperatures beyond that of traditional SiC based coated particle fuels. This effort also seeks to reduce anticipated minor actinide (MA) losses during fabrication by developing techniques that minimize the time that these fuels are exposed to high temperatures during fabrication. Tests have been conducted on both kernel production and fabrication of the ceramic matrix. Kernel coating studies are now starting with combined composite fuel manufacture to begin by the end of this year.

Traditional techniques for compact manufacture require long sintering times at temperatures of at least two-thirds the melting temperature of the material. In order to control the purity of samples and limit the time that kernels are exposed to high temperatures, a combustion synthesis process has been tested to form the ceramic matrix by using a direct exothermic reaction of zirconium and graphite powders. The ignition and adiabatic temperatures of this combustion synthesis process have been measured at approximately 1200°C and 2500°C respectively. A relationship has been developed between the initial powder size, applied pressure, and compact heat rate to achieve high density compacts with good mechanical strength. Cylindrical compacts (12 mm diameter) of pure, stoichiometric ZrC have been produced with up to 92% theoretical density (TD). This high density was accomplished by employing a method of uniaxial pressing at a minimum of 5.2 MPa similar to hot pressing to provide an additional driving force for sintering. These high density samples were produced with smaller size zirconium and graphite powders of approximately 3 and 44 microns respectively.

Kernels of uranium carbide for use in the composite fuel are produced using a high current (greater than 75 A) rotating electrode mechanism. The process involves an electric arc used to melt a small portion of a spinning electrode made of UC or mixed carbide. The centrifugal force acting on the melt flings it into a surrounding inert gas medium where it forms a sphere to minimize surface energy and is quenched in water, kerosene, or other medium. Electrodes of uranium or mixed carbide for the process are again produced by a combustion synthesis process to minimize the time exposed to high temperature. To control the purity of the starting powders, uranium metal is hydrided at a temperature of 200°C then mixed with graphite powders. The cylindrical compacts were heated only for 15 min. to initiate and ensure the combustion reaction is complete as later confirmed through x-ray diffraction of the as fabricated compact. This method produced samples with average TD of 83% but particle production tests showed that the electrodes did not hold together and fragmented into small particles only about few 10s of micron or less. Better sintering of the electrodes was achieved by a longer hold time of two hours to give approximately 88% TD. Despite the small difference in density, the electrodes did produce a significant fraction of larger size particles (kernels) and at least 25% by mass of kernels in the range 300 to 800 micron. The differences in electrode performance is attributed to changes in microstructure that occur with sintering—namely the shrinkage of very small pores. Additional testing is underway to optimize the process and reduce the sintering time required to produce electrodes suitable for particle production.

This effort supports two Ph.D. graduate students and two female undergraduate students. It has further proved successful at building a stronger link between USC and the nearby Savannah River National Laboratory (SRNL) resulting in SRNL staff co-teaching a related course on nuclear materials and plans are underway to have students perform work at SRNL using mixed carbides including minor actinides to examine their volatility during fuel manufacture.

High Throughput Analysis of the Low Dose Radiation Transcriptome*

Michael A. Langston¹, Elissa J. Chesler² and Brynn H. Voy²

¹ Department of Computer Science, University of Tennessee, Knoxville, TN 37996

² Biological Sciences Division, Oak Ridge National Laboratory, Oak Ridge, TN 37831-6445

Program Scope

The tools of molecular biology and the evolving tools of genomics can now be exploited to study the genetic regulatory mechanisms that control cellular responses to a wide variety of stimuli. These responses are highly complex, and involve many genes and gene products. The main objectives of this research project center on understanding these responses by (1) developing novel graph algorithms that exploit the innovative principles of fixed parameter tractability in order to generate distilled gene sets, (2) producing scalable, high performance parallel and distributed implementations of these algorithms utilizing cutting-edge computing platforms and auxiliary resources, (3) employing these implementations to identify gene sets suggestive of co-regulation, and (4) performing sequence analysis and genomic data mining to examine, winnow and highlight the most promising gene sets for more detailed study.

Our primary target is the elucidation of genetic regulatory mechanisms that control cellular responses to low dose ionizing radiation (IR). A low-dose exposure, as defined here, is an exposure of at most ten centigrays (rads). While the net health risk of low dose exposures continues to be debated, recent findings support the concept of risk even at very low doses. We aim to use genome scale gene expression data after IR exposure in vivo to identify the pathways that are activated or repressed as a tissue responds to the radiation insult. The driving motivation is that knowledge of these pathways will help clarify and interpret physiological responses to IR, which will advance our understanding of how low dose radiation exposures pose an increased risk to human health.

This research is of long-term significance to DOE and the nation at large. Understanding the health risks of exposure to low levels of radiation is critical if we are to protect the nation's workforce while making the most effective use of our national resources. The National Academy of Sciences recently issued a report [1] summarizing the most current evidence of the health effects of low levels of IR. This report supports the concept of a "linear-no-threshold" risk model, which holds that even the smallest doses of IR have the potential to increase the risk of cancer. Over the next several decades, it is expected that the majority of radiation exposures associated with human activity will be low dose in nature. These may arise from medical diagnostics, hazardous waste abatement, handling materials for nuclear weapons and power systems, and even terrorist acts such as dirty bombs. The major type of exposures will be low dose ionizing radiation (primarily X-radiation and gamma-radiation) from fission products.

DOE's Office of Biological and Environmental Research has a long-standing interest in low dose radiation research, with particular recent concentration on molecular mechanisms and pathways [2]. Microarrays and other advances in technology provide a means to begin to extract such mechanisms and pathways without *a priori* knowledge of genes that might be involved. By focusing on gene co-regulation and putative network mechanisms, we seek to characterize radiation-induced perturbations of normal physiological processes. This should greatly enhance our understanding of low dose radiation's effects at all levels of biological organization, from genes to cells to tissues and finally to organisms.

* This work is supported by the EPSCoR and Low Dose Radiation Research Programs, with UT-Battelle LLC the managing organization of ORNL for the U.S. DOE.

Recent Progress

Guilt by association, the assumption that genes with similar expression patterns participate in common cellular functions, drives a growing body of effort to extract regulatory pathways from microarray data [3]. As noted in [4], “partitioning genes into closely related groups has thus become the key mathematical first step in practically all statistical analyses of microarray data.” The general tenet is that genes encoding proteins participating in a common pathway will display correlated expression levels when analyzed at sufficient scale, and that the identities and known functions of these genes can be used to highlight existing and assimilate new functional information. A number of recent studies validate this concept, demonstrating that genes co-expressed across multiple conditions are more likely to represent common functions than would be expected by chance alone [5-7]. To date the computational methods to extract such patterns lag far behind the general agreement about their utility.

Clustering includes a wide variety of algorithms for organizing groups of genes with similar expression patterns into a format that is easy to interpret. Virtually all clustering algorithms begin with a similarity metric (e.g., Pearson’s correlation coefficient) between the expression levels of all pairs of genes in the analysis. There are several important limitations, however, to the vast majority of clustering algorithms that lie in contrast to the realities of biology. The clusters produced are typically disjoint, requiring that a gene be assigned to only one cluster. Also, most measures of similarity used by clustering algorithms do not permit the recognition of negative correlations, which are common and meaningful. As an alternative to assigning genes to clusters, the correlation matrix of expression data can be converted into a graph consisting of nodes (genes) connected by edges (gene-gene correlations). Applying a threshold to the matrix restricts the graph to only those edges likely to represent biologically meaningful relationships. The resulting graph (relevance network) contains many dense subgraphs of tightly interconnected genesets that represent the greatest potential for identifying members of common pathways. Without a systematic means to extract the aggregate relationships between multiple genes, however, many of the most interesting relationships remain embedded within the sea of correlations.

To remedy this, we have developed a computational approach that exploits graph theoretical algorithms to identify comprehensively the tightly connected subsets of genes present in relevance networks. In the most extreme case, in which a subgraph contains all possible edges between vertices in the subgraph, this structure is called a *clique*. In terms of gene expression, clique represents the most trusted potential for identifying a set of interacting genes [8]. Solving clique, however, is an *NP*-complete problem, and a classic graph-theoretic problem in its own right. We have developed novel graph algorithms that employ fixed-parameter tractability and vertex cover to solve immense instances of clique efficiently. We have applied these algorithms to identify differential gene relationships, that is, gene-gene interactions that are induced or repressed by in vivo exposure to low dose ionizing. Six strains of inbred laboratory mice were exposed to 10 cGy of X-rays, after which gene expression changes in spleen were profiled using microarrays. We employed our graph theoretical-based toolchain for identifying overlapping subsets of genes with tightly correlated expression levels, and worked to exploit the biological insight that this method provides [9].

Future Plans

To form a graph from a correlation matrix, a cutoff value, or threshold, must be chosen above which an edge connecting two genes is created, and below which the two genes are considered unconnected. This decision is of critical importance, as clique results are highly dependent on the starting graph. We propose specific study of three possible approaches to thresholding: ontological distance, statistical, and graph structure. In all cases, the criterion for successful thresholding will be the ability to capture biologically relevant cliques while minimizing cliques with no biological

meaning. This raises the question of how “biological meaning” will be defined. This is an issue with which all current approaches to extracting co-regulated genes must deal, since too little is known about the comprehensive biology of any genome to establish a concrete, proof-of-principle data set, especially for higher eukaryotes. In lieu of that, the state of the art is to determine whether predicted sets of co-regulated genes map to a common biological function, based on their gene ontology (GO) annotation. Therefore we will score the biological meaning of cliques and other subgraphs by determining the degree to which they are enriched for specific GO categories. The biological accuracy of various thresholds will be determined in part by the degree to which the thresholds produce cliques that are enriched for genes with common functional assignments. We will use GoTreeMachine [10], a tool created by our colleagues at ORNL, to identify statistically significant GO enrichments from dense gene sets. GoTreeMachine returns the statistical probability that a set of genes is significantly enriched in one or more GO categories. Using the IR data set, each threshold method will be applied, and GO enrichment of generated cliques compared. We do not rule out the possibility that using more than one method may be necessary in practice. If methods disagree, this may indicate something about the experimental data that needs to be reexamined.

To account for the many sources and varieties of noise inherent in data generated with current microarray technology, we will utilize our recently-developed clique relaxation technique to identify what we term “paracliques” [11]. Informally, a paraclique is an extremely densely-connected subgraph, but one that may be missing a small number of edges and thus is not, strictly speaking, a clique. In our application, this corresponds to a very highly intercorrelated group of putatively co-regulated genes whose transcript expression levels, as reflected in real and surely somewhat dirty microarray data, show highly significant but not necessarily perfect pair-wise correlations. Let us illustrate, beginning with a clique C of size k , where k is perhaps the size of the largest clique in the list. We set a connectivity factor, f , at some value strictly less than k . We also set an edge weight bound, b , at some value strictly less than the threshold, t , used to build the correlation graph. We now consider each non-clique vertex, v , in turn. We mark v if and only if it is adjacent to at least f vertices in C and if and only if the weight of the correlation coefficient on any “missing” edge is at least b . (Recall that the coefficients were used to build an edge-weighted graph that was later replaced by an unweighted graph via the use of a high-pass filter. Thus the weight of any edge missing from the unweighted graph is still available.) After each vertex has been considered, we define a paraclique, P , to be the union of C and the set of all marked vertices. We remove P from the graph and iterate.

We will continue the development of our tools using a data set we recently collected that focuses on the biological response to in vivo exposure to low doses of ionizing radiation (IR). Accumulating evidence suggests that the genes and pathways altered by lower doses are not merely a subset of those altered by higher doses [12]. Therefore low dose IR may exert its own unique set of cellular responses. Initially we will focus on microarray data from spleens of mice exposed to an acute low dose of IR in vivo. These exposures are part of an ongoing DOE-funded project on which Dr. Voy is the PI, designed to determine the extent to which varying genetic background alters the response to IR as defined by the gene expression profile. Dr. Voy’s laboratory has already analyzed the spleen and skin data to identify differentially expressed genes, that is, genes with expression levels that increase or decrease in response to IR exposure. These data indicate that multiple pathways respond to IR. In spleen, for example, differentially expressed gene sets are enriched in genes involved in apoptosis, regulation of transcription, and many novel, uncharacterized genes. A significant percentage (~ 22%) of genes that are differentially expressed in at least one strain upon IR exposure encode products that mediate immunity, suggesting that low doses of IR may initiate an immune response.

References

- [1] N. R. C. Committee to Assess Health Risks from Exposure to Low Levels of Ionizing Radiation, "Health Risks from Exposure to Low Levels of Ionizing Radiation: BEIR VII Phase 2," National Academies Press, Washington, DC, 2005.
- [2] DOE, "Low Dose Radiation Research Program - Molecular Mechanisms and Pathways," <http://www.science.doe.gov/grants/FAPN04-21.html>.
- [3] D. K. Slonim, From patterns to pathways: gene expression data analysis comes of age, *Nature Genetics*, vol. 32 Supplement, 2002, 502-508.
- [4] V. Cherepinsky, J. Feng, M. Rejali, and B. Mishra, Shrinkage-based similarity metric for cluster analysis of microarray data, *Proc Natl Acad Sci U S A*, vol. 100 (17), 2003, 9668-73.
- [5] N. Bhardwaj and H. Lu, Correlation between gene expression profiles and protein-protein interactions within and across genomes, *Bioinformatics*, vol. 21 (11), 2005, 2730-8.
- [6] H. Ge, Z. Liu, G. M. Church, and M. Vidal, Correlation between transcriptome and interactome mapping data from *Saccharomyces cerevisiae*, *Nat Genet*, vol. 29 (4), Dec, 2001, 482-6.
- [7] H. H. Yang, Y. Hu, K. H. Buetow, and M. P. Lee, A computational approach to measuring coherence of gene expression in pathways, *Genomics*, vol. 84 (1), 2004, 211-7.
- [8] A. J. Butte, P. Tamayo, D. Slonim, T. R. Golub, and I. S. Kohane, Discovering functional relationships between RNA expression and chemotherapeutic susceptibility using relevance networks, *Proc Natl Acad Sci U S A*, vol. 97 (22), Oct 24, 2000, 12182-6.
- [9] B. H. Voy, J. A. Scharff, A. D. Perkins, A. M. Saxton, B. Borate, E. J. Chesler, L. K. Branstetter, and M. A. Langston, Extracting gene networks for low dose radiation using graph theoretical algorithms, *PLoS Computational Biology*, vol. 2 (7), 2006, e89.
- [10] B. Zhang, D. Schmoyer, S. Kirov, and J. Snoddy, GOTree Machine (GOTM): a Web-Based Platform for Interpreting Sets of Interesting Genes using Gene Ontology Hierarchies, *BMC Bioinformatics*, vol. 5, 2004, 16.
- [11] E. J. Chesler and M. A. Langston, Combinatorial genetic regulatory network analysis tools for high throughput transcriptomic data, *Proceedings, RECOMB Satellite Workshop on Systems Biology and Regulatory Genomics*, San Diego, 2005.
- [12] E. Yin, D. O. Nelson, M. A. Coleman, L. E. Peterson, and A. J. Wyrobek, Gene expression changes in mouse brain after exposure to low-dose ionizing radiation, *Int J Radiat Biol*, vol. 70 (10), 2003, 759-775.

Recent DOE Sponsored Publications

- F. N. Abu-Khzam, M. A. Langston, P. Shanbhag, and C. T. Symons, Scalable parallel algorithms for FPT problems, *Algorithmica*, vol. 45, 2006, 269-284.
- N. E. Baldwin, E. J. Chesler, S. Kirov, M. A. Langston, J. R. Snoddy, R. W. Williams, and B. Zhang, Computational, integrative and comparative methods for the elucidation of genetic co-expression networks, *Journal of Biomedicine and Biotechnology*, vol. 2, 2005, 172-180.
- M. A. Langston, L. Lan, X. Peng, N. E. Baldwin, C. T. Symons, B. Zhang, and J. R. Snoddy, "A combinatorial approach to the analysis of differential gene expression data: the use of graph algorithms for disease prediction and screening," in *Methods of Microarray Data Analysis IV, Papers from CAMDA '03*, K. F. Johnson and S. M. Lin, Eds. (Boston: Kluwer Academic Publishers, 2005, 223-238.
- B. Zhang, N. C. VerBerkmoes, M. A. Langston, E. Uberbacher, R. L. Hettich, and N. F. Samatova, Detecting differential and correlated protein expression in label-free shotgun proteomics, *Journal of Proteome Research*, vol. 5, 2006, 2909-2918.
- J. D. Eblen, I. C. Gerling, A. M. Saxton, J. Wu, J. R. Snoddy, and M. A. Langston, "Graph algorithms for integrated biological analysis, with applications to type 1 diabetes data," in *Clustering Challenges in Biological Networks*: World Scientific, 2007, to appear.

A Grid-enabled Framework for Ensemble Inverse Modeling*

Zhou Lei¹, Gabrielle Allen¹, Tefvik Kosar¹, Guan Qin⁴, Frank Tsai³, Christopher White^{1,2}

¹ Center for Computation & Technology, Louisiana State University

² Department of Petroleum Engineering, Louisiana State University

³ Department of Civil and Environmental Engineering, Louisiana State University

⁴ Institute of Scientific Computing, Texas A&M University

E-mail: {zlei, cdwhite, gallen, kosar}@cct.lsu.edu, guan.qin@tamu.edu, ftsai@lsu.edu

Program Scope

The economic impact of inaccurate predictions is substantial, especially in petroleum industry which is notorious for its investment with high risk. Ensemble inverse modeling is a fundamental methodology for model parameter value determination and accurate performance predictions, extensively adopted by reservoir monitoring, groundwater modeling, weather forecasting, *etc.* However, ensemble inverse modeling is highly computing-intensive due to large-scale iterative model simulation and data assimilation.

Grid computing technologies promise large-scale computing and data processing capability with cost efficiency by cooperating geographically distributed, heterogeneous, and self-administrative resources. Our efforts focus on developing an easy-to-use grid-enabled framework, which will provide overall performance of underlying computing facilities to efficiently conduct ensemble inverse modeling. Various applications, such as reservoir performance studies, groundwater modeling, nuclear waste processing, and hurricane tracking, will take advantage of this framework. The essential issues to achieve this goal include underlying resources' computing capability integration, massive data manipulation, effective data assimilation algorithms, and easy-to-use integrated operating environment.

Recent Progress

A prototype of a grid-enabled framework has been provided to support large-scale ensemble inverse modeling. We have already identified the workchart of such a framework, implemented an efficient execution management model for modeling iterations across a grid, developed a data archive tool for massive data manipulation, implemented Ensemble Kalman Filter (EnKF) to support effective data assimilation, and accomplished a grid portal to ease user interaction. These achievements have been used for subsurface modeling studies.

The framework workchart is illustrated in Figure 1. It is a multi-layer structure. The first layer is initial dataset collection, including observation (or experiment) data, history data, experience data, simulation results, and expert interaction. A web interface, *i.e.*, grid portal, is adopted for these inputs. The second

*Sponsored by U.S. Department of Energy (DE-FG02-04ER46136) and Louisiana Board of Regents (DOE/LEQSF(2004-07)-ULL), a part of Ubiquitous Computing and Monitoring System (UCoMS) for Discovery and Management of Energy Resources project.

layer is grid middleware, which is in charge of data and execution management across a grid. Base model generation and simulation are conducted by underlying computing resources. Model updating is carried out by the third layer, which employs various pluggable algorithms (*e.g.*, Genetic Algorithm and EnKF) to analyze simulation results with the help of realtime/archive dataset. If simulated models are not satisfied, updated models are generated and further simulations are needed. Otherwise, post processing is used for conclusion making and/or visualization.

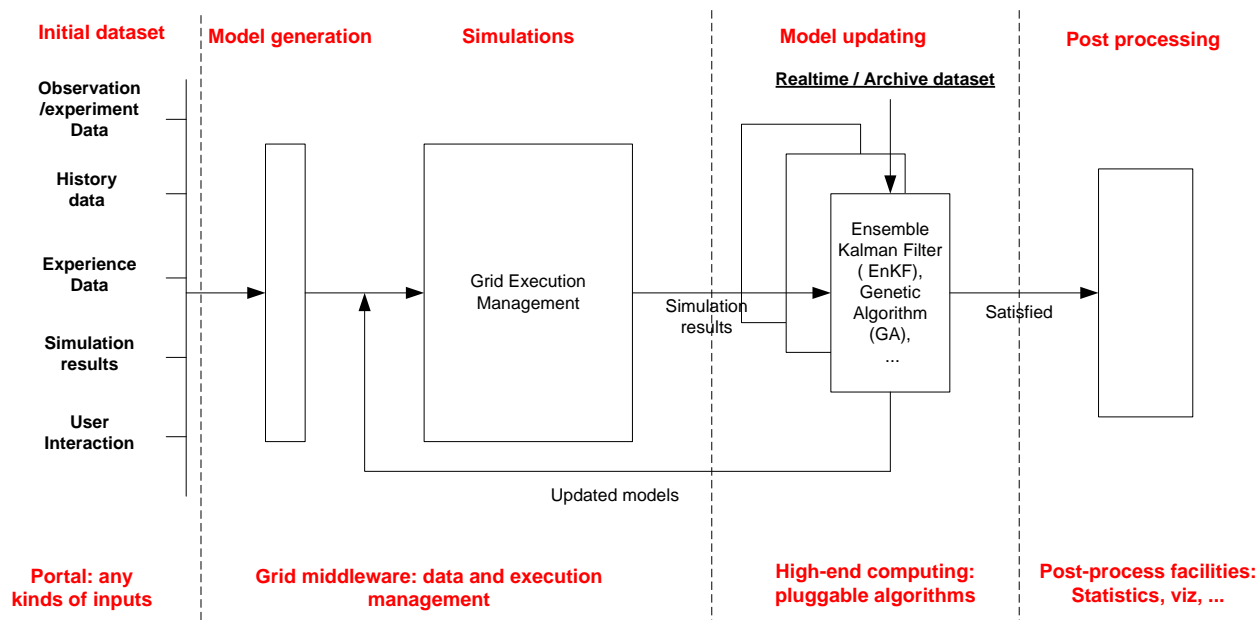


Figure 1: Grid-enabled framework for ensemble inverse modeling.

An efficient execution model across a grid has been presented and implemented. The crucial requirement for ensemble inverse modeling is to make decision on whether or not further simulations are needed based on the results of previous simulation iteration(s). It is a challenging issue to efficiently manage simulation synchronization and multiple iterations within inverse modeling in a grid environment. The dynamic assignment with task container (DA-TC) execution model has been presented to incorporate grid resources for each inverse modeling iteration with the following major advantages: 1) Turnaround time of each iteration is significantly reduced due to dynamically load balancing; 2) Execution reliability is upgraded as task assignment is based on resource runtime status; 3) Execution monitoring and steering is greatly improved. This execution model is built on existing grid middleware toolkits, such as Condor and Globus Toolkit.

Data management plays an important role, which covers both data collection and model generation. A GAT-based (Grid Application Toolkit) archive tool has been developed for data collection. It integrates metadata service and replica logical service for data location with adaptive file transfer capabilities. The GAT design means that the tool is not tied to any particular service implementation or paradigm, *e.g.*, the GAT can adaptively choose various data transfer protocols, *e.g.*, gridftp, scp or http. This feature provides flexibility and portability across different grid environments and options for future extensibility. Once the appropriate datasets have been staged, structured loadable models are generated, which are used for simulation runs.

As the first pluggable data assimilation algorithm in the framework, an EnKF filter has been implemented. EnKF method is widely adopted in subsurface modeling (*e.g.*, oil reservoir and groundwater studies). It reduces a nonlinear minimization problem in a large parameter space to a statistical minimization problem in the ensemble space by changing objective function minimization with multiple local minima. The ensemble members are loosely organized with independency, which is well suited in a grid environment. Our EnKF implementation was primarily designed for oil reservoir studies. Combined with grid execution model and data management mentioned above, it has been used to solve waterflooding problems.

A grid portal, built on top of GridSphere and GridPortlets, provides the entry point to conduct advanced reservoir studies, although its long-term goal is a generic interface for ensemble inverse modeling. First of all, the portal deals with security. A Grid Security Infrastructure certificate is retrieved from a proxy to provide authentication to access grid resources. Secondly, the portal provides web pages to specify input data sources, simulator, computation resources, and so on. Then, a user can submit the job and view the results via this portal.

Future Plans

To accomplish the ultimate goal, *i.e.*, contributing an integrated toolkit with end-to-end service for various inverse modeling applications, we come up with future plans as follows: 1) enhancing the research and development on four components of the framework: data manipulation, execution management, data assimilation algorithms, and portal based interaction environment; 2) seamlessly integrating these components into an all-in-one toolkit; 3) providing extensive supports on applications, such as subsurface modeling and weather forecasting.

Efforts on each component will provide different strategies with common operation interface to adapt various kinds of applications. For instance, data-intensive and computing-intensive applications need different execution management mechanisms or configurations. We also need to develop data assimilation algorithms to meet extensive model inversion requirements. Data management component should allow a user to customize model generation mechanisms for his/her specific needs.

The upcoming toolkit will be operated by a comprehensive grid portal. This portal encapsulates the complexity of grid computing and inverse modeling workflow, providing a user a friendly web interface. Through this portal, a user is allowed to specify dataset sources, specific simulator, computation nature (data-intensive or compute-intensive), data assimilation algorithms, and other parameters. All components will be integrated seamlessly into this framework. Once a user launches inversion process, all the other operations will be transparent to this user.

We also plan to put efforts on application support. Success of a toolkit is decided by its extensive adoption. We will work closely with application scientists to facilitate their research as well as promote this toolkit. Meanwhile, the quality of this toolkit will be improved according to the feedbacks from application community.

References

1. Allen, G. *Building a Dynamic Data Driven Application System for Hurricane Forecasting*. Proceedings of ICCS 2007, Y. Shi et al. (Eds.): ICCS 2007, Part I, LNCS 4487, pp. 1034-1041, 2007.
2. Allen, G.; Davis, K. and et al. *The gridlab grid application toolkit: Towards generic and easy application programming interfaces for the grid*. Proceedings of the IEEE, 93:534-550, March 2005. No.3.
3. Tarantola, A. *Inverse Problem Theory and Methods for Model Parameter Estimation*. Society for Industrial and Applied Mathematics, Philadelphia, 2005.
4. Evensen, G. *The ensemble kalman filter: Theoretical formulation and practical implementation*, Ocean Dyn., vol. 53, no. 4, pp. 334-367, 2003.
5. Foster, I.; Kesselman, C. and Tuecke, S. *The anatomy of the grid: enabling scalable virtual organizations*. International Journal of High Performance Computing Applications, pp. 200-222, 2001, 15(3).
6. He, N.; Reynolds, A. C. and Oliver, D.S. *Three-dimensional reservoir description from multiwell pressure data and prior information*. In SPE Annual Technical Conference and Exhibition, Denver, CO, October 1996, SPE 36509.
7. Tsai, F. *Geophysical parameterization and parameter structure identification using natural neighbors in groundwater inverse problems*. Journal of Hydrology, vol. 308, pp. 269-283, 2005.
8. Zhang, D.; Lu, Z. and Chen, Y. *Dynamic reservoir data assimilation with an efficient, dimension-reduced kalman filter*. SPE Journal, pp. 108-117, Mar 2007.

DOE Sponsored Publications in 2005-2007

1. Allen, G.; Chakraborty, P.; et al. *A Workflow Approach to Designed Reservoir Study*. Accepted by The 2nd Workshop on Workflows in Support of Large-Scale Science Monterey Bay California, June 27-29 2007.
2. Duff, R.; El-Khamra, Y. *Real Time Simulation in Grid Environments: Communicating Data from Sensors to Scientific Simulations*. 2007 Digital Energy Conference & Exhibition, Houston, TX. April 11-12, 2007.
3. Li, X.; White, C.D.; et al. *Queues: Using Grid Computing for Simulation Studies*. 2007 Digital Energy Conference & Exhibition, Houston, TX. April 11-12, 2007.
4. Duff, R. *Observation and Modeling of Identified Regimens of Torsional Vibration*. 2007 American Association of Drilling Engineers, Houston, TX, April 10- 12, 2007.
5. Lewis, L.; Xie M.; et al. *Resource Management for Multicluster Grids*. 2007 Louisiana Academy of Science Conference, Baton Rouge, March 16, 2007.
6. Lei, Z.; Allen, G.; et al. *Utilizing Grid Computing Technologies for Advanced Reservoir Studies*. Supercomputing 2006: 151.
7. Lewis, J.; Allen, G.; et al. *Developing a Grid Portal for Large-scale reservoir Studies*. Annual Argonne Undergraduate Symposium. Nov. 3-4, 2006.
8. Lewis, J.; Allen, G.; et al. *Building an Application Portal for Geoscience*. LSU Summer Undergraduate Research Program. August 3, 2006.
9. Pena, S.; Huang, D.; et al. *A Generic Task-Farming Framework for Reservoir Analysis in a Grid Environment*. The Processings of International Conference of Parallel Processing (ICPP) Workshops 2006: 426-434.
10. Lei, Z.; Huang D.; et al. *ResGrid: A Grid-aware Toolkit for Reservoir Uncertainty Analysis*. The Processings of Conference on Cluster and Grid Computing (CCGrid) 2006: 249-252.
11. Lei, Z.; Huang, D.; et al. *Leveraging Grid Technologies For Reservoir Uncertainty Analysis*. High Performance Computing Symposium (HPC06), Huntsville, Alabama. April 2-6, 2006.
12. Huang, D.; Allen, G.; et al. *Getdata: A Grid Enabled Data Client for Coastal Modeling*. High Performance Computing Symposium (HPC06), Huntsville, Alabama. April 2-6, 2006.
13. Kalla, S.; White, C.D.; et al. *Consistent Downscaling of Seismic Inversions to Cornerpoint Flow Models*. Society of Petroleum Engineering Paper 79676.

Properties of Ferroelectric Nanostructures: A Combined Theoretical and Experimental Approach

Sergey Lisenkov, Laurent Bellaiche and Huaxiang Fu

Department of Physics, University of Arkansas, Fayetteville, Arkansas 72701, USA

Program Scope

Complex ferroelectric oxides are key materials for actuators, sensors, and energy storage. They are specifically relevant to the Department of Energy's missions in energy efficiency and transportation technology, as dielectrics in capacitor components used in power distribution systems. However, the ferroelectric, dielectric and electromechanical properties required for a specific application are not always available in a pure perovskite material. This has led to considerable interest in tuning towards a desired behavior via nanostructuring of ferroelectrics, including epitaxial heterostructures, superlattices and three-dimensionally confined ferroelectric nanodots. The main objective of that award is to develop a research program aimed at determining and understanding properties of ferroelectric nanostructures. To reach it, we want to develop and use first-principles-based schemes, as well as collaborate with well-known experimentalists (e.g., Dr. Streiffer's group at ANL).

Recent Progress

Examples of recent progress are given below:

1) *Atomistic approach for computing depolarizing energy in low-dimensional ferroelectrics.* An atomistic approach allowing an accurate and efficient treatment of depolarizing energy and field in any low-dimensional ferroelectric structure was developed. Application of this approach demonstrates the limits of the widely used continuum model. Moreover, implementation of this approach within a first-principles-based model revealed an unusual phase transition – from a state exhibiting a spontaneous polarization to a phase associated with a toroid moment of polarization – in a ferroelectric nanodot for a critical value of the depolarizing field. The use of this approach also explained the dependency of the dipoles' patterns on the nanostructure's dimensionality and boundary conditions.

2) *Domain evolution in ferroelectric ultrathin films.* A first-principles-based method was used to reveal the electric-field-induced evolution of the recently discovered 180 degrees

stripe domains [1] in ultrathin films. This evolution involves (i) the lateral growth of majority dipole domains at the expense of minority domains with the overall stripe periodicity remaining unchanged; (ii) the creation of surface-avoiding *nanobubbles* via the “breaking” of minority stripe domains; and (iii) the formation of a single monodomain state.

3) *Phase diagrams of epitaxial ultrathin films and superlattices.* A first-principles-based scheme was developed for $(\text{Ba}_x\text{Sr}_{1-x})\text{TiO}_3$ systems. This method was used to determine the phase diagram of epitaxial (001) BaTiO_3 ultrathin films and of (001) $\text{BaTiO}_3/\text{SrTiO}_3$ superlattices of different periods. In particular, the effects of surface/interface, thickness and electrical boundary conditions on the temperature-misfit strain phase diagrams of thin films were revealed. We further found that short-period superlattices exhibit a phase diagram that resemble that of (001) BaTiO_3 thin films under short-circuit-like conditions, while original domain patterns with unusual atomistic features occur in the long-period superlattices.

4) *Ferroelectric nanodots: properties and applications.* A first-principles-based approach was used to show (i) that stress-free *isolated* ferroelectric nanodots under open-circuit-like electrical boundary conditions maintain a vortex structure for their local dipoles when subject to a transverse inhomogeneous static electric field, and, more importantly, (ii) that such field leads to the solution of a fundamental and technological challenge, namely an efficient control of the direction of the macroscopic toroidal moment. Moreover, different phases were predicted in nanodots that are *embedded* in a polarizable medium, depending on the ferroelectric strengths of the material constituting the dot and of the medium. In particular, novel states, exhibiting coexistence between two kinds of order parameters or possessing a peculiar order between dipole vortices of adjacent dots, were discovered.

Future Plans

We will continue to look for novel and technologically-important effects in ferroelectric nanostructures, and, in particular, determine how atomic ordering and size-effects affect their dielectric loss in the GHz-THz regime.

References

[1] S. K. Streiffer, J.A. Eastman, D.D. Fong, C. Thompson, A. Munkholm, M.V.R. Murty, O. Auciello, G.R. Bai and G.B. Stephenson, Phys. Rev. Lett. **89**, 067601, (2002).

DOE Sponsored publications in 2005 - 2007

1) “Low-dimensional ferroelectrics under different electrical and mechanical boundary conditions,” I. Ponomareva, I.I. Naumov and L. Bellaiche, Phys. Rev. B **72**, 214118 (2005).

- 2) "Phase Diagrams of Epitaxial BaTiO₃ Ultrathin Films From First Principles," B.-K. Lai, Igor A. Kornev, L. Bellaiche and G. J. Salamo, *Appl. Phys. Lett.* **86**, 132904 (2005).
- 3) "Morphotropic phase boundary of heterovalent perovskite solid solutions: Experimental and theoretical investigation of PbSc_{0.5}Nb_{0.5}O₃-PbTiO₃," R. Haumont, A. Al-Barakaty, B. Dkhil, J.M. Kiat and L. Bellaiche, *Phys. Rev. B* **71**, 104106 (2005).
- 4) "A combined theoretical and experimental study of the low temperature properties of BaZrO₃," A.R. Akbarzadeh, I. Kornev, C. Malibert, L. Bellaiche and J.M. Kiat, *Phys. Rev. B* **72**, 205104 (2005).
- 5) "Atomistic treatment of depolarizing energy and field in ferroelectric nanostructures," I. Ponomareva, I.I. Naumov, I. Kornev, Huaxiang Fu and L. Bellaiche, *Phys. Rev. B* **72**, 140102(R) (2005).
- 6) "Properties of GaN/ScN and InN/ScN superlattices from first principles," V. Ranjan, S. Bin-Omran, D Sichuga, R. S. Nichols, L. Bellaiche and A. Alsaad, *Phys. Rev. B* **72**, 085315 (2005).
- 7) "Study of Potassium-Sodium-Niobate Alloys: A Combined Experimental and Theoretical Approach," J. Attia, L. Bellaiche, B. Dkhil, P. Gemeiner and B. Malic, *Journal de Physique IV* **128**, 55 (2005).
- 8) "Spontaneous polarization in one-dimensional Pb(Zr,Ti)O₃ nanowires " I. Naumov and H. Fu, *Phys. Rev. Lett.* **95**, 24702 (2005).
- 9) "Ferroelectricity of perovskites under pressure," I. Kornev, P. Bouvier, P.-E. Janolin, B. Dkhil, J. Kreisel and L. Bellaiche, *Phys. Rev. Lett.* **95**, 196804 (2005).
- 10) "Controlling Toroidal Moment by Means of an Inhomogeneous Static Field: An Ab Initio Study," S. Prosandeev, I. Ponomareva, I. Kornev, I. Naumov and L. Bellaiche, *Phys. Rev. Lett.* **96**, 237601 (2006).
- 11) "Electric-field induced domain evolution in ferroelectric ultrathin films," B.-K. Lai, I. Ponomareva, I. I. Naumov, Igor A. Kornev, Huaxiang Fu, L. Bellaiche and G. J. Salamo, *Phys. Rev. Lett.* **96**, 137602 (2006).
- 12) "Influence of the growth direction on properties of ferroelectric ultrathin films," I. Ponomareva and L. Bellaiche, *Phys. Rev. B* **74**, 064102 (2006).
- 13) "Finite-temperature properties of (Ba,Sr)TiO₃ systems from atomistic simulations, " L. Walizer, S. Lisenkov and L. Bellaiche, *Phys. Rev. B* **73**, 144105 (2006).
- 14) "Symmetry breaking at the nanoscale and diffuse transitions in ferroelectrics: A

comparative study of $\text{PbSc}_{1/2}\text{Nb}_{1/2}\text{O}_3$ and $\text{PbZr}_{0.6}\text{Ti}_{0.4}\text{O}_3$,” J. Iniguez and L. Bellaiche, Phys. Rev. B **73**, 144109 (2006).

15) “Phase diagram of $\text{Pb}(\text{Zr,Ti})\text{O}_3$ solid solutions from first principles,” I. A. Kornev, L. Bellaiche, P.-E. Janolin, B. Dkhil and E. Suard, Phys. Rev. Lett. **97**, 157601 (2006).

16) “Properties of ferroelectric nanodots embedded in a polarizable medium: Atomistic simulations,” S. Prosandeev, and L. Bellaiche, Phys. Rev. Lett. **97**, 167601 (2006).

17) “Influence of the growth direction on properties of ferroelectric ultrathin films,” I. Ponomareva and L. Bellaiche, Phys. Rev. B **74**, 064102 (2006).

18) “The nature of ferroelectricity under pressure,” I. A. Kornev and L. Bellaiche, Phase Transitions **80**, 385 (2007).

19) “Asymmetric screening of the depolarizing field in ferroelectric thin film,” S. Prosandeev and L. Bellaiche, Phys. Rev. B **75**, 172109 (2007).

20) “Theoretical phase diagram of ultrathin films of incipient ferroelectrics,” A. R. Akbarzadeh, L. Bellaiche, J. Iniguez, and D. Vanderbilt, Appl. Phys. Lett. **90**, 242918 (2007).

21) “Tensors in ferroelectric nanoparticles: First-principles-based simulations,” S. Prosandeev, I. Kornev and L. Bellaiche, Phys. Rev. B **76**, 012101 (2007).

22) “Characteristics and signatures of dipole vortices in ferroelectric nanodots: First-principles-based simulations and analytical expressions,” S. Prosandeev and L. Bellaiche, Phys. Rev. B **75**, 094102 (2007).

23) “Domain evolution of BaTiO_3 ultrathin films under electric field: a first-principles study,” B.-K. Lai, I. Ponomareva, I.A. Kornev, L. Bellaiche and G. J. Salamo, Phys. Rev. B **75**, 085412 (2007).

24) “Vortex-to-Polarization Phase Transformation Path in $\text{Pb}(\text{Zr,Ti})\text{O}_3$ Nanoparticles,” I. Naumov and H. Fu, Phys. Rev. Lett. **98**, 077603 (2007)

25) “Effects of vacancies on properties of disordered ferroelectrics: a first-principles study,” L. Bellaiche, J. Iniguez, E. Cockayne and B.P. Burton, Phys. Rev. B **75**, 014111 (2007).

26) “Phase diagrams of $\text{BaTiO}_3/\text{SrTiO}_3$ superlattices from first principles”, S. Lisenkov and L. Bellaiche, Phys. Rev. B **76**, 020102(R) (2007).

27) “Modelling of nanoscale ferroelectrics from atomistic simulations,” I. Ponomareva, I. Naumov, I. Kornev, H. Fu and L. Bellaiche, Invited Review, Current Opinion in Solid State and Materials Science **9**, 114 (2005).

**ADDRESSING SYSTEM INTEGRATION ISSUES REQUIRED FOR THE
DEVELOPMENT OF DISTRIBUTED WIND-HYDROGEN ENERGY SYSTEMS**

Dr. Michael D. Mann and Dr. Hossein Salehfar, Nilesh Dale, Christian Biaku, Andrew Peters,
Tae-hee Han, Dr. Kevin Harrison (NREL), Dr. Eduardo Hernandez Pacheco (Intel)
School of Engineering and Mines, University of North Dakota, Grand Forks, ND 58202

Program Scope

Wind generated electricity is a variable resource. Hydrogen can be generated via electrolysis as an energy storage media and fuel, but is costly. Advancements in power electronics and system integration are needed to make electrolysis a more viable system. Therefore, the long-term goal of the efforts at the University of North Dakota is to merge wind energy, hydrogen production, and fuel cells to bring emission-free and reliable power to commercial viability. The primary goals include

1. Expand system models as a tool to investigate integration and control issues.
2. Examine long-term effects of wind-electrolysis performance from a systematic perspective.
3. Collaborate with NREL to design, integrate, and quantify system improvements by implementing a single power electronics package to interface “wild” AC to PEM stack DC requirements.

The specific objective includes modeling, simulation and verification of wind to hydrogen energy system with proton exchange membrane (PEM) electrolyzer using Renewable energy Power system Modular Simulator (RPM-Sim).

Recent Progress

A primary accomplishment was completion of electrolysis and fuel cell test facility which provided the capability to perform the heart of the proposed experimental work. The experimental facilities to address Goal 2 have been completed. The system is designed around a 6-kw PEM electrolysis stack that was purchased from Proton Energy Systems. Current work has focused on gathering fundamental information for understanding and optimizing electrolyzer performance. The impact of system operating temperature on key operating parameters within the stack has been investigated. On the system level, a new hydrogen drying system and electrochemical compression are being studied.

Independent PEM electrolyzer and fuel cell models have been developed in a format compatible with RPM-SIM. These models have been integrated into NREL’s existing RPM model using a new inverter module developed at UND. Case studies are being analyzed to identify issues associated with close coupling these systems. Results are also being used as input to develop improved power control systems.

We were not able to obtain a permit form the city to install the 17.5 kW wind turbine that was donated to the UND School of Engineering and Mines on the UND campus. Therefore, we will not use the wind turbine as a part of this project.

One of the deliverables that were stated in our original proposal is to develop a detailed model that is compatible with NREL’s RPM-Sim software for performance studies of PEM Fuel cells and electrolysis units in hybrid networks. The model has been developed in the VIS-Sim programming environment. In addition to working with RPM-SIM, this model also has the capability to run independently for PEM fuel cell and electrolysis studies under different operating conditions of temperature, pressure and humidity. Modeling results for the fuel cell and electrolysis modules were summarized in previous reports. Work during the last year integrated the fuel cell model with a wind turbine, diesel engine, and village load.

The UND PEM electrolysis system is designed to allow the precise control over operating temperature, hydrogen system pressure, water resistivity, water flow, stack current and safety. A temperature control unit (chiller) controls the inlet DI water temperature thereby providing control of the operating temperature of electrolyzer. This system is designed to allow higher temperature testing by maintaining DI water temperature with the chiller while using a heater provided in oxygen-water phase separator. Early work focused on operating temperature to provide data that can allow peak efficiency to be obtained regardless of operating current. This will be beneficial in variable power sources such as renewable energy. As shown in figure 1, for a given current, voltage drops as temperature increases. This increases stack efficiency as activation and ohmic losses (irreversible potentials) are reduced. At higher temperature the stack produces more hydrogen at a given current.

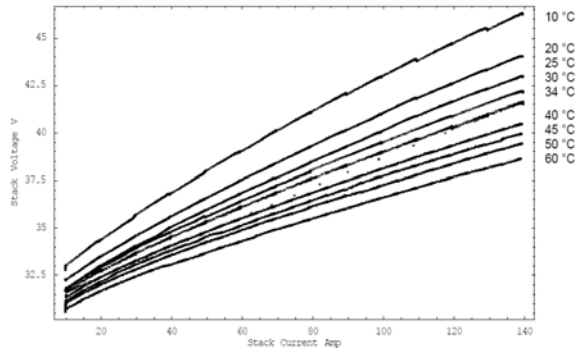


Figure 1. Characteristic curves at constant cathode pressure (165 psi) at temperature from 10 °C to 60 °C.

A number of studies have been performed on the Ballard Power Systems 1.2 kW PEM fuel cell. To investigate the performance of 1.2 kW PEM fuel cell stack, electrochemical impedance spectroscopy (EIS) studies were performed using a frequency response analyzer. We investigated the response of the PEM fuel cell in the presence of large amplitude test signals, up to and including amplitudes higher than the direct current drawn from the fuel cell, requiring a current reversal. At both high and low frequencies the size of the amplitude of the test signal resulted in noticeable variation in the impedance of the fuel cell. Results from these ongoing studies are being used to develop equivalent circuit models for analysis of voltage stability, short circuit conditions, transient responses, power quality, protection schemes, and optimizing dynamic operational performance. Several control algorithms are employed in fuel cell systems for protection and to enhance the quality of power generated. An investigation of the cathode purge process showed that for the Ballard Nexa™, the cathode purge results in a voltage change of 0.08 V per cell within the load range studied. This results in a sudden change of 9% in voltage when the fuel cell is not loaded. If the fuel cell is loaded this percentage increases. The shape of the decay curve changes with the loading on the fuel cell.

Assuming all cells in a stack behave alike simplifies modeling efforts, allowing single cell models to be utilized to represent stack performance. However, based upon transport and other considerations that occur at the stack level some variance can be accepted. Ten cells were taken at different locations in the stack and the impedance data measured. It was found in the Nyquist and Bode magnitude plots that the membrane resistances were unchanged. However, the activation resistance had changed. Identifying and understanding the differences between the cell and stack level will provide designers information to help identify which design aspects can result in the most significant improvement. Improving membrane and electrode porosity, developing better catalysts

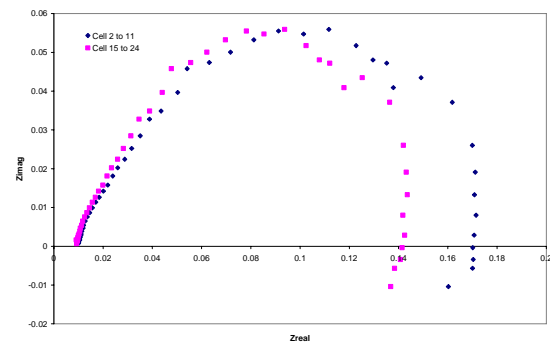


Figure 2: A comparison of the Nyquist plot of a group of the cells taken at different locations in the 1.2 kW PEM fuel cells.

and improving channel design will minimize losses and improve efficiency.

A study was conducted on the charge transfer coefficient (CTC) of the oxygen electrode (anode) of a 6kW PEM electrolyzer stack to determine its temperature dependence. Studies at UND found that variation of CTC from the symmetry factor is significant enough to impact the estimation of the activation overpotential. Figure 3 shows the variation of the anode charge transfer coefficient with temperature. Clearly there is an upward trend with temperature which could be the result of reaction modification or changes in electrode properties with temperature. The behavior of the CTC shows that the better performance observed for the electrolyzer stack at higher temperatures is not solely reliant on the increased membrane conductivity but also depends on the CTC. The upward trend observed in the value of the CTC is an indication that the kinetic characteristics improved as well with temperature.

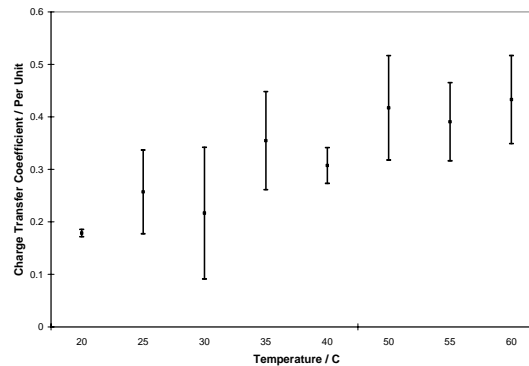


Figure 3: Variation of anode CTC with temperature.

Future Plans

ESI Studies of Electrolyzer: Very little work has been performed using EIS to analyze PEM electrolysis stacks because power supplies of required rating lack the wide frequency bandwidth required to conduct full range EIS studies. The primary limitation is a power system able to generate the high level of DC required to run the electrolysis stack at full load (140 A at 50 Volts) while applying the test signal (10 A at 0.01 to 20 kHz) required to perform the EIS analysis. Existing systems are typically restricted to either low current applications at the required frequency, or low frequency at the required current. Figure 4 shows the basic EIS experimental set up. A prototype of this system has been tested for a base DC up to 1A with AC signals up to 0.02 A and 300-4000Hz superimposed on the DC. The system generated output with no visual distortions over this frequency range. Our group plans to scale this system using their existing 200 A DC power supply and the Solartron frequency response analyzer currently being procured.

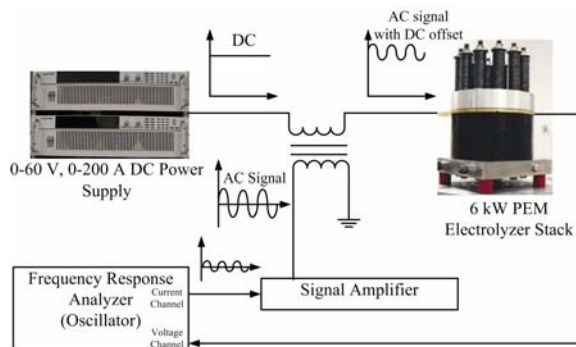


Figure 4. Prototyped EIS experimental schematic to be scaled up for proposed work.

Hydrogen Dew Point Control System: An adsorption drying system is generally used to remove water vapor from the hydrogen product gas. They can achieve a dew point of -65 °C, or less than 5 parts per million (ppm) water vapor, in the hydrogen product gas (99.9995% pure hydrogen). The two-tube desiccant system uses one tube at a time to dry the hydrogen from the PEM stack. At full operating current an orifice at the top of the drying assembly diverts roughly 10% of the dried hydrogen down the opposite tube to remove the adsorbate from the adsorbent. An alternative method to reduce and control the dew point of the hydrogen gas has been developed. Thermoelectric coolers (TECs) are used to cool saturated hydrogen gas as it travels through a large-surface-area cold plate, allowing the water vapor to condense in Stage 1 and sublime in Stage 2. The experimental system is currently being assembled at UND and details and results will be presented in open literature soon.

The following major papers, reports, and presentations have been given to disseminate the results of this work

- *Semi-Empirical Model for Determining PEM Electrolyzer Stack Characteristics*, Harrison, K., Pacheco, E.H., Mann, M.D., and Salehfar, H., *J. of Fuel Cell Science and Technology*, **2006**,3,220-223
- *An Advanced PEM Fuel Cell Performance Prediction Model*, Pacheco, E.H.; Biaku, C.; Peters, A.; Salehfar, H.; Mann, M.D., *Journal of Power Sources*, **2006**, (in review)
- *Addressing System Integration Issues Required for the Development of a Distributed Hydrogen Energy System*, Harrison, K.; Mann, M.D., Salehfar, H., *Abstract and presentation at AWEA Conference*, Pittsburgh, PA, June 4-7, **2005**.
- *Modeling of a PEM Fuel Cell Performance*, Biaku, C., Pacheco, E.H., Peters, A., Harrison, K., Mann, M.D., Salehfar, H., *Poster presented at Living the Life of the Mind – Fourth Annual Scholarly Activities Forum*, Grand Forks, ND, March 22-24, **2005**.
- *Addressing System Integration Issues Required for the Development of a Distributed Hydrogen Energy System*, Mann, M.D., Salehfar, H., Harrison, K., Biaku, C., Peters, A., Dale, N., *Abstract at the 2005 DOE EPSCoR Conference*, Morgantown, WV, June 12-14, **2005**
- *A Semi-Empirical Study of the Temperature Dependence of the Anode Charge Transfer Coefficient of a 6-kW PEM Electrolyzer*, Biaku, C.Y.; Dale, N.V.; Mann, M.D.; Peters, A.J; Salehfar, H.; Han, T., *Int. Journal of Hydrogen Energy*, **2007**, in review
- *Rational Approximations*, Pacheco, E.H., Mann, M.D., *Journal of Power Sources* **2004** 128 (1): 34-44
- *Dynamic Scheduling of Wind Energy for Hydrogen Production by Electrolysis*, Peters, R.R., Stevens, B.; Mann, M.D.; Salehfar, H., *Proceedings of 37th North American Symposium*, October 23-25, **2005**, Ames, IA
- *Dynamic Model Development of a Fixed Stall control Wind Turbine as Start-Up*, Peters, R.R.; Muthumuni, D.; Bartel, T.; Salehfar, H.; Mann, M., *Proceedings of 2006 Power Engineering Society General Meeting*, June 18-22, **2006**, Montreal, Canada
- *Electrolysis: Information and Opportunities for Electric Power Utilities*, Kroposki, J.; Levene, J.; Harrison, K.; Sen, P.K.; Novachek, F., NREL/TP-581-40605, September **2006**
- *Addressing System Integration Issues Required For The Development of a Distributed Wind-Hydrogen Energy System*, AWEA WINDPOWER Conference May, **2006**
- *PEM Electrolysis Hydrogen Production System Design For Improved Testing And Optimization*, Dale, N.V., Biaku, C.Y., Mann, M.D., Salehfar H., *NHA Annual Hydrogen Conference*, San Antonio, March **2007** (Poster also)
- *Electrochemical Compression Of Product Hydrogen From PEM Electrolyzer Stack*, Dale, N.V., Biaku, C.Y., Mann, M.D., Salehfar H., *NHA Annual Hydrogen Conference*, San Antonio, March **2007** (Poster also)
- *Analysis of Impedance Data of a Partially Loaded 1.2 kW PEM Fuel Cell Stack*, Biaku, C.Y., Dale, N.V., Mann, M.D., Salehfar H., *NHA Annual Hydrogen Conference*, San Antonio, March **2007** (Poster also)
- *Electrochemical compression of hydrogen from renewable wind-PEM electrolysis generation systems*, Dale N.V., Biaku, C.Y., Mann, M.D., Salehfar H., *AWEA WINDPOWER Conference*, Los Angeles, June **2007** (Poster also)
- *A Study of Low Pressure Fuzzy Logic Wind Hydrogen System for Off-Grid Applications*, Biaku, C.Y., Han, T., Mann, M.D., Salehfar H., *AWEA WINDPOWER Conference*, Los Angeles, June **2007** (Poster also)
- *Power Electronics for Interfacing of Wind Turbine and Electrolyzer for Hydrogen Generation*, Peters, A.J., Biaku, C.Y., Dale, N.V., Salehfar H., Mann, M.D., *AWEA WINDPOWER Conference*, Los Angeles, June **2007** (Poster also)

Novel Quantum Phenomena in Layered Ruthenates

Zhiqiang Mao

zmao@tulane.edu

Physics Department, Tulane University, New Orleans, LA 70118

Program Scope

Strongly correlated oxides have been the subject of intense study for the last two decades. Many of these materials exhibit exciting new properties and enhanced functionality: examples include high temperature superconductivity in cuprates and colossal magnetoresistance in manganites. Recently, perovskite-related ruthenates have become a new focus within this field. They exhibit a rich variety of fascinating ordered ground states, unprecedented for a transition metal oxide series. Spin-triplet superconductivity, metamagnetic quantum criticality, itinerant ferromagnetism, antiferromagnetic Mott insulating, and half-metallic behavior were all found in close proximity to one another. These diverse ground states originate from the strong interplay of charge, spin, lattice, and orbital degrees of freedom. They offer a unique opportunity to tune the system and study the physics of novel quantum phases. Since the active lattice and orbital degrees of freedom can lead to giant responses to small perturbations, the ground state properties of the ruthenates are extremely sensitive to impurities. Controlled studies of new phases require samples of exceptionally high quality. This project aims at searching for novel quantum phenomena in ruthenate materials using “superclean” high-quality single crystals, grown by the floating-zone technique, and investigating the underlying physics.

Recent Progress

We observed exciting properties in multi-layered ruthenates $\text{Sr}_4\text{Ru}_3\text{O}_{10}$ and $\text{Sr}_3\text{Ru}_2\text{O}_7$ in our early studies. $\text{Sr}_4\text{Ru}_3\text{O}_{10}$ shows a ferromagnetic transition at $T_c \approx 100$ K; followed by a second transition at $T^* \approx 50$ K [1]. Below T^* , a first order metamagnetic transition is induced by an in-plane magnetic field. Our experiments revealed that this metamagnetic transition occurs via a phase separation process with magnetic domain formation [2,3] (see Fig.1a) This phase separation process results in very unusual transport properties: a) the magnetoresistivity shows switching behaviors; b) the resistivity displays non-metallic temperature dependence within the transition region which is in sharp contrast with the Fermi liquid ground state outside the transition region. This work was published in *Physical Review Letters* **96**, 077205 (2006). Recently, we made a remarkable progress in understanding why the in-plane magnetic field can induce such a metamagnetic transition in the ferromagnetic ground state [3,4]. We performed systematic electronic and magnetic property measurements on $\text{Sr}_4\text{Ru}_3\text{O}_{10}$ under high magnetic fields and different field orientations in collaboration with Dr. Luis Balicas’ group at National High Magnetic Field Lab and Dr. Salamon’s group at University of Illinois at Urbana-Champaign. We observed evidences for the Fermi surface reconstruction (see Fig. 1b) and a transition from two-fold to four-fold symmetry in the in-plane anisotropy of magnetoresistivity across the metamagnetic transition (see Fig. 1c). These results suggested that the metamagnetism in $\text{Sr}_4\text{Ru}_3\text{O}_{10}$ is orbital dependent; ferromagnetic and metamagnetic bands coexist. This finding provides important information for the study of orbital-related physics. A part of these results have been published in *Physical Review B* **75**, 094413 (2007) and **75**, 094429 (2007). In

addition, we performed neutron scattering measurements on $\text{Sr}_4\text{Ru}_3\text{O}_{10}$ single crystals in collaboration with Wei Bao at Los Alamos National Laboratory. We have found preliminary evidences that the metamagnetic transition in $\text{Sr}_4\text{Ru}_3\text{O}_{10}$ involves a structure phase transition.

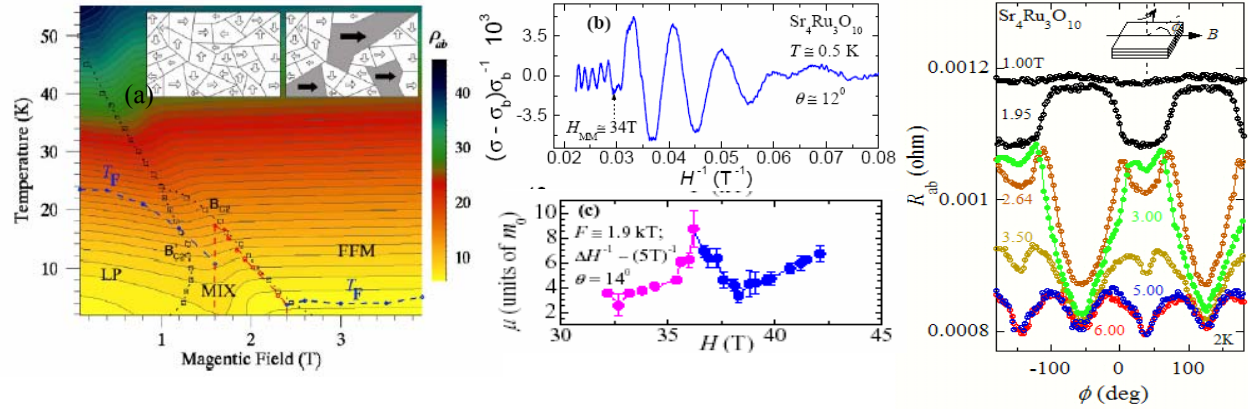


Figure 1: (a) Contour plot of in-plane resistivity as a function of magnetic field ($\parallel ab$ -plane) and temperature. LP: lowly polarized phase; FFM: forced ferromagnetic phase; MIX: mixed phase; T_F : Fermi liquid temperature. The resistivity shows a non-metallic temperature dependence in the mixed phase area marked by red dashed lines. Left inset illustrates ferromagnetic domains of the uniform LP phase; right inset shows the coexistence of the ferromagnetic domains of the LP phase and FFM domains (marked by the black arrows) [3]. (b) Top panel: The SdH signal $(\sigma - \sigma_b)/\sigma_b$, where $\sigma_b = 1/\rho_b$ is the background conductivity (the field is aligned at 12 degree relative to the c -axis); the metamagnetic transition field with this field orientation is about 34 T). Bottom panel: FFT spectrum of the oscillatory component of ρ_{zz} for fields above and below 34 T [4]. (c) In-plane angle dependence of the magnetoresistance. A two-fold to four-fold symmetry transition in the in-plane anisotropy was observed across the metamagnetic transition. The curves at 1T and 1.95 T are shifted for clarity.

$\text{Sr}_3\text{Ru}_2\text{O}_7$ shows a metamagnetic quantum phase transition [5,6] We previously performed tunneling studies on $\text{Sr}_3\text{Ru}_2\text{O}_7$ to study its Fermi surface properties near the quantum phase transition. We observed unusual oscillations in tunneling magnetoresistance. Systematic investigation of this feature suggests that it likely originates from unusual surface electronic states, which strongly couple with applied magnetic field. In addition, we have studied the magnetic ground state properties of $\text{Sr}_3\text{Ru}_2\text{O}_7$ through Ti doping. Our results reveal that small amounts of Ti suppress the characteristic peak in magnetic susceptibility near 16 K and result in a sharp upturn in specific heat. The metamagnetic quantum phase transition and related anomalous features are quickly smeared out by small amounts of Ti. These observations provide strong evidence for the existence of competing magnetic fluctuations in the ground state of $\text{Sr}_3\text{Ru}_2\text{O}_7$.

Future plans

As discussed above, $\text{Sr}_4\text{Ru}_3\text{O}_{10}$ is of particular interest; it is an ideal system to study novel physics associated with metamagnetic behavior, electronic inhomogeneity, orbital ordering, orbital dependence of magnetic interaction, and spin-lattice coupling. We will perform the following research to further clarify its underlying physics:

- Make larger $\text{Sr}_4\text{Ru}_3\text{O}_{10}$ single crystals and carry out further neutron scattering measurements on this material through collaboration with Dr. Bao to systematically investigate the characteristics of the structure transition near the metamagnetic transition and identify its magnetic structure.

- Investigate orbital ordering properties of $\text{Sr}_4\text{Ru}_3\text{O}_{10}$ using a resonant x-ray scattering technique in collaboration with Dr. Islam at Argonne National Lab. $\text{Sr}_4\text{Ru}_3\text{O}_{10}$ shows strong magnetoelastic coupling [7] and its metamagnetic transition is likely to involve suppression of orbital ordering, so structure studies under magnetic field for this material is highly desired. Resonant x-ray scattering is an ideal technique to probe orbital ordering since it is directly sensitive to the anisotropy of the orbitals of the resonating atom.
- Perform both in-plane and out-of-plane electronic transport measurements on ultra-pure $\text{Sr}_4\text{Ru}_3\text{O}_{10}$ crystals to further characterize the effect of domain structure on transport properties. Our current measurements have focused on in-plane transport properties. We have not made any measurement on the out-of-plane transport properties near the metamagnetic transition. A natural extension of the current work is to systematically investigate the dependence of magnetoresistivity steps on field orientation. We plan to carry out this measurement by adding a rotating sample stage to our existing ^3He cryostat. Such studies may provide information on the orientation of magnetic domains.

The unusual oscillations seen in the tunneling magnetoresistance of $\text{Sr}_3\text{Ru}_2\text{O}_7$ suggests that the surface of this material may have unusual electronic states, which couple with applied magnetic field. Further investigation on this phenomenon may reveal a novel quantum phase. We will perform the following studies on this material to clarify its underlying physics.

- Carry out systematic tunneling measurements on junctions prepared on differently oriented crystallographic surfaces. Tunneling measurements on precisely oriented crystals will allow us to systematically study the anisotropic properties of this oscillation behavior.
- Measure the dependence of the oscillation on field orientation. A striking difference in oscillation pattern between $H//c$ and $H//ab$ has been observed, which implies that the oscillations depend on field orientation. The most direct way for probing the field orientation dependence of the oscillation is to perform the measurement on the same junction at the same cooling-down with a rotator. We will perform this measurement by adding a rotating sample stage to our existing ^3He cryostat.
- Extend the tunneling measurements to higher field. If this oscillation is truly associated with critical fluctuations, the oscillation behavior is expected to diminish when the applied field is well above the critical field (~ 8 T). This measurement will be performed in collaboration with Drs. Luis Balicas at NHMFL.
- Characterize the surface electronic and magnetic properties of pure and Ti-doped $\text{Sr}_3\text{Ru}_2\text{O}_7$ using soft x-ray resonant magnetic scattering (SXRMS) through collaboration with Dr. Ederer. Our group has investigated the effect of nonmagnetic Ti^{4+} impurities on the bulk electronic and magnetic properties of $\text{Sr}_3\text{Ru}_2\text{O}_7$. We observed evidence that both antiferromagnetic (AFM) and ferromagnetic (FM) fluctuations coexist in the ground state of pure $\text{Sr}_3\text{Ru}_2\text{O}_7$. Small amounts of Ti doping quickly suppresses the AFM correlations, leaving the system in a state dominated by FM correlations [8]. More interestingly, we found that Ti-doping suppresses the oscillations in the tunneling magnetoresistance; no oscillations were observed when the doping level is above 0.1%. Systematic comparison of surface electronic and magnetic properties between pure and Ti-doped $\text{Sr}_3\text{Ru}_2\text{O}_7$ might provide insight into the mechanism of this new phenomenon.
- Carry out systematic scanning tunneling microscope (STM) and X-ray photoelectron spectroscopy (XPS) measurements on both pure and Ti-doped $\text{Sr}_3\text{Ru}_2\text{O}_7$ samples in collaboration with Dr. Diebold.

- Use orbital-resolved soft x-ray absorption (SXAS) and soft x-ray emission spectroscopy (SXES) to study the electronic band properties of Sr_2RuO_4 , $\text{Sr}_3\text{Ru}_2\text{O}_7$, and $\text{Sr}_4\text{Ru}_3\text{O}_{10}$ through collaboration with Drs. Ederer and Freeland.

References

- (1) M.K. Crawford, R.L. Harlow, W. Marshall, Z. Li, G. Cao, R.L. Lindstrom, Q. Huang, and J.W. Lynn, *Phys. Rev. B* **2002**, 65, 214412.
- (2) Z.Q. Mao, M. Zhou, J. Hooper, V. Golub, and C.J. O'Connor, *Phys. Rev. Lett.* **2006**, 96, 077205.
- (3) D. Fobes, M.H. Yu, M. Zhou, J. Hooper, C.J. O'Connor, M. Rosario, and Z.Q. Mao, *Phys. Rev. B* **2007**, 75, 094429.
- (4) Y.J. Jo, L. Balicas, N. Kikugawa, E.S. Choi, K. Storr, M. Zhou, and Z.Q. Mao, *Phys. Rev. B* **2007**, 75, 094413.
- (5) S.A. Grigera, R.S. Perry, A.J. Schofield, M. Chiao, S.R. Julian, G.G. Lonzarich, S.I. Ikeda, Y. Maeno, A.J. Millis, and A.P. Mackenzie, *Science* **2001**, 294, 329-332.
- (6) S. A. Grigera, P. Gegenwart, R. A. Borzi, F. Weickert, A. J. Schofield, R. S. Perry, T. Tayama, T. Sakakibara, Y. Maeno, A. G. Green, and A. P. Mackenzie, *Science* **2004**, 306, 1154-1158.
- (7) R. Gupta, M. Kim, H. Barath, S.L. Cooper, and G. Cao, *Phys. Rev. Lett* **2006**, 96, 067004.
- (8) J. Hooper, M. H. Fang, M. Zhou, D. Fobes, N. Dang, Z. Q. Mao, C. M. Feng, Z.A. Xu, M.H. Yu, C. J. OConnor, G. J. Xu, N. Andersen, M. Salamon, *Phys. Rev. B* **2007**, 75, 060403.

Publications in 2005-2007

Competing magnetic fluctuations in $\text{Sr}_3\text{Ru}_2\text{O}_7$ probed Ti doping, J. Hooper, M.H. Fang, M. Zhou, D. Fobes, N. Dang, Z.Q. Mao, C.M. Feng, Z.A. Xu, M.H. Yu, C.J. O'Connor, G.J. Xu, N. Anderson, and M. Salamon, *Phys. Rev. B* **2007**, 75, 060403 (*Rapid Communication*).

Phase diagram of the electronic states of trilayered ruthenate $\text{Sr}_4\text{Ru}_3\text{O}_{10}$, D. Fobes, M.H. Yu, M. Zhou, J. Hooper, C.J. O'Connor, M. Rosario, and Z.Q. Mao, *Phys. Rev. B* **2007**, 75, 094429.

Orbital-dependent metamagnetic response in $\text{Sr}_4\text{Ru}_3\text{O}_{10}$, Y.J. Jo, L. Balicas, N. Kikugawa, E.S. Choi, K. Storr, M. Zhou, and Z.Q. Mao, *Phys. Rev. B* **2007**, 75, 094413.

Phase separation in the itinerant metamagnetic transition of $\text{Sr}_4\text{Ru}_3\text{O}_{10}$, Z.Q. Mao, M. Zhou, J. Hooper, V. Golub, and C. J. O'Connor, *Phys. Rev. Lett.* **2006**, 96, 077205.

Critical current of the Sr_2RuO_4 - $\text{Sr}_3\text{Ru}_2\text{O}_7$ eutectic system, J. Hooper, M. Zhou, Z.Q. Mao, Y. Liu, R. Perry, and Y. Maeno, *Phys. Rev. B* **2006**, 73, 132510.

Tunneling magnetoresistance studies of $\text{Sr}_3\text{Ru}_2\text{O}_7$, J. Hooper, M. Zhou, Z.Q. Mao, R. Perry, and Y. Maeno, *Phys. Rev. B* **2005**, 72, 134417.

Homestake Ultra-Low Background Counting Facility and Detection of Double-Beta Decay to Excited States

Dongming Mei¹, Christina Keller¹, Yongchen Sun¹, Zhongbao Yin¹, Kevin Lesko², Yuen-dat Chan², Al Smith², Gersende Prior², Robert McTaggart³, Barbara Szczerbinska⁴, Andrew Alton⁵, William M. Roggenthen⁶

1: The University of South Dakota; 2: Lawrence Berkeley National Laboratory; 3. South Dakota State University; 4: Dakota State University; 5: Augustana College; 6: South Dakota School Mines & Technology.

Program Scope

The Homestake Mine in western South Dakota is being considered as a site for a Deep Underground Science and Engineering Laboratory (DUSEL). Many of the physics, geosciences, and geomicrobiology experiments in the facility will be funded by DOE and will benefit the missions of this agency. In support of these programs, physics faculty in South Dakota and scientists at Lawrence Berkeley National Laboratory (LBNL) have been working together to establish a multidisciplinary research cluster to provide baseline characterization for physics and geosciences/geomicrobiology experiments at the Homestake Mine through an Ultra-Low Background Counting Facility, including gamma-ray and radon measurements. The proposed project utilizes two low-background germanium detectors with massive shielding underground to carefully analyze the materials for low background experiments. Those low background experiments, such as $\beta\beta$ decay [1-3], solar neutrino [4], geoneutrino [5], and dark matter [6-7], must control the purity of *all* the materials used in the construction of the detector. In the majority of materials around us, the level of ^{238}U and ^{232}Th is on the order of 0.1 – 1 part per million. For the next generation of low background experiments, the purity of the materials in the detector needs to be at a level five orders of magnitude smaller or 1 – 10 parts per trillion for ^{238}U and ^{232}Th contamination. Measuring such low counting rates is a very challenging task that will be best accomplished by using large (~3.3 kg), high purity germanium (HPGe) detectors, which have recently become commercially available in sufficiently large sizes. Because of their extremely high purity, outstanding energy resolution and high detection efficiency, the low background HPGe detectors can provide the screening measurements with sensitivity at the necessary level at a deep underground laboratory. As applied in the detection of double-beta decay to excited states, our simulations show that with two low background detectors placed face to face, a few isotopes (^{76}Ge , ^{130}Te and ^{82}Se , etc) can be measured with a half life of $\sim 10^{23}$ years. Theoretical estimates of double beta decay to excited states for those isotopes should be around a half life of $\sim 10^{22}$ years. Thus, it is likely this would be the first experiment to detect this decay and to extract experimentally the Nuclear Matrix Element (NME) values for those isotopes. In the worst case scenario, we will set the world's best limit on this process.

Recent Progress

A powerful ultra-low background counting facility for material screening is crucial to the success of many DUSEL underground experiments dealing with extremely rare-occurring processes that are of great scientific importance. In order to reach the ultimate sensitivity (e.g. in dark matter searches and nuclear double beta-decay), only materials with the lowest possible radioactive impurity can be used in fabricating the experimental devices, and the entire experiment must be located in a deep underground site. The US high energy and nuclear physics communities have indicated a strong intention to play a leading role in future neutrino and dark matter experiments as part of the DUSEL program. It is clear that in order to fulfill this exciting mission it is necessary to have an advanced and deep underground ultra-low background facility to support the construction and R&D efforts of the approved and/or proposed projects. The Homestake Mine, home to the first solar neutrino experiment, provides an excellent

opportunity to host DUSEL, as well as the required ultra-low background laboratory facility. Indeed, due to the depth of the mine, this facility may become the world's most advanced low background counting facility and will draw international collaborators interested in low background measurements. The facility can be made self-sufficient after development, with an operating budget which pays for itself out of user fees to a broad community of end-users, which may include among others the public health sector, homeland security, environmental monitoring, geomicrobiology, isotope geology, ancient ^{14}C dating, and semiconductor manufacturers. LBNL is leading DUSEL at Homestake and other DUSEL related physics projects such as double-beta decay, low-energy neutrinos, and dark matter experiments. The facility will also provide a convenient conduit for present and future South Dakota physics faculty to directly support and participate in experiments at Homestake. In addition to low background counting, detectors in this facility can also be used to perform important physics experiments, such as studying the nuclear double-beta decay to excited-state process, a topic which has recently drawn both strong experimental and theoretical interests. Experimentally, it is a great advantage to be able to detect unambiguously the gamma-rays from the de-excitation of the daughter nucleus to its ground state, as proposed in our method. One can also differentiate between the right-handed current and the mass mechanism mode by this measurement, as the former will be enhanced and the latter highly suppressed. The measurement will also allow one to check the validity of the various theoretical models used in performing NME calculations for double beta-decay (e.g. those based on quasi-particle random-phase approximation (QPRA)) which have claimed that the results will depend only weakly on the actual nuclear structural parameters. The outcome of this measurement can also contribute to our knowledge about nuclear structure in this mass region as a whole, and possibly can support and extend the predictive power for some of the theoretical models. In summary, the success of the Early Implementation Plan and a potential Homestake DUSEL, in partnership with LBNL and operated in South Dakota will benefit greatly from such an ultra-low background counting facility. LBNL scientists and South Dakota physicists will build a close working relationship because of this facility.

3. Future Plans

The goals and objectives may be accomplished through the completion of four significant tasks, which are summarized below.

Task 1: Implementation of a Database of the background components inside the Homestake deep underground sites: Characterization of the environmental background components (in particular neutrons, gamma-rays, muons, and radon contamination in the air and in the water) in different levels at the Homestake Mine is an important first step in opening the facility to physics experiments. Existing information will be collected, coordinated, and analyzed. Subsequently, a campaign of new relevant measurements in the different levels will be initiated with the aim of covering missing data, and resolving possible inconsistencies. This is particularly important for the neutron and gamma-ray background components. Different techniques and detectors will be employed and results compared. This will allow development of a consistent database of the relevant background components in different levels. Equipment capable of measuring neutrons and radon will be acquired for preliminary screening at the 300 ft level. A continuous radon measurement will be carried out at the 4850 ft level using silicon photodiode detectors [8].

Task 2: Development of a standard library of background simulation codes: Building on the work done in Task 1, reliable and well-tested Monte Carlo simulation codes will be developed to identify and quantify the components of the background in a variety of experiments and of the typical backgrounds in underground sites. From this, a coherent library of codes will be developed for users of the different laboratory levels, which will be necessary for the design of the underground experiments. This research effort will contribute to an exchange of information and optimize the expertise among the different participants. The simulation codes will also contribute to the interpretation of additional data collected in Task 1. Thus, Task 1 and Task 2 are complementary efforts. In addition to personnel costs, an upgrade of

computing infrastructures will be required for hosting the libraries, implementing a common access to the libraries, and providing a mirroring system for the libraries.

Task 3: Construction of the Homestake Ultra-Low-Background Counting Facilities: This task is the primary goal of this proposal and will significantly strengthen the research infrastructure in South Dakota. This facility will include a development of background rejection techniques, active and passive shielding, veto systems, atmosphere control systems to reduce radon levels, pulse shape discrimination techniques, and low background detectors. The deliverables of this research activity will be a worldwide value and coordinated system of US facilities for ultra-low background measurement applications in rare event physics and in other fields such as environmental physics and geophysics. Figure 1 shows a conceptual design of the ultra-low background facility.

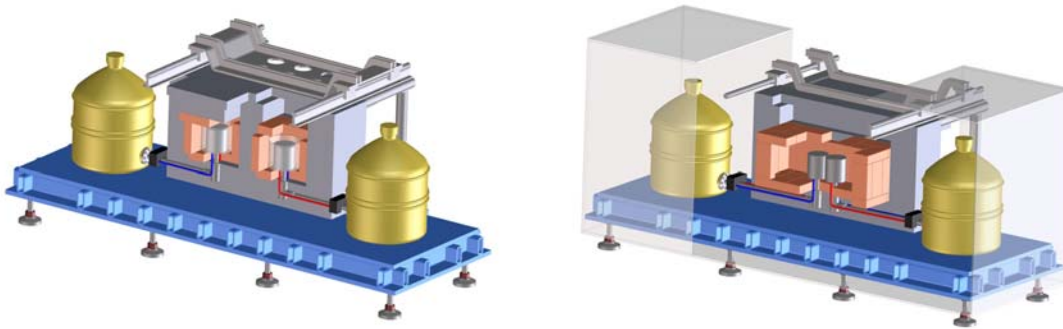


Fig. 1 Conceptual Design of Low-Background Counting Facility. Configuration on the left is used for materials screening. Configuration on the right is used for double-beta decay to excited states experiments.

Task 4: Detection of double beta decay to excited states for several isotopes: The decays of interest include: (1) $^{76}\text{Ge}(\beta\beta 2\nu)^{76}\text{Se}(0_1^+)$; (2) $^{100}\text{Mo}(\beta\beta 2\nu)^{100}\text{Ru}(0_1^+)$; (3) $^{130}\text{Te}(\beta\beta 2\nu)^{130}\text{Xe}(0_1^+)$; and (4) $^{150}\text{Nd}(\beta\beta 2\nu)^{150}\text{Sm}(0_1^+)$. The deliverable of this research activity is a better understanding of double beta decay schemes for various isotopes and a constraint on the uncertainty of the theoretical calculations for nuclear matrix elements for neutrinoless double beta decay.

We will adopt a phased approach to build this Ultra-low Background Counting Facility at Homestake. In Phase I (years 1-3 and funded by this proposal), the planned counting facility will consist of a clean room, γ -rays shield, neutron shield, radon measurement, two low background detectors, and a data acquisition system. The scientific objectives in Phase I are (1) to measure the environmental backgrounds and characterize the experimental site for incoming DUSEL experiments; (2) to screen the materials that will be used for DUSEL low background experiments; (3) to help maintain homeland security by monitoring events potentially associated with nuclear terrorism and nuclear accidents; and (4) to detect double beta decay to excited states for several isotopes. The technical goals in Phase I are (1) to count the contamination of ^{238}U and ^{232}Th in a level of 10^{-12} g/g for various materials and (2) to characterize the materials that will be used for incoming experiments of DUSEL.

If Phase I is funded, the counting facility will be upgraded by building an ultra-pure water pool to further shield muon-induced neutrons from rock, adding two low background detectors to enhance the detection efficiency for counting various isotopes, and adding α/β counters which are essential to the material surface contamination counting for double beta decay and dark matter experiments in Phase II (years 4 –

6). In this phase of the project, the sensitivity will be increased by a factor of at least 10 compared to Phase I.

References:

- [1] Majorana Collaboration, nucl-ex/0311013, 2003.
- [2] Arnaboldi et al., *Astropart. Phys.* 20, 91 2003 .
- [3] EXO Collaboration, <http://ktlesko.lbl.gov/LOI-PA> , 2006
- [4] CLEAN Collaboration, <http://ktlesko.lbl.gov/LOI-PAC> , 2006
- [5] Nikolai Tolich et al., <http://ktlesko.lbl.gov/LOI-PAC>, 2006
- [6] XENON Collaboration, <http://ktlesko.lbl.gov/LOI-PAC> , 2006
- [7] SuperCDMS Collaboration, <http://ktlesko.lbl.gov/LOI-PAC>, 2006
- [8] Gutierrez JL et al., *Applied Radiation and Isotopes*, 2004 Feb-Apr 60 (2-4) :583-587.

DOE Sponsored Publications in 2005 – 2007

1. D.-M. Mei, S. R. Elliott, V. M. Gehman, A. Hime and K. Kazkaz, Neutron Inelastic Scattering Processes as Background for Double-Beta Decay Experiments, Nucl-ex/0704.0306 (2007), accepted for publication in *Phys. Review C*.
2. D.-M. Mei and A. Hime, Muon-induced Background Study for Underground Laboratorie, PRD 73, 053004 (2006).
3. S. R. Elliott, V. M. Gehman, K. Kazkaz, D.-M. Mei and A. R. Young, Pulse shape analysis in segmented detectors as a technique for background reduction in Ge double-beta decay experiments, NIM A 558 (2006) 504.
4. D.S. Akerib (Co-chair), E. Aprile (Co-chair), E.A. Baltz, M.R. Dragowsky, P. Gondolo, R.J. Gaitskell, A. Hime, C.J. Martoff, D.-M. Mei, H. Nelson, B. Sadoulet, R.W. Schnee, A.H. Sonnenschein and L.E. Strigari, Deep Underground Science and Engineering Lab S1 Dark Matter Working Group Report, astro-ph/0605719
5. D.-M. Mei, A. Hime, S.R. Elliott, V.M. Gehman and K.Kazkaz, Depth-Sensitivity Relation (DSR) for Underground Laboratories, Particles and Nuclei, Proceedings of the seventeenth International Conference on Particles and Nuclei, Santa Fe, New Mexico, 23-30 October 2005.

Optoelectronic Properties of Carbon Nanostructures

John W. Mintmire and Thushari Jayasekera

Department of Physics, Oklahoma State University, Stillwater, OK, 74078

Program Scope

Solar energy is our major long-term renewable energy source, and photovoltaic devices are the most direct way of converting solar energy to electricity. The demand for solar energy has grown steadily over the past 20 years with growth rates of 20-25% per year, reaching a production level of 427 MW in 2002. Despite fifty years of research and innovation with concomitant reductions in the price of silicon-based photovoltaic devices, semiconductor photovoltaics still account for a small fraction of total world energy production, in large part because of the high costs of processing silicon-based semiconductor devices. Organic semiconductors represent a less expensive alternative to inorganic semiconductors such as silicon. Conjugated polymers are attractive as alternative semiconductors for photovoltaic cells because they are strong absorbers and can be deposited on flexible substrates at low cost. Photovoltaic devices based on organic, carbon based nanostructures offer the possibility of developing low cost, easily processed thin films of polymeric materials which function as photovoltaic materials. Such devices can be competitive with other sources of energy if power efficiencies of the order of 10% can be obtained.

One major approach for efficient polymeric photovoltaic cells lies in the use of bulk heterojunctions, which mix two different organic polymeric materials which act as donor and acceptor semiconductors. In these bulk heterojunctions the donor polymer typically acts as the light absorber, creating an electron-hole pair and then donating the excited electron to the acceptor polymer. A deep theoretical understanding of the physical processes at work in these materials will require a knowledge of the electron states near the Fermi level for both the donor and acceptor. Our DOE EPSCoR research program will use first-principles electronic structure methods to study the electronic properties of these materials.

Materials with extended, delocalized π -electron systems, such as carbon nanotubes and conjugated polymers, are of particular interest for solar photochemistry applications. Organic photovoltaic devices based on blends of single-walled carbon nanotubes (SWNTs) and soluble poly(3-octylthiophene) (P3OT) have been reported with open circuit voltages of 0.7-0.9 V. (1-4) One of the most critical problems of photovoltaics is improvement of the photoinduced charge separation, which is frequently limited in polymer optoelectronic materials because of the low exciton diffusion length. It was proposed that the photovoltaic response of these devices was based on the introduction of internal polymer/nanotube junctions, which in turn allowed enhanced charge separation in the composite as a result of photoinduced charge transfer from the P3OT to the SWNT with good transport properties.

This project is part of our research group's long-range research program in the electronic and structural properties of low-dimensional materials. The aim of our current DOE EPSCoR program is to use forefront computational tools to study the electronic structures of potential photovoltaic polymers and carbon nanotube structures, with the goal of providing characteristic data for these materials that will be of use to experimentalists and other theorists in developing better bulk heterojunction photovoltaic devices. Our specific goals for this project include carrying out first-principles simulations for a range of conjugated polymer donor systems and carbon nanotube acceptor systems, investigating possible low band-gap donor systems, and using results from our first-principles band structure simulations as input to calculations of the electron and hole transport properties in nanostructured materials. This work will be carried out in collaboration with the Computational Chemical Sciences (CCS) Group at Oak Ridge National Laboratory, which has active programs in computational studies of nanoscale materials.

Recent Progress

We have carried out studies of low-dimensional structures such as polymers and SWNTs using all-electron first-principles methods, taking advantage of the helical symmetry of these structures. Recent reports by Kymakis, et al. (1-4) suggest that mixtures of single-walled carbon nanotubes and P3OT represent an alternative class of organic semiconducting materials that can be used to manufacture organic photovoltaic cells with improved performance. We have used poly(3-methylthiophene) (P3MT) as a model system for P3OT and the other polyalkylthiophenes. We have calculated the electronic band structure of several SWNTs and P3MT using the first-principles, all electron self-consistent density functional method described above. Figure 1 depicts a comparison of the calculated band structures for P3MT, a semiconducting (17,1) SWNT, and a (10,10) armchair metallic SWNT. Both of the SWNTs have diameters of roughly 1.4 nm, and the (17,1) SWNT has a calculated band gap of roughly 0.7 eV. If we assume minimal

electron-hole pair binding in the polythiophene, then an exciton on the polythiophene backbone could dissociate and transfer an electron to multiple “subbands” in the (17,1) SWNT.

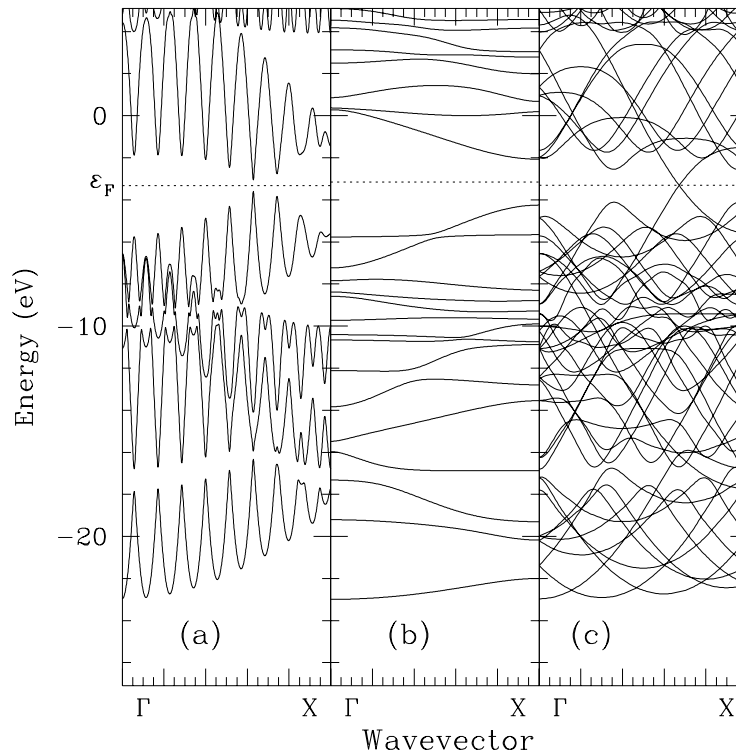


FIG. 1 First-principles valence band structures of (a) (17,1) semiconducting SWNT (b) P3MT (with dihedral angle of 147.5°), and (c) (10,10) armchair metallic SWNT.

If SWNTs are used as acceptor polymers in bulk heterojunction photovoltaic materials, then understanding their electron (and to some extent hole) transport properties is important in understanding their optoelectronic properties in photovoltaic devices. The effective mass is a quantity directly related to charge transport properties. Using what is commonly denoted as the graphene sheet model for SWNTs, we can derive a linear relation between carrier effective mass, m^* , and distance in energy from the Fermi level of the form

$$m^* = \frac{4}{3} \frac{\hbar^2}{a^2 V_{pp\pi}} \left(\frac{\epsilon_m}{V_{pp\pi}} \right). \quad (1)$$

We have numerically calculated the effective mass of charge carriers in SWNTs using our first-principles band structure results and compared these with the predictions of the graphene sheet model. Our results also agree with semiclassical results (5; 6) as well as with other first-principles results. (7) Figure 2 shows the effective mass of charge carriers calculated for several SWNTs based on our first-principles results. The effective mass of larger diameter SWNTs shows rough agreement with the graphene sheet model as expected. Also, the effective mass of holes and electrons related by particle-hole symmetry are similar in magnitude in the SWNTs.

We are also working on calculating overall transport properties of nanostructured materials with potential application in photovoltaics and other devices. We can apply nonequilibrium Green’s function techniques for the system in conjunction with results from our first-principles electronic structure calculations to calculate the current through the system using the Landauer formalism. (8) As a preliminary project using this approach, and also to participate in the emerging research area of graphene nanoribbon systems, (9; 10) we have studied electron transmission through multi-terminal graphene nanoribbon junctions.

We calculated the effect of several different lattice vacancies on the electron transmission in a T-shaped nanoribbon device (Figure 3) and compared these results with similar calculations for a bare zigzag nanoribbon, as depicted in Figure 4. A single lattice vacancy creates conductance dips in the low energy region, because of the quasibound states around the vacancy site. The energy of the bound state is related to the position of the lattice vacancy relative to the edge of the device, and can be explained in terms of the alternate atomic structure of the graphene lattice.

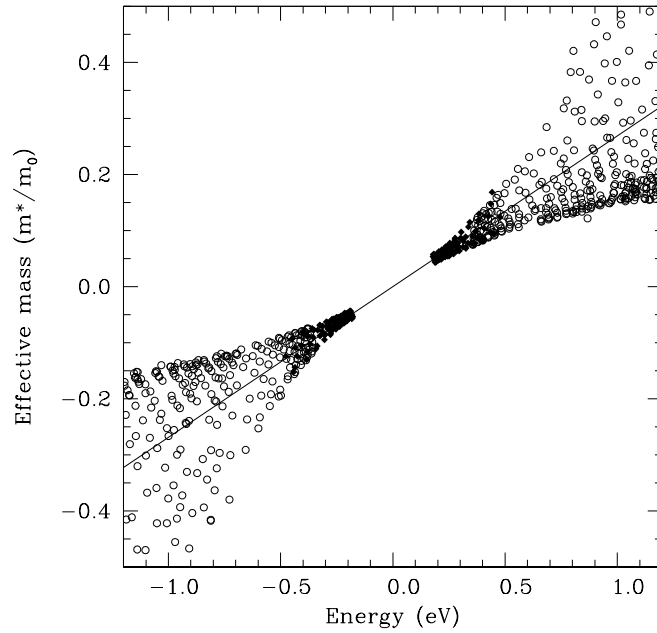


FIG. 2 Calculated effective masses of electron (positive values) and hole (negative values) carriers for several SWNTs at van Hove singularities near the Fermi level. Solid diamonds denote results for band extrema nearest the Fermi level, and open circles denote masses for further extrema. The solid line shows the effective mass of charge carriers in these SWNTs as calculated from the graphene sheet model (Eq. 1) using $V_{pp\pi} = -2.7$ eV.

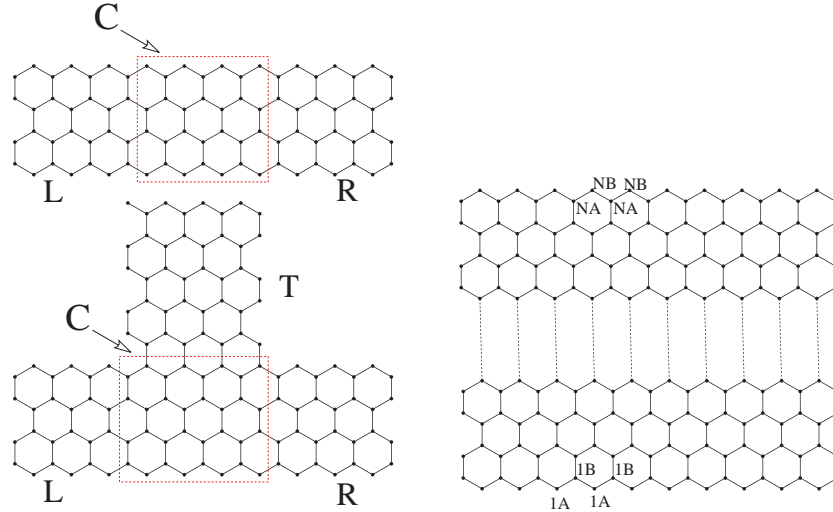


FIG. 3 Left panel shows the lattice configuration of a bare zigzag nanoribbon (up) and a nano-graphene T-junction device (down). Central region (boxed) is the conductor region, C which is attached to two leads (L and R) in the bare zigzag nanoribbon and three leads, (L, T, and R) in the T-junction device. Right panel shows the alternate A(B) lattice structure of the conductor region. The conductor region is made of N dimer lines. A zigzag nanoribbon with N dimer lines is terminated with 1A-type atoms and NB-type atoms.

Future Plans

We are also interested in the transport and other electronic properties of multiwalled carbon nanotube systems, and have begun some preliminary work on model double-wall carbon nanotube (DWNT) systems. Several electronic structure calculations have been reported on DWNTs constructed from coaxial combinations of armchair SWNTs. However, calculations on combinations of chiral SWNTs are computationally impractical using standard translational

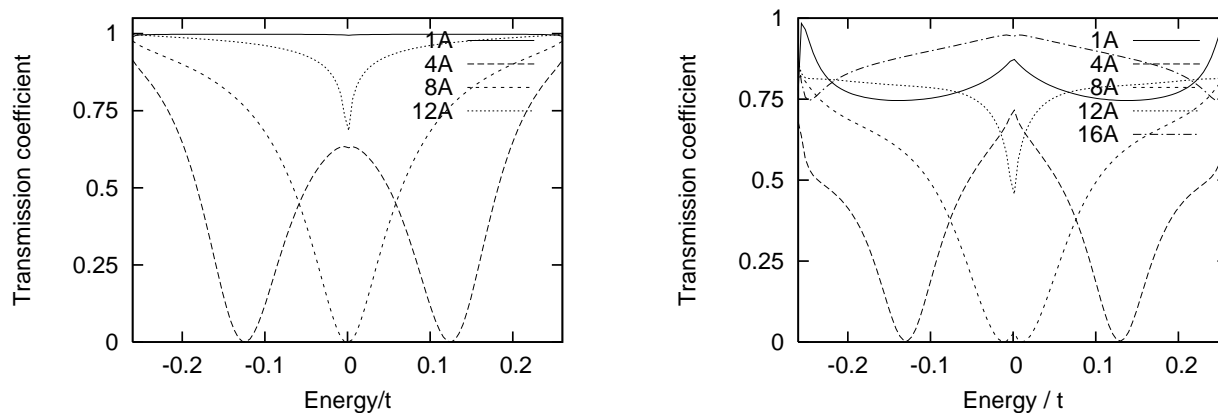


FIG. 4 Left panel shows the transmission coefficients of electrons in a bare zigzag nanoribbon with 16 dimer lines in the presence of single lattice vacancies. Right panel shows the transmission coefficients of electrons towards lead R in a T-shaped nano graphene device in the presence of single lattice vacancies. The zigzag-type leads are made of 16 dimer lines and the armchair type lead is made of 14 dimer lines. Electrons are injected from zigzag-type lead L.

band structure codes because of the large unit cell sizes required. The use of helical symmetry reduces the size of the unit cell overcoming the difficulty of calculating the electronic properties of chiral DWNTs. We have begun preliminary studies of the cohesive energies of chiral DWNTs. We plan to continue this work by calculating transport properties of DWNTs in collaboration with Vincent Meunier at ORNL. Other work will be carried out in collaboration with the ORNL group on transport properties of electroactive polymers with backbone dihedral angle disorder.

References

- [1] Kymakis E, Alexandrou I and Amaratunga G A J, 2002 *Synth Met* **127** 59.
- [2] Kymakis E and Amaratunga G A J, 2002 *Appl Phys Lett* **80** 112.
- [3] Kymakis E, Alexandrou I and Amaratunga G A J, *J Appl Phys* 2003, 93, 1764.
- [4] Kymakis E AND Amaratunga G A J, *Synth Met* 2003, 142, 161.
- [5] Pennington G. and Goldsman N, 2003 *Phys Rev B* **68** 45426.
- [6] Pennington G and Goldsman N, 2005 *Phys Rev B* **71** 205318.
- [7] Zhao G L, Bagayoko D and Yang L, 2004 *Phys Rev B* **69** 245416.
- [8] Datta S, *Electronic Transport Properties of Mesoscopic Systems* (Cambridge University Press, Cambridge, England, 1995).
- [9] Berger C, Song Z M, Li X B, Wu X S, Brown N, Naud C, Mayo D, Li T B, Hass J, Marchenkov A N, Conard E H, First P N, deHeer W A, 2006 *Science* **312** 1191
- [10] Wakabayashi K, 2001 *J Phys Soc Japan* **71** 2500.

DOE sponsored publications in 2007

- “First-Principles Properties of Organic Photovoltaic Materials”, T. Jayasekera, M. S. Monigold, S. L. Elizondo, and J. W. Mintmire, *Int. J. Quantum Chem.* 2007, in press
- “Effect of Single Lattice Vacancies on Transport in Multiterminal Graphene Nanodevices”, T. Jayasekera and J. W. Mintmire, *Int. J. Quantum Chem.* 2007, in press.

**Surface Anchoring of Nematic Phase on Carbon Nanotubes:
Nanostructure of Ultra-High Temperature Materials**

PI: Dr. Amod A. Ogale

Professor, Chemical Engineering, and

Dy. Director, Center for Advanced Engineering Fibers and Films

ogale@clmson.edu

Associated Students: Rebecca Alway-Cooper, Marlon Morales, Daniel Sweeney

Program Scope

Nuclear energy is a dependable source of electricity for the US because of the large size of the plants and their continuous periods of operation [1]. However, only 20% of electricity produced in the US is from nuclear source, whereas France produces almost 70%. Nuclear power also has the second-lowest production cost of the major sources of electricity (1.7 cents/kWh) in comparison to that of hydro (0.5 cents/kWh), coal (1.9 cents/kWh), natural gas (5.87 cents/kWh), and petroleum (5.39 cents/kWh) (1). Because fuel supply sources are available domestically, nuclear energy can be a strong domestic industry that can reduce dependence on foreign energy sources.

All commercial nuclear power plants have extensive security measures to protect the facility from intruders (1). However, additional research efforts are needed to increase the process safety of nuclear energy plants to protect the public in the event of a reactor malfunction. It has been envisioned that the next generation nuclear plant (NGNP) will consist of a helium-cooled nuclear reactor that will operate in the range 650-1000°C [2]. One of the most important safety design requirements for this reactor is that it must be inherently safe, i.e., the reactor must shut down safely in the event that the coolant flow is interrupted [2]. This next-generation *Gen IV* reactor must operate in an inherently safe mode such that the off-normal temperature may reach 1500°C due to coolant-flow interruption. Metallic alloys used currently in reactor internals (e.g., control-rods) will melt at such temperatures.

Structural materials that can resist such ultra-high temperatures are carbon fibers and carbon-matrix composites because they do not melt; however, radiation-damage effects on carbon fibers are poorly understood. This research is directed toward the fundamental understanding of the mechanisms of surface anchoring of the liquid crystalline precursors and the resulting “pinning” of the graphene layers by carbon nanotubes that could lead to neutron-damage resistance of the resulting carbon fibers. The goal of the proposed research is to generate novel carbonaceous nanostructures for radiation-stability in ultra-high temperature materials. The nanostructures are expected to generate high crystallinity, but not anisotropy, so that dimensional changes do not result in distortion.

Recent Progress

Among high performance materials, the graphitic form of carbon is known to possess the highest thermal resistance in a non-oxidizing environment. Graphite does not have a measurable melting point; it is known to sublime at about 3600°C [3]. Although graphite

has been used in nuclear environment for almost 50 years by DOE, DoD, and NASA, unfortunately, polygranular graphite is not suitable for structural applications because they do not possess adequate strength, stiffness or toughness that is required of structural components such as reaction control-rods, upper plenum shroud, and lower core-support plate [2,4]. For structural purposes, composites consisting of strong carbon fibers embedded in a carbon matrix are needed. Such carbon/carbon (C/C) composites have been used in aerospace industry to produce missile nose cones, space shuttle leading edge, and aircraft brake-pads [5]. However, radiation-tolerance of such materials is not adequately known because only limited radiation studies have been performed on C/C composites, which suggest that pitch-based carbon fibers have better dimensional stability than that of polyacrylonitrile (PAN) based fibers [6]. The thermodynamically-stable state of graphitic crystalline packing of carbon atoms derived from mesophase pitch (rather than PAN) leads to a greater stability during neutron irradiation. The severe axial orientation of graphene layers obtained from mesophase pitch precursors results in highly directional properties such as unusually high axial tensile modulus and axial thermal conductivity. However, the compressive strength of such fibers is an order of magnitude lower than its tensile strength, due to the severe anisotropy. In recent studies, cosponsored by NSF-funded project, we incorporated carbon multiwall nanotubes (MWNT) into mesophase pitch in a very dilute concentration of up to 0.3 wt% [7]. Carbon fibers derived from pure mesophase pitch displayed a highly anisotropic structure. In contrast, as displayed the presence of 0.1 wt% and 0.3 wt% nanotubes in the mesophase pitch led to a texture that was increasingly isotropic (random) in the plane. We emphasize that our research strategy calls for the addition of these nanotubes in a very dilute concentration, only about 0.3 wt%. Therefore, the materials are not cost-prohibitive. Carbonaceous nanostructures provide ultimate thermal conductivity and are also of interest to Air Force in thermal management.

Our recent data of MWNT-modified carbon fibers indicates that the compressive strength of the nanotube-reinforced fibers is at least equivalent or slightly improved, as compared with pure mesophase-based carbon fibers [8]. Moreover, it is noteworthy that the ratios of recoil compressive strengths to tensile strength of nanostructured fibers are much higher (the difference is at least 10% or higher) than those for the commercial counterparts and even than those for PAN-based commercial carbon fibers. This suggests that nanotubes are helping to reduce anisotropy in carbon fibers, which has typically resulted in very high tensile strength but very poor compressive strength.

Future Plans

This DOE-EPSCoR project, which was recently initiated in May 2007, has started to investigate the novel nanostructures that are being synthesized in carbon fibers using transmission electron microscopy (TEM) and atomic force microscopy (AFM) at Clemson University. Thermal conductivity measurements on single filaments will be performed at South Carolina State University.

Mechanisms of neutron-damage for such ultra-high temperature materials will be investigated in collaboration with Lab researchers at ORNL. Collaboration has been

planned with ORNL researchers from the Carbon Materials group headed by Dr. Tim Burchell. The irradiation studies will be done by ORNL collaborators using the High Flux Isotope Reactor (HFIR) to address their primary objective of determining radiation damage tolerance. It is planned that all of the irradiation studies will be conducted by ORNL collaborators using standard procedures developed from their extensive research expertise in radiation-damage in nuclear graphites. Rabbit irradiation capsules and an irradiation temperature of 600°C will be targeted, allowing comparison with prior data for carbon-carbon composites. The target irradiation dose will be 2-4 displacements per atom (dpa), which corresponds to 2-4 cycles in the HFIR. Post irradiation examination (PIE) of the samples will indicate the extent to which structural manipulation has influenced the neutron irradiation stability.

References

- [1] www.nei.org website for Nuclear Energy Institute, Washington, D.C. 20006-3708
- [2] W. R. Corwin, *Advanced Reactor, Fuel Cycle, and Energy Products Workshop for Universities*, Workshop for Universities, Gaithersburg, MD, June 16-17, 2005
- [3] J. P. Scahffer, A. Saxena, S. Antolovich, T. H. Sanders, and S. B. Warner, *The Science and Design of Engineering Materials*, 2nd Ed., WCB-McGraw Hill, Boston, 1999
- [4] T. D. Burchell, , MRS Bulletin, 22(4), 29-35 (1997)
- [5] J. D. Buckley and D. D. Edie, *Carbon-Carbon Materials and Composites*, NASA Reference Publication 1254, 1992.
- [6] T. D. Burchell, W. P. Eatherly, J. M. Robbins and J. P. Strizak, J. Nuclear Materials, 191-194, 295-299 (1992)
- [7] A. A. Ogale*, D. D. Edie, and A. Rao, US Patent 7,153,452, issued Dec 2006
- [8] Y.S. Lee, A. A. Ogale, Young Rack Ahn, Chang Hun Yun, Chong Rae Park, *Fibers and Polymers*, 7(10), 85-87, 2006.

DOE-Sponsored Publications

None from the current project as it was initiated only recently in May 2007

Preparation and Study of Novel Ru Dyes for Dye Sensitized Solar Cells (DSSCs)

Joshua J. Pak, Dominic X. Denty, Stephanie Pritchard, Lisa Lau, Anna Hoskins, Alan W. Hunt and Rene G. Rodriguez

pakjosh@isu.edu, rodrrene@isu.edu, huntalan@isu.edu

Department of Chemistry, Idaho State University, Pocatello, ID 83209-8023

Program Scope

The steady development of new and improved organic and inorganic semiconductors is rapidly reaching the point where they will soon become part of the next generation of optoelectronic devices, especially for thin film solar cell applications. Since Grätzel's initial discovery of solar photovoltaics based on semiconductor nanocrystals sensitized by light-harvesting dyes,¹ there have been rapid increases in the analysis and manufacture of progressively more efficient DSSCs. A current research trend suggests that these DSSC devices may present cost effective alternatives to purely inorganic systems in the near future.² The most efficient DSSC thus far reported in the literature was constructed with a highly porous anatase TiO₂ semiconducting film, deposited onto a transparent conducting glass anode, sensitized by Ru(II)(4,4'-dicarboxy-2,2'-bipyridine)₂(NCS)₂ (also known as N₃ dye), an acetonitrile electrolyte solution of I⁻/I₃⁻, and a Pt counter-electrode. The photocurrent measured at 100 mW/cm² of simulated solar intensity (AM 1.5) was about 10 mA/cm² with an open circuit voltage near 0.7 V. The overall efficiency of the cell was about 10%, and under defused daylight conditions it yielded around 12% efficiency.

Although a large number of organic and organometallic dyes have been used as sensitizers, a wide variation of quantum yields have been reported. Of these, ruthenium polypyridyl dyes appear to be the most promising, with nearly 100% of the absorbed photons converted to conduction band electrons. According to Benkő *et al.*, injection of an electron from the excited state in the dye into the semiconductor occurs 70% of the time from the ¹MLCT state on a femtosecond time scale, while 30% of the injection comes from the ³MLCT state on a picosecond time scale.³ It should therefore be possible to alter the rate of intersystem crossings by varying the nature of the ligands which, in turn, will change the relative energies of the two states and/or change the nature of the vibrational structure of these systems. If the conduction band of TiO₂ is sufficiently lower in energy than the excited state of the dye, the rate of electron injection is faster than the photonic decay of the dye excited state, allowing more efficient operation of the DSSC.

Recent Progress

A series of DSSCs have been constructed at Idaho State University, employing both synthetic and natural dyes. The best solar cell constructed at ISU to date was a 2 cm² cell employing N₃ dye. It had an overall conversion efficiency of greater than 8% using a 50 W halogen spotlight to simulate the solar spectrum.² The open circuit voltages, short circuit currents, and fill factor values are competitive with those reported in the literature.² This group has also constructed the highest efficiency solar cell based on a fruit dye. A 2 cm² dye cell employing dye extracted from the skin of the mangosteen fruit, native to Malaysia and other

Asian countries, had an overall conversion efficiency of ~ 2%. We are currently preparing a manuscript containing the above results for a publication.³

Most of the Ru dyes studied so far are simple Ru(II) complexes namely, N_3 and $Ru(dcbpy)_3^{2+}$ systems. From our studies, we discovered that when the electronic structure of a ligand in $Ru(bpy)_3L^{2+}$ system was varied, there were significant changes in the relationship between 1MLCT and 3MLCT , and therefore between the carrier lifetimes. For example, when L was varied from simple 2,2'-bipyridine to 4,4'-di(phenylethynyl)-2,2'-bipyridine, we observed an increase of 3MLCT lifetime from 719 ns to almost 2275 ns.⁴

Future Plans

Although we have learned a considerable amount from previous studies, it is necessary for us to systematically examine the dyes. As a series of novel ligands and their respective Ru complexes are being synthesized, and respective DSSCs will be constructed to test their optoelectric behaviors. To our best knowledge, there has not been a thorough investigation into the differences in the energy levels of 1MLCT and/or 3MLCT of the dye sensitizers, the energy levels of the TiO_2 conducting band, and the energies associated with the redox couple. We are conducting a systematic investigation involving; 1) factors affecting the electron energy levels, lifetimes and injection efficiencies based on dye structures and properties, 2) electron collection from the dye and their transport to the conducting electrode through TiO_2 layer, and 3) electron conduction to regenerate the dye sensitizer via redox couple. Knowledge from these investigations will provide a better understanding of energetic requirements for organic dyes, nanocrystalline anodes, and their interfaces. This, in turn, will ultimately aid in improved device design, construction, and efficiency of DSSCs.

References

1. "A low-cost, high-efficiency solar cell based on dye-sensitized colloidal titanium dioxide films." B. O'Regan, M. Grätzel, *Nature* **1991**, 335, 737.
2. "Solar Energy Conversion by Dye-Sensitized Photovoltaic Cells." M. Grätzel, *Inorg. Chem.* **2005**, 44, 6841.
3. "Comparison of the Conversion Efficiency in Dye Sensitized Solar Cells made from Mangosteen Fruit and Mangostin." Lisa D. Lau, Ebner Manuel, Anna Hoskins, R. Rodriguez, and A. Hunt In preparation.
4. "Modulating Excited-State Lifetimes in $[Ru(II)(bpy)_2L]^{2+}$ Systems." J. T. Bateman, T. Baker, A. C. Colson, D. P. Stay, M. Herring, R. G. Rodriguez, J. J. Pak *Lett. Org. Chem.* Submitted.

DOE Sponsored Publication in 2005-2007

1. "Modulating Excited-State Lifetimes in $[Ru(II)(bpy)_2L]^{2+}$ Systems." J. T. Bateman, T. Baker, A. C. Colson, D. P. Stay, M. Herring, R. G. Rodriguez, J. J. Pak *Org. Lett.* Submitted.
2. "Rapid and Size Control Synthesis of $CuInS_2$ Nanoparticles via Microwave Irradiation." Gardner, Joseph S.; Shurdha, Endrit; Lau, Lisa D.; Wang, Chongmin; Rodriguez, Rene G.; Pak, Joshua J. *J. Nanoparticle Research*, Submitted.
3. "Pulsed-Spray Radiofrequency PECVD of $CuInS_2$ Thin Films." Rodriguez, Rene G.; Pulsipher, Daniel J. V.; Lau, Lisa D.; Shurdha, Endrit; Pak, Joshua J.; Jin, Michael H.;

4. "Facile synthesis of 4,4',5,5'-tetraiododibenzo-24-crown-8 and its highly conjugated derivatives." Endrit Shurdha, Jaime L. Mayo, and Joshua J. Pak, *Tetrahedron Letters* **2006**, *47*, 233-237.
5. "Microwave-assisted preparation of Chalcopyrite nanoparticles from molecular single source precursors." Endrit Shurdha, Joseph Gardner and Joshua J. Pak, 2006, Patent Pending (No. 4005).

Preparation and Study of I-III-VI₂ Nanoparticles and Thin Films

Joshua J. Pak, Joseph Gardner, Endrit Shurdha, Ian Kihara, Lisa Lau, Anna Hoskins, Alan W. Hunt and Rene G. Rodriguez
pakjosh@isu.edu, rodrene@isu.edu, huntalan@isu.edu
Department of Chemistry, Idaho State University, Pocatello, ID 83209-8023

Program Scope

Ternary I-III-VI₂ nano-materials, particularly of Chalcopyrite CuIn_xGa_{1-x}Se(S)₂, are important components of next-generation PV devices. It has been proposed that inclusion of nanocrystalline semi-conductors such as Chalcopyrite in PV devices can dramatically improve the efficiency of photon conversion (quantum dot solar cell)¹ enable low-cost deposition of thin films,² and provide sites for exciton dissociation³ and pathways for electron transport.⁴ Chalcopyrite nano-materials are more resistant to degradation from electron, proton, and alpha particle radiation than the corresponding bulk materials, a requirement for space based solar cells.⁵⁻⁷

Recent Progress

Using microwave irradiation, the preparation of Chalcopyrite nanoparticles from single source precursors (SSP) has been accomplished.⁸ Particularly, colloidal Chalcopyrite (CuInS₂) nanocrystals have been produced by microwave-assisted decomposition of the single-source molecular precursors (PR₃)₂CuIn(SEt)₄ (R = Ph, alkyl) in the presence of alkylthiol ligands in dioctyl phthalate as a solvent. We observed nanoparticle formation temperature as low as 115 °C at 5 minute microwave irradiation. Using this technology, we are able to prepare Chalcopyrite nanoparticles at dramatically lower reaction temperatures and shorter reaction time over the conventional thermolysis techniques. In addition, we have achieved better control over nanoparticle size by controlling the reaction temperatures, times, and ligand concentrations. The resulting nanoparticles exhibit expected properties such as room-temperature fluorescence.

Future Plans

Currently, we are examining several aspects of CuInS₂ and its related materials. First, we are interested in preparing thin films and nanoparticles containing varying ratio of In/Ga/Al. Incorporation of varying amount of Ga and/or Al into ternary system such as CuInS₂ is not only important in terms of controlling the energy levels (bandgaps) of resulting materials but also presents unique synthetic challenges for preparing and respective molecular SSPs. Second, we have prepared fluorinated SSPs in order to dissolve SSPs in super critical CO₂ from which we will prepare nanoparticles, thin films, and their composite materials.⁹

References

1. Luque and A. Martí, *Phys. Rev. Lett.*, 78, 5014 (1997).
2. C. Eberspacher, K.L Pauls, C. V. Fredric, 29th *IEEE Proceedings*.

3. U. W. Huynh, X. Peng, A. P. Alivisatos, *Adv. Mater.*, 11, 923 (1999); W. U. Huynh, J. J. Dittmer, A. P. Alivisatos, *Science*, 295, 2425 (2002).
4. M. Grätzel, *Prog. Photovoltaics*, 8, 171 (2000).
5. S. Marcinkevičius, R. Leon, B. Čechvičius, J. Siegert, C. Lobo, B. Magness, W. Taylor, *Physica B*, 314, 203 (2002).
6. R. J. Walters, G. P. Summers, S. R. Messenger, A. Freundlich, C. Monier, F. Newman, *Prog. Photovolt*, 8, 349 (2000).
7. N. A. Sobolev, A. Cavaco, M. C. Carmo, M. Grundmann, F. Heinrichsdorff, D. Bimberg, *Phys. Stat. Sol B*, 224, 93 – 96 (2004).
8. J. S. Gardner, E. Shurdha, C. Wang, L. D. Lau, R. G. Rodriguez, J. J. Pak, *J. Nanoparticle Research*, (Submitted 2007).
9. M. Nanu, J. Schoonman, A. Goossens, *Adv. Funct. Mater.*, 15, 95 (2005).

DOE Sponsored Publication in 2005-2007

1. “Modulating Excited-State Lifetimes in [Ru(II)(bpy)₂L]²⁺ Systems.” J. T. Bateman, T. Baker, A. C. Colson, D. P. Stay, M. Herring, R. G. Rodriguez, J. J. Pak *Org. Lett.* Submitted.
2. “Rapid and Size Control Synthesis of CuInS₂ Nanoparticles via Microwave Irradiation.” Gardner, Joseph S.; Shurdha, Endrit; Lau, Lisa D.; Wang, Chongmin; Rodriguez, Rene G.; Pak, Joshua J. *J. Nanoparticle Research*, Submitted.
3. “Pulsed-Spray Radiofrequency PECVD of CuInS₂ Thin Films.” Rodriguez, Rene G.; Pulsipher, Daniel J. V.; Lau, Lisa D.; Shurdha, Endrit; Pak, Joshua J.; Jin, Michael H.; Banger, Kublinder K.; Hepp, Aloysius F. *Plasma Chemistry and Plasma Processing* **2006**, 26(2), 137-148.
4. “Facile synthesis of 4,4',5,5'-tetraiododibenzo-24-crown-8 and its highly conjugated derivatives.” Endrit Shurdha, Jaime L. Mayo, and Joshua J. Pak, *Tetrahedron Letters* **2006**, 47, 233-237.
5. “Microwave-assisted preparation of Chalcopyrite nanoparticles from molecular single source precursors.” Endrit Shurdha, Joseph Gardner and Joshua J. Pak, 2006, Patent Pending (No. 4005).

Impact of atmospheric aerosols on nocturnal boundary layer temperatures

Falguni Patadia, U. S. Nair, R. T. McNider (PI), S. A. Christopher, K. A. Fuller, R. M. Welch, D. A. Bowdle, M. Newchurch

Program Scope

Analysis of surface temperature observations shows decreasing diurnal temperature range (DTR) accompanied by an increase in minimum temperature^{1,2} (Karl et al., 1993; Vose et al., 2005). It has been suggested that enhanced downwelling longwave radiation, forced by increasing atmospheric concentration of green house gases, is mostly responsible for these observed changes. However other processes such as changes in cloud cover, land use and atmospheric aerosol loading may also be important. Even though several studies have focused on the shortwave aerosol forcing, very few address the longwave aerosol forcing and its impact on the nocturnal boundary layer which may be important for explaining the observed trends in DTR. Processes that lead to diurnal asymmetries in aerosol optical depth, including hygroscopic growth of aerosols, variations in vertical distribution and emissions rates all impact nocturnal boundary layer temperature. Numerical modeling and observational studies are required to understand how these processes impact boundary layer temperature.

Recent progress

A modeling system for studying the impact of aerosols on nocturnal boundary layer was developed. Thus modeling system consists of the Regional Atmospheric Modeling System (RAMS) coupled with the Fu-Liou radiative transfer scheme and an improved aerosol optical model is utilized to quantify nocturnal aerosol longwave radiative forcing. The OPAC³ package is used to parameterize the aerosol characteristics and the hygroscopic growth of aerosols and also its vertical distribution. The OPAC defines several different categories of aerosol types of which the continental clean, continental average, continental polluted and urban polluted categories are utilized in the simulations. OPAC aerosol model was modified to include improved observations of optical properties of sulfate aerosols and size distributions.

The modified RAMS modeling system is used for examining the impact of atmospheric aerosols on nocturnal boundary layer temperatures. Data collected during the CASES99 field experiment was used to initialize and validate numerical modeling simulations used in this study. For aerosol loading characteristic of urban conditions, numerical modeling simulations show enhancement of nocturnal downwelling longwave radiation in excess of 2.5Wm^{-2} . During the first night of the simulation, nocturnal minimum increases in excess of 0.25K corresponding to this increase in downwelling longwave radiation. However, during day, aerosol loading causes a decrease in the maximum temperature of about 2K. The increase in nocturnal minimum during the second night is significantly smaller, on the order of 0.09K. Note that the study addresses the impact of aerosol longwave radiative forcing only under observed wind conditions. Prior studies^{4,5} show that under favorable wind regimes, the magnitudes of aerosol longwave forcing estimated from the modeling experiments can lead to significant increases in surface temperature.

Future Plans

Future plans for this project include the conduct of a short field project to observationally quantify aerosol longwave radiative forcing and its impact on nocturnal boundary layer development. Numerical modeling studies are being extended to include other processes that create diurnal asymmetries in aerosol depths.

References

- (1) Karl, Thomas R., Phillip D. Jones, Richard W. Knight, George Kukla, Neil Plummer, Vyacheslav Razuvayev, Kevin P. Gallo, Janette Lindsey, Robert J. Charlson, and Thomas C. Peterson, 1993: A new perspective on recent global warming: asymmetric trends of daily maximum and minimum temperature. *Am. Meteor. Soc.*, 74, 1007- 1023.
- (2) Vose, R. S., D. R. Easterling, and B. Gleason (2005), Maximum and minimum temperature trends for the globe: An update through 2004, *Geophys. Res. Lett.*, 32, L23822, doi:10.1029/2005GL024379.
- (3) M. Hess, P. Koepke, and I. Schult (1998): Optical Properties of Aerosols and clouds: The software package OPAC, *Bull. Am. Met. Soc.*, 79, 831-844.
- (4) Walters, J. T., R. T. McNider, X. Shi, W. B. Norris, and J. R. Christy (2007), Positive surface temperature feedback in the stable nocturnal boundary layer, *Geophys. Res. Lett.*, 34, L12709, doi:10.1029/2007GL029505.
- (5) Shi, X., R. T. McNider, D. E. England, M. J. Friedman, W. Lapenta, and W. B. Norris (2005), On the behavior of the stable boundary layer and role of initial conditions, *Pure Appl. Geophys.*, 162, 1811–1829.

DOE Sponsored publications in 2006-2007

Walters, J. T., R. T. McNider, X. Shi, W. B. Norris, and J. R. Christy (2007), Positive surface temperature feedback in the stable nocturnal boundary layer, *Geophys. Res. Lett.*, 34, L12709, doi:10.1029/2007GL029505.

Thermochemical Conversion of Woody Biomass to Fuels and Chemicals

Hemant P. Pendse,¹ M. Clayton Wheeler,¹ William J. DeSisto,^{1,3} Brian G. Frederick,^{2,3} and Adriaan van Heiningen¹

hpendse@umche.maine.edu, cwheeler@umche.maine.edu, wdesisto@umche.maine.edu,
brian.frederick@umit.maine.edu, avanheiningen@umche.maine.edu

Chemical and Biological Engineering,¹ Chemistry,² and Laboratory for Surface Science and Technology,³ University of Maine, Orono, Maine 04469

Our newly established DoE EPSCoR research cluster is implementing new catalyst R&D infrastructure and addressing fundamental science and engineering pathways for *thermochemical conversion* of woody biomass to fuels and chemicals, an area of increasing importance to Maine's forest products industry. The technical focus is on thermal upgrading of biomass (yellow paths illustrated in Figure 1) through syngas and pyrolysis oils. Major roadblocks in thermally upgrading pyrolysis oil, a complex highly-oxygenated liquid, include improving the heating value through catalytic oxygen removal, identifying favorable reaction pathways, and developing production methods for optimum upgrading. Roadblocks for syngas conversion include shifting and narrowing the product distribution, tar removal or developing tar-tolerant catalysts, and integrating new technologies with existing facilities in Maine.

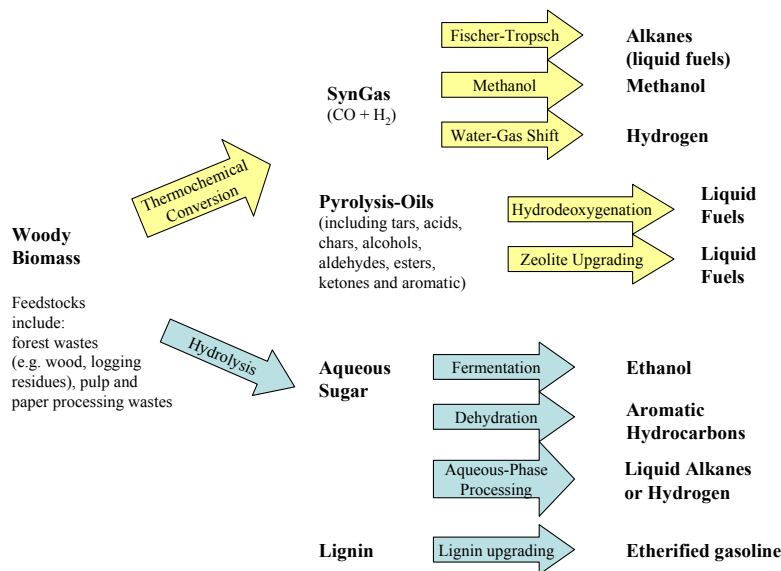


Figure 1. Pathways for production of fuels and chemicals from biomass

Our *multi-disciplinary, multi-institutional* research cluster is part of a larger Forest Bioproducts Research Initiative at the University of Maine which is addressing one of the seven key areas of Maine's Science and Technology Action Plan. This research will enable wood product industries to diversify their products to include biomass derived fuels and chemicals by helping to (1) understand the composition and properties of woody biomass derived pyrolysis oil (2) improve the heating value of pyrolysis oil and improve properties related to transportability through catalytic hydrodeoxygenation (3) overcome economic barriers to Fischer-Tropsch Liquids (FTL) synthesis by reducing stringent current syngas cleaning requirements, and (4) improve quality of FTL.

Scientific and Technical Merit highlights include: (1) an innovative combinatorial screening micro-array platform integrated with vibrational spectroscopies, (2) synthesis and physical characterization of novel size-selective catalyst/supports using engineered mesoporous (1-10 nm diameter pores) materials, (3) advances in fundamental knowledge of novel support/multi-metal catalyst systems tailored for pyrolysis oil and syngas upgrading, (4) rapid ink-jet synthesis techniques for micro-support/catalyst library generation, and (5) characterization of woody biomass-derived pyrolysis oils.

The research cluster is organized into four core areas that are integrated and interdependent upon one another as shown in Figure 2. Each core area is led by an individual PI. Area 1 is identifying critical reaction pathways to be studied through experiments and interactions with forest product industries and R&D community. Area 2 is exploring synthesis and physical characterization of novel integrated support/catalyst materials with combined reaction and separation capabilities. Area 3 is developing highly novel combinatorial approaches to catalyst design. Area 4 is advancing fundamental understanding of reaction kinetics and mechanisms to quantify performance parameters, such as conversion and selectivity, used in Area 1 for optimizing reaction engineering, and providing motivation for more detailed investigations of surface reactions.

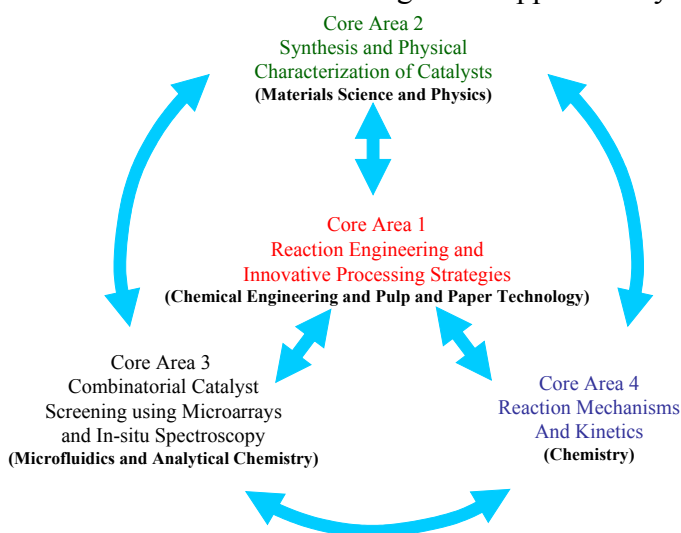


Figure 2. The overall integration of the cluster is based upon four Areas of Expertise.

There are three major research Thrusts in this project: Micro-Array Combinatorial Catalyst Screening (MACCS), Fischer-Tropsch Liquids, and Pyrolysis Oils. The Thrusts include contributions from each of the Core Areas, interactions with four graduate students and a post-doc, and collaborations with DOE, two Maine small businesses and Colby, Bates, and Bowdoin Colleges. Table 1 shows the major research tasks of each thrust and how those tasks integrate across the Core Areas. The MACCS thrust is focused on developing a microhotplate combinatorial screening platform integrated with vibrational spectroscopies. This development involves both feedforward and feedback interactions with the other Core Areas and research thrusts. The FTL thrust is taking advantage of the existing knowledge base in FTL catalysts to evaluate and qualify our novel micro-array combinatorial catalyst screening (MACCS) approaches. The physical properties and performance of bulk catalysts will be compared to those of catalyst micro-arrays synthesized using ink-jet printing techniques. In addition to MACCS qualification, we are focusing on FTL support/catalyst systems for size-selectivity and tar tolerance. The Pyrolysis Oil thrust is focused on fundamental kinetics and mechanistic understanding that will contribute to the development of support/catalyst systems for hydrodeoxygenation of pyrolysis oils.

Table 1: Future Plans and Integration of Research Thrusts across Core Areas

	Thrust 1	Thrust 2	Thrust 3
Title	Micro-Array Combinatorial Catalyst Screening	Fischer-Tropsch Liquids from Biomass-Derived Syngas	Pyrolysis Oil Upgrading and Characterization
Core Area 1 Reaction Engineering	Define representative compounds, processing conditions, and thermodynamics as input for combinatorial studies. Define catalyst compositional matrices.	Compare effects of tar-like contaminants such as benzene on bulk catalyst activity.	Create pyrolysis oil from Maine biomass. Study kinetics and reaction products for model compounds (furfural and guaiacol). Characterize bulk hydro-deoxygenation catalysts using purchased and in-house produced pyrolysis oils.
Core Area 2 Catalyst Synthesis and Characterization	Synthesize compositional matrix for inkjet catalysts. Identify catalyst/support systems for bulk synthesis.	Synthesize and physically characterize bulk and inkjet deposited catalysts.	Synthesize and physically characterize bulk catalysts.
Core Area 3 Combinatorial Platform Integration and Methods	Develop microhotplate platform. Integrate inkjet deposition system. Couple microarray with FTIR and Raman. Analysis of combinatorial data.	Synthesize micro-support/catalysts on MACCS platform and evaluate arrays using model compounds	Synthesize micro-support/catalysts on combi platform and evaluate arrays using model compounds.
Core Area 4 Fundamental Reaction Mechanisms	Compare bulk to micro-support/catalyst performance and properties. Determine critical input parameters for catalytic screening evaluation.	Correlate bulk activity with model compounds to combinatorial results.	Correlate bulk activity with model compounds to combinatorial results. Characterize complex products and identify model compounds for pyrolysis oil upgrading.

Design and Implementation of Multi-Hop Wireless and Sensor Networks for the Ubiquitous Computing and Monitoring System (UCoMS)

Hongyi Wu, Dmitri Perkins, Nian-Feng Tzeng, and Magdy Bayoumi

The Center for Advanced Computer Studies
University of Louisiana at Lafayette
{wu, perkins, tzeng, mab}@cacs.louisiana.edu

Project Scope

This project is a subtask of the Ubiquitous Computing and Monitoring System (UCoMS), which aims to provide integrated and cross-disciplinary solutions for more efficient methods of energy resource discovery. A key requirement for the UCoMS project and the effective discovery and management of energy resources is real-time data acquisition, data processing, and decision-making. This sub-project focuses on the use of a quickly-deployable two-layer hierarchical wireless networking system that can be used in the often harsh conditions encountered during energy resource discovery. The top-level wireless network is a high-bandwidth multi-hop wireless network (called a mesh network), which acts a backhaul network for transmitting data over long distances. The lower-level network comprises wireless-enabled sensor nodes that can be used for monitoring, data collection, as well as intrusion detection. The project has both scientific and technological goals. The scientific objectives are (1) to identify a fundamental set of principles that enable the design and application of multi-hop wireless networks in the harsh environmental conditions and (2) to use these principles to develop protocols and algorithms for self-organizing mesh and sensor ad hoc networks to be used for monitoring, data collection and distribution, location tracking, and real-time communication. The technological objective of the project is to build a fully functional prototype of the wireless and sensor network that demonstrates that the scientific research results (i.e., principles and algorithms) actually work in real environments.

Recent Progress

Mesh Networks

- **Wireless Mesh Testbed.** A wireless mesh testbed comprising seven (7) custom multihop wireless routers has been deployed, covering approximately 70 acres on the main campus of University of Louisiana at Lafayette. Each wireless router has two IEEE 802.11 a/b/g radio cards. Currently, the testbed has been evaluated using standards TCP (i.e., FTP) and UDP-based applications. The second phase of the testbed deployment will include (1) the deployment eight additional routers, (2) the design of flexible tools for monitoring and evaluating link-level and end-to-end performance, and (3) implementation of multipath routing and link-layer coding techniques for improving network quality-of-service.
- **Performance Modeling and Prediction.** The performance of mesh networks depends upon several factors. Such factors may be controllable (e.g., as system or protocol parameters, traffic load, network size, protocol design, network density, and channel assignments) while others may be uncontrollable (e.g., node mobility, channel quality, signal propagation characteristics). This component of our work has focused on modeling and predicting protocol and overall system performance as a function of such factors. In particular, using a statistical design of experiments approach we have developed first and second order linear regression models and non-linear artificial neural network models that can be used to estimate the performance of ad hoc networking systems over a wide range of scenarios [1, 2]. A scenario is defined as a single combination of factors and their respective values. Moreover, our models are able to quantify the main effects of each factor as well as the two-interaction effect of each factor pair.
- **A General Performance Index.** Evaluating and comparing the performance of dynamic wireless networks by comparing individual performance metrics over different scenarios is a non-trivial task and often leads to erroneous conclusions regarding which protocol or system configuration yields the best overall system performance. To this end, we have proposed a general performance index, which is a mathematical function that aggregates performance results from multiple response metrics into a single scalar value that quantifies overall system performance, leading to more objective evaluations and comparisons. We have illustrated the advantages of the proposed performance index by comparing two ad hoc networking systems over a wide range of networking scenarios. Based on the results of this analysis, we also developed an empirical model that

characterizes the relationship between the proposed performance index, four response metrics (packet delivery ratio, end-to-end delay, routing overhead, and jitter) and four influential factors (node mobility, offered load, network size, and routing protocol) [3].

- **S-Box: A Scalability Analysis Framework.** The scalability of adaptive protocols designed for multihop wireless networks is a key design issue for achieving large-scale deployments of mesh networks. In this work, we have propose a scalability index which aggregates the performance of multiple metrics into a single scalar value, while considering the correlation between individual metrics, the application-level requirements, and the network properties. The proposed index can be used as a measure of the protocol or system scalability with respect to any number of metrics. We further proposed S-Box, a general “black-box” type scalability analysis model for ad hoc routing protocols, which can be used to evaluate protocol scalability using the statistical design of experiments. S-Box provides a convenient and systematic way to address practical scalability problems [4].
- **Protocol Design and Analysis.** Channel arbitration is a key factor in the design of broadcast wireless networks [5]. Contention-based protocols (e.g., IEEE 802.11) have low delay at low load but poor channel efficiency at high load. Collision-free protocols, such as TDMA are able to achieve better channel efficiency at high loads but result in longer delays at low loads. In this work, we have proposed a hybrid medium access control (MAC) protocol based on distributed TDMA (HDTP) for multi-hop wireless networks. The hybrid protocol seeks to overcome limitations of TDMA under low or dynamic traffic load. By using static TDMA slot assignment and dynamic transmission schedule for real traffic situations, HDTP can achieve low delay at low load and high channel efficiency at high load. As a result, our hybrid protocol adapts well to a wide range of dynamic traffic load. We have developed analytical and simulation models of HDPT, and we are currently studying its performance in relation to hybrid medium access control protocols.
- **Prioritized Medium Access Control (P-MAC).** For P-MAC investigation, we have proposed an effective protocol based on the binary countdown approach, in order to differentiate packets in multiple Service Classes (SC's) based on their priority levels, thus providing different levels of service. It is the first attempt, to our best knowledge, to implement such an algorithm for service differentiation and to support absolute prioritization in distributed wireless networks, which cannot be achieved by any existing MAC protocols (such as IEEE 802.11e). Our analytic model, validated via simulation, shows that P-MAC can effectively support traffic differentiation as well as achieve very low packet dropping (both renegeing and blocking) probabilities when the traffic load is below the channel capacity. If the network is overloaded, P-MAC can still maintain an extremely stable and high channel throughput (in sharp contrast to other MAC protocols, such as the IEEE 802.11 protocol family including IEEE 802.11e) [5, 13, 14, 15].
- **Optimal Data Transmission in Heterogeneous Wireless Networks.** An important optimization issue in the ubiquitous and integrated wireless communication system is how to minimize the overall communication cost by intelligently utilizing the available heterogeneous wireless technologies while at the same time meeting the quality of service requirements of mobile users. Our research first identifies the cost minimization problem to be NP-hard. We then present an efficient minimum-cost data delivery algorithm based on linear programming (LP), with various constraints such as channel bandwidth, link costs, delay budgets, and user mobility taken into consideration. Extensive simulations are carried out to evaluate the proposed cost minimization scheme. Our results show that the proposed LP approach can effectively reduce the overall communication cost, with small overhead (< 3%) for signaling, computing, and handoff [8].

Sensors and Sensor Networks

- **Energy-efficient Routing in Sensor Networks.** Energy efficiency is a critical design issue in wireless sensor networks, where each sensor node relies on its limited battery power for data acquisition, processing, transmission, and reception. Our research studies an integrated approach on power control and load balancing, aiming at even distribution of the residual energy of the sensors and thus prolonging the lifetime of overall wireless sensor networks. More specifically, an Integer Linear Programming (ILP) algorithm, a Distributed Energy Efficient Routing (DEER) protocol, and a neural network based approach are proposed for time-driven sensor networks. A Residual Energy-based Traffic Splitting (RETS) protocol is introduced for event-driven sensor networks. We have carried out extensive simulations to evaluate the proposed energy efficient communication protocols, unveiling that the proposed DEER and RETS approaches can effectively distribute energy consumption evenly among the sensor nodes to prolong the network lifetime by up to 200% or more, when compared with other approaches in the literature [6].

- **RFID-based 3-D Positioning Schemes.** Our research on RFID-based 3-D positioning schemes aims to locate an object in a 3-dimensional space, with reference to a predetermined arbitrary coordinates system, by using RFID tags and readers. We have proposed two positioning schemes, namely, the active scheme and the passive scheme, for locating an RFID reader and an RFID tag (which is attached to the target object), respectively. Both approaches are based on a Nelder-Mead nonlinear optimization method that minimizes the error objective functions. We have carried out analyses and extensive simulations to evaluate the proposed schemes, with results showing that both schemes can locate the targets with acceptable accuracy [7]. The effectiveness of our proposed approaches is verified experimentally using the IDENTEC RFID kits.
- **Automated Scene Surveillance by Network of Sensors and Data Fusion.** Our developed surveillance framework includes object processing units, an object detection module, and a multi-agent tracking system for scene understanding. A region agent segments an image using the foreground mask, with each segment sent to an object processing unit for processing and tracking. When an object approaches the border of the area monitored by a region agent, the agent communicates with another proper agent to pass along its carried information, in support of object detection. As multiple types of sensors call for data fusion to combine information gathered by those sensors for accurate target interpretation, we have pursued effective data fusion techniques [9, 10]. The energy reduction framework we derived, aims to reduce the number of queries for the sensor energy status dispatched by cluster heads. Two types of information aggregates with respect to energy readings are possible: range-based and location-based ones, as detailed in two publications [11, 12].

Future Plans

Fast handoff techniques for 802.11-based Multi-hop Wireless Networks

To support real-time voice and video communication in a wireless network with mobile users requires a fast method to change the mesh router or AP to which a mobile station (MS) is connected. This process is called handoff. Previous work on reducing handoff in 802.11 wireless LANs have all assumed a wired backhaul or distribution system. However, in wireless mesh system the backhaul communication is done over a wireless channel. We have proposed the Backhaul-aided Seamless Handoff (BASH) protocol designed to take advantage of the mobiles ability to access the standard AP and wireless backhaul channel simultaneously. Our preliminary design and results show that BASH is able: (1) to reduce channel probing time by using the backhaul channel as a common channel (2) to shorten authentication time by utilizing the transitivity of the trust model and pre-authentication.

Performance Prediction and Analysis

In most ad hoc networks, user-level devices (e.g., laptops and PDAs) will also serve as mobile routers capable of forwarding packets on behalf of distant nodes. This means that the general CPU must be shared between host applications and network layer functions. Much of the previous work on routing protocol development, however, has not considered available CPU explicitly. In this work, we are studying the impact of host CPU capacity on the performance of ad hoc networks using analytical and empirical-based models. The analysis by queuing theory show the performance of ad hoc networks is substantially dependent on the available CPU capacity, path length, buffer size, and packet arrival patterns. Using a statistical design of experiments approach, we quantify the effects of each factor. In the next phase of this work, we intend to evaluate the effectiveness of available CPU capacity as a route selection metric in the existing Ad Hoc On-Demand Distance Vector routing protocol.

CDMA-based Wireless Mesh Network

The code division multiple access (CDMA) technology has been recently introduced into mesh wireless networks for improving channel efficiency. Several distributed CDMA code assignment schemes have been proposed, where different codes are assigned to adjacent point-to-point pairs in order to avoid multiple access interference. Such approaches, however, do not maximize the capacity of a CDMA system, because the sender transmits to one receiver only. In the next phase of this project, we will explore novel approaches to allow multiple data frames be transmitted from a sender to multiple receivers simultaneously, thus increasing network capacity and decreasing data delivery delay. To this end, we propose two CDMA-based medium access control schemes, the PNO (Pseudo Noise Only) scheme and the PPO (PN Plus Orthogonal) scheme, for highly efficient data transmission in mesh wireless networks, especially for those networks serving as communication backbone and thus experiencing high traffic load. The performance of our proposed schemes will be evaluated via both analysis and simulations, and compared with IEEE 802.11 and other CDMA-based schemes under the same channel bandwidth.

Performance Prediction and Analysis

The uplink scheduling in the WiMAX system is unique, due to its adaptive total bandwidth, quality-of-service (QoS) requirement, short scheduling delay budget, and frame-based data arrival and service. In the next phase of this project, we plan to develop a simple and efficient two-phase uplink scheduling algorithm tailed for WiMAX. It combines Weighted Round Robin (WRR) and Earliest Deadline First (EDF) algorithms, aiming to strike the balance between delay requirement and fair bandwidth allocation. In order to gain deep understanding of and insights into the two-phase scheduling algorithm, we will establish an elegant queuing system to derive in theory the performance metrics in terms of packet drop rate, throughput, and fairness. Extensive simulations will be carried out on the basis of a broad set of parameters according to WiMAX physical layer standard WirelessHUMAN-SCa. In simulations, we will consider both popular Poisson traffic and practical bursty traffic that is modeled by the Markov Modulated Poisson Process (MMPP) for comprehensive evaluation.

DOE-Sponsored Publications for 2005-2007

- [1] M. Totaro and D. Perkins, "Statistical Design of Experiments for Analyzing Mobile Ad Hoc Networks," in *Proceedings of the 8th ACM/IEEE International Symposium on Modeling, Analysis and Simulation of Wireless and Mobile Systems*, pp. 159-168, 2005.
- [2] A. Moursy, I. Ajbar, D. Perkins, and M. Bayoumi, "Building Empirical Models of Multi-hop Wireless Networks," accepted for presentation in the SCS/IEEE International Symposium on Performance Evaluation of Computer and Telecommunication Systems, July 2007.
- [3] I. Ajbar and D. Perkins, "A Performance Index and Statistical Model for Evaluating Multihop Wireless Networks," accepted for presentation in the IEEE International Conference on Computer Communications and Networks, August 2007.
- [4] Y. He, D. Perkins, and B. Huang, "S-Box: A Scalability Analysis Framework for Ad Hoc Routing Protocols," submitted for possible publication.
- [5] Y. Li, H. Wu, N.-F. Tzeng, D. Perkins, and M. Bayoumi, "MAC-SCC: A Medium Access Control Protocol for Mobile Ad Hoc Networks," *IEEE Transactions on Wireless Communications*, vol. 5, pp. 1805-1817, July 2006.
- [6] Y. Wang, H. Wu, and N.-F. Tzeng, "Energy-Efficient Communications in Wireless Sensor Networks: An Integrated Approach on Power Control and Load Balancing," accepted for publication in *International Journal on Ad Hoc & Sensor Wireless Networks*.
- [7] C. Wang, H. Wu, and N.-F. Tzeng, "RFID-Based 3-D Positioning Schemes," in *Proceedings of 26th Annual IEEE Conference on Computer Communications (IEEE INFOCOM)*, pp. 1235-1243, 2007.
- [8] H. Chen, H. Wu, S. Kumar, and N.-F. Tzeng, "Minimum-Cost Data Delivery in Heterogeneous Wireless Networks," accepted for publication in *IEEE Transactions on Vehicular Technology*.
- [9] R. Aguilar-Ponce, A. Kumar, J. TecpanecatI-Xihuitl, and M. Bayoumi, "Automated Object Detection and Tracking for Intelligent Visual Surveillance Based on Sensor Network," *Artificial Intelligence and Integrated Intelligent Information Systems: Emerging Techniques and Applications*, Idea-Group Press, 2006.
- [10] R. Aguilar-Ponce, A. Kumar, J. TecpanecatI-Xihuitl, and M. Bayoumi, "A Network of Sensors Based Framework for Automated Visual Surveillance," *Journal of Networks and Computer Applications*, Elsevier (scheduled to appear in 2007).
- [11] M. Bhattacharyya, A. Kumar, and M. Bayoumi, "A Framework for Assessing Residual Energy in Wireless Sensor Network," *International Journal of Sensor Networks*, vol. 2, 2007, pp. 256-272.
- [12] M. Bhattacharyya, A. Kumar, and M. Bayoumi, "Design and Analysis of Energy Reference Metric in a Cluster Based Wireless Sensor Network," in *Proceedings of IEEE International Conference on Circuits and Systems for Communications (ICCS '06)*, July 2006.
- [13] H. Wu, A. Utgikar, and N.-F. Tzeng, "SYN-MAC: A Distributed Medium Access Control Protocol for Synchronized Wireless Networks", in *ACM Mobile Networks and Applications Journal (MONET)*, Vol. 10, No. 5, pp. 627-637, 2005.
- [14] L. Pan and H. Wu, "Performance Evaluation of The SYN-MAC Protocol in Multihop Wireless Networks", accepted for presentation in the International Conference on Computer Communications and Networks (ICCCN), August 2007.
- [15] X. Cao, L. Pan, and H. Wu, "Enhanced Synchronized Medium Access Control Protocol for Wireless Ad Hoc Network", accepted for presentation in the International Conference on Computer Communications and Networks (ICCCN), August 2007.

Dynamic and Deterministic Lightpath Scheduling in Next-Generation WDM Optical Networks

Byrav Ramamurthy

Department of Computer Science and Engineering

University of Nebraska-Lincoln

Lincoln NE 68588-0115

Email: byrav@cse.unl.edu

1. Program Scope

The next-generation wavelength-division multiplexing (WDM) optical networks will be a key enabler for many high-end applications, including those using Grid technologies, by provisioning end-to-end lightpaths in an on-demand manner. Unlike previous optical bandwidth consumers, end users largely control these new applications and thus the bandwidth demands come directly from the end users' requests. Such demands are usually dynamic, which means that the network operation based on the assumption of static or predictable demands will be considerably inefficient. In addition, many end users need guaranteed lightpath connections during a specified period of time in future. They usually prefer to make advance reservations for end-to-end lightpaths with predefined service durations where the starting time of the lightpath demand can be days to weeks in the future. Such an advance reservation of a lightpath is called scheduling of a lightpath and correspondingly the lightpath itself is termed as a scheduled lightpath demand (SLD).

Many SLDs arrive in a dynamic manner. We distinguish between these dynamic scheduled lightpath demands (D-SLDs) as opposed to the concept of static scheduled lightpath demands (S-SLDs), where the whole set of lightpath demands is available before any actual provisioning happens in the network. Therefore, the time schedule of every S-SLD is known in advance for the network control plane. We study the problem of bandwidth allocation for D-SLDs in this paper. For the purpose of scheduling, we assume that the network time is slotted. The duration of a scheduled lightpath is measured in number of time slots. Each time slot has equal length.

In practical network operation, many end users require deterministic services. By a deterministic service, we mean that after submitting a request for a lightpath, a user expects a deterministic answer to whether the request can be accommodated and if so, the precise schedule information for the request. Deterministic service provisioning in the presence of D-SLDs may be inefficient in terms of network resource utilization. Unlike S-SLDs, arrivals of D-SLDs cannot be precisely predicted and thus resource allocation for D-SLDs is difficult to be optimized as a whole. Although the deterministic answer returned for a D-SLD can be optimal at the current time, the resource allocation in the network may still become sub-optimal with the arrivals of future D-SLDs. Interestingly, before a D-SLD is physically provisioned in the network, any adjustment carried out on the resources reserved for this D-SLD, e.g., rerouting and reassignment of wavelength, will not disrupt its service. Therefore, we have the opportunity to perform re-optimization for all D-SLDs scheduled to be set up in the future. In this paper, we propose that resources reserved for scheduled lightpaths be re-optimized before they are physically provisioned so that better network performance can be achieved.

D-SLDs can be classified into two main types. We use two example applications to characterize them respectively. The first is to schedule a real-time, collaborative scientific experiment. A lightpath is scheduled between the data collecting and data processing facilities at a fixed startup time for fixed duration, e.g., 9:00-10:00AM on Monday. We term such a demand to be of the time-fixed type. In the second example, a financial institution demands a scheduled lightpath on a weekly basis to backup its huge database to a data depot facility in a different city. The transfer takes up to one hour. It specifies a loose starting time window, say 1:00-5:00AM on Saturdays, during which any lightpath starting time is acceptable. We term such a demand to be of the time-window type.

We propose an efficient approach to schedule both time-fixed and time-window D-SLDs. We propose a dynamic lightpath scheduling algorithm to schedule a coming demand in a timely manner. We further develop novel re-

optimization techniques to the scheduled lightpaths that have not been physically provisioned. The simulation results show that 30%-60% of blocking can be eliminated by our re-optimization approach.

2. Recent Progress

We consider WDM wavelength-routed mesh networks, where a set of reconfigurable optical cross-connects (OXCs) are interconnected by optical fibers. To facilitate lightpath scheduling, the network time is slotted. A time slot is a minimum time unit in the network, each having an equal and fixed length. The wavelength availability in a time slot is independent of its availability in other time slots. As a result, a wavelength can be reused over different links as well as multiple time slots. We assume the network is under wavelength continuity constraint.

A D-SLD is denoted by a 5-tuple, (s, d, t, e, x) , where s and d denote source and destination nodes of the demand, t and e denote the starting time slot and duration of the demand respectively, and x is the maximum lightpath length in order to confine the optical impairs and end-to-end delay. The time-fixed D-SLD has fixed starting time, while the starting time of the time-window demand can be any value in a range of contiguous time slots. However once a time-window D-SLD is scheduled, its starting time cannot be altered. A lightpath admitted in the network is in either a *scheduled* state or an *in-service* state. *Scheduled* state indicates that its starting time, routing and wavelength assignment have been determined, but the lightpath has not been physically provisioned. *In-service* state implies that the lightpath is currently being used for data transmission. Figure 1 shows an example of lightpath reservation system. The horizontal axis represents the time line and the vertical line represents different wavelengths.

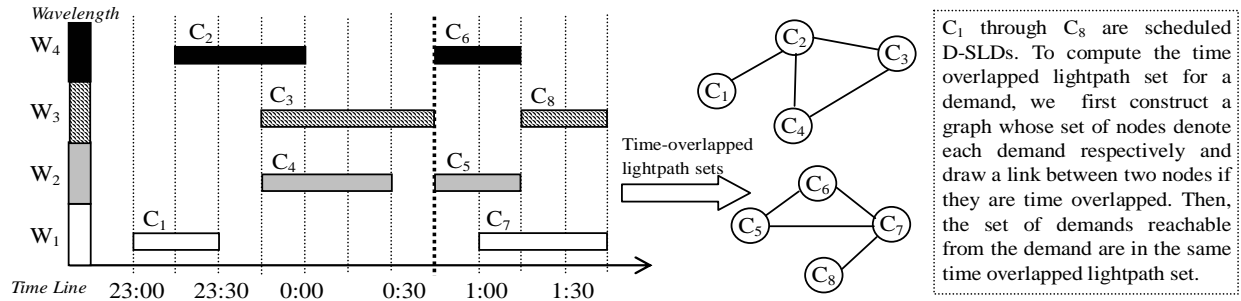


Figure 1 An example of lightpath reservation system.

Given a network topology, the wavelength availability information in each time slot, and a D-SLD request, the dynamic lightpath scheduling problem is to determine the starting time for the D-SLD and assign a route and wavelength (RWA) for the lightpath with the objective of reducing the network blocking probability.

We propose a two-phase approach to schedule a D-SLD. In phase I, our approach schedules the starting time and conducts RWA for the D-SLD with a load-balancing objective. The load balancing objective is expressed as:

minimizing $\text{MAX}_{t \leq i \leq m, l \in L} u_l^i$, where L is the set of links in the network, and t and m are the starting and ending time slot of

the D-SLD respectively. u_l^i represents the number of used wavelengths on the link l in time slot i . Given this D-SLD, we first compute k -shortest paths between its source and destination whose lengths are not greater than the maximum path length (x) of the demand. These paths are used as candidate routes for the demand. We use a slotted first-fit (*SFF*) scheme for wavelength assignment. Given a route, *SFF* picks the first common wavelength that is available on every link on the path during all the time slots between its starting and ending time. After computing the load balancing objective values iteratively on each candidate path over each possible starting time slot, our approach chooses the solution that minimizes the load balancing objective value. If the D-SLD is blocked in phase I, our approach enters phase II where the re-optimization procedure starts.

The objective of our approach in phase II is to eliminate the blocking generated in phase I. This is achievable because we can re-provision those scheduled lightpaths for re-optimization. The re-provisioning is risk-free since they are not in-service yet. First, the re-optimization procedure finds the time-overlapped lightpath set of the blocked demand. The time-overlapped lightpath set is a set containing all the lightpaths correlated to each other in terms of their service time (Figure 1 explains how to compute the time-overlapped lightpath set). Second, the re-optimization procedure sorts all the demands in the time-overlapped lightpath set according to a specific ordering scheme (as

explained in next paragraph). Third, it releases all the lightpaths in the set and tries to re-provision them (including the blocked demand) one by one in the sorted order with our load-balancing objective. If all the demands are provisioned successfully, the blocked is removed. Otherwise, the blocked demand in Phase I remains blocked and we restore the existing lightpaths to their original states.

The ordering scheme used in the re-optimization procedure of Phase II has a significant effect for our approach. We use a combination of multiple keys for ordering. Given a set of scheduled lightpaths, we first sort them according to the non-decreasing order of their starting time. If two lightpaths have the same starting times, we break the tie by sorting them according to the non-decreasing order of the number of hops on their minimum-hop paths. If they are still tied, we break the tie by sorting them according to the non-decreasing order of their service durations. Therefore, the lightpaths are sorted according to the rules of the earliest starting time first, maximum hop first, and longest duration first with decreasing priorities.

Below, we present numerical results of our proposed approach for on demand lightpath reservation. We conduct simulation experiments on a 24-node, 84 link network. The duration of each time slot is set to 15 minutes. In each simulation we simulate 100,000 D-SLDs consisting of a mix ratio of 7:3 of *time-fixed* and *time-window* demands. The window size of the time-window demands is uniformly distributed in the range [4, 48] time slots. The duration of D-SLDs is measured in number of time slots and is a weighted non-uniform distribution in the range [1, 50]. The distribution of the inter-arrival time and the starting times of D-SLDs are Poisson processes. We use two metrics for comparison, blocking probability (BP) and service blocking probability (SBP). The service blocking probability is measured as the ratio of the sum of the durations of blocked D-SLDs to the sum of the durations of all the D-SLDs. Because D-SLDs may have different durations, SBP provides a fair measurement on the network performance. We conduct our experiments in the cases with 8, 16, 32, and 64 wavelengths. The path length constraint is set to 600km, which is considered as a typical reach distance of all-optical signals.

Figure 2 plots BP and SBP of lightpath scheduling approaches with and without re-optimization in those test cases with 8 wavelengths. Other cases achieve similar results. As shown in the figure, the approach with re-optimization reduces both the blocking probability and the service blocking probability significantly. Table 1 presents the average improvement under different experimental settings. On average, compared to the approach without re-optimization, our approach eliminates 49.8%, 58.9%, 58.8%, and 54.7% blockings in phase II for different cases. The performance gain in terms of service blocking probability remains at the same level.

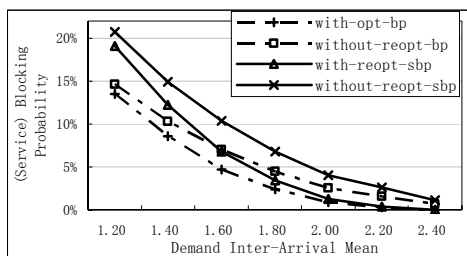


Figure 2 Results of approach with and without re-optimization in the network with 8 wavelengths.

W	Average Improvement	
	Blocking Probability	Service Blocking Probability
8	49.8%	51.8%
16	58.9%	59.9%
32	58.8%	59.1%
64	54.7%	51.8%

Table 1. Performance improvement by re-optimization.

3. Future Plans

In this study we addressed dynamic lightpath scheduling problem. We considered both time-fixed and time-window D-SLDs. Compared to predefined static demands, the unpredictable dynamic demands have a very limited potential for optimization. We proposed an efficient two-phase lightpath scheduling scheme to reduce about half of the blockings in the network with advance reservation. This is a great performance improvement for those network users who require both dynamic and deterministic scheduled lightpath services.

In this study, we did not consider the lightpath protection required for D-SLDs. However, such application usually require strict backup for the working lightpaths. Future work should focus on the lightpath scheduling problem under protection requirements. Also, we have not considered the ability to switch and schedule capacity in the form

of wavelength bands or wavebands. We propose to study the implications of waveband switching on our scheduling algorithms.

We plan to investigate the end-to-end issues emerging from the mutual interactions between the bandwidth-on-demand service-capable optical WDM network substrate layer and the application-driven highly reconfigurable higher layer in our future work. In particular, we will focus on the DOE UltraScience Net and its capabilities for our investigation. We will also plan to transition our results to the DOE ESnet which is the Department of Energy's high-speed production network.

4. Acknowledgments

The author thanks his former Ph.D. students, Dr. Xi Yang (USC/ISI East), Dr. Lu Shen (Juniper Networks) and Dr. Ajay Todimala (MAX) for their help with the simulation results presented here. The author also thanks Dr. S. V. Nageswara (Nagi) Rao, Oak Ridge National Labs for his suggestions towards improving this work.

References

1. W. Reinhardt, "Advance reservation of network resources for multimedia applications," in *Proc. of the 2nd International Workshop on Advanced Teleservices and High Speed Communication Architectures (IWACA'94)*, Heidelberg, Germany, Oct. 1994.
2. D. Wischnik and A. Greenberg, "Admission control for booking ahead shared resources," in *Proc. of IEEE INFOCOM '98*, San Francisco, CA, USA, Mar. 1998.
3. L. Wolf, L. Delgrossi, R. Steinmetz, S. Schaller, H. Wittig, "Issues of reserving resources in advance," in *NOSSDAV, Lecture Notes in Computer Science*, pp. 27-37, Springer, Durham, NH, USA, Apr. 1995. Springer.
4. A. Schill, S. Kuhn and F. Breiter, "Resource reservation in advance in heterogeneous networks with partial ATM infrastructures," in *Proc. of the IEEE INFOCOM '97*, pp. 612-619, Kobe, Japan, Apr. 1997.
5. R. Guerin and A. Orda, "Networks with advance reservations: The routing perspective," in *Proc. of the IEEE INFOCOM '00*, pp. 118 – 127, Tel-Aviv, Israel, Mar. 2000.
6. A. Maach and A. Hafid, "Resources reservation in advance in slotted optical networks," in *Proc. of the Third International Conference on Optical Communications and Networks (ICOON 2004)*, Hong Kong, China, Nov. 2004.
7. J. Kuri, N. Puech, M. Gagnaire, E. Dotaro, R. Douville, "Routing and wavelength assignment of scheduled lightpath demands", *Journal of Selected Areas in Communications (JSAC)*, vol. 21, no. 8, pp. 1231-1240, Oct. 2003.
8. J. Kuri, N. Puech, M. Gagnaire, and E. Dotaro, "Routing foreseeable lightpath demands using a tabu search metaheuristic," in *Proc. of IEEE GLOBECOM 2002*, Taipei, Taiwan, Nov. 2002.
9. B. Wang, T. Li, X. Lou, Y. Fan, and C. Xin, "On service provisioning under a scheduled traffic model in reconfigurable WDM optical networks," in *Proc. of IEEE BroadNets '05*, Boston, MA, USA, Oct. 2005.
10. S. Figueira, N. Kaushik and S. Naiksatam, "Advance reservation of lightpaths in optical-network based Grids," in *Proc. of IEEE BroadNets/GridNets 2004*, San Jose, CA, USA, Oct. 2004.
11. E. Bouillet, J-F. Labourdette, R. Ramamurthy and S. Chaudhuri, "Lightpath re-optimization in mesh optical networks," *IEEE/ACM Transactions on Networking*, Apr. 2005.
12. I. Chlamtac, A. Ganz, and G. Karmi, "Lightpath communications: an approach to high bandwidth optical WAN's," *IEEE Transactions on Communications*, vol. 40, pp. 1171-1182, July 1992.

Advances in the Fundamental Understanding of Coal Combustion Emission Mechanisms

Wayne S. Seames,¹ Mark R. Hoffmann,² John Hershberger,³ Uwe Burghaus,³ Michael D. Mann,¹ Frank Bowman,¹ David T. Pierce,² and Evguenii I. Kozliak²

wayne.seames@und.nodak.edu, John.Hershberger@ndsu.nodak.edu, mhoffmann@chem.und.edu

University of North Dakota, Depts. of Chemical Engineering (¹) and Chemistry (²), Grand Forks, ND 58202; North Dakota State University, Dept. of Chemistry, Fargo, 58105 (³)

Program Scope

Addressing the balance between maintaining low processing costs and mitigating environmental impacts will be one of the primary issues facing future sustainability for coal utilization. A fundamental understanding of the factors most important to small-size PM emissions is necessary for the development of cost effective technologies that will mitigate the environmental impact of the substantial quantities of coal consumed for power generation. The ND DOE EPSCoR IIP formulates an interrelated set of projects focused on improving our understanding of the fundamental chemistry that determines the emissions profile of particulate matter (PM) and trace inorganic compounds during coal combustion (this is the program's 1st year). A balance of multi-scale experimental and theoretical/computational studies focus on how inorganic compounds and fine fragmentation PM (FPM_{2.5}) are formed during the coal combustion process and how the reaction products transform to their ultimate fates as emitted flue gas or collected fly ash. Three focus areas to properly understand trace element (TE) behavior are included: 1) Formation mechanisms and 2) partitioning of inorganic compounds during combustion as well as 3) post-emission mechanisms. Much of our work focuses on macro-scale modeling of TE interactions during combustion plus generating key data necessary to render these models useful through experimentation and molecular-scale computations.

Recent Progress (for the 1st year of the project)

FOCUS AREA 1: FORMATION MECHANISMS

Modeling. A modular structure is being developed for a first principles-based model of the behavior of TEs during pc-combustion to accommodate both existing and new sources of data. Because these models rely upon information generated in other tasks of this project as well as existing data and models, activities during the reporting period have focused on obtaining information on existing models and data stores. Data acquisition and database development activities will continue during the next reporting period.

Molecular scale experiments. Physical property data are being generated for their use in modeling. We have devised a method that utilizes a graphite furnace atomic absorption spectrometer (GFAA) as the experimental platform for reducing condition physical property data measurements. The other aspect of this project is making small transient metal-containing molecules such as diatomic metal hydride and oxide species in order to study their kinetics. Currently, the AIO molecule (generated in situ via multiphoton photolysis of Al(CH₃)₃ followed by reaction of the atomic Al formed with O₂ or N₂O) is under investigation.

Large-scale experiments. A static high temperature materials test chamber has been designed and is under construction as a prototype of a 2-stage high temperature drop-tube furnace (HTDF) we intent to build in this project. This chamber's ultimate use will be to study the corrosion and degradation mechanisms of materials used in gasifiers and in oxy-combustion PC combustors. It

is being built to similar specifications as the first stage of an HTDF that we will use to generate additional physical property data.

Computational chemistry. An upgrade of our preferred variant of multireference perturbation theory for molecular electronic structures, i.e. second-order generalized Van Vleck perturbation theory (GVVPT2), has been made for the description of molecules relevant to the study of coal combustion. Specific molecular systems were examined and a few chosen for computational study, e.g., reactions of some of the transition metal monohydrides, i.e., CrH, FeH, TiH, MnH, with the small atmospherically relevant molecules NO, NO₂ and OH. Large scale multireference configuration interaction calculations (MRCISD) have been performed on CrH and FeH and on NO and NO- to provide calibration data for studies on the whole potential energy surfaces, which will be performed using GVVPT2.

FOCUS AREA 2: PARTITIONING MECHANISMS

A portion of this task is to gain a better understanding of the formation mechanisms of fine fragmentation ash particles. Baseline size-segregated samples of particles were extracted from the combustion of Blacksville bituminous coal in a 19kW downflow combustor's post combustion zone using a Dekati low pressure impactor. These samples were then examined qualitatively and quantitatively under scanning electron microscopes at Argonne National Laboratory (ANL). Based on these results, a design of experiments' matrix was developed for parametric study of particles in order to examine postulated formation mechanisms.

The adsorption of *n*-butane and *iso*-butane on HOPG (highly-oriented pyrolytic graphite) has been studied by molecular beam scattering and thermal desorption spectroscopy (TDS). The initial adsorption probability, S_0 , decreases with impact energy, E_i , and is independent of surface temperature, T_s , i.e., molecular adsorption is present. The adsorption probability (S) increases with coverage (Θ), which is most distinct at large E_i and low T_s . Thus, precursor mediated (adsorbate assisted) adsorption is concluded. Coverage-dependent kinetics parameters have been obtained by directly fitting the TDS curves.

FOCUS AREA 3: POST-EMISSION MECHANISMS

We have begun developing a macro-scale model for trace elements in the plume from coal combustion stack emissions. The SCICHEM reactive plume model forms the core modeling framework on which our model will be built. SCICHEM accounts for both plume dispersion and plume chemistry for gas, aqueous, and particulate phases. Information on the speciation, partitioning, and reactions of these compounds is being gathered to help define the model parameters for these processes.

As a screening step for the chemical activity of silica [SiO₂/Si(100)], which is often used as a support, thermal desorption spectroscopy data have been gathered for a variety of gases such as *n*-nonane, *n*-hexane, *n*-butane, *iso*-butane, ethane, CO₂, CO, O₂, and H₂. Whereas the alkanes with chain lengths larger than three adsorb with large binding energies ($E_d = 50-70$ kJ/mol), the activity towards the other probe molecules was found to be negligible (< 24 kJ/mol) down to adsorption temperatures of 95 K. The adsorption of *n*- and *iso*-butane has also been studied by molecular beam scattering and found to follow standard precursor-mediated adsorption dynamics.

Our proposed method for characterization and fractionation of organic carbon (OC) with a

focus on frequently omitted polar species was validated. This was performed using three model PM materials of different origin and composition: wood smoke PM, diesel exhaust SRM 2975, urban PM SRM 1649. While wood smoke PM consists mainly of organic OC (61%), the portion of OC in both diesel exhaust and urban PM was found to be 10 %. Diesel exhaust PM consists mainly (90%) of elemental carbon while the major constituents of urban PM are inorganics.

We have compared organic solvent extraction to hot pressurized (e.g., subcritical) water (HPW) extraction which allows for the separation of polar and non-polar organics using low and high temperatures, respectively. The major advantage of HPW is in the use of a single solvent, thus eliminating artifacts of organic solvents in carbon determination. Moreover, water allows for efficient extraction of polar species. The results show that the overall recoveries of OC, using both solvent extraction methods, are comparable. The extraction efficiencies of overall OC were ca. 50% suggesting that 50% of OC is not extractable and thus remains irreversibly bound within the matrices of the PM. A higher portion of OC was obtained in the first (low-temperature) HPW fraction, due to higher polarity of water compared to methanol. Thus, a significant portion of OC is polar even for the relatively non-polar matrices such as diesel exhaust PM.

Future Plans

FOCUS AREA 1. By varying the delay between the vaporization pulse and the probe pulse, we will obtain the time-resolved kinetic profile of the metal hydride species. Initial work will be on species such as MnH, CdH, and CrH, as spectroscopic information is readily available. Subsequent work will expand these studies to other metals of interest, such as AsH and SbH. These species are expected intermediates in the near char reduced environment for TEs liberated that are organically associated or part of inclusions. Reactions with a variety of species, including O₂, CO, NO, NO₂, H₂S, and small hydrocarbon molecules, will be investigated.

Clean graphite (HOPGE) and metal covered graphite surfaces will be used to determine the adsorption probabilities on unburned entrained PM carbon. Then, CaO and Fe₂O₃ surfaces will be sampled to examine the possibility of adsorption at or near the active cationic reaction site.

Experiments will be continued using the Graphite Furnace AA as an in situ simulation of burning char particles (reducing environment high in carbon, 1700 – 2100 K). Simulated inorganic particles (silica, silica-al particles coated with the target elements) will be inserted into the graphite furnace which will then be rapidly heated to establish vapor-liquid-solid partitioning. The vapor phase concentration will then be measured using the spectroscopic techniques inherent in the GFAA.

Because the GFAA/FAA experimental setup described above will not be sufficient to generate all of the data required for the models, a 2-stage high temperature drop-tube furnace (HTDF) will be designed and fabricated specifically for this project. Fabrication of the high temperature materials test chamber is approximately 70% complete and will be finished and commissioned during the next reporting period. We will then move on to the construction of the HTDF. The HTDF will indirectly heat the 1st stage combustion environment up to 2400 K. As such it will be capable of simulating the reducing environment of the near-char pyrolysis that initially impact inorganic elemental partitioning and forms of occurrence during coal combustion. It will also be capable of simulating the entire combustion zone of the furnace – by

allowing small-scale combustion at realistic combustion temperatures. The 2nd stage will be capable of simulating conditions in the near combustion environment as the particles transition from reducing to oxidizing or the post-combustion zone conditions (lower temperatures, longer residence times). The data generated will be used in macro-scale modeling

In computational chemistry (i.e., molecular-scale modeling), we expect to make significant progress on the computer program realizing a local orbital variant of GVVPT2 (i.e., one of the original year 1 goals) using the new Graphical Unitary Group Approach (GUGA) framework in the upcoming year. We will conduct computational examination of the reaction paths postulated for combustion involving main group oxo-acids (of As, Sb, and Se).

In FOCUS AREA 2, to examine the postulated formation and partitioning mechanisms, particle examination will be performed. Parametric experiments changing the temperature- and fuel-to-oxygen ratio will be run in order to quantify their effects on the fine-fragmentation particle size range. Mass samples will be collected to form a particle size distribution (PSD) and determine if there is a shift of mass from the fine-fragmentation mode (FFM) to either the larger supermicron mode or the smaller ultrafine mode. Coal ash particles will also be gathered to be analyzed by a scanning electron microscope (SEM). The formation mechanisms are then determined and quantified from the SEM images by qualitatively viewing the shapes.

In investigating post-emission mechanisms (FOCUS AREA 3), the extracted fractions will be characterized during the next reporting period by GC/MS with specific attention to polar species. The distribution of different functional groups with regard to their polarity will be also studied using nuclear magnetic resonance spectroscopy.

DOE Sponsored Publications

1. Funk, S., Nurkic, T., Burghaus, U.; Reactivity screening of silica. *Applied Surface Science* **253** (2007) 4860-4865.
2. Kadossov, K., Goering, J., Burghaus, U.; Molecular beam scattering of n-/iso-butane on graphite (HOPG), measurements. In progress, submittal expected spring, 2007.
3. Song, J.; Apra, E.; Khait, Y. G.; Hoffmann, M. R. High level ab initio calculations on the NiO₂ system. *Chem. Phys. Lett.* 2006, 428, 277-282.

Software Development

1. aoints – a new C language program to calculate integrals over atomic basis function of arbitrary angular momentum using Obara-Saika recursion.
2. propints; properties – two new C language programs to calculate multipole integrals up to hexadecapoles, compatible with aoints.
3. gvvpt2g – a new C language program to calculate second-order multireference perturbation theory corrections to molecular electronic structure, using GVVPT approach, in the GUGA framework.

Ro-vibrational Relaxation Dynamics of PbF Molecules

Neil Shafer-Ray, Greg Hall, and Trevor Sears
shaferry@physics.ou.edu, gehall@bnl.gov, sears@bnl.gov

Program Scope

In 1950 Purcell and Ramsey suggested that the electron might have a CP-violating electric dipole moment (EDM) proportional to its spin angular momentum[1]. This possibility initiated an ongoing hunt for the e-EDM. This hunt has been spurred on by the recognition of the importance of CP-violation to the formation of a matter-dominated universe[2] as well as by the marked difference in the prediction of the magnitude of the e-EDM by Supersymmetry[3] and the Standard Model[4].

The current limit on the e-EDM is 1.6×10^{-27} e-cm as determined in a Ramsey beam resonance study of the Tl atom[5]. The PbF molecule provides a unique opportunity to search for an even smaller moment. The molecule's odd electron, heavy mass, and large internal field combine to give it an intrinsic sensitivity to an e-EDM that is over three orders of magnitude bigger than that of the Tl atom[6]. In addition to this increased intrinsic sensitivity, the ground state of the PbF molecule allows for a "magic" electric field at which the magnetic moment vanishes[7]. All of these advantages create an opportunity to significantly lower the current limit on the e-EDM. These advantages can only be realized if an intense source of ground-state PbF molecules can be created. The scope of this project is to (1) create a rotationally cold molecular beam source of PbF, (2) achieve a continuous ionization scheme for sensitive state selective detection of the PbF molecule.

Recent Progress

Previous workers have created the PbF molecule by cracking PbF_2 [8–12], by reaction of fluorine with lead[13–16], and by the reaction of NF_3 with lead in a continuous discharge[17]. We have discovered that the reaction of molten lead with MgF_2 leads to the efficient production of PbF. Our reactor source is shown in Fig 1. It consists of a nozzle constructed from MgF_2 . Inside this nozzle is a small removable vessel in which lead pellet is placed. When the nozzle is heated to temperatures above 900°C , the reaction of this lead with the MgF_2 vessel creates PbF. An inert buffer gas is used to carry this PbF product into the vacuum chamber. The yield of PbF created in this way is comparable to the production we achieved using a $\text{Pb}+\text{F}_2$ flow reactor. The MgF_2 reactor has the advantage of both simplicity and stability.

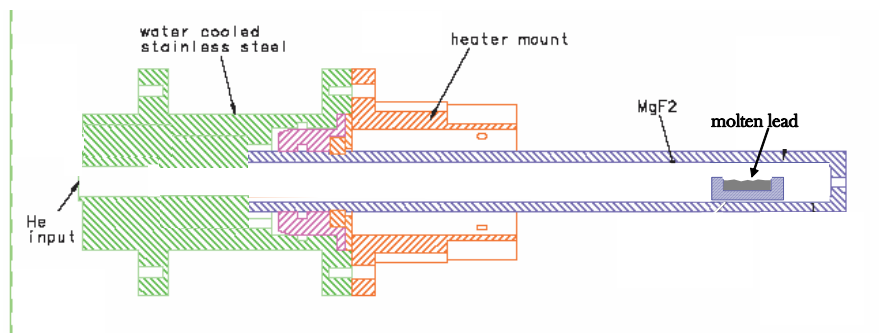


Figure 1: Pb+ MgF_2 reactor.

Because of the weak intensity of our PbF source as compared to an atomic beam source, it is desirable to choose an extremely sensitive detection scheme. Our first attempt at such a scheme was 1+1 ionization of the molecule via the B-state of PbF[18]. Unfortunately, the short lifetime of the B-state made rotational-state-resolution impossible. Despite the failure of this strategy for state-selective detection, we were able to use this 1+1 ionization scheme to determine the ionization potential of the molecule.

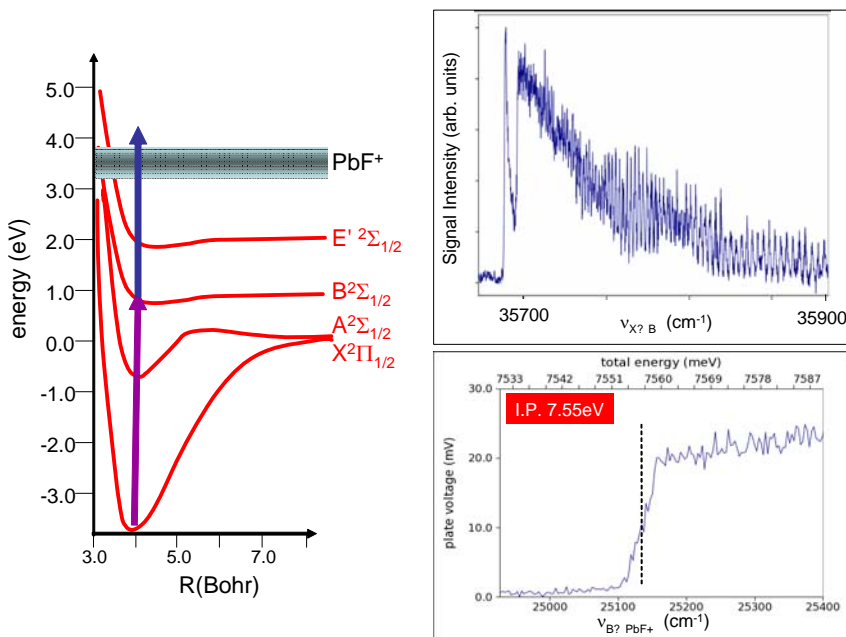


Figure 2: 1+1 REMPI of PbF via the X-B transition

After B-state ionization proved an ineffective tool for state selective detection, we developed the ionization scheme shown in Figure 3. The scheme is doubly resonant, requiring three sources of laser radiation. The first laser is used to drive the X→A transition at 436.7 nm. The second laser, at 476.7 nm, is used to drive the A→E' transition that we have begun to characterize. The third source of laser radiation is a frequency doubled Nd:YAG laser that drives the E' state to ionization. To attempt to characterize the vibrational structure of the E' state, we fixed the frequency of laser radiation driving the X→A transition to the Q-branch pile up at 22897cm^{-1} and scanned the laser driving the A→E' transition. The resulting vibrational structure is irregularly spaced and difficult to interpret. A second vibrational level, centered at 442nm, shows similar rotational structure as does the transition at 476.7nm whereas vibrational bands at 455nm and 463nm show no rotational structure

indicating a very short E' -state lifetime.

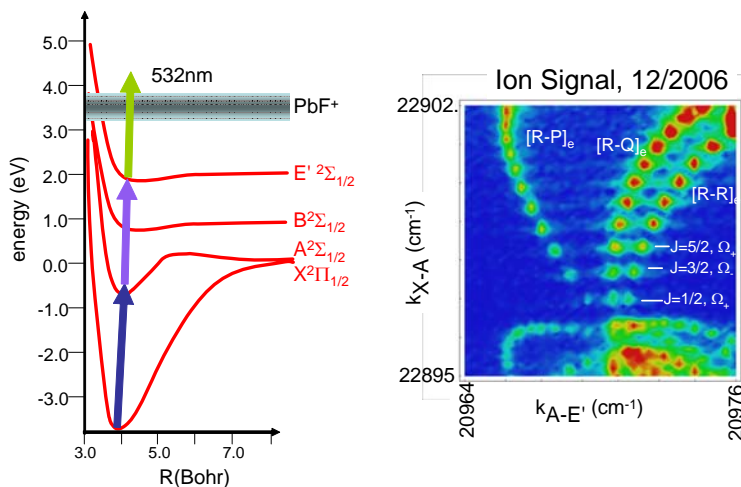


Figure 3: 1+1+1 REMPI of PbF via the $X \rightarrow A$ and $A \rightarrow E'$ transitions.

Future Plans

In our present set up, the rotational state distribution of the PbF molecules entering our vacuum system is hot, with only 1 molecule in 10^4 in the ground state. Because only the ground state of the molecule is useful to an e-EDM measurement, it is important to gain back this loss in population. We have already observed that when Neon is used as a carrier gas, the population of ground-state PbF is enhanced by a factor of two, whereas the backing pressure of He has little affect on the rotational state distribution. When the heavier noble gasses (namely Ar, Kr, and Xe) are used, the ground state of PbF is diminished, presumably because of the loss due clustering of the radical with the inert gas. We have begun construction of a new pumping system that will allow us to create a true supersonic molecular beam. When this machine is completed, we will be able to determine if Neon can be used to rotational cool the PbF molecule.

We are also working to improve our detection scheme. Our current laser system operates at just 10Hz, creating a detection duty cycle of 10^{-5} . This five-order-of-magnitude loss in sensitivity is not acceptable for an e-EDM experiment. To remedy this problem, we plan to implement a continuous or pseudo-continuous source of laser radiation in order to drive the $X \rightarrow A$, $A \rightarrow E'$, and $E' \rightarrow \text{PbF}^+$ transitions. We have carried out saturation curves on each of the three transitions and the lifetime of the E' state has been measured. We are now in the process of engineering an optical bench in order to state-selectively ionize a large fraction of the PbF molecules entering the focussed waist of cw and pseudo-cw laser radiation.

[1] E. Purcell and N. Ramsey, Phys Rev **78**, 807 (1950).

[2] Sakharov, JETP Lett **5**, 24 (1967).

- [3] R. Arnowitt, B. Dutta, and Y. Santoso, Phys. Rev. D **64**, 113010 (2001).
- [4] F. Hoogeveen, Nuclear Physics **B341**, 322 (1990).
- [5] B. Regan, E. D. Commins, C. J. Schmidt, and D. DeMille, Physical Review Letters **88**, 71805 (2002).
- [6] M. Kozlov, V. Fomichev, Y. Y. Dmitriev, L. Labzovsky, and A. Titov, J. Phys. B: At. Mol. Opt. Phys. **20**, 4939 (1987).
- [7] N. Shafer-Ray, Physical Review A **73**, 34102 (2006).
- [8] Rochester, Proc. R. Soc. London A **153**, 407 (1936).
- [9] F. Morgan, **49**, 47 (1936).
- [10] R. Barrow, D. Butler, J. Johns, and J. Powell, Proceedings of the Physical Society of London **73**, 317 (1958).
- [11] S. Singh, Indian J. of Pure Appl. Phys. **5**, 292 (1967).
- [12] D. Lumley and R. Barrow, Journal of Physics B **10**, 1537 (1977).
- [13] C. Dickson and R. Zare, Optica Pura y Aplicada **10**, 157 (1977).
- [14] R. Green, L. Hanko, and S. Davis, Chemical Physics Letters **64**, 461 (1977).
- [15] F. Melen and I. Dubois, Journal of Molecular Spectroscopy **124**, 476 (1987).
- [16] J. Chen and P. Dagdigian, J Chem Phys **96**, 1030 (1992).
- [17] K. Ziebarth, K. Setzer, O. Shestakov, and E. Fink, Journal of Molecular Spectroscopy **191**, 108 (1998).
- [18] C. McRaven, S. Poopalsingham, and N. Shafer-Ray, Physical Review A **75**, 024502 (2007).

Recent Publications

1. N.E. Shafer-Ray, *Possibility of zero-g-factor paramagnetic molecules for the measurement of the electron's electric dipole moment*, Phys. Rev. A, **73**, 034102 (2006.)
2. C. McRaven, P. Sivakumar, N.E. Shafer-Ray, *Multi-photon ionization of lead monofluoride resonantly enhanced by the $X_1^2\Pi_{1/2} \rightarrow B^2\Sigma_{1/2}$ transition*, Phys. Rev. A. **75** 023502 (2007.)

(The publications here are relevant publications in the last two years, but are not the result of DOE funded research.)

Fabrication of Cu-In-S Nanoparticles and Clusters

Pamela Shapiro, shapiro@uidaho.edu, University of Idaho Moscow, ID 83844-2343

i) Program Scope

The original objective of this research project was to prepare monodisperse chalcopyrite nanoparticles in a size-selective manner for use in third-generation quantum dot-based solar cells.

These nanoparticles were to be formed from compounds of general formula $(R_3P)_2Cu(\mu-ER')_2In(SR')_2$ ($E = S, Se$),¹ which have been used as single source precursors (SSPs) for the chemical vapor deposition of thin films of the photovoltaic material $CuInE_2$ ²⁻⁶ and for the solvothermal synthesis of $CuInE_2$ nanoparticles.^{7,8} We planned to use calixarene macrocyclic templates to control the size of the nanoparticles produced *via* the thermal decomposition of the SSPs.

ii) Recent Progress

We discovered a photochemical route to chalcopyrite nanoparticles.⁹ UV irradiation of solutions of the SSPs $(oct_3P)_2Cu(\mu-SR)_2In(SR)_2$ ($R = Et, t-Bu$) in a variety of solvents (dioctylphthalate, toluene, pentane) with a 200W mercury arc lamp afforded ultrafine (1-2 nm) $CuInS_2$ particles (Figure 1).

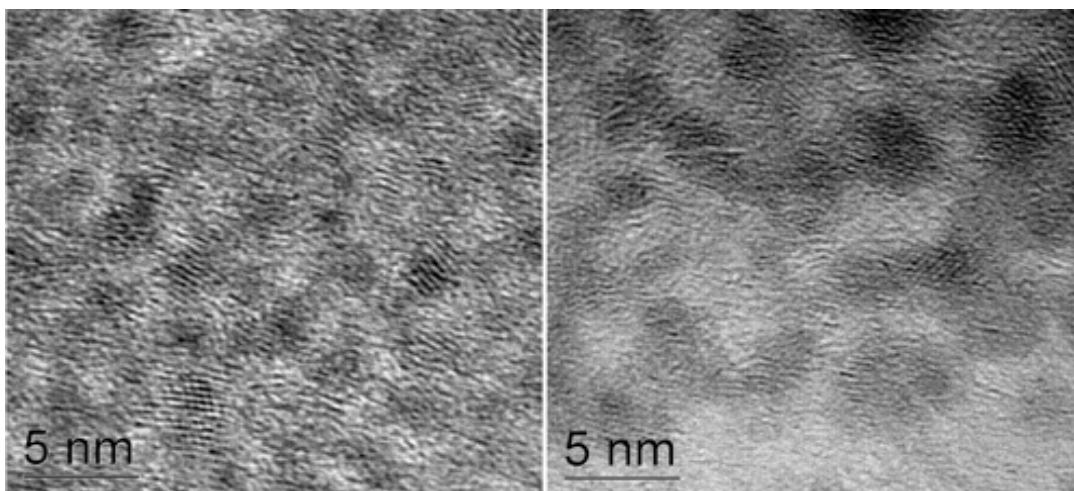


Figure 1. TEM micrographs of $CuInS_2$ nanoparticles formed from $(P_{oct_3})_2CuIn(S^tBu)_4$ by (a) photolysis in dioctylphthalate (DOP), (b) thermolysis at 170°C in DOP.

Over the course of the photolysis the UV-vis absorption onset of the solutions shifted to longer wavelengths, indicating particle growth. Consistent with this,

the color of the solutions changed from colorless to yellow to orange to red (Figure 2).

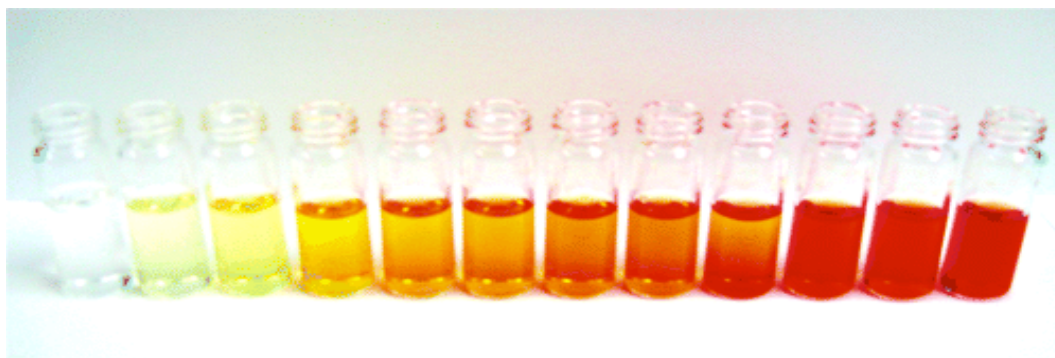


Figure 2. Vials of samples from the irradiation of 20 mM solutions of $(\text{Poct}_3)_2\text{CuIn}(\text{SEt})_4$ in DOP for (from left to right) 0. 2. 4. 6. 8. 11. 21. 30. 50. 74. 124. and 218 h.

Curiously, the shape and position of the emission band of the products did not change over the course of the photolysis, although its intensity increased. The powder XRD pattern of the nanoparticles was consistent with that of bulk CuInS_2 (roquesite) (Figure 3).

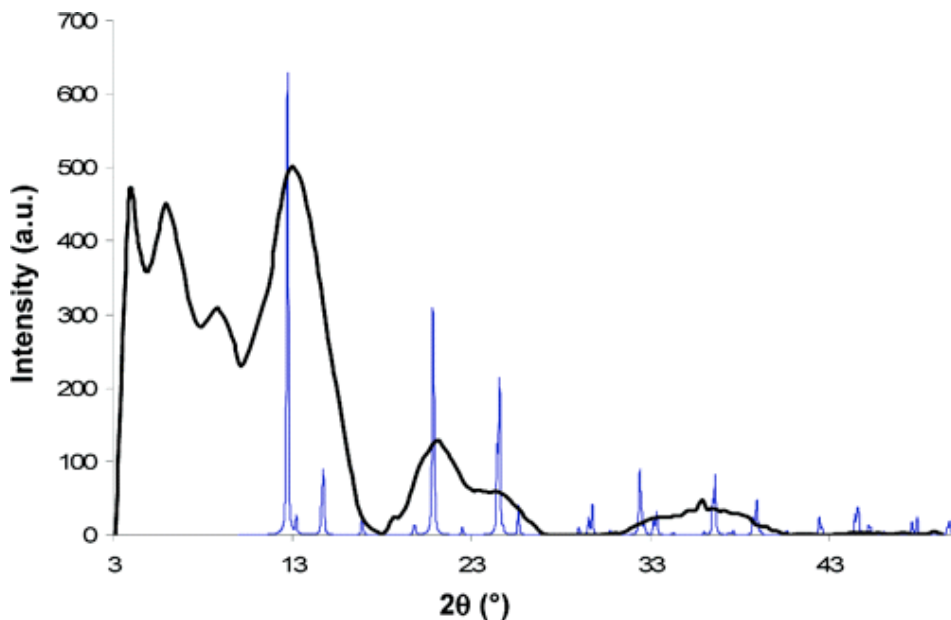


Figure 3. XRD pattern of nanoparticles (black) with calculated XRD pattern of bulk CuInS_2 (roquesite) (blue).

Since precursor photodecomposition is complete within five hours, we recently explored the possibility of isolating and structurally characterizing clusters formed during the initial stages of the photolysis. Clusters $\text{Cu}_9\text{In}_{10}\text{S}_9(\text{SEt})_{21}(\text{PPh}_3)_3$ (**1**) and $\text{Cu}_{11}\text{In}_6\text{S}_7(\text{StBu})_{15}$ (**2**) (Figure 4) were isolated

from the 5-7 hr photolysis of toluene solutions of $(\text{Ph}_3\text{P})_2\text{CuIn}(\text{SEt})_4$ and $(\text{Ph}_3\text{P})_2\text{CuIn}(\text{S}^t\text{Bu})_4$, respectively.¹⁰ Cluster **1** is an incomplete supertetrahedral T4-like cluster and exhibits the adamantoid structure of bulk CuInS_2 (with one copper atom and one indium atom in swapped positions) and an inorganic core of formula $\text{Cu}_9\text{In}_{10}\text{S}_{30}$. Cluster **2** has a copper rich core with the formula $\text{Cu}_{11}\text{In}_6\text{S}_{22}$. Photolysis of $(\text{Ph}_3\text{P})_2\text{CuIn}(\text{SCH}_2\text{CH}_2\text{C}(\text{O})\text{OMe})_4$ under similar

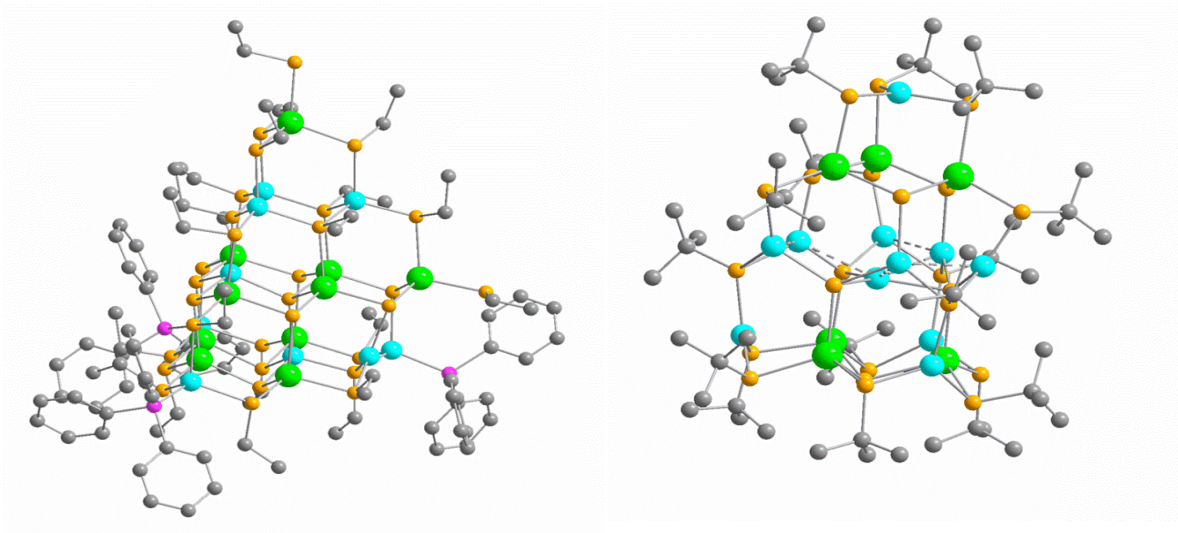


Figure 4. Ball and stick drawings of the molecular structures of clusters 1 (left) and 2 (right). Color scheme: Cu (blue), In (green), S (orange), P (pink), C (grey). Hydrogen atoms are omitted for clarity

conditions produces red, rhombohedral crystals in good yield. Due to the quasi-periodicity of the lattice in these crystals, we have not yet obtained a single-crystal X-ray structure of this material.

iii) Future Plans

We plan to develop HPLC/MS methods for analyzing the cluster products in order to determine the selectivity of reaction and to see if we can optimize cluster yield by fine-tuning the reaction conditions. We also plan to determine the mechanisms of SSP decomposition and cluster growth. Using monochromatic radiation from pulsed Nd:YAG and dye lasers, we will explore the effect of the wavelength and the intensity of the radiation on the selectivity of the photolysis and determine if we can control the size of the cluster products by controlling these parameters. Finally, we plan to apply this method to cluster synthesis from other precursors in order to explore the effect of varying the thiolate ligands, the phosphine ligands, the

chalcogens (S,Se,Te), the group 11 metals (Cu,Ag) and the group 13 metals (B, Al, In, Ga) on the structures of the clusters.

iv) References

- (1) Hirpo, W.; Dhingra, S.; Sutorik, A. C.; Kanatzidis, M. G. *J. Am. Chem. Soc.* **1993**, *115*, 1597-1599.
- (2) Banger, K. K.; Cowen, J.; Hepp, A. F. *Chem. Mater.* **2001**, *13*, 3827-3829.
- (3) Banger, K. K.; Hollingsworth, J. A.; Harris, J. D.; Cowne, J.; Buhro, W. E. et al. *Appl. Organomet. Chem.* **2002**, *16*, 617-627.
- (4) Banger, K. K.; Harris, J. D.; Cowen, J. E.; Hepp, A. F. *Thin Solid Films* **2002**, *403-404*, 390-395.
- (5) Banger, K. K.; Jin, M. H.-C.; Harris, J. D.; Fanwich, P. E.; Hepp, A. F. *Inorg. Chem.* **2003**, *42*, 7713-7715.
- (6) Hollingsworth, J. A.; Banger, K. K.; Jin, M. H.-C.; Harris, J. D.; Cowen, J. E. *Thin Solid Films* **2003**, 63-67.
- (7) Castro, S. L.; Bailey, S. G.; Raffaele, R. P.; Banger, K. K.; Hepp, A. F. *Chem. Mater.* **2003**, *15*, 3142-3147.
- (8) Castro, S. L.; Bailey, S. G.; Raffaele, R. P.; Banger, K. K.; Hepp, A. F. *J. Phys. Chem. B* **2004**, *108*, 12429-12435.
- (9) Nairn, J. J.; Shapiro, P. J.; Twamley, B.; Pounds, T.; von Wandruska, R.; Fletcher, T. R.; Williams, M.; Wang, C.; Norton, M. G. *NanoLett* **2006**, *6*, 1218-1223.
- (10) Williams, M.; Okasha, R. M.; Nairn, J. J.; Twamley, B.; Afifi, T. H. *Chem. Commun.* **2007**, early view.

v) DOE sponsored publications in 2006-2007

- (1) Williams, M.; Okasha, R. M.; Nairn, J. J.; Twamley, B.; Afifi, T. H.; Shapiro, P. J. *Chem. Commun.*, published on the web: 25 May 2007.
- (2) Nairn, J. J.; Shapiro, P. J.; Twamley, B.; Pounds, T.; von Wandruska, R.; Fletcher, T. R.; Williams, M.; Wang, C.; Norton, M. G. *NanoLett* **2006**, *6*, 1218-1223.

Key Physical Mechanisms in Nanostructured Solar Cells

Principal Investigator: Valeria Gabriela Stoleru, Materials Science and Engineering, University of Delaware, Newark, DE; gstoleru@udel.edu

Co-Principal Investigator: Christiana B. Honsberg, Electrical and Computer Engineering, University of Delaware, Newark, DE; honsberg@udel.edu

Collaborator: Andrew G. Norman, National Renewable Energy Laboratory, Golden, CO; andrew_norman@nrel.gov

A. Pancholi and Y. C. Zhang, Materials Science and Engineering, University of Delaware, Newark, DE

Program Scope

Nanostructured solar cells (which include quantum dot-, quantum well-, and quantum wire-based solar cells) have attracted significant interest in recent years since they offer the promise of both high efficiency and low cost, offering a way to reach thermodynamic efficiency limits as well as cost targets. High efficiency is achievable because nanostructured materials are required in order to implement several advanced-concept solar cell designs which can exceed the one-junction Shockley-Queisser efficiency limit, such as solar cells utilizing the two-photon absorption and impact ionization processes, and the quantum well or the intermediate band solar cells, which incorporate multiple-energy levels. Further, through processes such as up/down conversion, they allow improvement of existing solar cell efficiencies through the addition of coatings containing nanostructures. In addition to their efficiency potential, nanostructured solar cells offer the promise of low cost since substantial research efforts are focused on developing low-cost self-assembly approaches to fabricate nanostructures.

While generalized efficiency-limit calculations have predicted high efficiencies for nanostructured solar cells, substantial fundamental theoretical and practical challenges still exist in their implementation. A central factor hindering their development are the theoretical and experimental unknowns regarding the excitation, recombination, and transport properties of solar cells. The goal of the proposed research is to theoretically and experimentally investigate the excitation, recombination, and transport properties on which advanced concept solar cells rely. More specifically, the goal of the project is to study physical and loss mechanisms in nanostructured solar cells and determine properties of nanostructures required for high efficiency solar cells, develop optimum solar cell designs based on experimental findings, and determine the most important properties of the nanostructured solar cells. The proposed work primarily focuses on nanostructure based intermediate band solar cells using multiple absorption and multiple energy level approaches.

Recent Progress

Both structural and optical characterization of multi-stacked strain compensated $\text{In}_{0.47}\text{Ga}_{0.53}\text{As}/\text{GaAs}_{1-x}\text{P}_x$ quantum dot structures were grown on (311)B GaAs substrates by using metal organic vapor phase epitaxy. The structures chosen as a model system for investigating intermediate band solar cells consist of 50 layers of (In,Ga)As quantum dots separated by GaAsP barriers ~ 10 nm thick, in which the phosphorus content was varied between 0.8 and 18%.

A typical TEM micrograph of the structures studied is shown in Fig. 1. The image shows the formation of pseudomorphic, dislocation-free arrays of vertically-coupled quantum dots, with average height and lateral extent of ~ 4 nm and 40-50 nm, respectively.

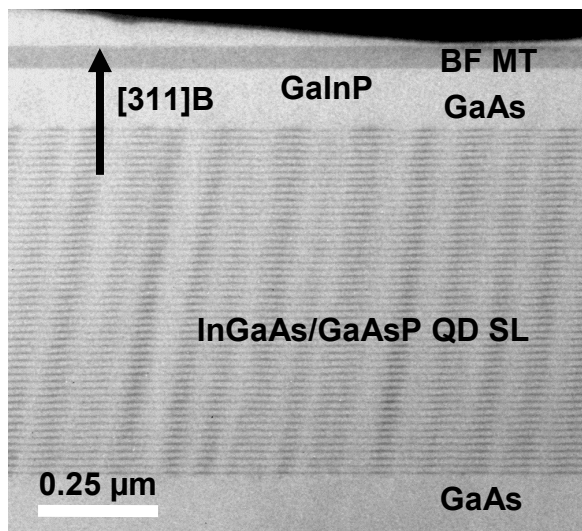


Figure 1: Transmission electron micrograph of multi-stacked InGaAs/GaAsP quantum dot structure (A.G. Norman, NREL)

Temperature and excitation dependent time-integrated and time-resolved photoluminescence (PL) measurements have been conducted and analyzed. We observe reduced PL linewidth in the samples with phosphorus containing barriers compared to the similar structure with no phosphorus in the barrier, indicating more uniform QD size distribution, as illustrated in Fig. 2. This may be due to the strain compensation effect in which the residual compressive strain of buried QD layer does not have a strong effect on the growth of the next QD layer. The increase in PL linewidth with excitation density is due to more quantum dots contributing to PL spectrum with increase in excitation density. Although the dots still form a vertical self-alignment, the sizes of the subsequent layer dots are not necessarily larger than the dot in previous layer as they usually do in the multi-stacked (In,Ga)As/GaAs uncompensated QD structures.

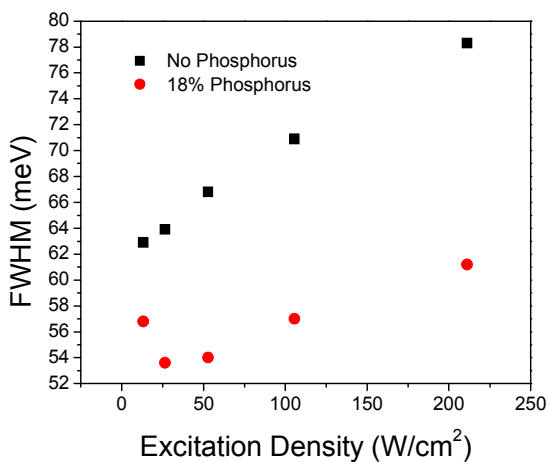


Figure 2: PL linewidth comparison between samples with 18 % P to no P in barrier layers.

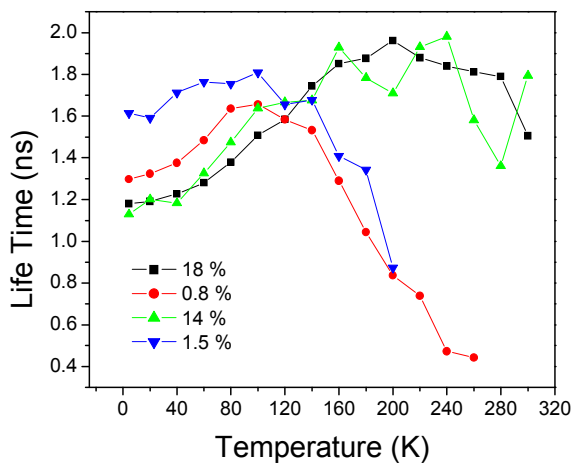


Figure 3: Temperature dependent TRPL on samples with different P barrier composition.

From time-resolved measurements we also found an increased radiative lifetime at room temperature in samples with higher phosphorus content in the barrier layer (see Fig. 3), which may be due to (i) the lower dislocation density as a result of strain compensation and/or (ii) strong carrier confinement in the QDs provided by the barrier. We also studied the effect of electronic coupling on radiative lifetime in the multi-stacked QD structures. An attempt is being made to calculate the energy levels of these structures theoretically by using an eight band $\mathbf{k}\cdot\mathbf{p}$ formalism in which the strain is incorporated and compare the results with the experimentally measured data.

We also measured low temperature ($T = 77$ K) polarization dependent PL from the cleaved edges on all samples. The QD ground state emission was identified to be transverse electric (TE) mode dominated, indicating the dominant transition from the electron ground state to the heavy-hole ground state. Unlike the dots grown on GaAs (001) substrate, where the TE mode of the field is parallel to the dot base (i.e. the sample surface), the TE mode of the electric field showed $\sim 5\text{-}6^\circ$ deviation from the sample surface for the dots grown on GaAs (311)B substrate, as shown in Fig. 4(b). This can be attributed to the shape anisotropy of the dots resulted by the substrate orientation, as verified by the structural transmission electron microscopy analysis. A schematic explanation is provided in Fig. 4(a). The dots grown on (311)B substrates are also aligned at about 9° to the surface normal, which is not the case for the dots grown on (001) substrates. Based on a continuous elasticity model, this inclination angle can be explained by a surface strain field driven by the buried dot. Our studies provide information about the optical anisotropy and spatial ordering of QDs which may be useful in designing the optical coupling for solar cells based on QDs grown on off-oriented substrate.

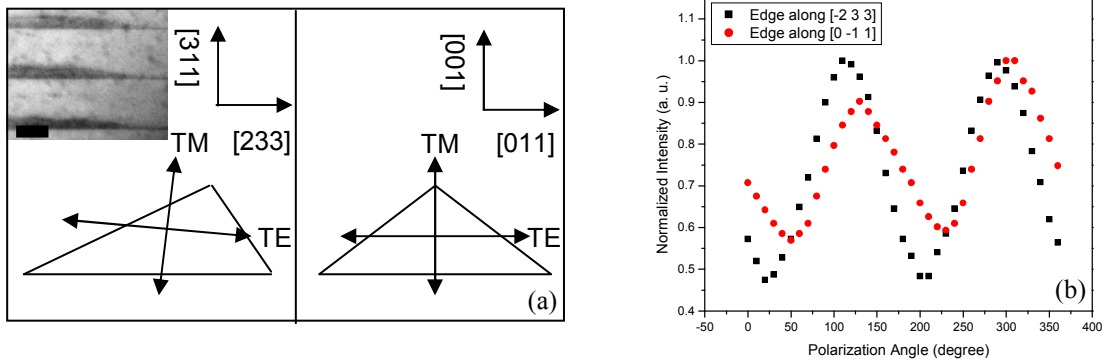


Figure 4: (a) Schematic explanation for asymmetric QDs grown on (311)B GaAs substrate. (Inset: TEM micrograph with asymmetric QD [A.G. Norman, NREL]); (b) Edge emission polarization of QD structure grown on (311)B substrate.

Light I-V curve (Fig. 5(a)) shows that by adding P to barrier layers to achieve strain balance leads to a significant increase in V_{OC} . We also observe reduced current density in Si doped InGaAs/GaAsP QD superlattice (SL) cell in comparison to control cells, which is probably associated with the Si δ -doping. Effective quantum efficiency curves (Fig. 5(b)) show that both InGaAs/GaAs and InGaAs/GaAsP QD SL devices have photoresponses extended to longer wavelengths than those of the control cells.

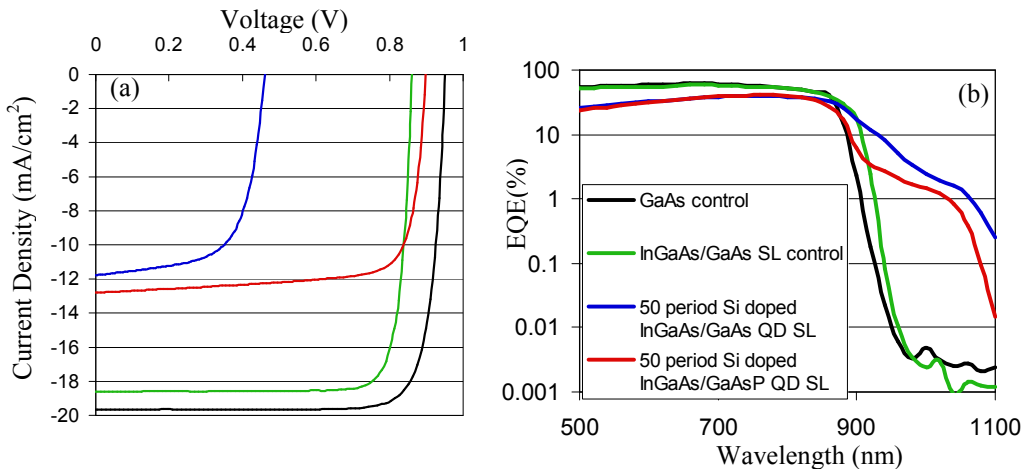


Figure 5: (a) I-V curve and (b) Quantum efficiency for various solar cells devices [A.G. Norman, NREL]

Future Plans

The goal of the proposed project is to demonstrate physical mechanisms which have not been previously observed in high efficiency nanostructured photovoltaic solar cells, to experimentally characterize the structures and the devices in order to determine the impact and the causes of non-idealities, to develop models which include non-idealities and can be used to determine device design rules and optimum solar cell structures based on the new physical mechanisms, and finally, to experimentally implement optimized device structures. The research plan is divided into several components:

- (1) Growth and characterization of quantum well and quantum dot nanostructures;
- (2) Theoretical studies, growth and characterization of quantum well- and quantum dot-based devices, in order to facilitate the demonstration of radiative coupling between multiple quasi-Fermi levels in nanostructured multiple energy level solar cells;
- (3) Theoretical studies, growth and characterization of devices in order to support the demonstration of: (a) transport of carriers in solar cells in which the nanostructures (quantum wells, quantum wires, or quantum dots) are spaced such that their wavefunctions do not overlap, and (b) transport of carriers in closely-spaced quantum dot nanostructures;
- (4) Modeling, growth, fabrication, and characterization of quantum dot- and quantum well-based solar cell devices.

Recent Publications

1. Y.C. Zhang, A. Pancholi, V.G. Stoleru, Size-dependent radiative lifetime in vertically stacked (In,Ga)As quantum dot structures, *Appl. Phys. Lett.* **90**, 183104 (2007).
2. A. Pancholi, Y.C. Zhang, H. Shah, J. Boyle, P. Pancholi, A.G. Norman, V.G. Stoleru, Carrier dynamics in multi-stacked $\text{In}_{0.47}\text{Ga}_{0.53}\text{As}/\text{GaAs}_{1-x}\text{P}_x$ quantum dot solar cells structures, submitted to MRS Fall 2007 Meeting, Boston, Nov. 2007.
3. Y.C. Zhang, A. Pancholi, H. Shah, J. Boyle, P. Pancholi, A.G. Norman, V.G. Stoleru, Optical anisotropy of InGaAs/Ga(As,P) quantum dots grown on GaAs (311)B substrates, submitted to MRS Fall 2007 Meeting, Boston, Nov. 2007.
4. J. Boyle, V.G. Stoleru, Bandstructure engineering in InAs/GaAsSb/GaAs quantum dots for optoelectronics and photovoltaics, submitted to MRS Fall 2007 Meeting, Boston, Nov. 2007.

EPSCOR program at OCHEP

Flera Rizatdinova, Mike Strauss
Oklahoma State University, The University of Oklahoma

The Oklahoma Center for High Energy Physics (OCHEP), an inter-university center for research and education in High Energy Physics (HEP) has been established and is fully operational with the support from a DOE EPSCOR implementation grant. The center is composed of three universities, Oklahoma State University (OSU), the University of Oklahoma (OU), and Langston University (LU), with all active high energy physicists in the state of Oklahoma participating as members in the center. The two major objectives of the DOE EPSCOR grant were (1) to initiate an experimental HEP program at OSU and (2) to establish a Grid Computing Facility at OU. These two objectives have been accomplished. The OSU experimental HEP group is now an official member of the D0 Collaboration at Fermilab and the ATLAS Collaboration at CERN. OU and LU are part of the Southwest Tier 2 Center for ATLAS and is contributing actively to Large Hadron Collider (LHC) and Tevatron data processing and Monte Carlo simulation.

1 Progress of the OCHEP experimental projects

In the past three years, the OCHEP experimental group has performed research at the D0 experiment at the Tevatron and at the ATLAS experiment at the LHC.

Members of OCHEP have made significant contributions to the D0 experiment through their research and leadership roles in crucial areas of the experiment. These are:

- **Discovery of the single top quark production.** Recently, the D0 experiment has announced the evidence of the single top quark production [1]. The primary OCHEP contributor was S. Jain, a postdoctoral fellow working together with OU professor Dr. P. Gutierrez. She has also investigated the production of single top quarks through flavour-changing neutral current interactions. These results are summarized in [2]. Dr. Rizatdinova finalized her analysis on ratio of the branching fraction $t \rightarrow Wb$ to the total branching fraction $t \rightarrow Wq$. This measurement published in [3] sets a new limit on the mixing of the top quark with possible undiscovered fermions.
- **Higgs boson searches.** OCHEP member Dr. Khanov from OSU leads the D0 Collaboration efforts in searches for both Standard Model (SM) and non-SM Higgs bosons as a co-convenor of the D0 Higgs group. Several papers have been submitted to the publication under his leadership. He also conducted a search for the associated SM Higgs production ($p\bar{p} \rightarrow WH$) where Higgs decays to a pair of W bosons. The result [4] represents the world's best upper limit on Higgs boson production in this mode. OU group (Prof. Gutierrez, Drs. S. Jain, A. Pompos and S. Hossain) are looking for a charged Higgs boson production in the top quark decays.

- **Discovery of the B_s oscillations.** B. Abbot, P. Gutierrez and M. Strauss from OU are active participants of the B-physics group at D0. Abbot served as a co-convenor of this group, and later served as a convenor of B mixing and lifetime subgroup. D0 has published the first evidence for B_s oscillations [5] with the frequency consistent with the SM expectations.
- **Tracking and trigger at D0.** One of the most important areas of the D0 experiment is identifying charged particles and measuring their position and momentum. Dr. Strauss is a co-convenor of the tracking group. Under his leadership, Dr. Khanov and Dr. Rizatdinova adapted the newly installed silicon tracker layer into tracking software, and studied the tracking performance of the upgraded tracker. Postdoctoral fellow A. Pompos from OU was in charge of the trigger operations and the maintenance of the trigger lists for the whole experiment.

Research interests of the OCHEP group at the LHC are focused on understanding the mechanism for electroweak symmetry breaking (EWSB). One primary focus is on the search for a heavy charged Higgs boson predicted by extensions of the SM. Presence of heavy flavor jets is a characteristic feature for many physics channels involving charged Higgs boson production and decay. At ATLAS, OCHEP members mainly contribute to:

- **b -tagging algorithms.** Drs. Rizatdinova and Khanov have implemented and tuned a simple b -tagging algorithm that has been initially developed by them for the D0 experiment. The tagging performance of the algorithm has been studied. Currently, the algorithm became a one of the default ATLAS b -tagging algorithms.
- **Upgrade of the pixel detector.** Drs. Rizatdinova's and Skubic's interest in hardware development is focused on vertex detectors. They are committed to pixel detector research and development to improve the characteristics of the existing pixel detector. In August 2006, OCHEP members together with colleagues from Ohio State University irradiated four optoboards with PIN and VCSEL arrays from various vendors using 24 GeV protons at CERN. It was found that responsivity of PIN diodes went down by factor of 2. All VCSEL arrays except the one died after irradiation to the level of SLHC doses. The next step is the creation of the test stand for further measurements of the PIN diodes lifetimes.

2 Progress of the OCHEP theoretical projects

The OCHEP theoretical group is involved in cutting edge research in a wide range of theoretical HEP topics. The focus is on phenomenology of Higgs boson physics, physics of extra dimensions, neutrino masses and oscillations, Grand Unified theories, dark matter, PT-symmetric quantum field theory, and the Casimir effect. A brief summary of these projects completed in the last three years is given below.

- **A new Higgs doublet model** has been proposed by Dr. Nandi and his graduate student Gabriel. It provides an alternative mechanism for tiny mass of neutrinos and

predicts new signals for Higgs boson at LHC. One of the features of this model is that it predicts that the SM Higgs boson will decay to two practically massless Higgs bosons [6].

- **Unification of all the SM particles in extra dimensions** has been considered by Dr. Nandi and his collaborators. Dr. Nandi together with his colleagues constructed a model based on the $SU(8)$ gauge symmetry in six dimensions with $N = 2$ supersymmetry. The model predicts unification of the Yukawa couplings for the third family fermions with the gauge couplings at the unification scale of 2×10^{16} . They also constructed a model which unifies the Higgs couplings of the NMSSM with the gauge couplings, which predicts an interesting implications for the Higgs mass and top quark mass [7].
- **Fermion mass hierarchy and flavour violation.** Dr. Babu with his collaborators have constructed realistic models of quark and lepton masses in the context of the anomalous $U(1)$ flavor symmetry of string origin employing the Froggati-Nielsen mechanism [8]. The model predicts observation of $\mu \rightarrow e\gamma$ decay by ongoing experiments. It also predicts that EDM of neutron and electron should be close to the current experimental limits.
- **Post-sphaleron baryogenesis.** Dr. Babu has proposed a new mechanism for generating the baryon asymmetry of the universe [9]. In this scheme, a SM singlet scalar field S which has a mass of order of 100 GeV decays directly into baryons and antibaryons and produces asymmetry. S couples to $\Delta B = 2$ operator via exchange of colored scalars, which arise naturally in Pati-Salam SM extension. Babu's model predicts the LHC should see colored scalars carrying baryon number with masses of order of TeV. It also predicts existence of neutron-antineutron oscillations that are within the reach of the next generation experiments.
- **Supersymmetric model building.** Dr. Babu has addressed the tachyonic slepton problem of anomaly mediated supersymmetry breaking models. Babu with his collaborators proposed an $SU(3)$ family symmetry for lepton fields, which provides positive squared masses for sleptons. In a second project an extra $U(1)$ symmetry was suggested that is broken along with SUSY at the TeV scale. Both models are easy to check at the LHC.
- **Nonperturbative quantum field theory** is the focus area of Dr. Milton. Specifically, he has helped to set new limits on monopole masses, studied the temperature and local divergence structure of quantum vacuum energy, and developed new alternative non-Hermitian quantum field theories which may have an important implications in describing new physics.
- **Electroweak symmetry breaking** Dr. Kao is investigating a mechanism by which particles acquire their masses, the reasons why top quark is so heavy and neutrino is so light, supersymmetry between bosons and fermions.

3 Grid computing

OCHEP institutions have been chosen by ATLAS management to be part of the Southwest Tier 2 facility. OCHEP has purchased and deployed a large computing cluster with 45 dual P4 Xeon nodes as part of facility encompassing diverse computing resources. This facility serves as a regional analysis center with a significant effort devoted to Tevatron and LHC experiments.

4 Conclusions

OCHEP is fully operational. Faculty members, postdocs and graduate students have published 114 research articles and have presented 77 talks at national and international conferences during three years of the EPSCOR support.

References

- [1] V. M. Abazov et al. [D0 Collaboration], Phys. Rev. Lett. 98, 181802 (2007)
- [2] V. M. Abazov et al. [D0 Collaboration], submitted to Phys. Rev. Lett. (hep-ex/0702005)
- [3] V. M. Abazov et al. [D0 Collaboration], Phys. Lett. B 639, 616 (2006)
- [4] V. M. Abazov et al. [D0 Collaboration], Phys. Rev.Lett. 97, 151804 (2006)
- [5] V. M. Abazov et al. [D0 Collaboration], Phys. Rev.Lett. 97, 021802 (2006)
- [6] S. Gabriel and S. Nandi, hep-ph/0610253
- [7] I. Gogoladze, T. Lu, Y. Mimura and S. Nandi, Phys. Rev. D72, 055006 (2005)
- [8] K.S. Babu and T. Enkhbat, Nucl. Phys. B708, 511 (2005)
- [9] K.S. Babu, R.N. Mohapatra and S. Nasri, Phys. Rev. Lett. 97, 131301 (2006)

“Phase II: The Next Generation Thermoelectric Materials for Solid State Cooling & Power Generation Applications“

Terry M. Tritt (PI), Joe Kolis*, Murray Daw, Fivos Drymiotis**,
Catalina Marinescu and Apparao Rao
Clemson University, Dept. of Physics & Astronomy, Clemson, SC 29634

* Department of Chemistry, Clemson University

** New Hire Supported by DOE Phase I program

I.) Program Scope:

The demand for alternative energy technology to reduce our dependence on fossil fuels along with their environmental impacts leads to very important regimes of research, including that of high temperature energy harvesting via the direct recovery of waste heat and its conversion into useful electrical energy. Thus, the development of higher performance thermoelectric (TE) materials for power generation from waste heat recovery or solar energy conversion is becoming ever more important. As an example, solar cell and thermoelectric cooperative devices can be used in a solar energy system to transform stored heat from a thermal bath storage system into useful electrical energy. Also, a TE device can be directly coupled to a solar collector/concentrator system. An excellent overview of the state of the art TE materials, as well as an overview of recent developments is given in the following references. [1, 2]

Over the past decade there has been a heightened interest in the field of TE's driven by the need for more TE efficient materials for both electronic refrigeration and power generation. [3, 4] Some of the research efforts focus on minimizing the lattice thermal conductivity while other efforts focus on materials that exhibit large power factors. Refrigeration aspects include applications such as cooling electronics (e.g. CPU chips) and optoelectronics (IR detectors and laser diodes) for enhanced performance. [5] The modular aspects of TE cooling devices make them applicable to a wide range of uses. One of the largest current markets incorporates TE cooling devices into automotive seat coolers. Power generation applications are especially important in deep space missions (NASA) where the need for a reliable long-term power source is an absolute necessity. Other technologies such as fuel cell batteries or solar power are not feasible for many of these applications. Given the recent energy needs experienced in the United States there is even a more pressing need to investigate alternative energy conversion technologies, such as thermal to electrical energy conversion from natural heat gradients that TE technologies can provide. The incorporation of TE power generation from recovery of the large amount of waste heat ($\approx 2/3$ of generated power) from an automobile's exhaust or engine and harvesting this into usable "on-board" electrical energy can provide a reduced demand for fossil fuels and reduce their detrimental impact on the environment. [6] In addition, the possibilities within the solar energy conversion technologies may even be much more important. It is not likely that any single technology can solve all the nation's energy needs of the 21st century. It is most probable that it will be a combination of many technologies, one of which we believe will be TE energy conversion.

II.) Recent Progress:

The major programmatic impacts of Phase I funding was the hiring of a new faculty member and the acquisition of several major pieces of experimental equipment. Prof. Drymiotis was a new faculty hire under the Phase I part of the program. He was able to establish a state-of-the-art bulk materials synthesis laboratory. We were able to acquire several major pieces of equipment for enhancement of the research infrastructure. These include: (a) a Netzsch 457 laser flash diffusivity system, (b) a Netzsch

404 high temperature DSC (these two combined allow for high temperature thermal conductivity measurements on bulk materials) (c) a Thermal Technology hot isostatic press to provide high quality densified polycrystalline materials, (d) a Rigaku X-Ray Diffraction apparatus, (e) an Ulvac ZEM-2 high temperature resistivity and Seebeck measurement system and (f) a UV-visible spectrometer that was used to determine the position of the surface plasmon absorption peak Bi nanowires (10 nm).

One of our major scientific successes in Phase I of this DOE Implementation program has been the ability to synthesize thermoelectric nanocomposite materials. A nano-composite is a bulk material, that may weigh several grams, which is comprised of a bulk matrix of one thermoelectric material that has had a large fraction of nanomaterials incorporated into the bulk phase. This second phase of nanomaterials is typically also a good TE material, which may be the same composition as the host or may be very different. A requirement is that one must be able to synthesize large quantities of the nanomaterials that will eventually be incorporated into the nanocomposite, typically via a hot pressing technique of the nanomaterial and the bulk phase.

Using CVD or Hydrothermal Methods: We have been very successful in using both CVD (chemical vapor deposition) methods and hydrothermal methods to synthesize large amounts of TE nanomaterials. For example, we used a CVD method to grow large amounts (100's of mg) of the TE material, PbTe and doped PbTe as shown in Figure 2 below. [7] It is apparent from Figure 1 that the PbTe nanoparticles are about 100 nm cubic particles. We are able to grow large quantities of size selective particles ranging from about 50 nm up to 2 μm or so. The composition and phase purity is confirmed by X-Ray diffraction measurements as shown in Figure 1.

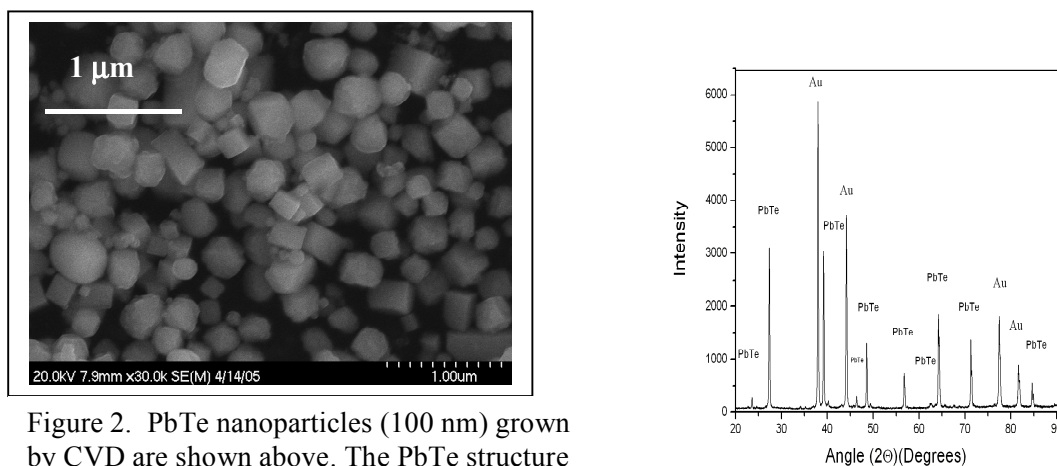


Figure 2. PbTe nanoparticles (100 nm) grown by CVD are shown above. The PbTe structure is confirmed by X-Ray (right).

We have used CVD methods in order to obtain large yield growth of nanostructures of several TE materials including Bi_2Te_3 . In addition, we have also used solvothermal and hydrothermal methods in order to yield large quantities (grams per growth) of other TE materials such as: PbTe, Bi_2Te_3 , Bi_2S_3 and CoSb_3 . Skutterudite nanomaterials were also grown via this technique, such as CoSb_3 . The techniques are described in more detail elsewhere. [24, 8] The nanomaterials can vary in size from several nanometers to submicron and subsequently even several micron size materials, depending on the material and the conditions. These materials are then incorporated into a bulk structure using our hot pressing capabilities and investigated as a bulk composite made up of the parent material and the incorporated nanostructured material. In addition, we have synthesized large amounts of nanoscaled CoSb_3 and mixed with other non-reactive nanomaterials though hot pressing. Incorporating these nanoparticles into a composite should lower the lattice thermal conductivity. Results on each system will be presented. It has been known since the 1980s that the ZT for highly disordered PbTe alloys with a

mean grain size of 1 μm could be $\sim 10\%$ higher than the equivalent single-crystal value. In addition, we believe that investigations of the interface of these nanostructures and its role after hot pressing could be very interesting scientifically. We have recently developed a technique with which the hydrothermal techniques are used to grow the nanostructures directly onto seed particles. [9] The seed particles can be either nanoparticles or small particle size-grains. This has been performed successfully in the PbTe system and these results will be discussed.

III.) Future Plans:

An exciting possibility for increasing the efficiency is based on preparing thermoelectric materials that includes an inherent nanophase component. This research direction has been motivated by several recent theoretical and experimental investigations. It was proposed by Hicks *et al.* that an increase in ZT can be expected due to an increase in the electronic DOS per unit volume in quantum-well structures. [10] The results from an experimental measurement of a 2-D PbTe/Pb_{1-x}Eu_xTe quantum well system found such a large increase in the figure of merit confirming this prediction. [11] Thus, by shrinking conventional thermoelectric materials to the nanoscale it may be possible to convert these materials into higher efficiency materials. [12, 13] Certainly low dimensional structures of TE materials have shown to possess higher ZT values than their bulk counterparts such as the PbTe quantum dot structures [14] and the Bi₂Te₃/Sb₂Te₃ superlattice materials have already been shown to be quite feasible. [15] Therefore we plan to:

- Develop methods of synthesis and investigate thermally stable phases of TE materials embedded with nanoparticles of a semiconducting phase (e.g. rare-earth oxides).
- Utilize current method of hydrothermal and solvothermal synthesis of nanostructures in order to incorporate these nanostructures into a matrix of a high ZT filled TE materials, thus forming a TE nanocomposite. Hopefully, point defect, strain field and two-phase effects will yield significant reductions in the lattice thermal conductivity. Investigate effect of nanoparticle size and density of nanoparticles on phonon scattering; and investigate κ_L reduction by employing distributed particle sizes to scatter phonons over a broad spectrum.
- Utilize spark plasma sintering techniques to form highly densified TE nano-composite materials. Investigate role of overall density on the specific thermoelectric properties of the nano-composites.
- Develop the TE phenomenology of composites through investigation of effects of microstructure and bandgap on thermopower and electrical conductivity in order to provide the basis for identifying and evaluating the relevant transport mechanisms that can contribute to the enhancement in the power factor, $\alpha^2 T/\rho$.
- Characterize the structural, electrical and thermal properties; and subsequently analyze and model the TE properties. This will occur over a broad range of temperature from 10 K up to temperatures as high 1400 K.

Summarizing, the proposed composites and nano-composites will contain selective second TE phases or nano-inclusions, and that the microstructure and local composition must not change at high temperatures (e.g, 600-800°C). The role of the specific nanoparticles, size and/or density of nanoparticles and the interface effects and interface materials will be a major focus of our Phase II investigations. The composites to be designed are to have the following material characteristics:

IV. References:

1. *Harvesting Energy through Thermoelectrics: Power Generation & Cooling*, special edition MRS Bulletin, Vol. **31**, 2006 guest editors: Terry M. Tritt and M. A. Subramanian.

-
2. G. S. Nolas, J. Sharp and H. J. Goldsmid, *Thermoelectrics: Basic Principles and New Materials Developments*, Springer New York (2000)
 3. The reader is referred to many of the recent MRS Proceedings on the topic of thermoelectric materials and energy conversion technologies. MRS Proceedings, **478** (1997), **545** (1998), **626** (2000), **691**(2001), **793** (2003) and **886** (2005)
 4. Terry M. Tritt, (volumes editor): "*Recent Trends in Thermoelectric Materials Research*", Semiconductors and Semimetals, Volumes **69**, **70** and **71**, Treatise editors, R. K. Willardson and E. Weber, Academic Press, New York, (2000)
 5. Andrew W. Allen, Detector Handbook, *Thermoelectrically Cooled IR Detectors Beat the Heat*, Laser Focus World, Volume **33**, pS15, March issue 1997.
 6. *Thermoelectric Materials for Space and Automotive Power Applications*, J. Yang and T. Caillat, special edition MRS Bulletin, Vol. **31**, 2006
 7. B. Zhang, J. He and Terry M. Tritt, Appl. Phys. Lett., **88**, 043119 (2006)
 8. X. Ji, J. W. Kolis and Terry M. Tritt unpublished
 9. Bo Zhang, J. He and **Terry M. Tritt**, Appl. Phys. Lett., **88**, 043119 (2006)
 10. Hicks et al., Phys Rev B, **47**, 12727 (1993).
 11. Hicks et al., Phys Rev B, **53**, R10493 (1996).
 12. M.S. Dresselhaus, G. Chen, M.Y. Tang, R.G. Yang, H. Lee, D.Z. Wang, Z.F. Ren, J.P. Fleurial, and P. Gogna, Mater. Res. Soc. Symp. Proc. 886, 170056 (2005)
 13. Terry M. Tritt, *et.al.*, MRS Fall 2005, MRS Proceedings Volume **886**, p53 (2005)
 14. T.C. Harman, P.J. Taylor, M.P. Walsh, and B.E. LaForge, Science **297**, 2229 (2002).
 15. R. Venkatasubramanian, E. Siivola, T. Colpitts, and B. O'Quinn, Nature **413**, 597 (2001).

V.) DOE Sponsored Publications (Selected Highlights): 2004-2007

Synthesis and Thermoelectric Properties of "Nano-Engineered" CoSb₃ Skutterudite Materials

P. N. Alboni, X. Ji, J. He, N. Gothard, J. Hubbard, and Terry M. Tritt Jour Elec. Materials, (2007) in press

Solution-chemical synthesis of nano-structured Bi₂Te₃ and PbTe thermoelectric materials

X. Ji, J. He, B. Zhang and Terry M. Tritt Jour Elec. Materials, (2007) in press

Laser-assisted Synthesis and Optical Properties of Bismuth Nanorods

Jason Reppert Rahul Rao; Malcolm Skove; Jian He; Matthew Craps; Terry Tritt; Apparao M Rao, Chem. Phys. Lett., in press

Size-Selective High-yield Growth of Lead Telluride (PbTe) Nanocrystals Using a

CVD Technique, Bo Zhang, J. He and Terry M. Tritt, Appl. Phys. Lett., **88**, 043119 (2006)

Controlled Two-Dimensional Coated Nanostructures for Bulk Thermoelectric Composites

B. Zhang, J. He, X. Ji and Terry M. Tritt, Amar Kumbhar Appl. Phys. Lett., **89**, 163114 (2006)

Selected for The Virtual Journal of Nanoscale Science & Technology (*Oct. 30, 2006 issue*)

Sample Probe to Measure Resistivity and Thermopower in the Temperature Range: 300 – 1000 K

V. Ponnambalam, S. Lindsey, N. S. Hickman and Terry M. Tritt, Rev. of Sci. Instrum, **77**, 073904 (2006)

Thermoelectric properties of the new polytelluride Ba₃Cu_{1-δ}Te₁₂,

Abdeljalil Assoud, Stephanie Thomas, Brodie Sutherland, Huqin Zhang, Terry M. Tritt, Holger Kleinke, Chem. Mater. **18**, pp 3866-06 (2006)

New Directions in Bulk Thermoelectric Materials Research.

Terry M. Tritt MRS Fall 2005, MRS Proceedings Volume **886**, p53 (2006)

Ubiquitous Computing and Monitoring System (UCoMS) for Discovery and Management of Energy Resources

University of Louisiana at Lafayette, Louisiana State University, and Southern Univ. at Baton Rouge
URL – <http://www.ucoms.org>

Project Scope

This UCoMS research is funded by U.S. DoE and Louisiana Board of Regents, involving faculty members from three Louisiana institutions (with the project key investigators listed in the footnote below). The project involves three research areas: wireless and sensor networks, Grid computing, and applications, with the goals of creating new knowledge to push forward the technology forefronts on pertinent research topics, developing and disseminating software codes and toolkits for the research community and the public, and establishing system prototypes and testbeds for evaluating innovative techniques and methods. It targets at the petroleum applications to arrive at technical solutions for production data logging and processing, reservoir development optimization, and infrastructure monitoring and intrusion detection. Such applications require intensive computing, large storage space, and/or high speed, real-time data acquisition, calling for collaborative effort of investigators with diverse background and technical skills exemplified by this research team [24].

The ultimate goal of this UCoMS project lies in deriving an end-to-end solution for a petroleum production application. The end-to-end solution involves sensor data gathering and wireless transmission, sensor data storage following the WITSML standard format, reservoir simulation using the computational Grid testbed established with gathered live data as its inputs, and outcomes visualization for production management use. The goal is to be achieved by fulfilling ten technical milestones: (1) to develop and evaluate efficient and energy-saving sensor networks, (2) to design and assess high-bandwidth and reliable wireless communication protocols, (3) to develop and test Grid application toolkits and relevant Cactus thorns, (4) to pursue and implement enhanced resource information and data management services for computational Grids, (5) to implement and demonstrate reservoir simulation studies using the Grid, (6) develop and evaluate outcome visualization software, (7) to develop and implement a unified Grid portal for steering and managing implemented infrastructure, functions and software, (8) to design and fabricate an energy-saving sensor processors, (9) to implement and evaluate object recognition and tracking techniques for monitoring use with video data, and (10) to develop and evaluate efficient Grid task execution management service.

Recent Progress

This UCoMS research cluster has made considerable progress in all the three research areas: wireless and sensor networks, Grid computing, and applications, in terms of new knowledge creation, software code development and dissemination, and system prototypes and testbeds establishment. Industrial and academic partners in the areas of petroleum production testing and petroleum IT application have been formed successfully. Collaborative work among investigators from participating institutions has yielded the establishment of a Grid testbed comprising computer clusters at Center for Advanced Computer Studies (CACS, UL Lafayette) and at Center for Computation & Technology (CCT, LSU) for application program execution. A wireless mesh network has been developed and deployed at the UL campus as a key testbed for evaluating and fine-tuning new techniques and algorithms in connection with wireless and sensor networks developed by UCoMS researchers. A unified Grid portal has been developed and implemented for steering and managing

This project was supported in part by the U.S. Department of Energy under Award Number DE-FG02-04ER46136, and by the Board of Regents, State of Louisiana under Contract No. DOE/LEQSF(2004-07)-ULL. Key investigators of this project include: Nian-Feng Tzeng (lead PI), Magdy Bayoumi, Hongyi Wu, Gabrielle Allen, Dmitri Perkins, Chris White, Zhou Lei, Boyun Guo, Edward Seidel, John Smith, and Douglas Moreman. The project is directed by Michael Khonsari (with Louisiana Board of Regents). Questions regarding this article can be directed to the lead PI at tzeng@cacs.louisiana.edu or through phone no. (337)482-6304.

implemented infrastructure, functions and software, through collaborative effort extensively by investigators from three involved institutions [23]. The standardized data format for sensor data acquisition and storage has been ironed out by UL and LSU investigators, following the WITSML (Wellsite Information Transfer Standard Markup Language) standard, facilitating the development of Cactus thorns for automatic parallel processing of applications inputted with those data. Key project progress is highlighted in sequence.

- **Unified UCoMS Portal.** As a diverse research cluster, UCoMS encompasses various disciplines each with its new techniques and software modules/tools together for an end-to-end solution, calling for a unified user-friendly interface to take advantage of UCoMS solutions. We have developed and deployed such a unified portal to steer computation-intensive reservoir simulation (which involves massive amounts of data), to control wireless sensor networks (to collect and process real-time data from production sites), and to manage reliable and high-bandwidth communications over a wireless mesh network (for streaming production data collected in the field to the computational and storage Grids) [23]. The portal has been largely completed, with certain new portlets to be added for expanding its capability called upon by users.
- **Wireless Mesh Network Testbed.** A wireless mesh network testbed has been completed, and it comprises 7 routers currently, each with two IEEE 802.11a/b/g radio cards, to cover approximately 70 acres on the UL campus. The testbed has been evaluated using video streams and large file transfers, and it will be expanded to contain 12-15 routers and to incorporate remote video surveillance cameras and sensor ad hoc networks.
- **Computational Grid.** A computational Grid has been established to include computer clusters located at CACS (namely, CANGrid and CANBlade), at CCT (namely, SuperMike and SuperHelix), and at the Thai National Grid. It enables the empirical evaluation of new Grid computing techniques and petroleum applications we have developed under this research cluster effort.
- **Research Outcomes and Publications.** The research cluster has yielded rich research findings, leading to impressive publications and presentations in major journals and various technical conferences. Research topics carried out are listed below according to the research areas.

Wireless and Sensor Networks

Six research topics in this area have been pursued by project investigators recently, including (1) An effective prioritized medium access control (MAC) protocol based on the binary countdown approach to differentiate packets in multiple service classes following their priority levels, achieving the support of different service levels for the first time [1], (2) Minimum-cost data delivery in heterogeneous wireless networks, which was identified to be NP-hard [2] and then was solved using linear programming (LP) for reducing the overall communication cost effectively, with small overhead (< 3%) for signaling, computing, and handoff, (3) Energy-efficient framework for wireless sensor networks, which are critical, given that each sensor node relies on its limited battery power for data acquisition, processing, transmission, and reception; our proposed framework aims to reduce the number of queries for the sensor energy status dispatched by cluster heads using two types of energy reading information aggregates: range-based and location-based ones, as detailed in two publications [3, 4], (4) Energy-efficient communications, realized via integrated power control and load balancing for even distribution of sensor residual energy, thus prolonging the lifetime of overall wireless sensor networks [5], (5) RFID-based 3-D positioning schemes, which can locate an object in a 3-dimensional space, with reference to a predetermined arbitrary coordinates system, by using RFID tags and readers, following the active and the passive positioning schemes [6], and (6) Automated scene surveillance by network of sensors and data fusion, which includes object processing units, an object detection module, and a multi-agent tracking system for scene understanding in our design to support object detection [7, 8].

Grid Computing

We have developed ResGrid to ease deployment of large-scale applications over a Grid [9]. In addition, we have designed and implemented a new information service and a suite of task manipulation tools for ResGrid performance improvement, with the former suitable for multicluster Grid environments [10] and the latter for manipulating tasks over the clusters (such as status tracking, task migration, task removal, task resubmission, etc.) [11]. Meanwhile, we have devised heuristic algorithms able to attain highly reliable

checkpointing arrangements in a mobile Grid, following our reliability-driven protocol [12], which is demonstrated to compare favorably with a baseline protocol where checkpointing arrangement is carried out by neutral heuristics. We also have developed one general framework for communicating live real-world drilling sensor data as inputs to simulation executed on the computational Grid, employing the Cactus open-source high-performance scientific computing code, with results displayed and recommendations provided [13]. Separately, we have arrived at a fast and scalable resource discovery mechanism, based on a distributed hash table (DHT) approach, in support of multi-attribute range queries for resource discovery in large-scale heterogeneous Grids [14].

Applications

Given the need to identify vibration and deformation modes in drilling applications, we have modeled the identified regimens of torsional vibration for accommodating various operating parameters [15]. As the abnormal production decline of a gas well could be due to a number of reasons, including liquid loading, we also have developed a more accurate method to diagnose the liquid loading problem [16]. Separately, pressure instability is one of the major threats in under-balanced drilling, possibly causing drilling failures. We have devised a mathematical model that can be incorporated with analyses of pressure data from real-time measurements during drilling for pressure instability analyses, with our key findings reported in [17]. In addition, we have developed a more accurate computer simulator, by combining the composite IPR model with Poettmann & Carpenter correlation, for predicting the well production rate, with oil and gas wells treated differently, to give rise to accuracy within 3.1% [18]. We also have arrived at an analytic model for inflow performance prediction of horizontal wells, with its details and results provided in [19]. We have demonstrated [20] a geostatistical study of 3-dimensional displacement in heterogeneous reservoirs using a parallel IMPES reservoir simulator, following a designed workflow [22]. Accurately analyzing various reservoir uncertainty factors is challenging due to its associated large-scale data manipulation and massive simulation runs which cannot be handled easily with typical computing resources. We have leveraged the computing Grid to address this challenge, with suitable data replication tools implemented for manipulating raw data and simulation results [21].

Future Plans

This research cluster is scheduled to complete on Aug. 14, 2007, with a renewal proposal submitted in February 2007 to seek for continuing funding from Aug. 15, 2007 to Aug. 14, 2010. Future research plans are outlined as follows. First, the unified portal developed will be enriched to include three portlets for controlling and managing the wireless mesh testbed, and for video monitoring and surveillance, and for Grid resource display and job scheduling, respectively. Second, testbeds and infrastructure will be expanded and enhanced, including (1) the incorporation of adaptive routing and data security software in our wireless mesh network testbed to permit evaluation of new techniques and protocols developed under this research, and (2) the extension of our developed computational Grid to add computing resources in other campuses (like Louisiana Tech) and possibly other countries as well (like Singapore and Poland), with additional Grid utilities and tools incorporated to ease execution of applications. Third, the research topics pursued under this project will be explored further; in particular, we shall (1) enhance our RFID-based positioning technique with low-cost ultrasound transceivers to arrive at highly accurate localization results, (2) improve our proposed CDMA-based wireless mesh network by means of new carrier sensing schemes, (3) expand our scalability evaluation to accommodate a more adequate correlation matrix of individual performance metrics for comparing different functions involved in the overall scalability index, (4) devise efficient checkpointing data derivation and transmission techniques for mobile Grids to lower checkpointing overhead, (5) implement a faster reservoir simulation code based on high-order finite difference methods for solving the Convection-Diffusion equation, and (6) complete our inflow performance evaluation of horizontal wells.

This DoE-sponsored research cluster seeks to continue the technical advances made through UCoMS' diverse and successful activities summarized above. We intend to complete a highly modularized end-to-end system solution for geoscience applications (noticeably, reservoir simulation and operational safety & security surveillance) via integrating various functional blocks already developed and those planned for development. The solution will have a broad impact on the discovery and management of energy resources nationwide.

DOE-Sponsored Publications (partial list for 2006-2007)

- [1] Y. Li, H. Wu, N.-F. Tzeng, D. Perkins, and M. Bayoumi, "MAC-SCC: A Medium Access Control Protocol for Mobile Ad Hoc Networks," *IEEE Transactions on Wireless Communications*, vol. 5, pp. 1805-1817, July 2006.
- [2] H. Chen, H. Wu, S. Kumar, and N.-F. Tzeng, "Minimum-Cost Data Delivery in Heterogeneous Wireless Networks," accepted for publication in *IEEE Transactions on Vehicular Technology*.
- [3] M. Bhattacharyya, A. Kumar, M. Bayoumi, "A Framework for Assessing Residual Energy in Wireless Sensor Network," *International Journal of Sensor Networks*, vol. 2, 2007, pp. 256-272.
- [4] M. Bhattacharyya, A. Kumar, M. Bayoumi, "Design and Analysis of Energy Reference Metric in a Cluster Based Wireless Sensor Network," *Proc. IEEE Int'l Conf. Circuits & Systems for Communications (ICCSC '06)*, July 2006.
- [5] Y. Wang, H. Wu, and N.-F. Tzeng, "Energy-Efficient Communications in Wireless Sensor Networks: An Integrated Approach on Power Control and Load Balancing," accepted for publication in *International Journal on Ad Hoc & Sensor Wireless Networks*.
- [6] C. Wang, H. Wu, and N.-F. Tzeng, "RFID-Based 3-D Positioning Schemes," *Proceedings of 26th Annual IEEE Conference on Computer Communications (IEEE INFOCOM '07)*, May 2007.
- [7] R. Aguilar-Ponce, A. Kumar, J. TecpanecatI-Xihuitl, and M. Bayoumi, "Automated Object Detection and Tracking for Intelligent Visual Surveillance Based on Sensor Network," *Artificial Intelligence and Integrated Intelligent Information Systems: Emerging Techniques and Applications*, Idea-Group Press, 2006.
- [8] R. Aguilar-Ponce, A. Kumar, J. TecpanecatI-Xihuitl, and M. Bayoumi, "A Network of Sensors Based Framework for Automated Visual Surveillance," *Journal of Networks and Computer Applications*, Elsevier (to appear in 2007).
- [9] Z. Lei, D. Huang, A. Kulshrestha, S. Pena, G. Allen, X. Li, R. Duff, S. Kalla, C. D. White, and J. R. Smith, "ResGrid: A Grid-aware Toolkit for Reservoir Uncertainty Analysis," *Proc. of IEEE International Symposium on Cluster Computing and the Grid (CCGrid 2006)*, May 2006, pp. 249-252.
- [10] L. Lewis, M. Xie *et al.*, "Resource Management for Multicluster Grids," *Proceedings of 2007 Louisiana Academy of Science Conference*, Mar. 2007.
- [11] S. Pena, D. Huang *et al.*, "A Generic Task-Farming Framework for Reservoir Analysis in A Grid Environment," *Proceedings of International Conference on Parallel Processing (ICPP) Workshops*, Aug. 2006, pp. 426-434.
- [12] P. J. Darby III and N.-F. Tzeng, "Peer-to-Peer Checkpointing Arrangement for Mobile Grid Computing Systems," accepted for presentation at 16th IEEE International Symposium on High Performance Distributed Computing (HPDC 2007) in June 2007.
- [13] R. Duff and Y. El-Khamra, "Real-Time Simulation in Grid Environments: Communicating Data from Sensors to Scientific Simulations," *Proc. 2007 Digital Energy Conference and Exhibition*, Paper No. SPE 107561, April 2007.
- [14] M. M. Ghantous, D. Smith, and N.-F. Tzeng, "FaSRed: Fast and Scalable Resource Discovery in Support of Multiple Resource Range Requirements for Computational Grids," submitted for possible presentation.
- [15] R. Duff, "Observation and Modeling of Identified Regimens of Torsional Vibration," *Proceedings of 2007 AADE (American Association of Drilling Engineers) National Technical Conference and Exhibition*, April 2007.
- [16] B. Guo and A. Ghalambor, "Characterization and Analysis of Pressure Instability in Aerated Liquid Drilling," *Journal of Canadian Petroleum Technology*, vol. 45, July 2006.
- [17] K. Sun, B. Guo, and A. Ghalambor, "An Analytical Solution for Aerated Mud and Foam Drilling Hydraulics in Deviated Holes," *Journal of Canadian Petroleum Technology*, vol. 45, Mar. 2006.
- [18] B. Guo, K. Lin, and A. Ghalambor, "A Rigorous Composite-IPR Model for Multilateral Wells," *Proceedings of SPE Annual Technical Conference and Exhibition (ATCE 2006)*, Paper No. SPE 100923, Sept. 2006.
- [19] B. Guo, J. Zhou, Y. Liu, and A. Ghalambor, "A Rigorous Analytical Model for Fluid Flow in Drain Holes of Finite Conductivity Applied to Horizontal and Multilateral Wells," *Proceedings of SPE 2007 Production Operations Symposium*, Paper No. SPE 106947, April 2007.
- [20] X. Li, C. White *et al.*, "Beyond Queues: Using Grid Computing for Simulation Studies," *Proceedings of 2007 Digital Energy Conference and Exhibition*, Paper No. SPE 106949, April 2007.
- [21] Z. Lei, D. Huang, A. Kulshrestha, S. Pena, G. Allen, X. Li, R. Duff, S. Kalla, C. D. White, and J. R. Smith, "Leveraging Grid Technologies for Reservoir Uncertainty Analysis," *Proceedings of High Performance Computing Symposium (HPC 2006)*, April 2006.
- [22] G. Allen *et al.*, "A Workflow Approach to Designed Reservoir Study," accepted for presentation in 2dn Workshop on Workflows in Support of Large-Scale Science, June 2007.
- [23] P. Chakraborty, A. Lewis, I. Jangjaimon, J. Lewis, I. Chang-Yen, Z. Lei, N.-F. Tzeng, and G. Allen, "A Grid-Oriented Infrastructure for Managing Energy Resources," submitted for possible presentation.
- [24] N.-F. Tzeng, M. Bayoumi, H. Wu, E. Seidel, G. Allen, D. Perkins, Z. Lei, B. Guo, A. Ghalambor, D. Moreman, "Techniques for Meeting the Communication and Computing Needs in Energy Resource Discovery and Management," submitted for possible presentation.

Experimental and Numerical Investigation of Flows in Expanding Channels

Peter Vorobieff and Vakhtang Putkaradze

kalmoth@unm.edu, vakhtang@unm.edu

Department of Mechanical Engineering

The University of New Mexico, MSC01 115, Albuquerque, NM 87131

Program Scope

In any machinery operating with fluids, expanding or contracting ducts are ubiquitous. In the simplest idealized case, a duct has planar walls, expanding or contracting in the $x - y$ plane, with the $x - y$ cross-section z -independent for some considerable range of z . For a slow-moving fluid flow in this geometry, a simple solution exists which can be described by analytical formulæ (Jeffery-Hamel, or JH, flow)^{1,2}. JH solutions are perhaps the most fundamental in fluid mechanics; they concern two-dimensional stationary flows of an incompressible viscous fluid in an idealized expanding (contracting) channel, or wedge. Moreover, modifications and generalizations of the JH similarity solution have provided analytical templates for a large variety of exact solutions of the 2D boundary layer equations for corner, wedge, sink, and other flows. In JH flows, the characteristic flow rate is usually described in terms of the Reynolds number $R = Q/\nu$, where Q is volume flux per unit length of the source in the z -direction and ν is the fluid kinematic viscosity. For a symmetric channel, the flow for small R is symmetric, with maximum velocity in the center. When the Reynolds number increases, this simple solution ceases to exist. The flow breaks the symmetry (bifurcates), with most of the fluid going in a thin layer along one wall. The fluid is prevented from utilizing the whole area of the expanding channel by a recirculation vortex which blocks the exit. In addition, secondary instabilities driven by this vortical motion develop in this flow. This proposal addresses the least studied regime of the intermediate Reynolds numbers separating the zones of low- R nearly-2D deterministic flow and high- R turbulent flow which can be assessed statistically. We study both the stationary bifurcations and the non-stationary transitional flow features. The understanding of the flow physics is achieved through a combination of experimental, theoretical and numerical studies. This study is also of interest as an experimental benchmark for numerical code validation.

Recent Progress

The subtly intricate nature of the JH solutions and their practical importance motivated many stability studies of JH flows. A serious problem for the stability analysis is the lack of realistic boundary conditions at the outlet, while the choice of different boundary conditions can lead to different results. This would tremendously complicate any purely theoretical investigation of the selection mechanism and solution stability in JH flow. However, these ambiguities related to the boundary conditions can be trivially resolved in experiment. Quite surprisingly, until the results of our work sponsored by the DOE EPSCoR grant were published, there had been no consistent experimental study of JH flows and their bifurcations.

Figure 1 presents a summary of the possible radial velocity profiles in wedge flows. The simplest are the pure inflow (“I”) and pure outflow (“O”) solutions, corresponding to a sink or a source at the narrowest contraction point of the channel. An asymmetric profile (IO) is also

known to be realized. Another symmetric profile with two inflow zones (IOI) is known from theory.

In our experiment, JH flows are realized in a long (38.6 cm in the direction parallel to the visualization axis) rectangular acrylic container placed inside a much larger water tank (total volume 60 l). The container has a 0.2 cm wide slit in the bottom. Two 10.2 cm long inclined walls are attached at a fixed angle to the bottom near the slit. Multiple containers were fabricated, with the angle between the walls varying from 12 to 60 degrees. The flow field is visualized by illuminating a planar section of the flow (corresponding to the $x - y$ plane), with a pulsed laser sheet. The fluid in the container (water) is seeded with a small volume fraction of tracer particles (titanium dioxide flakes). A high-resolution digital camera captures the images of the flow fields both for visualization purposes and for quantitative acquisition of the flow fields using particle image velocimetry (PIV)³.

Our results confirm the stability of the pure outflow (Fig. 1, “O”) solution, whenever it exists. As the flow rate in the outflow regime and the Reynolds number increase, a different solution is realized, with the radial velocity profile roughly corresponding to the asymmetrical solution (Fig. 1, “IO”). In reality, the velocity vectors in this flow are no longer oriented in the radial direction (as was the case for the low- R pure outflow). Instead, a large recirculating vortex forms and attaches itself to one of the walls. However, the large-scale structure of the flow remains spatially two-dimensional.

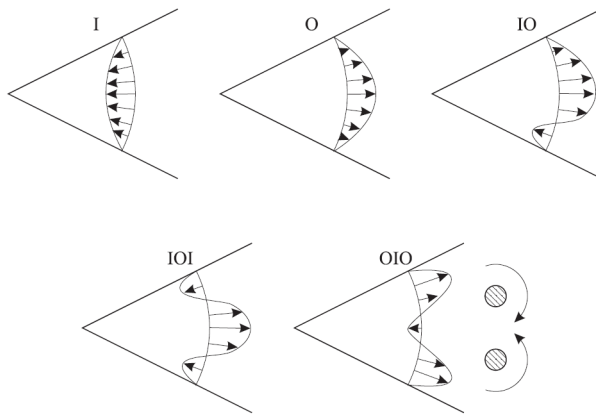


Figure 1. Flow regimes in different types of Jeffery-Hamel flows. Each type of flow is labeled by a different type of symbols I (inflow) and O (outflow).

We found that the value of the Reynolds number characterizing the transition between the symmetric radial outflow regime and the vortex-dominated asymmetric regime depends on the direction of the transition. In other words, as we increase the flow rate, the critical Reynolds number at which the flow transitions to the asymmetric regime is higher than the corresponding Reynolds number for the reverse transition as the flow rate is decreased – the phenomenon known as hysteresis. The existence of hysteretic transition between these flow regimes was quite surprising, as it has no explanation within the traditional JH theory.

Instead, we attribute the existence of this hysteresis to a temporally transient, convective (in the sense that it propagates downstream with the flow) instability. If this instability develops slowly enough, it is flushed out of the system without changing the flow pattern. However, if vortex roll-up due to this instability occurs on the same or smaller time scale as the time it takes for the fluid to exit the system, the flow is destabilized. The delay between the transition to vortex-dominated flow as the Reynolds number is increased is successfully explained by

invoking this destabilization mechanism.

Notably, secondary shear-driven instabilities of the large vortex manifested themselves as soon as the vortex formed. This observation was consistent with the results of separate shear-driven instability studies carried out in a novel quasi-two-dimensional shear flow generator based on a soap film tunnel⁴. In addition, that investigation revealed some features peculiar to soap film systems. Interaction with air surrounding the quasi-two-dimensional flow in the film of soap suspended between two nylon wires led to preferential removal of energy from vortices of large scales, and since in two-dimensional turbulence, unlike its better known three-dimensional analog, the energy cascade moves kinetic energy from smaller vortices to larger ones, this energy removal led to formation of fossil turbulence structures advected by the flow but no longer evolving.

Recently, an interesting stationary solution in JH flow geometry has been discovered⁵. The solution consists of periodically spaced vortices attached alternatively to either left or right walls. The boundary conditions for this solution have to be periodic in the inlet and outlet. The apparently nonphysical boundary conditions notwithstanding, we have managed to realize such a solution in our experiment. This solution is transient, but the time scale over which it decays (10 minutes) is much longer than the equilibration time for this regime. The decay of this solution happens when the inner vortex “squeezes out” the outer vortex and thus is due to the discrepancy in boundary conditions.

Future Plans

We will investigate the influence of boundary conditions on the selection of the morphology that is realized in the flow. The boundary conditions are known to influence the stability of the solutions. Specifically, we will use a combination of rotors/impellers, as shown in the last picture of Fig. 1 (label “OIO”), in an attempt to realize flow regimes that do not occur naturally in wedge flows. Also we will attempt to use similar forcing to re-stabilize the pure outflow solution at flow rates above the bifurcation boundary. We will conduct further studies of multi-vortex transient regimes.

References

- (1) Jeffery, G.B., “The Two-Dimensional Steady Motion of a Viscous Fluid,” *Phil. Mag.* Vol. 29 (6), pp. 455-465 (1915).
- (2) Hamel, G., “Spiralförmige Bewegungen zäher Flüssigkeiten,” *Jahresbericht Deutsch. Math. Verein* Vol. 25, pp. 34-60 (1916).
- (3) Grant, I., “Particle image velocimetry: A review,” *Proc. Inst. Mech. Eng., Part C: J. Mech. Eng. Sci.* Vol. 211 no.1, pp. 55-76 (1997).
- (4) Georgiev, D., and Vorobieff, P., “The slowest soap-film tunnel in the Southwest,” *Rev. Sci. Instrum.* Vol. 73 (3), pp. 1177-1184 (2002).
- (5) Kerswell, R.R., Tutty, O.R., and Drazin, P.G., “Steady nonlinear waves in diverging channel flow,” *J. Fluid Mech.* Vol. 501, pp. 231-250 (2004).

DOE Sponsored Publications

Holm, D.D., Putkaradze, V., Weidman, P. D., and Wingate, B., "Boundary effects on exact solutions of the Lagrangian-averaged Navier-Stokes equations," *Journal of Statistical Physics* vol. 113 (5/6), pp. 841-854 (2003).

Holm, D.D., Putkaradze, V., and Stechmann, S., "Rotating Cocentric Circular Peakons," *Nonlinearity* vol. 17, pp. 1-24 (2004).

Putkaradze, V., Durgin, T., Vorobieff, P., and Deshler, J., "Hysteresis in Jeffery-Hamel flows: experiments and theory", *American Physical Society, 57th Annual Meeting of the Division of Fluid Dynamics*, November 21-23, 2004, abstract #GP.002.

Korlimarla, A., and Vorobieff, P., "Evolution of a quasi-2D shear layer in a soap film flow," *American Physical Society, 57th Annual Meeting of the Division of Fluid Dynamics*, November 21-23, 2004, abstract #GG.008.

Vorobieff, P., and Putkaradze, V., "Instabilities, Bifurcations, and Multiple Solutions in Expanding Channel Flows," *Physical Review Letters* vol. 97, art. no. 144502 (2006).

Vorobieff, P., and Putkaradze, V., "Jeffery-Hamel flow: an experimental study of instabilities, bifurcations and multiple solutions," *American Physical Society, 59th Annual Meeting of the APS Division of Fluid Dynamics*, November 19-21, 2006, abstract #AO.009.

Nitsche, M., Holm, D.D., and Putkaradze, V., "Euler-alpha and vortex blob regularization of vortex filament and vortex sheet motion," *Journal of Fluid Mechanics* vol. 555, pp. 149-176 (2006).

Putkaradze, V., and Watanabe, S., "Extended boundary layer theory and modeling of flows in symmetric channel expansions," *Fluid Dynamics Research*, under consideration (2006).

Korlimarla, A., "Turbulence in two-dimensional shear flows," M.Sc. Thesis, The University of New Mexico (2006).

Putkaradze, V., and Watanabe, S., "A simple model for description of flows in symmetric channel expansions," *Physics Letters A*, in press (published online May 13, 2007).

Vorobieff, P., and Putkaradze, V., "Expanding channel flows: stability, bifurcations and boundary conditions," in preparation (2007).

Delaware Research Cluster: The Center for Spintronics and Biodetection

John Q. Xiao, Yi Ji, James Kolodzey¹ Branislav K. Nikolić, Edmund R. Nowak, Shouheng Sun²
 Department of Physics and Astronomy, University of Delaware, Newark, DE 19711

¹ Department of Electrical Engineering, University of Delaware, Newark, DE 19711

² Department of Chemistry, Brown University, Providence, RI

Center Overview

The scientific goals of the proposed Center for Spintronics and Biodetection (CSB) are to create, explore, understand, and apply novel nanomagnetic materials and phenomena. CSB research activities comprise three interrelated projects focused on: (1) revealing fundamental physics of generation, manipulation, and detection of low dissipation spin current. This includes addressing issues concerning spin transport across interfaces, through materials, and the effects of spin-orbit coupling, exchange interaction, electron-electron interactions, and radio-frequency fields, (2) identifying and controlling the electronic and magnetic mechanisms that lead to fluctuations and noise in magnetic nanostructures with the explicit objective of attaining pico-Tesla magnetic field detectivity at low frequencies from sensors based on spin-dependent tunneling structures, and (3) advancing magnetic nanotechnology for sensitive biodetection which includes fundamental materials issues involving synthesizing of stable monodisperse magnetic nanoparticles (NPs) with high moments for improved signal/noise ratio, and investigations of interactions between functionalized NPs and the magnetic sensor's surface and biological molecules. Another key aspect of CSB is the education and mentoring of students.

CSB is organized into two overlapping themes as illustrated in Figure 1 which also depicts CSB interactions at the investigator, University, State, and National levels. The Spintronics theme emphasizes fundamental spin related science. It is comprised of three experimental physicists and one theoretical/computational physicist. The Biodetection theme is focused on functionalizing nanoparticles, modeling their detection using spin dependent tunneling magnetic sensors, and device development. It consists of a chemist, a device physicist in electrical engineering, and shares a

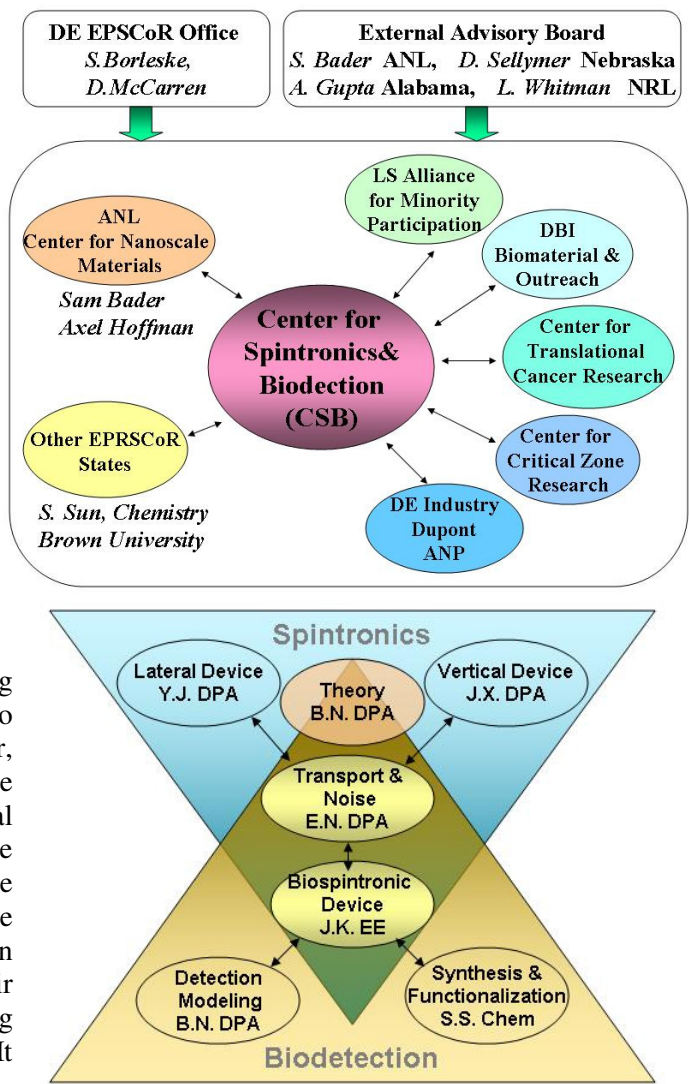


Figure 1, Program overview (top) and PIs (bottom) in the Center for Spintronics and Biodetection.

computational physicist from the Spintronics team. Understanding and advances in each theme are integrated into a biodetection technology as depicted by the overlapping triangles in Figure 1. CSB investigators will collaborate closely with scientists at Argonne National Laboratory, particularly Dr. Sam Bader’s group. All three projects will make use of the nanofabrication and characterization facilities at the Center for Nanoscale Materials at Argonne.

As indicated in Figure 1 CSB is well poised to collaborate with some existing Centers and Institutes in Delaware, as well as with industry. For example, CSB will collaborate with Delaware Biotechnology Institute on biomaterials efforts pertaining to human health and with the Center for Critical Zone Research related on nanoparticle transport and detection in plants and soil. Another collaboration involves the Center for Translational Cancer Research (CTCR), a recently established Center “without walls” to support clinical and basic scientific efforts in translational cancer research within the State of Delaware. CTCR researchers have a keen interest in using magnetic nanoparticles as tags for drug delivery and as therapeutic agents.

Research Overview

Recent theoretical, experimental, and technological efforts to gain control over electron spin, termed as spintronics, in metals [1,2,3] and semiconductors [4,5], for applications in information storage, transmission [6], and processing of classical [4] or quantum information [5] have brought about a plethora of fundamental and challenging problems for condensed matter physics. The utilization of spin transport may lead to a novel circuit logic where flipping spins requires less energy and suffers far less heat dissipation, which is one of the major obstacles for increasing the speed of conventional electronics because of the high energy cost of charge pile-ups. Such achievements will demand theoretical and experimental understandings of phenomena such as spin injection, spin accumulation, spin relaxation, spin currents and their interactions with the magnetization dynamics of ferromagnets in the presence of spin-orbit (SO) couplings, other relevant spin-dependent interactions, and electron-electron interactions. *Arguably one of the most intellectually challenging problems to emerge recently in condensed matter is how to generate, manipulate, and measure pure spin currents.*

The first project in the proposed center focuses on the fundamental physics of spin injection, spin accumulation, pure spin current generation, manipulation and detection, and spin Hall effects in metals. To achieve these objectives, we will combine theory and experiment on lateral and vertical structures where pure spin currents will be driven by electric current or rf field. By exploring these exciting phenomena, we hope to extend our basic understanding in nanostructured magnetic materials and lay the foundations for emerging technologies. The second project focuses on fluctuations in magneto-electronic materials systems in general and magnetic sensors based on spin-dependent tunneling in particular. Apart from its technological importance, fluctuations, or noise, are a useful probe of electronic and magnetic kinetic processes in nanoscale systems and devices. In the third project, we will demonstrate highly sensitive biodetection based on low noise sensors, address the fundamental material issues on fabricating stable and monodisperse magnetic nanoparticles with high magnetic moments for improved signal/noise ratio, and investigate the interaction between nanoparticle and sensor surface and biology molecules.

Project 1: Generation, Manipulation, and Detection of Pure Spin Current

Pure spin current (I^S) represents the flow of spin angular momentum that is not accompanied by net charge transport, as illustrated in Figure 2(c). This can be contrasted with traditional electrical charge current where equal numbers of spin- \uparrow and spin- \downarrow electrons propagate in the same direction, so that the charge current in that direction $I = I^\uparrow + I^\downarrow$ is unpolarized with $I^S = 0$ [Figure 2(a)]. Spin currents differ from familiar charge currents in two key aspects—they are time-reversal invariant and they transport a vector quantity, spin, instead of scalar charge. In metallic spintronic devices, ferromagnetic elements polarize electron spins, leading to a difference in charge currents of spin- \uparrow and spin- \downarrow [Figure 2 (b)]. Such *spin-polarized* charge currents are accompanied by a net *spin current* $I^S = \hbar/2e (I^\uparrow - I^\downarrow) \neq 0$, which can be created and detected in magnetic layered systems [1].

The generation of a pure spin current (Figure 2(c)) is the central objective in spintronics since zero charge current produces little power dissipation in the system and gives rise to intriguing spin physics. Pure spin currents have been generated in metals using nonlocal spin injection-detection schemes with lateral spin valves [7-10] or, recently, by exploiting theoretical suggestions [2, 11] for spin pumping where a precessing ferromagnet driven by a resonant rf magnetic field injects pure spin current into the adjacent metal through a junction. This latter effect is dubbed as the *spin battery effect* and has

been detected indirectly as an additional Gilbert-like damping in ferromagnetic resonance experiments [12,13]. We will first investigate the pure spin currents generated in lateral nonlocal spin valve structures (NLSV). We will then explore the spin battery effect with a new experimental scheme where microwave can be effectively coupled into a vertical magnetic structure. With lateral and vertical

structures, we will investigate the spin Hall effects of various materials or other spintronic devices where pure spin current injection is desired. The overarching objectives of this project are:

1. fundamental understanding of pure spin current generation and transport in the presence of spin-orbit coupling, exchange interaction, and electron-electron interaction;
2. fundamental understanding of spin dynamics in the presence of spin current and large angle excitation;
3. confirming and understanding of spin Hall effect in metals;
4. determination of spin diffusion length of various nonmagnetic and magnetic materials;
5. exploration of interfacial effects in pure spin current generation, transport, spin dynamics, and spin Hall effects.

Project 2: Fluctuations in Spin Dependent Tunneling Biosensors

The objective of this project is to provide fundamental insight into giant tunneling magnetoresistance and noise sources in spin dependent tunneling structures. The broader impact of the program is to greatly advance or enable the application of magnetic sensors for detecting biological, terrestrial, and extra-terrestrial magnetic anomalies at sub-Hz frequencies. The program leverages recent materials advances to develop magnetic tunnel junctions (MTJs) based on crystalline, rather than amorphous, tunnel barriers that operate at room temperature and are designed to provide extremely large signal with very low noise at low frequencies. These sensor elements would be the core of a reliable, inexpensive, low power, magnetic field detection system capable of detecting potentially sub-picoTesla fields at 1 Hz. A central goal of this research theme is to integrate the MTJ sensor elements together with functionalized magnetic nanoparticles (Project 3) into a magnetic biochip capable of detecting a single magnetic nanoparticle.

Project 3: Sensor Applications in Biology

The spin dependent magnetoresistive (MR) sensor developed above will allow highly sensitive detection of magnetic nanoparticles as magnetic field generated by the particles can affect the resistivity of the sensor circuit. If such magnetic nanoparticles are anchored on the sensor surface via biological interactions, then the combination of the sensor and magnetic nanoparticles can be used for highly sensitive bio-detection. Such magnetic nanoparticle based sensing devices will have many applications in

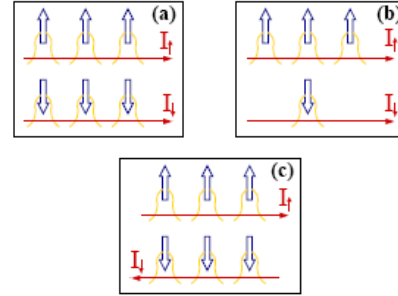


Figure 2 The classification of spin I^s and charge I currents in spintronic system corresponding to spatial propagation of spin- \uparrow and \downarrow electrons (represented as the Bloch wave-packets): (a) conventional unpolarized spin current $I^s = \hbar/2e (I^\uparrow - I^\downarrow) \equiv 0$ and charge current $I = I^\uparrow + I^\downarrow \neq 0$; (b) spin-polarized charge current $I \neq 0$ is accompanied also by spin current $I^s \neq 0$; and (c) pure spin current $I^s \neq 0$ arising when spin- \uparrow electrons move in one direction, while an equal number of spin- \downarrow electrons move in the opposite direction, resulting in zero charge current.

biodefense and diagnostics of various diseases as magnetic nanoparticles can be anchored on the surface through not only DNA hybridization, but also antibody-antigen and avidin-biotin interactions. The sensors operate at room temperature and the fabrication is compatible with standard CMOS technology. The detection system can be made as a portable and easily employed lab-on-a-chip and will have great advantage over the heavy and expensive microarray scanners.

Conventionally, the demonstrated biodetection using MR biosensors employed micron or submicron sized iron oxide doped polymer particles as labels. Such labels have very low magnetic moment density (~ 10 emu/cc), a value that is much less than that from the common iron oxide materials (~ 400 emu/cc). To achieve the ultrahigh biodetection sensitivity required for single molecules (such as DNA fragments), one needs to employ stable magnetic particles whose diameter is less than 20 nm with high magnetic moment for improved signal/noise ratio; to have these magnetic nanoparticles bond site specifically to the sensor surface via biological interactions; and to have the established correlation between nanoparticle-sensor distance and sensor signal. The MTJs proposed to be explored here could offer such solution. They offer excellent sensitivity and can detect single high moment magnetic nanoparticles (moment density higher than or similar to that from the common iron oxide). Furthermore, scalability of small MTJs will make it possible to integrate TMR biosensors into a high density MRAM-type arrays for screening thousands of different analytes simultaneously.

Reference

1. Maekawa, S. and T. Shinjo, eds. *Spin Dependent Transport in Magnetic Nanostructures*. 2002, Taylor & Francis: London.
2. Tserkovnyak, Y., A. Brataas, G.E.W. Bauer, and B.I. Halperin, *Nonlocal magnetization dynamics in ferromagnetic heterostructures*. *Reviews of Modern Physics*, 2005. 77(4): p. 1375-1421.
3. Brataas, A., G.E.W. Bauer, and P.J. Kelly, *Non-collinear magnetoelectronics*. *Physics Reports-Review Section of Physics Letters*, 2006. 427(4): p. 157-255.
4. Zutic, I., J. Fabian, and S. Das Sarma, *Spintronics: Fundamentals and applications*. *Reviews of Modern Physics*, 2004. 76(2): p. 323-410.
5. Awschalom, D.D., D. Loss, and N. Samarth, *Semiconductor Spintronics and Quantum Computation*. 2002, Berlin: Springer.
6. Awschalom, D.D. and J.M. Kikkawa, *Electron spin and optical coherence in semiconductors*. *Physics Today*, 1999. 52(6): p. 33-38.
7. Ji, Y., A. Hoffmann, J.E. Pearson, and S.D. Bader, *Enhanced spin injection polarization in Co/Cu/Co nonlocal lateral spin valves*. *Applied Physics Letters*, 2006. 88(5): p. 052509.
8. Garzon, S., I. Zutic, and R.A. Webb, *Temperature-dependent asymmetry of the nonlocal spin-injection resistance: Evidence for spin nonconserving interface scattering*. *Physical Review Letters*, 2005. 94(17): p. 176601.
9. Jedema, F.J., H.B. Heersche, A.T. Filip, J.J.A. Baselmans, and B.J. van Wees, *Electrical detection of spin precession in a metallic mesoscopic spin valve*. *Nature*, 2002. 416(6882): p. 713-716.
10. Valenzuela, S.O. and M. Tinkham, *Direct electronic measurement of the spin Hall effect*. *Nature*, 2006. 442(7099): p. 176-179.
11. Brataas, A., Y. Tserkovnyak, G.E.W. Bauer, and B.I. Halperin, *Spin battery operated by ferromagnetic resonance*. *Physical Review B*, 2002. 66(6): p. 060404.
12. Mizukami, S., Y. Ando, and T. Miyazaki, *The study on ferromagnetic resonance linewidth for NM/80NiFe/NM (NM = Cu, Ta, Pd and Pt) films*. *Japanese Journal of Applied Physics Part 1-Regular Papers Short Notes & Review Papers*, 2001. 40(2A): p. 580-585.
13. Mizukami, S., Y. Ando, and T. Miyazaki, *Ferromagnetic resonance linewidth for NM/80NiFe/NM films (NM = Cu, Ta, Pd and Pt)*. *Journal of Magnetism and Magnetic Materials*, 2001. 226: p. 1640-1642.

Estimating Soil Hydraulic Parameter Uncertainty and Heterogeneity Using Bayesian Updating and Neural Network Methods

Jianting Zhu¹, Ming Ye^{1,2}, Philip D. Meyer³, Yanxia Zhao¹, Ahmed E. Hassan¹, Feng Pan¹
Jianting.Zhu@dri.edu, mingye@scs.fsu.edu, Philip.Meyer@pnl.gov, Yanxia.Zhao@dri.edu,
Ahmed.Hassan@dri.edu, Feng.Pan@dri.edu

¹Division of Hydrologic Sciences, Desert Research Institute, Las Vegas, NV 89119, ²School of Computational Science & Department of Geological Sciences, Florida State University, Tallahassee, FL 32306, ³Pacific Northwest National Laboratory, Richland, WA 99352

Program Scope

Heterogeneity and uncertainty are the most significant hampering factors in modeling and predicting subsurface flow and contaminant transport. This program tries to complete a quantitative study to predict heterogeneous soil hydraulic properties and the associated uncertainties. We seek to address a number of important issues related to the hydraulic property characterizations. It involves extending a Bayesian updating method, developing innovative artificial neural network (ANN) models, postulating a new Bayesian geostatistical inference method, and combining these three methods to estimate heterogeneous soil hydraulic parameter fields. Specific objectives are to:

(1) Extend a Bayesian updating method to estimate the Department of Energy (DOE)'s Hanford site-specific probability distributions and associated statistics of hydraulic parameters for uncertainty analysis. The extension will eliminate the assumption that the parameters follow normal distributions.

(2) Develop innovative ANN-based pedo-transfer functions (PTFs) to estimate soil hydraulic parameters using "soft" data (e.g., particle size distribution and soil texture and bulk density etc.). The PTFs will incorporate parameter distributions obtained from the extended Bayesian updating method and eliminate the artificial correlation of output hydraulic parameters.

(3) Propose a new Bayesian geostatistical inference method to estimate spatial correlation scale of inputs to the developed neural network models. Heterogeneous input fields will be generated and fed to the neural network models to result in heterogeneous fields of soil hydraulic parameters that can be used for numerical simulation and uncertainty analyses.

The outcomes facilitate subsurface flow and contaminant transport modeling and improve the defensibility of model results. Systematic and quantitative consideration of the parametric heterogeneity and uncertainty can properly address and further reduce predictive uncertainty for contamination characterization and environmental restoration at DOE-managed sites such as the Hanford and other sites.

Recent Progress

The hydraulic property model of van Genuchten¹, which closely fits measured water-retention data of many types of unstructured soils², is used. van Genuchten's model for the soil water retention curve combined with the hydraulic conductivity function of Mualem³ can be expressed as follows,

$$\theta(h) = \theta_r + (\theta_s - \theta_r) \left[1 + (\alpha h)^n \right]^{-m} \quad (1)$$

$$K(h) = K_s \left\{ 1 - (\alpha h)^m \left[1 + (\alpha h)^n \right]^{-m} \right\}^2 \left[1 + (\alpha h)^n \right]^{-m/2} \quad (2)$$

where h is the soil water suction head [L], θ is the soil water content [L^3L^{-3}], θ_r is the residual water content [L^3L^{-3}], θ_s is the saturated water content [L^3L^{-3}], K_S is the saturated hydraulic conductivity [L/T], α is the shape factor, approximately equal to the inverse to the air entry value [L^{-1}], n is the pore size distribution index [-], and m is the empirical constant which can be related to n by $m = 1-1/n$.

The traditional neural network based PTFs utilize the objective function (denoted *Function 1*) (i.e., the sum of the squared errors of the neural network prediction of the soil hydraulic properties)

$$O_1(W, U) = \sum_{i=1}^{N_s} \sum_{j=1}^{N_o} \alpha_{ij} [\hat{Y}_{ij} - Y_{ij}]^2 \quad (3)$$

where N_s is the number of samples, N_o is the number of output parameters, W and U are weights of the hidden and the output layer of neural network model that are adjusted in the training process, Y_{ij} is the measured hydraulic parameters and \hat{Y}_{ij} is the predicted hydraulic parameters (i.e., θ_r , θ_s , α , n , or K_s), α_{ij} are weighting coefficients that can be assigned based on measurement error and confidence level of Y_{ij} and will not be adjusted in the neural network training process.

70-point data set of hydraulic properties has been gathered and compiled for the Hanford site. Using cokriging and the ANN approaches, site-specific PTFs in conjunction with a Bayesian method have been developed. The ANN models, which were based on the traditional objective function, used the cokriged heterogeneous fields of pedo-transfer variables as input to generate heterogeneous fields of the soil hydraulic parameters.⁴

We try to develop a suite of new neural network models to estimate soil hydraulic parameters. These neural networks have the same input and output variables, but different objective functions, which will incorporate sequentially the site soil hydraulic parameter measurements, parameter probability distributions, and parameter correlations. To incorporate the hydraulic parameter distributions, the objective function (denoted *Function 2*) is modified as

$$O_2(W, U) = \sum_{i=1}^{N_s} \sum_{j=1}^{N_o} \alpha_{ij} [\hat{Y}_{ij} - Y_{ij}]^2 + \sum_{j=1}^{N_o} \gamma_j [\hat{\mu}_j - \mu_j]^2 + \sum_{j=1}^{N_o} \delta_j [\hat{\sigma}_j^2 - \sigma_j^2]^2 \quad (4)$$

where γ_j , δ_j are weighting coefficients for the mean and variance, $\hat{\mu}_j$ and $\hat{\sigma}_j^2$ are the mean and variance of \hat{Y}_{ij} estimated by the neural networks, μ_j and σ_j^2 are the theoretical mean and variance of soil hydraulic parameter Y_j . The objective function defined in Eq. (4) enforces the adjusted neural network weights to predict soil hydraulic parameters following the specified probabilistic distributions.

In order to resolve the problem of unrealistic parameter correlations introduced by the neural networks, an objective function (denoted *Function 3*) is introduced to incorporate the parameter correlations among different hydraulic parameters

$$O_3(W, U) = \sum_{i=1}^{N_s} \sum_{j=1}^{N_o} \alpha_{ij} [\hat{Y}_{ij} - Y_{ij}]^2 + \sum_{j=1}^{N_o} \gamma_j [\hat{\mu}_j - \mu_j]^2 + \sum_{j=1}^{N_o} \delta_j [\hat{\sigma}_j^2 - \sigma_j^2]^2 + \sum_{i=1}^{N_o} \sum_{j=i+1}^{N_o} \epsilon_{ij} (\hat{C}_{ij} - C_{ij})^2 \quad (5)$$

Since non-conventional objective functions are used, new neural network algorithms are needed. In doing so, the computation of the derivatives of the objective function with respect to the neural network weights (i.e., W and U) is a key step in implementation of neural network models. This can be accomplished in two steps, (1) the derivative of the objective function with respect to the output hydraulic parameters, and

(2) the derivative of the output parameters with respect to the weights. Step 1) can be implemented as follows

$$\frac{\partial O_2}{\partial \widehat{Y}_{kl}} = 2\alpha_{kl}(\widehat{Y}_{kl} - Y_{kl}) + \frac{2\gamma_k}{N_S}(\widehat{\mu}_k - \mu_k) + \frac{4\delta_k}{N_S - 1}(\widehat{\sigma}_k^2 - \sigma_k^2)(\widehat{Y}_{kl} - \widehat{\mu}_k) \quad (6)$$

$$\begin{aligned} \frac{\partial O_3}{\partial \widehat{Y}_{kl}} = & 2\alpha_{kl}(\widehat{Y}_{kl} - Y_{kl}) + \frac{2\gamma_k}{N_S}(\widehat{\mu}_k - \mu_k) + \frac{4\delta_k}{N_S - 1}(\widehat{\sigma}_k^2 - \sigma_k^2)(\widehat{Y}_{kl} - \widehat{\mu}_k) \\ & + \frac{2}{N_S} \sum_{i=1}^{N_o} \sum_{j=i+1}^{N_o} \varepsilon_{ij} (\widehat{C}_{ij} - C_{ij}) \sum_{m=1}^{N_S} \left[\left(\delta_{ml} - \frac{1}{N_S} \right) \left(\delta_{jk} (\widehat{Y}_{jm} - \widehat{\mu}_j) + \delta_{ik} (\widehat{Y}_{im} - \widehat{\mu}_i) \right) \right] \end{aligned} \quad (7)$$

The second step is accomplished with the widely used back-propagation method.⁵

Using a synthetic data set calculated based on the multiple regression models of Rawls and Brakensiek⁶, we first test and investigate the ANN models with three different objective functions described above. Table 1 shows correlation coefficients between the original and the ANN model predicted hydraulic parameters for three different objective functions. We can see very good correlations using all objective functions are achieved.

Table 1: Correlation Coefficient between the original and the ANN predicted hydraulic parameters using synthetic data

	<i>Function 1</i>	<i>Function 2</i>	<i>Function 3</i>
θ_r	0.9833	0.9837	0.9834
$\ln(\alpha)$	0.9914	0.9918	0.9913
$\ln(n)$	0.9966	0.9962	0.9966
$\ln(K_S)$	0.9927	0.9922	0.9926

Next, 53-point hydraulic parameter set and the associated texture and bulk density data set collected from the Hanford site are used to train the ANN models. Table 2 shows correlation coefficients between the original and the ANN model predicted hydraulic parameters for three different objective functions. We can see a progressively better correlation trend when using objective function 2 and 3.

Table 2: Correlation Coefficient between the original and the ANN predicted hydraulic parameters using field measured data

	<i>Function 1</i>	<i>Function 2</i>	<i>Function 3</i>
θ_r	0.2044	0.5252	0.5498
θ_s	0.5651	0.6056	0.6649
$\log(\alpha)$	0.5273	0.6093	0.6436
$\log(n)$	0.6732	0.7251	0.7161
$\log(K_S)$	0.8654	0.8980	0.9000

Future Plans

The probability distributions of hyper-parameters of the soil hydraulic parameters from the Hanford site will be evaluated. We will extend the Bayesian updating algorithm to update the hyper-parameters without the restriction that the hyper-parameters follow normal distributions and then apply the developed algorithm to the parameters gathered

from the Hanford site. The estimation of posterior distributions of the parameter correlation scales will also be conducted.

We will continue to evaluate the ANN based PTF performance by incorporating various statistical features of the hydraulic parameters which can be better controlled for the synthetic cases before using and testing the successful PTFs to actual field hydraulic parameter data collected from the Hanford site. The testing will include, for example, adding some noise (measurement errors) to both input and output parameters of the synthetic data to investigate the effects of incorporating different objective functions on the ANN-based PTFs. After the synthetic case testing and evaluations, we will then use the parameter data sets from the available field measurements for extensive ANN training and validation. The ANN training and validation will be carried out in two scenarios, similar to the synthetic cases considered earlier, i.e., incorporating hydraulic parameter distributions, as well as incorporating both hydraulic parameter distributions and correlations in the ANN objective functions.

Using the estimated posterior distributions of hyper-parameters and the correlation scales, together with the developed PTFs, we can then generate spatially heterogeneous random hydraulic parameter fields that will be used for the numerical simulations of the vadose zone processes and compare the simulations with the observed field data at the Hanford site.

References

- (1) van Genuchten, M.Th., **1980**. A closed-form equation for predicting the hydraulic conductivity of unsaturated soils. *Soil Sci. Soc. Am. J.*, 44, 892–898.
- (2) Leij, F. J., W. B. Russell, and S. M. Lesch, **1997**. Closed-form expressions for water retention and conductivity data, *Ground Water*, 35(5), 848-858.
- (3) Mualem, Y., **1976**. A new model for predicting the hydraulic conductivity of unsaturated porous media, *Water Resour. Res.*, 12(3), 513-522.
- (4) Ye, M., R. Khaleel, M. G. Schaap, and J. Zhu, **2007**. Simulation of field injection experiments in heterogeneous unsaturated media using cokriging and artificial neural network, *Water Resour. Res.*, 43, W07413, doi:10.1029/2006WR005030.
- (5) Nelles, O., 2001. *Nonlinear System Identification*, Springer-Verlag, Berlin, Germany.
- (6) Rawls, W. J., and D. L. Brankensiek, **1985**. Prediction of soil water properties for hydrologic modeling, in *Proceedings of Symposium on Watershed Management*, pp. 293-299, American Society of Civil Engineers, New York.

DOE-EPSCoR Sponsored Publications in 2006-2007

Simulation of field injection experiments in heterogeneous unsaturated media using cokriging and artificial neural network, M. Ye, R. Khaleel, M. G. Schaap, and J. Zhu, *Water Resour. Res.*, 43, W07413, doi:10.1029/2006WR005030, **2007**.

Incorporating soil hydraulic parameter statistics in developing neural network based pedo-transfer functions, J. Zhu, M. Ye, P. Meyer, F. Pan, A. Hassan, and Y. Zhao, in preparation.

Author Index

Adams, Thad.....	46	Guo, Boyun.....	121
Adebisi, Rasheed.....	33	Hall, Greg.....	101
Allen, Gabrielle.....	52, 121	Hall, Jaclyn.....	37
Alley, Earl.....	37	Han, Tae-hee.....	60
Alton, Andrew.....	68	Harrison, Kevin.....	60
Alway-Cooper, Rebecca.....	76	Hassan, Ahmed.....	133
Ang, Simon.....	30	Hernandez, Rafael.....	37
Angst, Manuel.....	42	Hernández-Pacheco, Eduardo.....	60
Bader, Sam.....	14	Hershberger, John.....	97
Bang, Sookie.....	1	Hoffmann, Mark.....	97
Bass, Henry.....	33	Holmes, William.....	37
Bayoumi, Magdy.....	89, 121	Honsberg, Christiana.....	109
Bellaiche, Laurent.....	56	Hoskins, Anna.....	79, 82
Benson, Tracy.....	37	Hunt, Alan.....	79, 82
Berry, Devon.....	46	Jayasekera, Thushari.....	72
Biaku, Christian.....	60	Ji, Yi.....	129
Bond, Tariq.....	22	Katiyar, Ram.....	38
Bowdle, D.....	84	Keller, Christina.....	68
Bowman, Frank.....	97	Keppens, Veerle.....	42
Bromenshenk, Jerry.....	4	Khonsari, Michael.....	121
Burghaus, Uwe.....	97	Kihara, Ian.....	82
Cassibry, Jason.....	5	Kirkpatrick, Ron.....	5
Celik, Ismail.....	10	Knapp, Charles.....	5
Chan, Yuen-dat.....	68	Knight, Travis.....	46
Chesler, Elissa.....	48	Kolis, Joe.....	117
Christopher, S.....	84	Kolodzey, James.....	129
Chui, Siu-Tat.....	14	Kosar, Tefvik.....	52
Dale, Nilesh.....	60	Kozliak, Evguenii.....	97
Darby III, Paul.....	18	Lamberton, Jr., Gary.....	33
Daw, Murray.....	117	Langston, Michael.....	48
DeCuir, Jr., Eric.....	22	Lau, Lisa.....	79, 82
Denty, Dominic.....	79	Lei, Zhou.....	52, 121
DeSisto, Bill.....	86	Lesko, Kevin.....	68
Donovan, Richard.....	25	Liang, Kaiwen.....	37
Drymiotis, Fivos.....	117	Lisenkov, Sergey.....	56
Ekkebus, Allen.....	29	Lobach, Sergiy.....	46
Fred, Emil.....	22, 30	Luan, Yanbing.....	42
Frederick, Brian.....	86	Mann, Michael.....	60, 97
French, Todd.....	37	Manasreh, Omar.....	22, 30
Fu, Huaxiang.....	56	Mandrus, David.....	42
Fuller, K.....	84	Marinescu, Catalina.....	117
Gardner, Joseph.....	82	Mao, Zhiqiang.....	64
Gladden, Joseph (Josh).....	33	McNider, R.....	84
Gudkov, Vladimir.....	36	McTaggart, Robert.....	68

Mei, Dongming.....	68	Tritt, Terry.....	117
Meyer, Philip.....	133	Tsai, Frank.....	52
Mintmire, John.....	72	Tzeng, Nian-Feng.....	18, 89, 121
Mondala, Andro.....	37	van Heiningen, Adriaan.....	86
Morales, Marlon.....	76	Vasudevamurthy, Gokul.....	46
Moreman, Douglas.....	121	Vorobieff, Peter.....	125
Nair, U.....	84	Voy, Brynn.....	48
Narsingi, Kaushik.....	30	Wang, Andrew.....	30
Newchurch, M.....	84	Watts, Jenny.....	46
Nikolić, Branislav.....	129	Welch, R.....	84
Norman, Andrew.....	109	Wheeler, Clay.....	86
Nowak, Edmund.....	129	White, Christopher.....	52, 121
Ogale, Amod.....	76	White, Mark.....	37
Pak, Joshua.....	79, 82	Wu, Hongyi.....	89, 121
Pan, Feng.....	133	Wu, S. T.....	5
Pancholi, Anup.....	109	Xiao, John.....	129
Patadia, Falguni.....	84	Ye, Ming.....	133
Pendse, Hemant.....	86	Yin, Zhongbao.....	68
Perkins, Dmitri.....	89, 121	Zhang, Yong.....	109
Peters, Andrew.....	60	Zhao, Yanxia.....	133
Pierce, David.....	97	Zhu, Jianting.....	133
Prior, Gersende.....	68		
Pritchard, Stephanie.....	79		
Putkaradze, Vakhtang.....	125		
Qin, Guan.....	52		
Ramamurthy, Byrav.....	93		
Rao, Apparao.....	117		
Rizatdinova, Flera.....	113		
Rodriguez, Rene.....	79, 82		
Roggenthen, William.....	68, 82		
Salehfar, Hossein.....	60		
Sani, Rajesh.....	1		
Seames, Wayne.....	97		
Sears, Trevor.....	101		
Seidel, Edward.....	121		
Shafer-Ray, Neil.....	101		
Shapiro, Pamela.....	105		
Shurdha, Endrit.....	82		
Smith, Al.....	68		
Smith, John.....	121		
Stoleru, Valeria.....	109		
Strauss, Mike.....	113		
Sun, Shouheng.....	129		
Sun, Yongchen.....	68		
Sweeney, Daniel.....	76		
Szczerbinska, Barbara.....	68		
Trimble, Judy.....	29		

Participant List

Phil Ahrenkiel, South Dakota School of Mines and Technology
Sergey Aizen, University of Idaho
Gary April, University of Alabama
David Bagley, University of Wyoming
Richard Bajura, West Virginia University
Sookie Bang, South Dakota School of Mines and Technology
Mahdi Farrokh Baroughi, South Dakota State University
Kristin Bennett, U.S. Department of Energy, Office of Science
Mary Bissell, Los Alamos National Lab
Eldon Boes, Senate Committee on Agriculture, Nutrition and Forestry
Venkat Bommisetty, South Dakota State University
Tariq Bond, University of Arkansas
Stephen Borleske, Delaware EPSCoR
Jim Brainard, National Renewable Energy Laboratory
Alysia Bridgman, SC EPSCoR/IDeA
Jerry Bromenshenk, Montana Organization for Research in Energy
Stan Bull, National Renewable Energy Laboratory
Daryle Busch, KU Center for Environmentally Beneficial Catalysis
Thomas Butcher, Brookhaven National Laboratory
Jason Cassibry, University of Alabama, Huntsville
Kenneth Cassman, University of Nebraska
Ismail Celik, West Virginia University
Namas Chanda, University of Nebraska, Lincoln
Fred Choobineh, Nebraska EPSCoR
Siu-Tat Chui, University of Delaware
Bob Dalton, University of New Hampshire
Paul Darby III, University of Louisiana, Lafayette
Kalyan Das, Tuskegee University, Dept. Electrical Eng.
Asad Davari, WVU Tech
Satyen Deb, National Renewable Energy Laboratory
Eric DeCuir, Jr., University of Arkansas
Bill DeSisto, University of Maine
Nilesh Dhote, University of Alabama, Huntsville
Richard Donovan, Montana Tech of the University of Montana
Mildred Dresselhaus, Massachusetts Institute of Technology
Deb Easterly, Idaho State University
Louis Edwards, University of Idaho
Allen Ekkebus, ORNL
Randy Ellingson, National Renewable Energy Laboratory
Muhammad Farooq, West Virginia University
Sherry Farwell, South Dakota School of Mines and Technology
Barbara Ferris, National Renewable Energy Laboratory
Jerald Fletcher, West Virginia University, Natural Resource Analysis Center
Larry Ford, Idaho State University

Tom Foust, National Renewable Energy Laboratory
Emil Fred, University of Arkansas
Brian Frederick, University of Maine
Marie Garcia, Sandia National Laboratories
Bobi Garrett, National Renewable Energy Laboratory
Arlene Garrison, University of Tennessee
Jim Gershey, Louisiana Board of Regents
Joseph (Josh) Gladden, University of Mississippi
David Glickson, National Renewable Energy Laboratory
Richard Gostic, University of Nevada, Las Vegas
Julie Gostic, University of Nevada, Las Vegas
Eric Grulke, University of Kentucky
Vladimir Gudkov, University of South Carolina
Rand Haley, EPSCoR/IDeA Foundation
Melinda Hamilton, Idaho National Laboratory
Bruce Harmon, Ames Laboratory
Kevin Harrison, National Renewable Energy Laboratory
Robert Hawsey, Oak Ridge National Laboratory
Jian He, Clemson University
Stephen Herbert, University of Wyoming
Rafael Hernandez, Mississippi State University
David Hobbs, Montana Tech
James Hoehn, EPSCoR/IDeA Foundation
Haiping Hong, SDSM&T
Alan Hurd, Los Alamos National Laboratories
Ram Katiyar, University of Puerto Rico
Sudha Katiyar, University of Puerto Rico
Larry Kazmerski, National Renewable Energy Laboratory
Veerle Keppens, University of Tennessee
Michael Khonsari, Louisiana Board of Regents
Barbara Kimbell, University of New Mexico
Christopher Kitchens, Clemson University Chemical Engineering
Sophia Kitts, Oak Ridge Institute for Science and Education
Sarah Koerber, University of Idaho
Goutam Koley, University of South Carolina
David Koppenaal, Pacific Northwest National Laboratory
Mathieu Kourouma, Southern University and A&M College
Evguenii Kozliak, University of North Dakota
Rick Kurzynske, Director, Kentucky Statewide EPSCoR Program
Marjorie Langell, University of Nebraska
Mike Langston, University of Tennessee
Zhou Lei, Louisiana State University
Shuhui Li, University of Alabama
Ge Lin, West Virginia University
Sergey Lisenkov, University of Arkansas
Yanbing Luan, University of Tennessee
Ronald Madl, KSU/GRSC/BIVAP

Andrea Mammoli, University of New Mexico
Michael Mann, University of North Dakota
Omar Manasreh, University of Arkansas
Zhiqiang Mao, Tulane University
David McCarren, Delaware Biotechnology Institute
Monica Mehanna, University of Kentucky
Dongming Mei, University of South Dakota
John Mintmire, Oklahoma State University
Melody, Mountz, National Renewable Energy Laboratory
Walt Musial, National Renewable Energy Laboratory
Harold Myron, Argonne National Laboratory
Jonathan Naughton, University of Wyoming
Christie Nelson, Brookhaven National Laboratory
Vicki Nemeth, University of Maine/Maine EPSCoR
Tzeng Nian-Feng, Univ of Louisiana
Andrew Norman, National Renewable Energy Laboratory
Michael Nowak, Natl Energy Tech Lab
Amod Ogale, Clemson University
Frank Ogletree, Lawrence Berkeley National Lab
Joshua Pak, Idaho State University
Anup Pancholi, University of Delaware
Falguni Patadia, Department of Atmospheric Sciences, University of Alabama in Huntsville
Hemant Pendse, University of Maine
Dmitri Perkins, University of Louisiana at Lafayette, The Center for Advanced Computer Studies
Norm Peterson, Argonne National Laboratory
Sheri Powell, Alabama EPSCoR
Qiquan Qiao, South Dakota State University
John Quaranta, West Virginia University
Byrav Ramamurthy, University of Nebraska, Lincoln
James Rice, South Dakota EPSCoR
Flora Rizatdinova, Oklahoma State University
Mike Robinson, National Renewable Energy Laboratory
Rene Rodriguez, Idaho State University
Eric Rohlfing, Office of Basic Energy Sciences/DOE
Doug Schulz, North Dakota State University
Rick Schumaker, Idaho EPSCoR Office
Caterina Scoglio, Kansas State University
Wayne Seames, University of North Dakota
Neil Shafer-Ray, University of Oklahoma
Pamela Shapiro, University of Idaho
Susan Solomon, NOAA/ESRL Chemical Sciences
Daniel Sordelet, Ames Laboratory
Everett Springer, Los Alamos National Laboratory
Valeria Stoleru, University of Delaware
Mike Strauss, The University of Oklahoma
Ray Stults, National Renewable Energy Laboratory

Ray Teller, Argonne National Laboratory - IPNS
Keenan Thomas, University of South Dakota
Ed Tracy, National Renewable Energy Laboratory
Judy Trimble, Oak Ridge National Laboratory
Terry Tritt, Clemson University
Janet Twomey, Wichita State University
Nian-Feng Tzeng, University of Louisiana, Lafayette
Arthur Vailas, Idaho State University
Thomas Vogt, USC NanoCenter
Peter Vorobieff, University of New Mexico
Warren Washington, National Center for Atmospheric Research
Clay Wheeler, University of Maine
Daniel White, Institute of Northern Engineering
James Wicksted, OSU - Oklahoma EPSCoR
Sonya Wohletz, Los Alamos National Lab
Hongyi Wu, University of Louisiana, Lafayette
John Xiao, University of Delaware
Yong Zhang, National Renewable Energy Laboratory
Jianting Zhu, Desert Research Institute
John Ziagos, Lawrence Livermore National Laboratory